論文 / 著書情報
Article / Book Information

題目(和文)	フォトクロミック有機-無機複合材料の機能化と特性に関する研究 / 上田雅英
Title(English)	Studies on functionality and characteristics of photochromic organic-inorganic hybrids
著者(和文)	上田雅英
Author(English)	
出典(和文)	学位:博士(工学), 学位授与機関:東京工業大学, 報告番号:乙第3462号, 授与年月日:2000年7月31日, 学位の種別:論文博士, 審査員:市村 國宏
Citation(English)	Degree:Doctor (Engineering), Conferring organization: Tokyo Institute of Technology, Report number:乙第3462号, Conferred date:2000/7/31, Degree Type:Thesis doctor, Examiner:
学位種別(和文)	博士論文
Type(English)	Doctoral Thesis

Studies on Functionality and Characteristics of Photochromic Organic-Inorganic Hybrids

by
MASAHIDE UEDA

Chemical Resources Laboratory,
Tokyo Institute of Technology
2000

[contents]

Chapter 1

General Introduction

Amorphous Silicas [1)]

The phrase "as numerous as the grains of sand on the seashore" represents an excellent way to express a great multitude of anything. First and foremost, the phrase must be derived from the fact that there is a great deal of sand lying around the world. In addition, the large quantity of silicon binds up in countless different minerals, and it is easy to see why silicon is the most abundant of all elements except oxygen. In nature, silicon is usually found in the form of silica -SiO_2. Quartz is a crystalline form of pure silica, and silica gel, which is now widely used as absorbents, is a partially dehydrated form of polymerized colloidal silica.

Figure 1-1 shows the present commercial manufacturing methods for amorphous silica particles. Roughly speaking, amorphous silica can be produced by two different process; a liquid phase process and a gas phase one. The liquid phase process, which consists essentially of the gelation of an alkali silicate, produces several types of hydrated amorphous silica. Silica gel and precipitated silica are manufactured by the acid treatment of aqueous sodium silicate solution. Silica gels are formed by a reaction carried out under acidic conditions with a critical pH, whereas precipitated silicas are produced from alkaline solutions. Both of these products are in a class of materials known as hydrated silicas which contain 6 to 8 % of moisture. The chemical reaction is expressed by the following equation.

$$Na_2O/mSiO_2 + H_2SO_4 \rightarrow SiO_2/nH_2O + Na_2SO_4$$

The physical properties of silica gel are quite distinct from the other silicas. In contrast to precipitated silica, silica gels exhibit a high degree of porosity or pore volume and a very high surface area. In the manufacturing process, a colloidal silica suspension of silica is first formed, then the

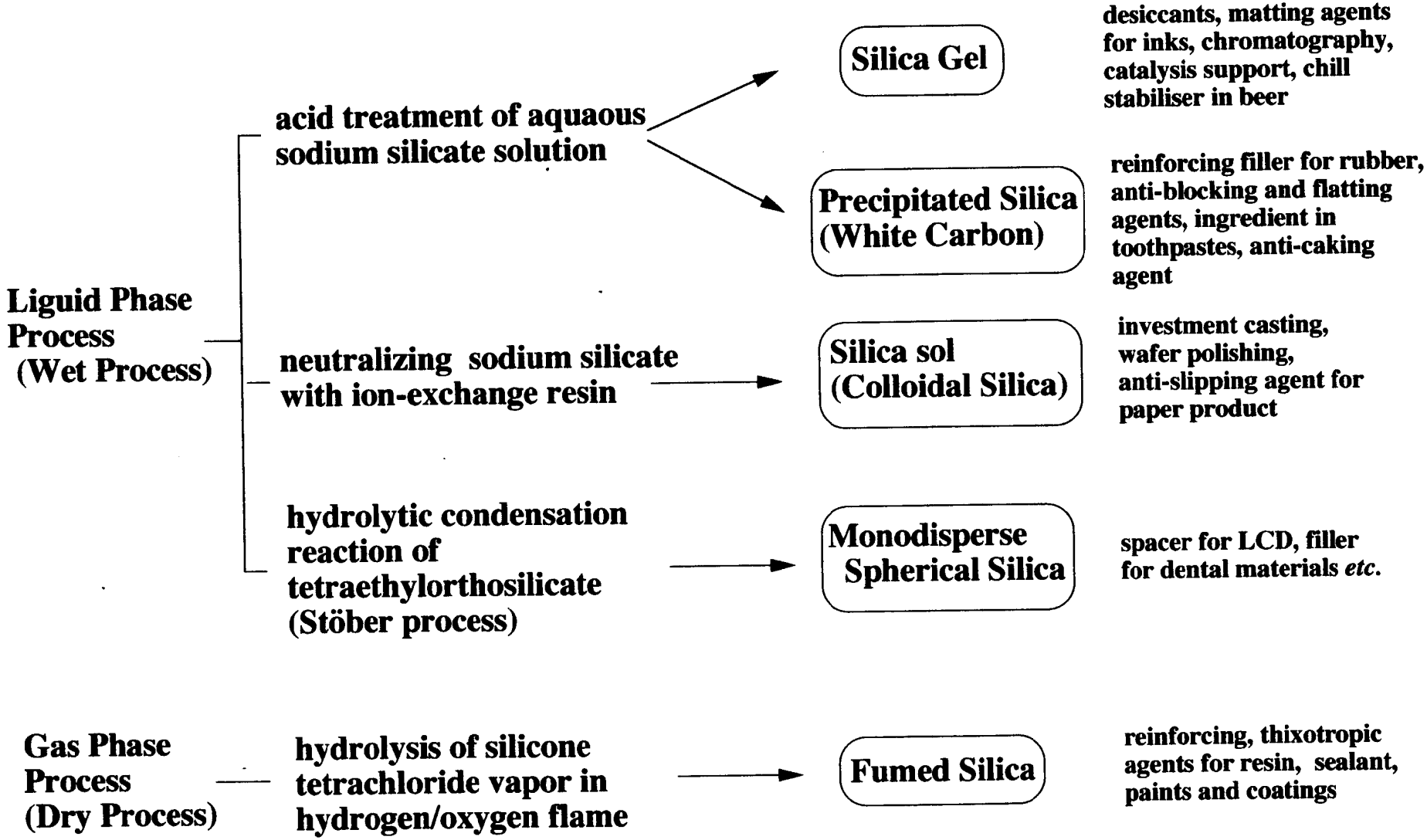

Figure 1-1 Manufacturing Methods and Applications of Amorphous Silica Particle

internal pores are filled with water producing hydrogels. Further processing yields either xerogels or aerogels. Xerogels are formed when hydrogels are dried and shrunk to reduce their porosity.[2] On the other hand, aerogels are formed when hydrogels are dried without shrinkage by replacing most of the water in the gel with alcohol to be subjected to be heated in an autoclave above the critical temperature of alcohol so that there is no meniscus between liquid and gas phases.[3] Generally, silica gels are compressed as they are dried. But, aerogels are an exception, and it is difficult to distinguish them from some precipitated silicas.

Precipitated silica has little gel characteristics in the strict sense of the term, because it is prepared under conditions which do not permit the formation of a continuous gel structure; for instance, by adding a precipitating salt, setting at low pH or freezing. The product is washed, filtered, dried and classified according to particle size and surface area. Changing such variables as reaction time, temperature, solution concentration and composition of reactants can readily vary the physical properties of precipitated silica.[4]

Silica sol, the so-called colloidal silica, is also obtained by neutralizing a water solution of sodium silicate with an acid and subsequently by removing various salts through an ion-exchange resin.[5] The most notable difference is that they come in aqueous dispersions of 15% to 50% solid which are commonly used in industry. Colloidal silicas differ greatly in physical properties from other specialty silicas by their very small particle size, which ranges from 5 nm to 50 nm. By comparison, this is nearly a thousand times smaller than silica gel or precipitated silica particles, although it is comparable in size to anhydrous fumed silica particles. Therefore, colloidal silica can be thought of a precursor to these hydrated silicas. Agglomeration and precipitation to larger particle forms is prevented by the maintenance of proper water contents and cation concentration, as well as environmental conditions, particularly temperature. Freezing or evaporation of the sol causes irreversible precipitation. Cations such as sodium and ammonium, in concentrations of less than 1 % by weight, create negative charges on silica surfaces, causing the particles to repel each other and prevent them from gelling.[6]

Monodisperse spherical silica is prepared from ammoniacal tetraethyl orthosilicate (TEOS) solution. This method was first reported by Stöber *et al.*[7] Detailed studies was made on the so-

called " Stöber process" as one of the interesting fields of study in sol-gel process.[8] The highly polymerized silica particles exhibit wide range of diameters up to several microns, depending on the initial solution conditions.[7,9]

Fumed silica (or pyrogenic silica) is synthesized by dry process. The vapor of silicone tetrachloride (STC) is hydrolyzed in oxygen -hydrogen premix flames to generate anhydrous silica.[10-12] The net reaction for the hydrolysis process to form fumed silica is as follows;

$$SiCl_4 + 2H_2 + O_2 \rightarrow SiO_2 + 4HCl$$

Very fine spheres of molten amorphous silicone dioxide are formed in the hydrolysis process, during which the molten spheres collide and fuse together to form branched, three-dimensionally chained aggregates. Very fine particles thus formed give rise to the formation of nonporous and amorphous silicas with large surface areas and high purity. Their particle sizes and surface areas can be controlled by changes in combustion conditions, while the purity of the fumed silica exceeds 99.9 %. The average particle size of original particle ranges from 7 nm to 40 nm and its specific surface area ranges from 50 m^2/g to 380 m^2/g.[13]

Surface-modification of Silica

These various types of amorphous silicas may be widely used as adsorbents, fillers and additives such as reinforcing, thixotropic, anti-blocking and flatting agents corresponding to their different characteristics (Figure 1-1). In the field of these applications, the interfaces between silica and surrounding materials play important roles in material properties (adhesion, wetting, colloid stabilization, chromatography, and catalysis *etc.*). Especially, silica fillers as a reinforcing agents of composite materials have been investigated and used for a long time. Extensive evaluations of silane coupling agents in glass-reinforced polyester and epoxy composites were motivated primarily by the objective of increasing the wet strength in glass-reinforced polymer composites.[14] Hundreds of organofunctional silanes have been developed for bonding virtually any polymer to silica in reinforced

composites.[15,16] Advanced analytical techniques have been also used to characterize the interphase and to provide direct evidence regarding the mechanism of bonding in such a particular system.[17-22] For bonding a given polymer to a silica filler, a silane is selected in such a way that the organofunctional group is capable of reactions or interactions with the polymer matrices. This interactions may result in covalent bonds of organofunctional group with polymer matrices, or they may consist of a co-polymerization reaction at the interphase, or formation of an interpenetrating polymer networks (IPN).

Another attention has been paid to extensively prepare graft polymers chemically bound to silica surfaces in order to stabilize colloidal silica in organic solvents. The formation of covalently bound polymer layers (*e.g.*, polystyrene,[23] poly(dimethylsiloxane),[24,25] poly(ethyleneoxide),[26,27] polyester,[28] poly(methyl methacrylate),[29] *etc.*) by polymerization reactions carried out on silica surfaces via suitable initiating, terminating or polymerisable groups or by reactions of surface silanol groups with chemically active chlorosilane or alkoxysilane groups of polymers.

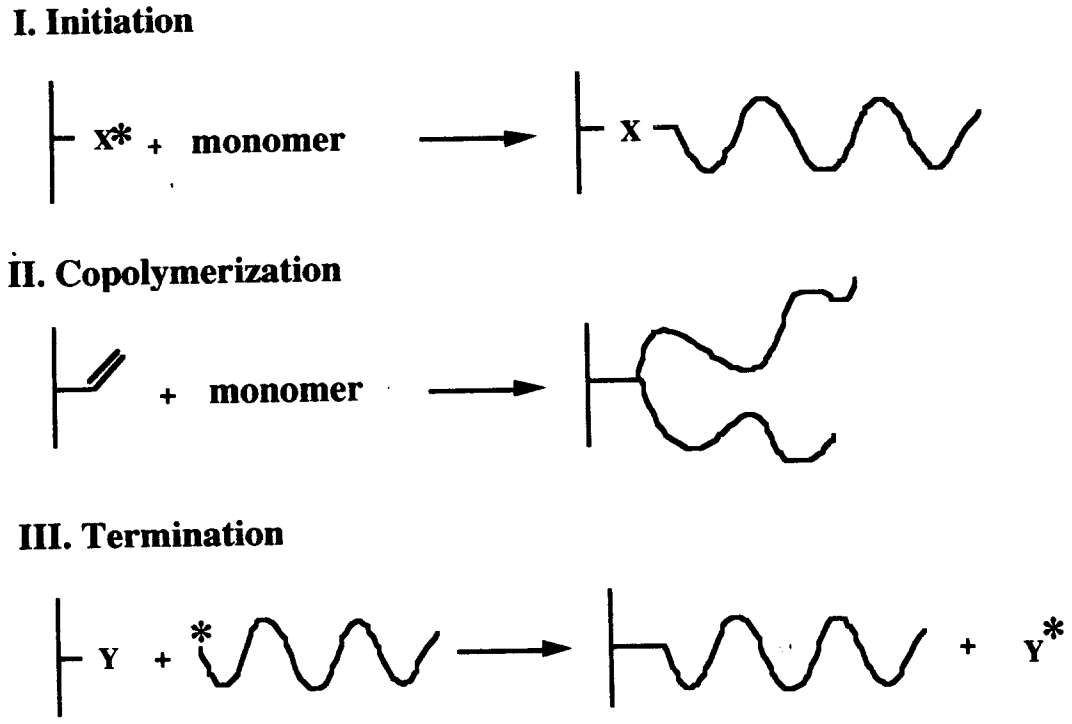

Figure 1-2 Polymerization reactions on silica surfaces.

(Asterisk indicates activated species)

As Figure 1-2 shows, one of the following principles may be applied to the grafting of polymers onto silica surfaces;[30]

(a) the initiation of polymerization from a silica surface using functional surface sites as catalysts in radical or ionic polymerization reaction.
(b) the propagation of polymerization on a silica surface modified with polymarizable, chemically bound groups which are capable of acting as monomers or comonomers in polymerization reactions.
(c) the termination of polymerization on a silica surface at functional surface sites which can deactivate growing polymeric chains.

Besides the aforementioned properties (adhesion, wetting, and colloid stabilization), various characteristics prepared for some applications including chromatography, adsorbent and catalysts have been advanced by surface modification with organofunctional chlorosilane or alkoxysilane on silica surfaces.[31-35] This implies that these properties can be often dramatically altered by the attachment of one or more layers of organic functional groups or polymer chains at the silica surface.[36] However, scarcely attention has been paid to integrate properties of inorganic silicas with the unique function of organic chemistry, although the sol-gel process has thrown such a way open (*vide infra*).

Functionality of Silica by Surface-modification with Photochromic Compounds

Systematic studies on the relationship between surface molecules and wettability revealed that contact angles of water droplets are markedly determined by chemical and conformational stuctures of molecular residues attached to an uppermost surfaces of substrates.[37] This fact has led Chaudhurt and Whitesides to achieve a demonstration that a water droplet runs uphill on a silica glass plate which is surface-modified with a long-chain silylating reagent to result in a gradient in the surface hydrophobicity.[38] Suzuki have proposed a concept concerning driving mechanism for micro-object based on a hydrophobic gradient of surfaces which is induced by external energy such as heat and

light.[39] This may offer a novel way to make micromachines workable by the dynamic regulation of surfaces at molecular levels and requires further studies on molecular surfaces responsive to external stimuli.

On the other hand, organic photochromic compounds undergo reversible color changes owing to their molecular structural modification upon light irradiation, accompanied by the alteration of their physical properties other than electronic absorption spectra such as molecular shape, polarity and so on.

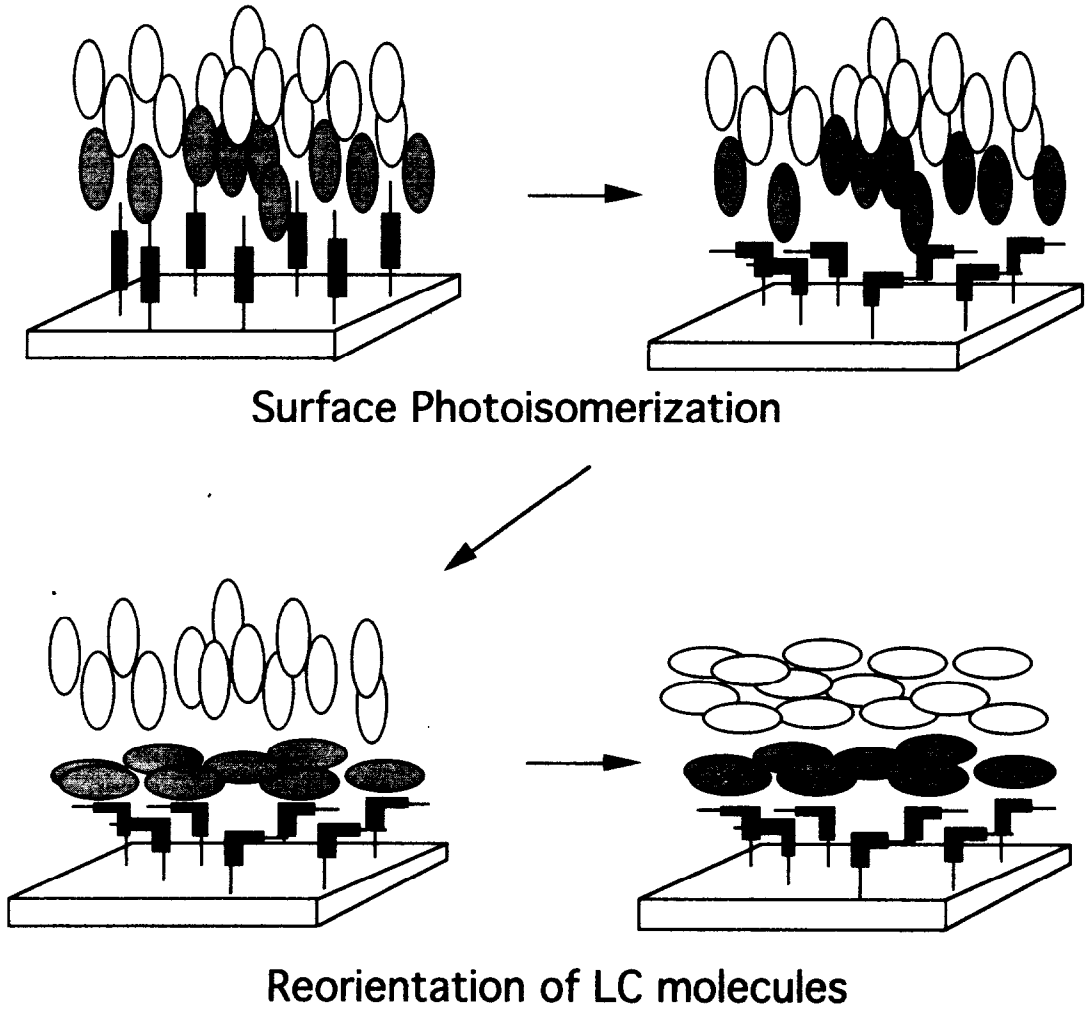

Figure 1-3 Illustrative representation of alteration of LC alignment between homeotropic and planar modes induced by the structural change of surface photochromic molecules, followed by the reorientation of LC molecules.

Photoinduced reversible changes have attracted extensive interest from a point of view of their applicability to photoregulation of molecular systems in versatile ways by appropriate combinations of photochromic molecules with various materials.[40] Systematic studies by Ichimura *et al.* revealed that the alignment of a numerous liquid crystal (LC) molecules is regulated by photochromic molecules (commander molecules) such as azobenzenes localized at topmost surfaces (command surfaces) of silica plates by the photoinduced structural alteration of the molecules.[41,42] The photoalignment involves the reversible alignment change between homeotropic (perpendicular) and planar (parallel) states as a result of the E/Z geometrical photoisomerization of commander molecules (Figure 1-3).[43] When actinic light for the E-to-Z photoisomerization is linearly polarized, liquid crystal (LC) molecules orient uniaxially to form a homogeneous alignment.[44,45] The second class of the alignment regulation has also been achieved by slantwise exposure for the E-to-Z photoisomerization with non-polarized light.[46] The third class consists of the azimuthal photocontrol of the alignment by linearly polarized light from a single light source.[47-50] This type of the photoalignment is performed only when command-molecules result in a planar LC alignment before photoirradiation. In these systems, photoactive molecules are reasonably referred to as " commander molecules " since their photofunctionality does not arise from the spectroscopic modification in a visible range, but from triggering structural as well as orientational alteration of a number of molecules or residues surrounding the photoactive molecules which are proposed to call "soldier molecules." [51] This means that macroscopic properties can be regulated by functional molecules localized on material surfaces with marked amplification of structural alteration of the surface molecules.

The stability of dispersions of colloidal silica is of great practical importance. It depends on various factors including dispersion media, pH, additives such as inorganic salts, surface-active reagents and polymers,[1, 52-54] and results from molecular interactions between colloidal surfaces and solvent molecules. As mentioned above, chemical modification of the silica surface has been undertaken to render the surface oleophilic in order to improve the dispersibility in organic solvents. So far, however, little attention has been paid to regulating colloidal stability in organic solvents by external stimulation, without the aid of additives.

In the first half of this thesis, the author examined the functionality of silicas by means of surface-modification. Especially in Chapters 3 and 4, the author proposes a novel photochemical approach for controlling the dispersibility of colloidal silica by surface treatment with photochromic molecules that displays a drastic polarity change upon UV irradiation (Figure 1-4). This opens a way to an alternative photoresponsive system in which photoinduced molecular structural alteration is converted into macroscopic change through a surface-mediated process.

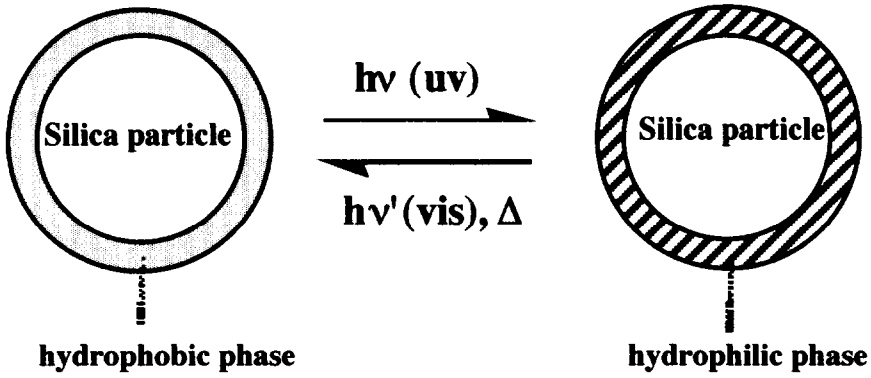

Figure 1-4 Polarity change of a colloidal silica surface by light stimulation

Sol-gel Process

When one considers the methods of integrating unique properties of inorganic silicas with vast functionality of organic chemistry, there are two different approaches; one is, as aforementioned, the surface modification of inorganic surfaces with organic molecules, while the other involves the incorporation of organic molecules into inorganic matrices. However, the latter method has the inherent difficulty to encapsulate organic molecules into inorganic silica matrices, *i. e.*, typical process temperatures employed between organic and inorganic materials has a very wide gap: Organic compounds can rarely survive at temperatures higher than 200 ℃, whereas typical operation temperatures for inorganic ceramic and glass can be well above 1000 ℃. Therefore, until recently doping has been limited to salts and oxide-additives, which can withstand elevated temperatures involved

in the melting procedures.

The late 1970s and early 1980s witnessed a dramatic change; the recognition that better ceramic materials can be obtained through the detailed tailoring of chemical aspects of polymerization led to a worldwide burst of activity and to the birth of what became known as "sol-gel science".[55-60] Although sol-gel transitions are, of course, well documented in many polymerization and precipitation phenomena, the terms "sol-gel materials", "sol-gel process", *etc.* are used today in connection with syntheses of inorganic materials from suitable monomers, passing indeed through sol, gel, and xerogel (dry gel) stages as shown in Figure 1-5.

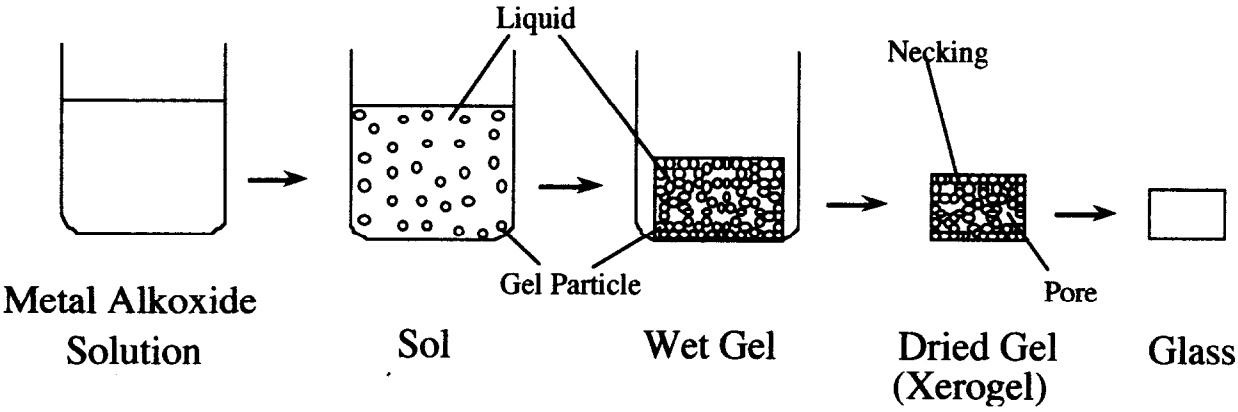

Figure 1-5 The sol-gel process

The sol-gel process consists of two main steps. In the first step, suitable metal alkoxides hydrolyze to cause condensation-polymerization at a room temperature to form a microporous glass (Xerogel) with a large surface area. For instance, the sol-gel process of TEOS, which produces silica matrix, can be described as follows:

$$\textbf{hydrolysis} \quad : Si(OC_2H_5)_4 + 4H_2O \rightarrow Si(OH)_4 + C_2H_5OH$$

$$\textbf{condensation} \quad : \quad Si(OH)_4 \rightarrow SiO_2 + 2H_2O$$

Therefore, the overall reaction is:

$$Si(OC_2H_5)_4 + 2H_2O \rightarrow SiO_2 + 4C_2H_5OH$$

In the second step, the porous glass is annealed at an elevated temperature in order to fill the pores. This results in a shrunken, nonporous glass.

The sol-gel method has received considerable attention because it possesses a number of desirable characteristics. It enables one to prepare glasses at far lower temperatures than that of conventional melting. Compositions, which are difficult to obtain by conventional means because of volatilization, high melting temperatures or crystallization problems, can be produced. In addition, the method is a high-purity process which leads to excellent homogeneity. Moreover, the sol-gel process is adaptable to producing bulk pieces as well as films,[61-63] fibers,[64] and powders.[7-9] Last but not least, the low processing temperatures enable one to dope the gel with organic molecules. During the past 15 years, it has been widely recognized that the use of low temperatures in this process allows the entrapment of organic compounds in an inorganic medium without either denaturing them or impairing their functionality. It became clear that the sol-gel process is a promising candidate for fulfilling a gap between inorganic and organic materials by virtue of the employment of an ambient temperature up to the xerogel stage. Prior to the sol-gel work, the incorporation of organic molecules in solids generally was limited to use of frozen solvents or organic polymer matrices. The sol-gel method represents a totally new type of organic/inorganic composite materials because the oxide matrix not only offers a significantly more ionic environment, but also it is thermally, chemically and dimensionally more stable, so that this method opens a way to various potential applications as described the following organic/inorganic composite materials (①: Polymer/inorganic hybrids and ②: encapsulation of organic molecules and enzymes).

Organic/Inorganic Composite Materials

① Polymer/inorganic hybrids

Sol-gel glass preparation has allowed the synthesis of hybrids of polymer and glasses which have variously been called ormosils (organically modified silicates),[65] ceramers[66] and hybrid polymers.

[67] The incorporation of organic polymers into an inorganic glass matrix via covalent bond is particularly interesting because new hybrid materials could have controllable combination of the properties of both organic polymers (soft and tough) and inorganic glasses (hard and brittle). Wilkes and co-workers have used sol-gel reactions carried out in solutions containing dissolved polymers or oligomers which carry silane groups.[66,68-71] These groups become incorporated into the forming silica, interlocking the two components. Many polymers such as poly(dimethylsiloxane),[68,69] poly(tetramethylene oxide),[70] poly(arylene ether ketone/sulfone),[71] polyimide,[72] and poly(acrylate)[73] were reported to be incorporated into SiO_2 glass network.

However, due to poor solvating properties of typical sol-gel formulations, homogeneous polymer solutions can be obtained by using a limited number of polymers. In order to solve problems related to solubility and homogeneity associated with performed polymers/sol-gel formations, Ellsworth and Novak have described the formation of inorganic-organic simultaneous interpenetrating networks (SIPNs),[74,75] wherein both inorganic glass and polymer formation occur concurrently as shown in the following scheme;

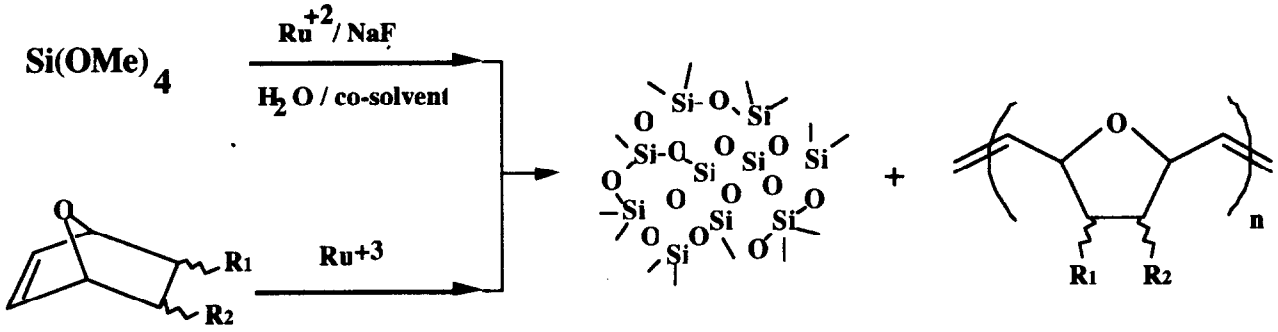

The simultaneous method gives very homogenous materials with a structure finer when compared with using preformed polymers.

Webster *et al.*, on the other hand, demonstrated that sol-gel processing allows for the preparation of aryl-bridged polysilsesquioxanes, which were microporous with surface areas as high as 1000 m^2/g and thermally stable up to 400 ℃ in air, and this property of the solid was related to the presence of rigid-rod organic spacers interspaced at regular intervals in the silicate framework.[76, 77]

As with most newly developed materials, however, it is not obvious what these hybrids will be good for. Unfortunately, the only application so far described is in scratch-proof coating for plastic lenses.[78] The aerospace industry is keenly interested in extending the maximum operating temperatures of polymer composites. High temperature polymers blended with glasses should give strong and tough materials with increased temperature resistance.

② Encapsulation of Organic Molecules and Enzymes

Avnir *et al.* demonstrated that the properties and advantages of doped sol-gel glasses which are of use for the applications are the following;[79,80]

1. Glasses are stable thermally, chemically and photochemically, especially when compared to plastic matrices, which have been the only materials used so far for encapsulation of organic molecules.
2. The encapsulated molecules are well protected again, much better than in plastics. For instance, their photodegradation is much suppressed, compared to solution.
3. The glasses are transparent well to UV light, allowing a whole array of photochemical, photophysical and optical applications.
4. The trapped molecules are either non-leachable, or, in some cases, leachable over a very long time period.
5. A sub-population of the non-leachable molecules is trapped close enough to a pore-surface to be able to interact with substrate molecules contained in pore space. It is this portion of trapped-yet-exposed molecules which allows the development of chemically active sol-gel glasses.

These dominant characteristics have led many applications such as chemical sensors (metal ion sensors,[81] pH sensors[81, 82]), photochemical hole-burning (PHB),[83, 84] non-linear optics,[85-87] solid-state dye lasers,[88-92] electro-optical liquid crystals,[93-95] organometallic catalysis,[96] bioactive glasses,[97-99] and so forth (Table 1-1).

Table 1-1
Applications by Encapsulation of Organic Molecules in Sol-Gel Glasses

Applications	Starting Materials	Trapped Molecules	Contents
Chemical Sensors	$Si(OCH_3)_4$	*o*-Phenanthrolin Dimethylglyoxime	Fe^{2+} (white → red) Ni^{2+} (colorless → red) Metal ion sensors
		Methyl orange, Methyl red, Bromothymol blue, *etc.*	A prototype of a pH meter based on a pH-sensing glass is constructed.
Photochemical hole-buring (PHB)	$Si(OC_2H_5)_4$	1,4-Dihydroxy-anthraquinone	PHB at 4.8 K
		Porphins (TPPS, TCPP, and TMPyP)	A photochemical hole is formed in the lowest transition of the Q band of TMPyP in the silica Film at 20K.
Non-linear optical materials	$Si(OCH_3)_4$	Polyaniline, Fluorescein, Coumarines, *etc.*	Third order nonlinear effects are observed.
Solid state dye laser	$Si(OC_2H_5)_4$ $Si(OCH_3)_4$ ORMOSILs*	Rhodamine-6G, -B, Coumarins, Oxazine-170, *etc.*	The dyes can be incorporated in in-organic environment without undesirable aggregation effects.
Glass dispersed liquid crystals (GDLC)	$C_2H_5Si(OC_2H_5)_3$ or Phenyl- (methyl) triacethoxysilane	Nematic liquid crystals	GDLC may have, in principle, the same performances as PDLC (polymer dispersed liquid crystals) for electro-optical devices.
Organometallic catalysis	$Si(OCH_3)_4$ CATB	$RhCl_3$, $PtCl_4$, and $CoCl_2$	Recyclable hydrogen transfer catalyst
Bioactive glass	$Si(OCH_3)_4$	Enzymes (glucose oxidase, trypsin, acid phosphatase *etc.*)	Some of entrapped enzymes shows remarkable enhancement in stability.

* Organic modified silicates

Characteristics of Trapped Molecules in Sol-gel Silica Matrices

Understanding of the reactivity of doped sol-gel glasses is intimately linked with understanding of the nature of the entrapment and the cage properties. So far, various spectroscopies have been employed to study the dopant cage properties and their evolution in time along the monomer ~ oligomer ~ sol ~ gel ~ xerogel transition.

The sol-gel processes and the evolution of various cage properties was first monitored with pyrene (Py) as a fluorescent probe because of the relatively long singlet lifetime, its distinct vibronic peaks in a fluorescence spectrum, the ability to form an excimer (Py*2) and the sensitivity of these

parameters to changes in environmental conditions ; especially, the ratio of the relative intensity of the first to the fifth peak in a fluorescent spectrum (I_1 / I_5) is sensitive to the environment polarity, since the ratio increases with increase in polarity.[100,101] Changes in microenvironmental polarity and structures around the probe molecules were detected and monitored from adsorption onto the surface of the growing SiO_2 particles up to the complete isolation in microporous cages.

The following conclusions were reached. On a molecular scale, geometric complexity and irregularity start to build up mainly after the gelation point. Two general patterns of behavior were observed, depending on the water to silane ratio. At low ratios, geometric irregularity and porosity build up gradually along the whole process, resulting first in an increase in pyrene emission intensity as aggregation became more pronounced, followed by a decrease in intensity as pyrene molecules became isolated. At high water to silane ratio, a smooth surface was formed, prior to the buildup of a porous structure. These results suggested that polymerization - gelation occurs at low water to silane ratios whereas the formation of a colloid followed by its gelation occurs at high water to silane ratios. The pyrene excimer disappears at the final xerogel stage, proving that the sol-gel process is an effective method for isolating organic molecules. The changes in microenvironmental polarity during the sol-gel process, as reflected by the I_1 / I_5 ratio, are due to pyrene aggregation and not due to the support itself.

Some other photophysical probes (*e.g.*, 7-azaindole,[102] 1- and 2-naphthols,[103, 104] pyrene-3-carboxaldehyde,[105] Rhodamine B,[106] and so on) were also used for following the sol-gel transitions. Zink *et al.* have reported the preparation of silica and aluminosilicate gels doped with bipyridyltriscarbonylchlororhenium (I) as a probe for cage rigidity, and demonstrated that large changes in the local gel structure occur during the aging period which increases the rigidity of the oxide skeleton.[107-109]

Table 1-2
van der Waals volume of photochromic probes and extra volume needed to isomerize

	trans, $\mathring{A}^3$	extra to isomerize, $\mathring{A}^3$
Azobenzene	**144**	**127**
m - Azotoluene	**170**	**166**
1, 1' - Azonaphthalene	**216**	**200**
4 - Ethoxyazobenzene	——	**127**
2, 2' - Azonaphthalene	**216**	**230**
Stilbene	**151**	**222**
4, 4' - Dinitrostilbene	**187**	**262**
4, 4' - Diphenylstilbene	**270**	**571**
Thioindigo	**197**	**212**
1, 3 - Di (1-pyrenyl) propane	——	**439**

However, there have been few systematic studies on the nature of interactions between guest molecules and silica matrices and flexibility of entrapped molecules. Photochromic reactions are influenced by properties of matrices including polarity, viscosity, acid-base interactions, free volume, *etc.* In particular, photochromic compounds with marked alternation of their molecular structure have been employed to elucidate microstructures of different polymer matrices, as the reaction rates of photochemical and thermal isomerizations of photochromic molecules are affected by the rigidity of matrices owing to their molecular shape changes.[110, 111] Victor and Torkelson have calculated these sweep volumes of several photoactive compounds after the method of Bondi (Table 1-2).[112]

Azobenzene photoisomerizes from E-isomer to Z-isomer, and the reverse process takes place photochemically or thermally. The photochemistry is relatively insensitive to fluid reaction media. The quantum yield for the photoisomerization is hardly affected by the nature of solvent.[113,114] Since the geometrical isomerization requires a sufficient free volume due to the remarkable alteration of

molecular structure, the efficiency of the isomerization in solid phase reflects the molecular mobility. Hence, azobenzene is a suitable photoactive probe to estimate the rigidity of matrices so that this type of photochromic probes has been widely employed to elucidate the microstructures of polymer solid matrices.[110-113, 115-118] In analogy with polymer matrices, the use of such photochromic molecules as photoprobes is of significance in obtaining information about microstructures of silica matrices prepared by sol-gel process.

Some reports dealt with the photochromic behavior of a fulgide and spiropyranes in sol-gel bulk materials.[119-123] However, these photochromic compounds seem to be inappropriate to estimate the rigidity of the matrix since the molecular movement associated with these 6 π electrocyclic reactions is very small and the photochromism of the spiropyrans is too markedly affected by the polarity of matrices. In Chapters 6-8 of this thesis, the author studied the photoinduced *trans-cis* isomerization and thermal *cis-trans* isomerization of azobenzene derivatives in sol-gel silica matrices.

Scope of the Present Thesis

The present thesis aims at studying on the functionality and characteristics of photochromic organic-inorganic hybrids. The author explored novel possibilities of silicas/organic composite by two different approaches, *i. e.*, by placing organic photochromic molecules *onto* and *into* silica matrices. In the first half of this thesis (Chapters 2-5), the author examined the functionality of silicas by means of surface-modification. In the second half (Chapters 6-9), the author investigated microenvironmental structures in sol-gel silica matrices by evaluating the reactivity of doped organic photochromic probes.

(Chapters 2-5: Functionality of Silica by Surface-modification with Photochromic Compounds)

Chapter 2 deals with revealing that azobenzene having an amino residue show good adsorptivity on a silica surface, and a silica surface adsorbing the azobenzene amphiphilic compound displays the ability to command the photoalignment of a nematic liquid crystal between homeotropic and planar modes.

Chapter 3 describes a novel photochemical approach for controlling the dispersibility of colloidal silica by surface adsorption of a calixresorcin[4]arene having azobenzene groups. A dipole moment change of azobenzene units on a surface of colloidal particles results in the photocontrol of the reversible alternation between dispersed and aggregated states of the particles in non-polar solvents. This provides a novel system for molecular amplification of photonic information.

Chapter 4 also deals with the photocontrolled aggregation of colloidal silica by surface-chemisorption of spirobenzopyran (SP) having a decamethylene spacer. When the photochromic particles are dispersed in carbon tetrachloride, UV irradiation induced flocculation, causing the sedimentation of the colloidal silica, while visible light irradiation recovered the dispersed state. In Chapter 5, the thermal reverse isomerization kinetics of SP attached to a silica surface through two different methylene spacers were studied and compared with those of their model compounds in various solvents in order to elucidate the surface environment. The photoinduced control of the dispersibility of the SP-modified colloidal silica will be discussed.

(Chapters 6-9: Characteristic of Trapped Molecules in Sol-Gel Silica Matrices)

Chapter 6 describes the *trans*-to-*cis* photoisomerization and the thermally induced the *cis*-*trans* reversion of 4-methoxy-4'-(2-hydroxyethoxy)azobenzene (MHAB) in sol-gel silica films prepared under various conditions. Furthermore, these photochemical and thermal isomerizations of MHAB in sol-gel films were compared with that in a poly(methylmethacrylate) (PMMA) film or in solutions.

In Chapter 7, sol-gel glass thin films were prepared from tetraethyl orthosilicate (TEOS) in the presence of MHAB, 4-methoxy-4'-(N-(3-triethoxysilylpropyl)carbamoylmethoxy)azobenzene (MTAB) and 4,4'-bis(N-(3-triethoxysilylpropyl)carbamoylmethoxy)azobenzene (DTAB). This chapter deals with the effect of covalent bond formation between a doping azobenzene moiety and silica matrices on the geometrical isomerization. The author expected that the introduction of silylation units at both sides of the azobenzene enhances considerably the suppression of reactivity of the chromophore.

Chapter 8 deals with revealing the marked differences in microenvironmental structures of sol-gel silica between bulk materials and thin films by means of evaluating the reactivity of doped three azobenzenes (MHAB, MTAB, and MTAB).

In Chapter 9, sol-gel films and monoliths were prepared by the hydrolysis of TEOS or tetramethyl orthosilicate (TMOS) in the presence of 1,3-bis(9-anthryl)propan-1-ol (BAP), bis(9-anthrylmethyl)amine (BAA) and intermolecular photodimer of BAA (DBAA). The intramolecular photodimerization of these dianthryl compounds as photoprobes was examined in sol-gel glasses and compared with those in solutions as well as in PMMA films. The purpose of this chapter is to obtain further information on the mobility of organic molecules embedded within sol-gel matrices. Moreover, studies of competitive photooxidation behavior of the anthracenes were also made to reveal the permeation of atmospheric oxygen into the inorganic matrices.

Finally, the summary of this work is presented in Chapter 10.

REFERENCES

1) R. K. Iler, in *The Chemistry of Silica*, Wiley, New York, 1979.

2) W. W, Barkas, *Trans. Farady Soc.*, **42**, 147 (1946).

3) S. S. Kistler, E. A. Fischer, and I. R. Freeman, *J. Am. Chem. Soc.*, **65**, 1909 (1943).

4) G. B. Alexander, R. K. Iler, and F. W. Wolter, U. S. Pat. 2,731,326 (Du Pont), 1956.

5) P. G. Bird, U. S. Pat. 2,244,325 (National Aluminate Co.), 1941.

6) D. Graham, *Chem. Reos.*, **41**, 441 (1947).

7) W. Stöber, A. Fink, and E. Bohn, *J. Colloid Interf. Sci.*, **26**, 62 (1968).

8) B. Karmakar, G. De, D. Kundu, and D. Ganguli, *J. Non-Cryst. Solids*, **135**, 29 (1991).

9) G. H. Bogush, M. A. Tracy, and C. F. Zukoski, *J. Non-Cryst. Solids*, **104**, 95 (1988).

10) H. Kloepfer, DBP 870242 (Degussa Corp.), 1942.

11) L. J. White, *Industrial and Engineering Chemistry*, **51**, 232 (1959).

12) Y. Mitani and M. Ushio, *Nippon Kagakukaishi*, 153 (1992).

13) H. Ferch, *Chem. Ing. Tech. Z.*, **48**, 11 (1976).

14) G. Tesoro and Y. Wu, *J. Adhesion Sci. Technol.*, **5**, 771 (1991).

15) E. P. Plueddemann, H. A. Clark, H. A. Nelson, and K. R. Hoffmann, *Mod. Plast.*, **39**, 135 (1962).

16) E. P. Plueddemann, in *Silane Coupling Agents*, Plenum Press, New York (1982).

17) H. Ishida and J. L. Koenig, *Polym. Eng., & Sci.*, **18**, 128 (1978).

18) H. Ishida, *Polym. Composites*, **5**, 101 (1984).

19) S. R. Culler, H. Ishida, and J. L. Koenig, *J. Coll. Inter. Sci.*, **106**, 334 (1985).

20) E. Nishio, N. Ikuta, T. Hirashima, and J. Koga, *Appl. Spectr.*, **43**, 1159 (1989).

21) N. Ikuta, T. Hori, H. Naitoh, Y. Kera, E. Nishio, and I. Abe, *Composite Interphases*, **1**, 455 (1993).

22) N. Nishiyama, K. Horie, and T. Asakura, *J. Coll. Inter. Sci.*, **129**, 113 (1989).

23) K. Bridger, D. Fairhurst, and B. Vincent, *J. Coll. Inter. Sci.*, **68**, 190 (1979).

24) J. Edwards, S. Lenon, A. F. Toussaint, and B. Vincent, *ACS Symp. Ser.*, **240**, 281 (1984).

25) L. G. Bricher, D. C. Kehoe, J. G. Matisons, R. St. C. Smart. and A. G. Swincer, *Langmuir*, **9**, 1609 (1993).

26) K. Bridger and B. Vincent, *Eur. Polym. J.*, **16**, 1017 (1980).

27) H. B. Ouada, H. Hommel, A. P. Legrand, H. Balard, and E. Papirer, *J. Coll. Inter. Sci.*, **122**, 441 (1988).

28) N. Tsubokawa, A. Kogure, and Y. Sone, *J. Polym. Sci.: Part A: Polym. Chem.*, **28**, 1923 (1990).

29) E. Schomaker, A-J. Zwarteveen, G. Challa, and M. Capka, *Polym. Commun.* **29**, 158 (1988).

30) R. Laible and K. Hamann, *Adv. Coll. Inter. Sci.*, **13**, 65 (1980).

31) M. L. Lee and B. W. Wright, *J. Chromatogr.*, **184**, 235 (1980).

32) J. Nawrocki and B. Buszewski, *J. Chromatogr.*, **449**, 1 (1988).

33) W. C. Moreira, Y. Gushiken, and O. R. Nascimento, *J. Coll. Inter. Sci.*, **106**, 334 (1985).

34) D. E. Leyden and G. H. Luttrell, *Anal. Chem.*, **47**, 1612 (1975).

35) P. Tundo, P. Venturello, and E. Angeletti, *J. Am. Chem. Soc.*, **104**, 6547 (1982).

36) J. D. Swalen, D. L. Allarea, J. D. Andrade, E. A. Chandross, S. Garoff, J. Israelachvili, T. J.

McCarthy, R. Murray, R. F. Pease, J. F. Rabolt, K. J. Wynne and H. Yu, *Langmuir*, **3**, 932 (1987).

37) G. M. Whitesides and P. E. Laibinis, *Langmuir*, **6**, 87 (1990).

38) M. K. Chaudhury and G. M. Whitesides, *Science*, **256**, 1539 (1992).

39) M. Suzuki, *Polym. Gels Networks*, **2**, 279 (1994).

40)K. Ichimura, in *Photochromism; Molecules and System*, Eds., H. Durr and H. Bouas-Laurent, Elsevier, Amsterdam, 1990, p.903.

41) K. Ichimura, T. Seki, Y. Kawanishi, Y. Suzuki, M. Sakuragi and T. Tamaki, In *Photo-reactive Materials for Ultrahigh Density Optical Memory*, Ed. M. Irie, Elsevier Science, Amsterdam, 1994, p. 55.

42) K. Ichimura, In *Polymers as Electrooptical and Photooptical Active Media*, ed., V. Shibaev, Springer-Verlag, Heidelberg, 1996, p. 138.

43) K. Aoki, Y. Kawanishi, T. Seki, M. Sakuragi, T. Tamaki and K. Ichimura, *Liq. Cryst.*, **19**, 119 (1995) and references therein.

44) Y. Kawanishi, T. Tamaki, M. Sakuragi, T. Seki, Y. Suzuki and K. Ichimura, *Langmuir*, **8**, 2601 (1992).

45) Y. Kawanishi, T. Tamaki, T. Seki, M. Sakuragi and K. Ichimura, *Mol. Cryst. Liq. Cryst.*, **218**, 153 (1992).

46) Y. Kawanishi, T. Tamaki and K. Ichimura, *ACS Symp. Ser.*, **537**, 453 (1994).

47) W. M. Gibbons, P. L. Shannon, S.-T. Sun and B. J. Swetlin, *Nature*, **351**, 49 (1991).

48) K. Ichimura, Y. Hayashi and N. Ishizuki, *Chem. Lett.*, 1063 (1992).

49) K. Ichimura, Y. Hayashi, H. Akiyama and N. Ishizuki, *Langmuir*, **9**, 3298 (1993).

50) K. Ichimura, Y. Hayashi, H. Akiyama, T. Ikeda and N. Ishizuki, *Appl. Phys. Lett.*, **63**, 449 (1993).

51) K. Ichimura, *Supramol. Sci.*, **3**, 67 (1996).

52) D. H. Napper, in *Polymeric Stabilization of Colloidal Dispersions*, Eds. R. H. Ottewill and R. L. Rowell, Academic Press, 1983.

53) H. De Hek and A. J. Vrij, *J. Colloid Interface Sci.*, **84**, 409 (1980).

54) B. Vincent, J. Edwards, S. Emmett and A. Jones, *Colloids Surfaces*, **18**, 261 (1986).

55) M. Yamane, S. Aso, and T. Sakaino, *J. Mater. Sci.*, **13**, 865 (1978)

56) S. Sakka and K. Kamiya, *J. Non-Cryst. Solids*, **42**, 403 (1980).

57) C. J. Brinker and G. W. Scherer, *J. Non-Cryst. Solids*, **70**, 301 (1985).

58) H. Dislich, *J. Non-Cryst. Solids*, **73**, 599 (1985).

59) G. W. Scherer, *Yogyo Kyoukaishi*, **95**, 21 (1987).

60) L. L. Hench and J. K. West, *Chem. Rev.*, **90**, 33 (1990).

61) C. J. Brinker, A. J. Hurd and K. J. Ward, in *Ultrastructure Processing of Advanced Ceramics*, eds. J. D. Mackenzie and D. R. Ulrich , Wiley, New York, 1988, p 223.

62) C. J. Brinker, A. J. Hurd, G. C. Frye, P. R. Schunk, and C. S. Ashley, *Nippon Seramikkusu Kyokai Gakujutsu Ronbunshi*, **99**, 862 (1991).

63) C. J. Brinker, A. J. Hurd, P. R. Schunk, G. C. Frye, and C. S. Ashley, *J. Non-Cryst. Solids*, **147/148**, 424 (1992).

64) K. Kamiya, Y. Iwamoto, T. Yoko, and S. Sakka, *J. Non-Cryst. Solids*, **100**, 195 (1988).

65) H. K. Schmidt, *J. Non-Cryst. Solids,* **73**, 681 (1985).

66) G. L. Wilkes, B. Orler, and H. Huang, *Polym. Prep.*, **26**, 300 (1985).

67) Y. Chujo. E. Ihara, S. Kure, K. Suzuki, and T. Saegusa, *Makromol. Chem., Macromol. Symp.*, **42/43**, 303 (1991).

68) H.-H. Huang, B. Orler, and G. L. Wilkes, *Polym. Bull.* **14**, 557 (1985).

69) H.-H. Huang, B. Orler, and G. L. Wilkes, *Macromolecules*, **20**, 1322 (1987).

70) R. H. Glaser and G. L. Wilkes, *Polym. Bull.*, **19**, 51 (1988).

71) B. Wang, G. L. Wilkes, J. C. Hedrick, S. C. Liptak, and J. E. McGrath, *Macromolecules*, **24**, 3449 (1991).

72) A. Morikawa, Y. Iyoku, and M. Kakimoto, *Polym. J.*, **24**, 107 (1992).

73) Y. Wei, D. Yang, and R. Bakthavatchalam, *Mater. Lett.*, **13**, 261 (1992).

74) M. W. Ellsworth and B. M. Novak, *J. Am. Chem. Soc.*, **113**, 2756 (1991).

75) M. W. Ellsworth and B. M. Novak, *Chem. Mater.*, **5**, 839 (1993).

76) K. J. Shea, D. A, Loy, and O. W. Webster, *Chem. Mater.*, **1**, 572 (1989).

77) K. J. Shea, D. A, Loy, and O. W. Webster, *J. Am. Chem. Soc.*, **114**, 6700 (1992).

78) H. Schmidt, B. Sieferling, G. Philip, and K. Deichmann, in *Ultrastructure Processing of Advanced Ceramics*, eds. J. D. Mackenzie and D. R. Ulrich, Wiley, New York, 1998, p 651.

79) D. Avnir, D. Levy, and R. Reisfeld, *J. Phys. Chem.*, **88**, 5956 (1984).

80) D. Avnir, S. Braun, and M. Ottolenghi, *A. C. S. Sym. Ser.*, **499**, 384 (1992).

81) R. Zusman, C. Rottman, M. Ottolenghi, and D. Avnir, *J. Non-Cryst. Solids*, **122**, 107 (1990).

82) C. Rottman, M. Ottolenghi, R. Zusman, O. Lev, M. Smith, G. Gong, M. L. Kagan, and D. Avnir, *Mater. Lett.*, **13**, 293 (1992).

83) T. Tani, H. Namikawa, K. Arai, and A. Makishima, *J. Appl. Phys*, **59**, 3559 (1985).

84) H. Inoue, T. Iwamoto, A. Makishima, M. Ikemoto, and K. Horie, *J. Opt. Soc. Am. B*, **9**, 816 (1992).

85) R. Reisfeld, *J. Non-Cryst. Solids*, **121**, 254 (1990).

86) M. Nakamura, H. Nasu, and K. Kamiya, *J. Non-Cryst. Solids*, **135**, 1 (1991).

87) J. I. Zink, B. Dunn, R. B. Kaner, E. T. Knobbe , and J. McKiernan, in *Materials for Nonlinear Optics - Chemical Perspectives*, eds. S. R. Marder, J. E. Sohn and G. D. Stucky, A. C. S. Washington, D. C. , 1991, ch. 36, p 541.

88) A. Makishima and T. Tani, *J. Am. Ceram. Soc.*, **69**, C-72 (1986).

89) D. Avnir, V. R. Kaufman, and R. Reisfeld, *J. Non-Cryst. Solids*, **74**, 395 (1985).

90) E. T. Knobbe, B. Dunn. P. D. Fuqua, and F. Nishida, *Appl. Op.*, **29**, 2729 (1990).

91) Y. Haruvy and S. E. Webber, *Chem. Mater.*, **4**, 89 (1992).

92) M. M. E. Severin-Vantilt and E. W. J. L. Oomen, *J. Non-Cryst. Solid*, **159**, 38 (1993).

93) J. M. Oton, A. Serrano, C. J. Serna, and D. Levy, *Liquid Crystals*, **10**, 733 (1991).

94) D. Levy, C. J. Serna, and J. M. Oton, *Mater. Lett.*, **10**, 470 (1991).

95) D. Levy, J. M. S. Pena, C. J. Serna, and J. M. Oton, *J. Non-Cryst. Solids*, **147/148**, 646 (1992).

96) A. Rosenfeld, D. Avnir, and J. Blum, *J. Chem. Soc., Chem. Commun.*, 583 (1993).

97) D. Avnir, S. Braun, O. Lev, and M. Ottolenghi, *Chem. Mater.*, **6**, 1605 (1994).

98) S. Shtelzer, S. Rappoport, D. Avnir, M. Ottolenghi, and S. Braun, Biotechn. *Appl. Biochem.*, **15**, 227 (1992).

99) S. A. Yamanaka, F. Nishida, L. M. Ellerby, C. R. Nishida, B. Dunn, J. S. Valentine, and J. I. Zink, *Chem. Mater.*, **4**, 495 (1992).

100) V. R. Kaufman, D. Levy, and D. Avnir, *J. Non-Cryst. Solids*, **82**, 103 (1986).

101) V. R. Kaufman and D. Avnir, *Langmuir*, **2**,717 (1986).

102) K. Matsui, T. Matsuzaka, and H. Fujita, *J. Phys. Chem.*, **93**, 4991 (1989).

103) T. Fujii, T. Mabuchi, and I. Mitsui, Chem. *Phys. Lett.*, **68**, 5 (1990).

104) T. Fujii, T. Mabuchi, H. Kitamura, O. Kawauchi, N. Negishi, and M. Anpo, *Bull. Chem. Soc. Jpn.*, **65**, 720 (1992).

105) K. Matsui and T. Nakazawa, *Bull. Chem. Soc. Jpn.*, **63**, 11 (1990).

106) N. Negishi, M. Fujino, H. Yamashita, M. A. Fox, and M. Anpo, *Langmuir*, **10**, 1772 (1994).

107) J. MaKiernan, J-C Pouxviel, B. Dunn, and J. I. Zink, *J. Phys. Chem.*, **93**, 2129 (1989).

108) B. Dunn and J. I. Zink, *J. Mater. Chem.*, **1**, 903 (1991).

109) J. I. Zink and B. S. Dunn, *Nippon Seramikkusu Kyokai Gakujyutsu Ronbunshi*, **99**, 878 (1991).

110) K. Horie and I. Mita, in *Advances in Polymer Science, Vol. 88,* ed. H. Fujita , Springer, Berlin, 1989, p. 77.

111) V. A. Krongauz, in *Photochromism Molecules and System*, eds., H, Dürr and H. Bouas-Laurent, Elsevier, Amsterdam, 1990, p. 793.

112) J. G. Victor and J. M. Torkelson, *Macromolecules*, **20**, 2241 (1987).

113) I. Mita, K. Horie and K. Hirao, *Macromolecules*, **22**, 558 (1989).

114) D. L. Ross and J. Blanc, in *Photochromism*, ed., G. H. Brown, Wiley-Interscience, New York, 1971, p. 516.

115) J. W. Pries and M. M. Sifain, *J. Polym. Sci. A-1*, **9**, 3161 (1971).

116) T. Naito, K. Horie, and I. Mita, *Macromolecules*, **24**, 2907 (1991).

117) C. P. S. Sung, I. R. Gould and N. J. Turro, *Macromolecules*, **17**, 1447 (1984).

118) W.-C. Yu, C. P. S. Sung, and R. E. Robertson, *Macromolecules*, **21**, 355 (1988).

119) V. R. Kaufman, D. Levy, and D. Avnir, *J. Non-Cryst. Solids*, **82**, 103 (1986).

120) D. Levy and D. Avnir, *J. Phys. Chem.*, **92**, 4734 (1988).

121) D. Levy, S. Einhorn, and D. Avnir, *J. Non-Cryst. Solids*, **113**, 137 (1989).

122) K. Matsui, T. Morohoshi, and S. Yoshida, *MRS Int. Mtg. Adv. Mater.*, **12**, 203 (1989).

123) D. Preston, J.-C. Pouxviel, T. Novinson, W. C. Kaska, B. Dunn, and J. I. Zink, *J. Phys. Chem.*, **94**, 4167 (1990).

Chapter 2

Alignment Photoregulation of a Nematic Liquid Crystal by Surface Adsorption of Aminoalkylated Azobenzenes

INTRODUCTION

As described in the general introduction (Chapter 1), systematic studies have revealed that the alignment of numerous liquid crystal (LC) molecules is regulated by photochromic molecules (commander molecules) localized at the topmost surfaces (command surfaces)of substrate plates by the photoinduced structural alteration of the molecules. The photoalignment regulation by command surfaces is affected by various factors[1-3] including photochromic moieties like azobenzenes, substituents at the commander molecules, spacers for attaching commander molecules to substrate surfaces, the nature of substrate surfaces and so forth. In particular, command surfaces prepared from photochromic polymer thin films demonstrate complicated features in the photoresponse[4] although this type of polymer surfaces possesses very practical significance. One of the factors influencing the responsiveness of LC photoalignment has been discussed based on the penetration of LC molecules into photoirradiated polymer thin films, leading to the randomization of photooriented azobenzene chromophores in polymer matrices. In this respect, the surface-selective modification of silica substrates with photochromic compounds[1] plays a crucial role since LC molecules cannot penetrate into the substrate matrix because of tightly networked structures.

The surface silylation of silica plates have carried out with the use of photochromic compounds having a triethoxysilyl residue.[1,2] Although this procedure affords versatile ways to the three types of the LC photoalignment regulation as mentioned in the Chapter 1, the structure of the command layers prepared by the silylation is not always well-defined because there is a possibility that triethoxysilyl compounds form oligosiloxanes during the preparation of silylation solutions for surface silylation.

On the other hands, some reports described that aliphatic amino residues bind firmly to a silica surface through hydrogen bond formation. The amino group of γ-aminopropylsilyl residues covalently attached to a silica surface through silylation interacts effectively with surface silanols[5,6] while intermolecular hydrogen bonding between an amine and a silica surface was suggested by the fact that the adsorptivity of allylamine on a silica is two magnitude greater than that of allyl methacrylate.[7] These have led us to prepare azobenzenes having an aminoalkyl residue to achieve the surface modification of a silica plate with azobenzene moieties by the adsorption through a hydrogen bond.

In this chapter, the author presents a simple and convenient method to prepare command surfaces by the adsorption of aminoalkylated azobenzenes on a silica surface. Since the binding site is an amino group, the surface can be covered with a single monolayer of the commander molecules, and silica surfaces become photoactive simply by placing a nematic LC containing the azobenzene amphiphile without any surface treatment before cell assemblage.

EXPERIMENTAL

Materials

Silica particles donated by Tokuyama Corp. were monodispersed particles of ca. 400 nm diameter with a BET nitrogen specific surface area of 6.1 m^2/g. Prior to adsorption experiment, they were dried under vacuum at 180°C for 5 hr. A nematic liquid crystal (DON-103), a mixture of p-alkoxyphenyl cyclohexanecarboxylates of TNI = 74°C, was gifted by Rodic Corp.

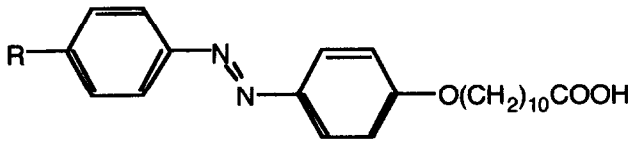

1 (a) 4AzC : R = C_4H_9, (b) 8AzC: R = C_8H_{17}, (c) 0AzC: R = H

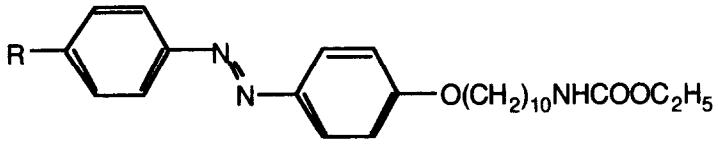

2 (a) 4AzU : R = C_4H_9, (b) 8AzU: R = C_8H_{17}, (c) 0AzU: R = H

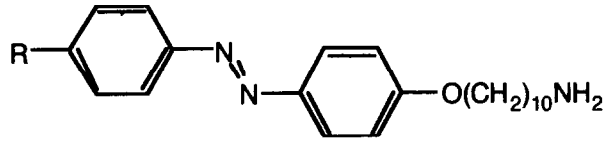

3 (a) 4AzA : R = C_4H_9, (b) 8AzA: R = C_8H_{17}, (c) 0AzA: R = H

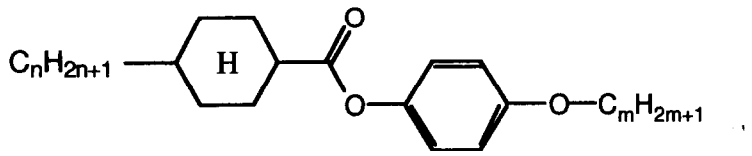

DON-103

Figure 2-1 Chemical structures of azobenzenes and a liquid crystal.

Azobenzenes (Figure2-2)

4-(10-aminodecyloxy)-4'-butylazobenzene (4AzA)

4-(10-Ethoxycarbonyldecyloxy)-4'-butylazobenzene was synthesized from 4-hydroxy-4'-butylazobenzene by the Williamson method and purified by repeated recrystallization from methanol to give crystals of mp 74-75°C. Calcd. for $C_{29}H_{42}N_2O_3$; C, 74.64; H, 9.07; N, 6.00%. Found: C, 74.67; H, 8.84; N, 5.94%. ^{1}H-NMR ($CDCl_3$) δ : 0.92 (3H, t, CH_3-C), 1.25 (3H, t, OCH_2CH_3), 1.2-1.9 (20H, m, -CH_2-), 2.28 (2H, t, CH_2(C=O)), 2.70 (2H, t, CH2-arom), 3.9-4.3 (4H, m, CH_2O-arom and (C=O)OCH_2), 6.95 (2H, d, H-arom), 7.26 (2H, d, H-arom), 7.82 (4H, d, H-arom). IR (KBr): 2910, 2850, 1760, 1240, 840 cm^{-1}. The ester was hydrolyzed to yield 4-(10-carboxydecyloxy)-4'-butylazobenzene (4AzC), followed by recrystallization from methanol to give crystals of mp 113-114°C. Calcd. for $C_{27}H_{38}N_2O_3$; C, 73.94; H, 8.73; N, 6.39%. Found: C, 74.43; H, 8.96; N, 6.42%. ^{1}H-NMR ($CDCl_3$) δ : 0.95 (3H, t, CH_3-C), 1.2-1.9 (20H, m, -CH_2-), 2.32 (2H, t, CH_2(C=O)), 2.67 (2H, t, CH_2-arom), 4.02 (2H, t, CH_2O-arom), 6.95 (2H, d, H-arom), 7.24 (2H, d, H-arom), 7.80 (4H, d, H-arom). IR (KBr): 2910, 2850, 1725, 1250, 850 cm^{-1}. A solution of an equimolar mixture of the azobenzenecarboxylic acid, triethylamine and diphenylphosphoryl azide was refluxed in tert-butyl alcohol for 7 hr, after the Sioiri's procedure,[8] to form the corresponding urethane derivative of mp 82-83°C. Calcd. for $C_{31}H_{47}N_3O_3$; C, 73.05; H, 9.29; N, 8.24%. Found: C, 72.87; H, 9.19; N, 8.83%. ^{1}H-NMR ($CDCl_3$) δ : 0.92 (3H, t, CH_3-C), 1.50 (9H, s, CH_3-C), 1.2-1.9 (20H, m, -CH_2-), 2.67 (2H, t, CH_2-arom), 3.10 (2H, m, CH_2-N), 4.02 (2H, t, CH_2O-arom), 4.45 (1H, br. NH), 6.99 (2H, d, H-arom), 7.28 (2H, d, H-arom), 7.83 (4H, d, H-arom). IR (KBr): 2920, 2830, 1690, 1250, 850 cm^{-1}. The urethane was subjected to mild acidic hydrolysis to be converted into the azobenzene bearing an amino residue which was recrystallized from acetonitrile. Calcd. for $C_{26}H_{39}N_3O$; C, 76.24; H, 9.60; N, 10.26%. Found: C, 75.90; H, 9.40; N, 10.12%. ^{1}H-NMR ($CDCl_3$) δ : 0.94 (3H, t, CH_3-C), 1.2-2.0 (20H, m, -CH_2-), 2.67 (4H, m, CH_2-arom and -CH_2-NH_2), 4.02 (2H, t, CH_2O-arom), 6.95 (2H, d, H-arom), 7.24 (2H, d, H-arom), 7.82 (4H, d, H-arom). IR (KBr): 3430, 2920, 2850, 1605, 1240, 850 cm^{-1}.

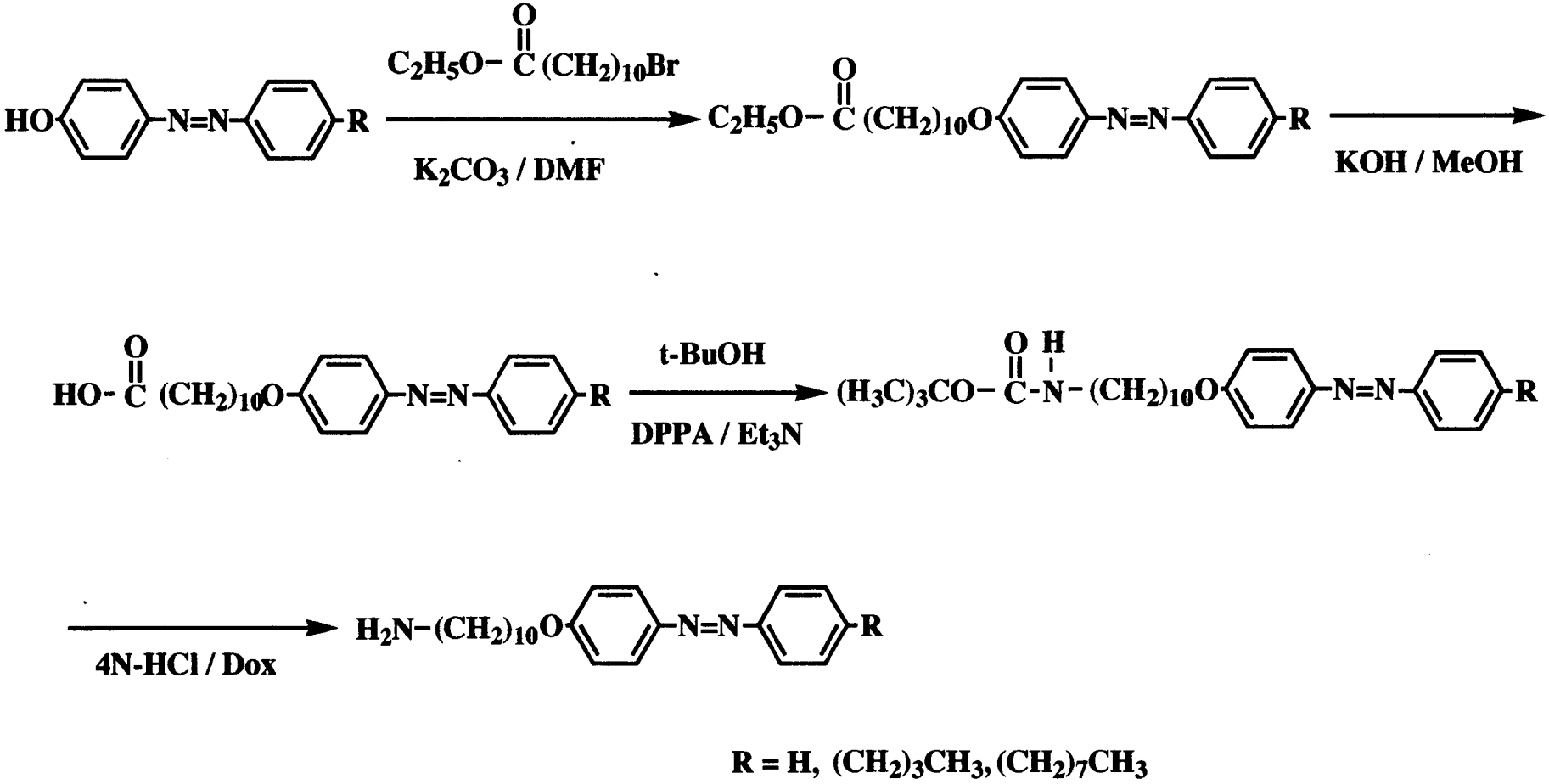

Figure 2-2 Synthetic pathways of azobenzenes

4-(10-aminodecyloxy)-azobenzene (0AzA) was prepared in the same way. Calcd. for $C_{22}H_{31}N_3O$; C, 74.79; H, 11.89; N, 8.84%. Found: C, 74.69; H, 11.71; N, 8.73%. ^{1}H-NMR ($CDCl_3$) δ : 1.2-2.0 (16H, m, -CH_2-), 2.67 (2H, t, -CH_2-NH_2), 4.02 (2H, t, CH_2O-arom), 6.95 (2H, d, H-arom), 7.24 (2H, d, H-arom), 7.82 (5H, m, H-arom). 4-(10-aminodecyloxy)-4'-octylazobenzene (8AzA) was obtained similarly. Calcd. for $C_{30}H_{47}N_3O$; C, 77.37; H, 10.17; N, 9.02%. Found: C, 76.98; H, 10.11; N, 8.83%. ^{1}H-NMR ($CDCl_3$) δ : 0.87 (3H, t, CH_3-C), 1.2-2.0 (28H, m, -CH_2-), 2.67 (2H, t, -CH_2-NH_2), 4.04 (2H, t, CH_2O-arom), 7.00 (2H, d, H-arom), 7.28 (2H, d, H-arom), 7.4-8.0 (4H, d, H-arom).

Adsorption on Silica Particles

Twenty milliliter of a dry benzene solution of an azobenzene with a known concentration was mixed with 1.00 g of silica particles in a glass tube and placed under mild shaking at 25°C for approximately 8 hr to reach an adsorption equilibrium. A silica suspension was centrifuged at 3000 rpm for 15 min to sediment the silica particles, and a supernatant was removed with care to monitor the concentration of azobenzene spectroscopically. The amount of azobenzene adsorbed on flocculated silica, W*i* (mmol/g), was calculated from the expression

$$Wi = V(Co\text{-}Ci)/Mi$$

where V = volume of a solution in mL, *Co* = an initial concentration of the azobenzene in mol/L, *Ci* = concentration of the azobenzene in the supernatant after centrifugation in mol/L and M*i* = silica weight in g.

Adsorption on Quartz Plates and Photoisomerization of Azobenzenes

Quartz plates (1 x 3 cm^2) were cleaned in a conventional way. Plates were immersed in benzene solutions of an azobenzene of concentrations in a range between 1 x 10^{-2} mol/L and 1 x 10^{-4} mol/L for 30 min, air-dried, and rinsed with fresh benzene several times. A surface-modified plate was irradiated at 365 nm from a Jasco CRM-FA Irradiator equipped with a 2 kW xenon arc lamp for the

photoisomerization of adsorbed azobenzene. Absorption spectra were taken on a Hitachi UV320 spectrometer.

Cell Fabrication and Liquid Crystal Photoalignment

A nematic liquid crystal (DON-103; Rodic) containing spherical glass spacers of 5 μ m diameter (Tokuyama Corp., SP-50F) was placed between two surface-modified quartz plates. The cell was irradiated alternately with UV light (365 nm) and blue light (440 nm) from a 500 W high pressure mercury arc. Alignment alteration was followed by monitoring transmitted light intensity of a He-Ne laser beam passed through a cell and a crossed polarizer (Figure 2-3).

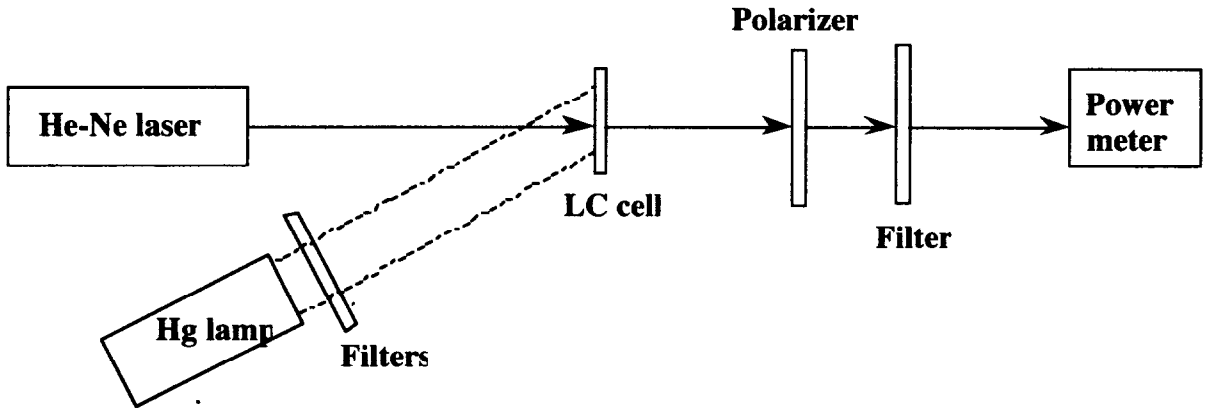

Figure 2-3 An experimental setup for the photoinduced alignment regulation.

RESULTS AND DISCUSSION

Adsorption on Silica Plates

As revealed previously, the photoinduced LC alignment between homeotropic and planar modes by surface azobenzenes attached through silylation is influenced markedly by various factors including a substituent and a spacer length.[2] An alkyl residue at the p-position of the E-azobenzene chromophore brings about homeotropic alignment effectively, while a longer spacer linking an azo-chromophore to a silica substrate surface plays an important role for the photoalignment control. Based on these observations, azobenzenes in this work were substituted with a butyl group at the *p*-position and a decamethylene spacer between the photoisomerizable group and a hydrophilic residue like carboxylic and amino groups (Figure 2-1). The amino compound (**3a**; 4AzA) was prepared from the corresponding carboxylic acid (**1a**; 4AzC) through the urethane (**2a**; 4AzU).

The adsorption behavior of the azobenzenes was examined by immersing a quartz plate in a 10^{-2} mol/L benzene solution, followed by rinsing the plate with benzene. A plate immersed in a 4AzA solution showed a distinct absorption spectrum due to the azobenzene chromophore, while 4AzC is adsorbed slightly on a silica surface (Figure 2-4). No surface adsorption was detected for 4AzU at all. As shown in Figure 2-4(a,), the absorbances are reduced gradually after successive washing out ultrasonically with fresh benzene. The azobenzene absorption bands disappeared almost completely after rinsing with ethanol. These indicates that the azobenzene having an amino group adsorbs physically on the surface through hydrogen bonding. Figure 2-4(a) furthermore indicates the followings: First, the red shift of the absorption maximum due to the π - π* transition from 338 nm to 352 nm is caused by the second rinsing with benzene. The absorption maximum of the latter is equivalent to that in a solution, while the blue shift of the absorption is ascribable to the face-to-face aggregation of the chromophores.[9] This implies that the partial desorption of the azobenzene upon rinsing leads to the reduction of the surface density of the chromophore, which results in an increase in isolated azobenzene molecules on the surface. Second, the ratio of the absorbance at 352 nm (A_l) to the one at about 250 nm (A_s) decreases by successive washing with benzene. Since the absorption

bands at the longer wavelength and the shorter wavelength are due to the longer and the shorter molecular axes, respectively, the ratio (A_l/A_s) is a measure of the conformational state of the azobenzene chromophore; the smaller ratio reflects the more perpendicular conformation of the chromophore on a surface.[2] The increase in A_l/A_s after repeated washing of the quartz plate suggests that the tilt angle (the angle contained by the molecular axis and the surface) of the azobenzene chromophore is enhanced by the partial desorption upon washing as a result of the decrease in the surface density.

This was supported by the absorption spectral change upon UV irradiation for the E/Z photoisomerization (Figure 2-5). Figure 2-5(a) shows the spectral changes of a plate after the first washing. UV irradiation causes the decrease in the π-π^* absorption band to give a photostationary state. Judging from the spectral shape after prolonged UV irradiation, the photostationary state contains approximately one third of the initial E-isomer since the decrease in the absorption at 352 nm is incomplete. This is more clearly recognized by the comparison with the spectral change of the plate which was subjected to repeated washing to result in the partial desorption, followed by UV irradiation. As shown in Figure 2-5(b), the absorption at 352 nm due to the E-isomer decreases efficiently after UV irradiation, and the absorption band at about 440 nm due to the n-π^* transition is intensified because of the sufficient formation of Z-isomer with an absorption coefficient larger than that of E-isomer. Thus, the partial desorption leading to the reduction of the surface density brings about the increase in free volume required for the E/Z photoisomerization.

The adsorption behavior of the azobenzene amphiphiles on a silica surface was determined UV-spectroscopically using colloidal silica in stead of a silica plate since amounts of the azobenzene adsorbed on silica plate are so minute that it is hard to obtain reliable absorbances. Colloidal silica was dispersed in benzene containing an azobenzene derivative to reach adsorption equilibrium, and the amount of adsorbed azobenzene was estimated by measuring a UV absorbance of a supernatant after the removal of silica particles by means of centrifugation. The results are shown in Figure 2-6. The adsorption capability is in the following order; 4AzA >> 4AzC $\geqq$ 4AzU. The adsorption behavior of 4AzA onto silica particles was well fitted with the Freundlich's equation,

$$\log W_i = \log K_f + (1/n)\log C$$

where K_f and n are adsorption constants. It was confirmed that the adsorbate (4AzA) has a strong affinity to silica surface since n = 3.44.

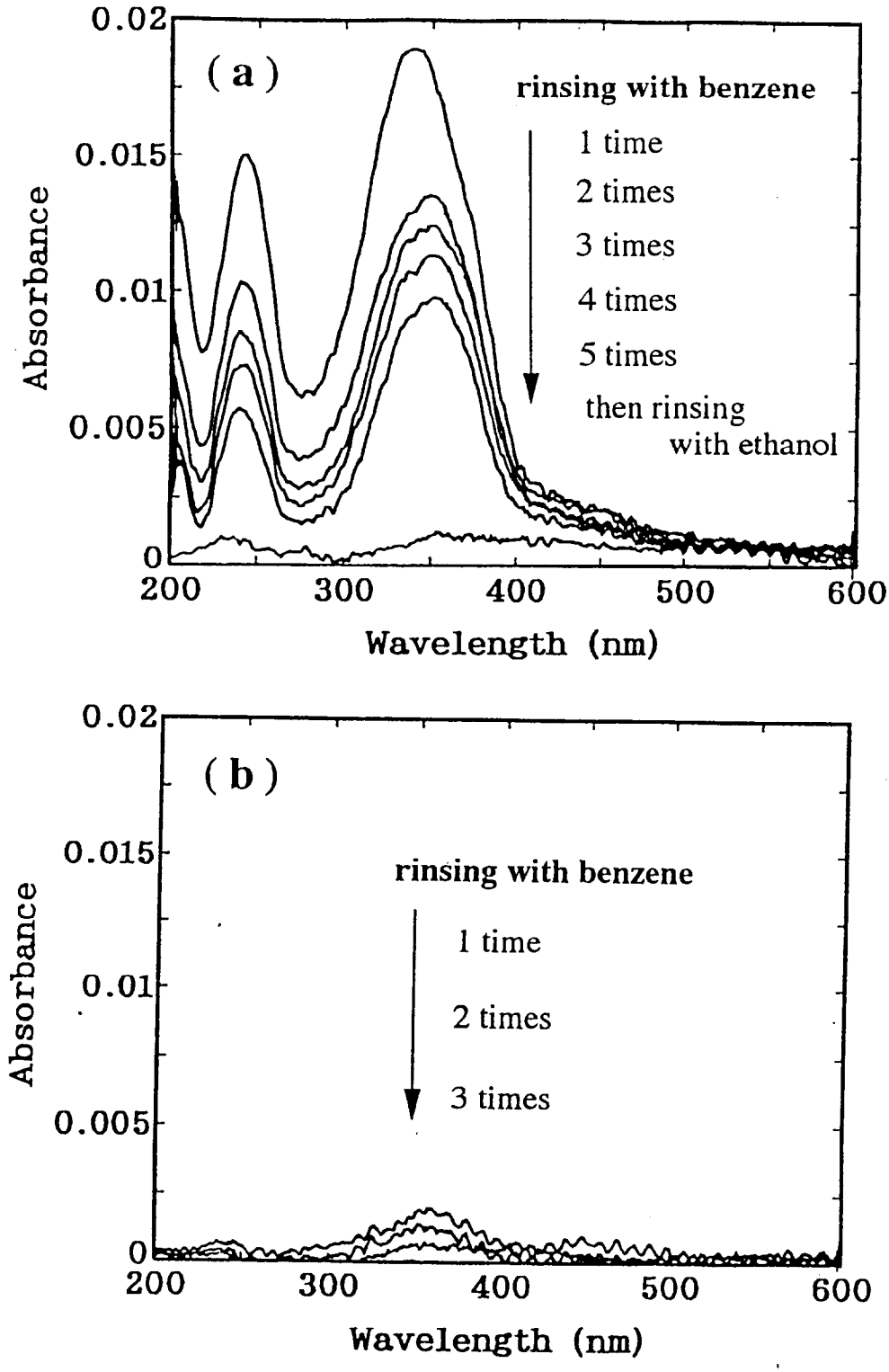

Figure 2-4 Absorption spectra of azobenzenes ((a): 4AzA, (b) :4AzC) adsorbed on quartz plates which were rinsed with fresh benzene repeatedly.

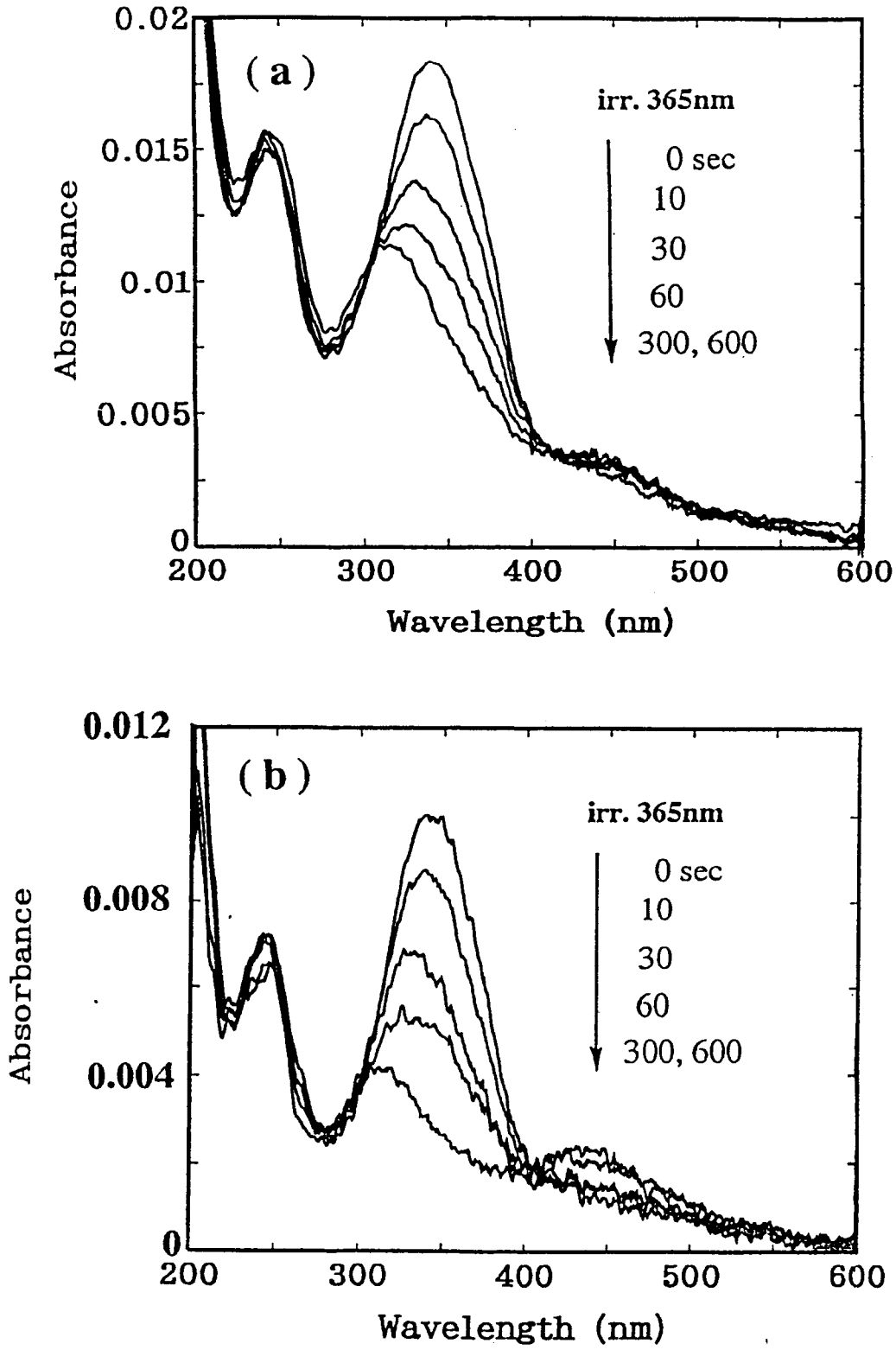

Figure 2-5 Absorption-spectral changes during UV irradiation of (a) a plate immersed in a 10^{-2} mol/L benzene solution of 4AzA, followed by rinsing with benzene once and (b) a plate rinsed with benzene four times after the surface adsorption.

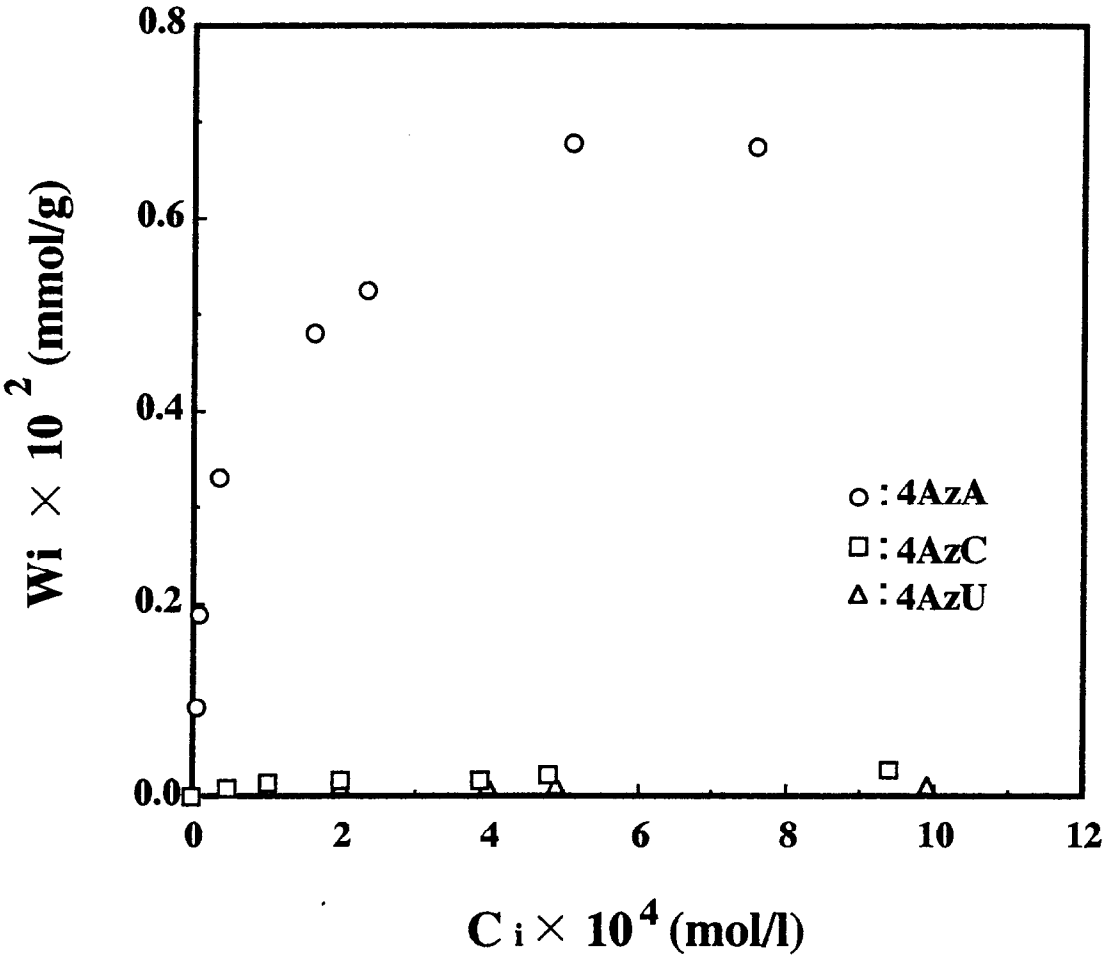

Figure 2-6 Adsorption isotherms of azobenzenes (-○-: 4AzA, -△-: 4AzU and -□-: 4AzC) on colloidal silica from benzene solutions.

Photoregulation of Liquid Crystal Alignment

Silica plates modified with 4AzA displayed the ability to regulate liquid crystal alignment between homeotropic and planar modes upon alternate irradiation with 365 nm light and 440 nm light. As presented in Figure 2-7, plates treated with benzene solutions of 4AzA in higher concentrations exhibit the reversible alignment alteration, although no photoresponse was observed for plates modified with a diluted (1×10^{-4} mol/L) benzene solution. It has already been shown that the photoregulation of LC alignment is determined by the surface density of commander molecules at a critical value.[2,10] At least one azobenzene molecule is needed on a surface area of 1 nm^2 for the photoalignment, and LC cells do not work when the density of the molecule is reduced less than this value. The treatment of a silica plate with a benzene solution of 1×10^{-2} mol/L 4AzA gave the surface coverage of roughly 2.5 molecules per 1 nm^2, as estimated by the UV-absorbance of the plate. This value is sufficiently larger than the critical one so that the surface exhibits the ability to perform the reversible alignment change.

A silica surface was treated with other azobenzenes bearing an aminoalkyl group to determine the photoresponsiveness of LC cells to reveal the substitutent effect of azobenzene chromophores. As shown in Figure 2-8, both 8AzA (**3b**) and 0AzA (**3c**) made the substrate surface photoactive to result in similar photoregulation of LC alignment. It should be noticed here that the surface adsorbed by 0AzA without an alkyl residue at the *p*-position is able to command the LC alignment upon photoirradiation. The effect of the substituent on the azobenzene moiety on the photocontrollability of LC alignment has been reported.[2] When a silica surface was modified with azobenzene silylating reagents, an alkyl substituent at the para-position of azo-moiety works favorably to make the alignment homeotropic so that the cell displays reversible photoalignment regulation. On the contrary, a silylating reagent having azobenzene skeleton without *p*-alkyl substituent produces planar alignment, and, as a result, no efficient homeotropic/ planar alignment photoregulation was attained. This is a marked contrast to the present results. In the case of the silylation, an azobenzene moiety was linked to a silica surface through a spacer, $(O(CH_2)_5CONH(CH_2)_3Si\text{-}O$. The photoactivity of 0AzA to command the alignment alteration is probably owing to the longer alkylene spacer.

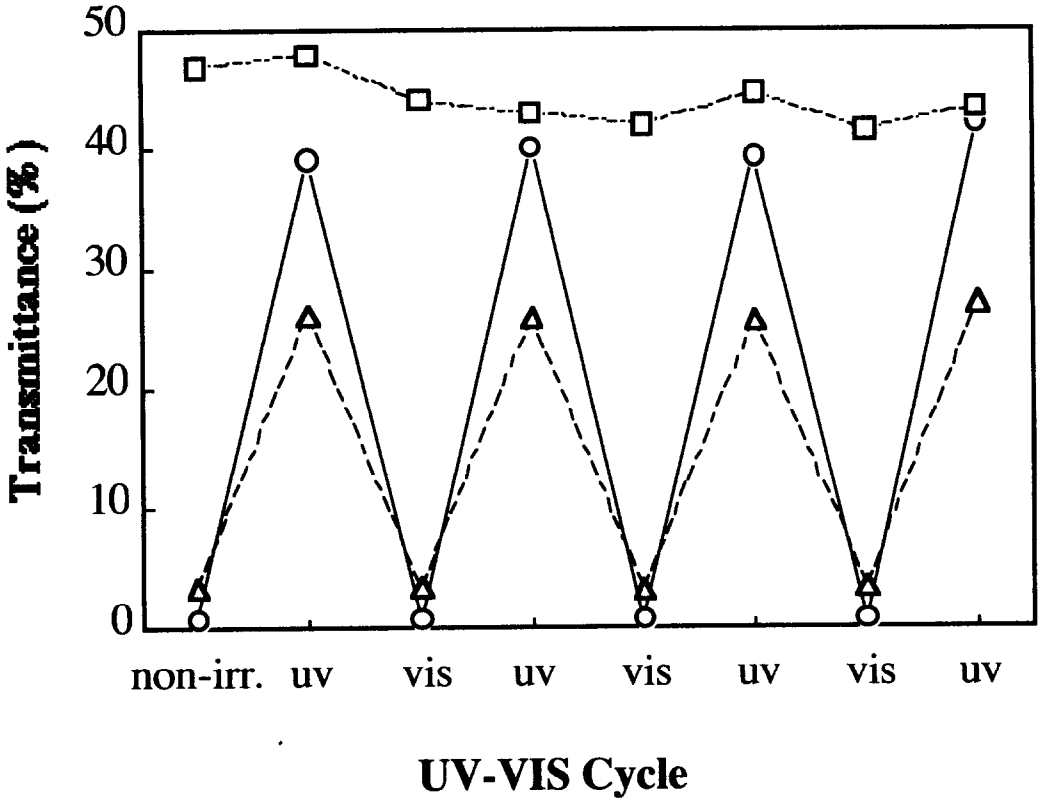

Figure 2-7 Reversible changes of transmitted light intensity of a probing linearly polarized He-Ne laser beam passed through a cell and a crossed polarizer upon alternate irradiation with UV and blue light. Substrate plates were treated with 1 x 10^{-2} mol/L (-○-), 1 x 10^{-3} mol/L (-△-) and 1 x 10^{-4} mol/L (-□-) benzene solutions of4AzA, respectively.

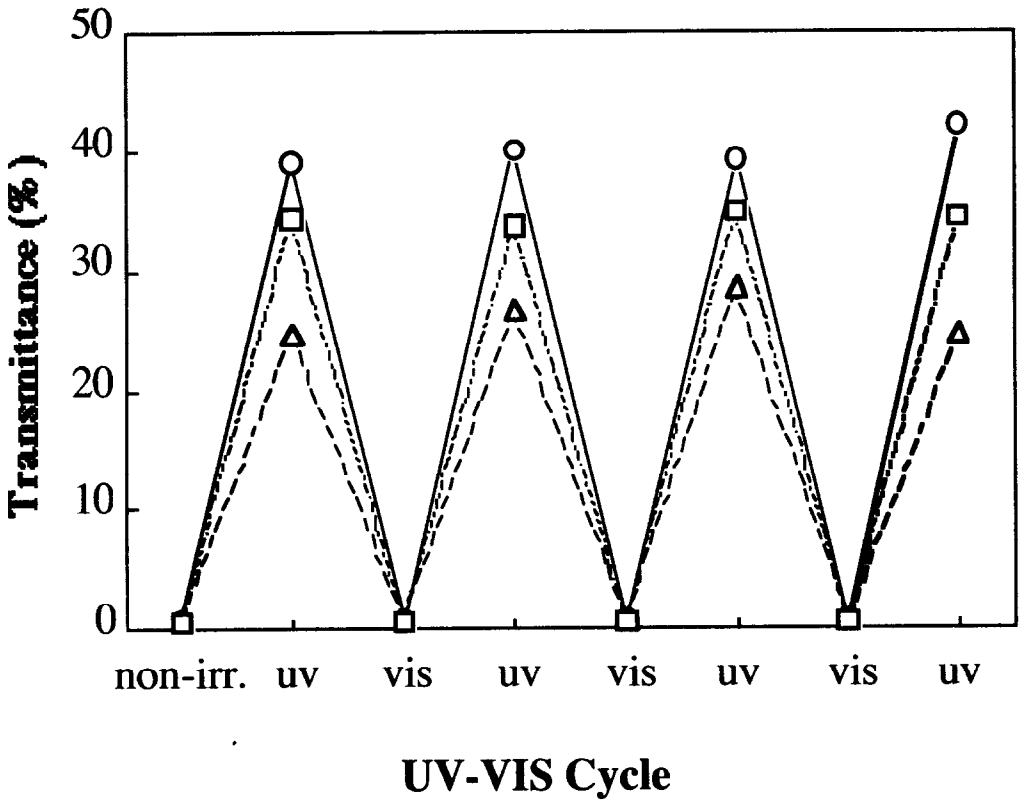

Figure 2-8 Reversible changes of transmitted light intensity of a probing linearly polarized He-Ne laser beam passed through a cell and a crossed polarizer upon alternate irradiation with UV and blue light. Substrate plates were treated with 1 x 10^{-2} mol/L benzene solutions of 4AzA (-○-), 0AzA (-△-) and 8AzA (-□-), respectively.

A similar spacer effect was observed for p-methoxyazobenzene.[11,12] When a silica substrate is modified with the *p*-substituted azobenzene through the same spacer incorporating an amide bond, the alignment of a nematic LC became random parallel so that no photocontrol of LC alignment was attained upon alternate UV-vis photoirradiation. On the contrary, the attachment of the same chromophore through a decamethylene spacer enabled us to achieve the reversible alignment regulation between homeotropic and planar modes. These facts may lead us to a clue for the molecular design to obtain a homeotropic alignment induced by a commander molecule by tethering a photochromic unit through a longer hydrophobic alkylene spacer.

In the meantime, it was found that a cell fabricated with plates treated with a 10^{-2} mol/L solution of 4AzA and filled with DON-103 becomes photoinactive after being kept standing for 10 days even in the dark. Because azobenzene-modified surfaces are so photofatigue-resistant that more than 1000 repetition cycles are possible upon alternate UV and visible light irradiation,[2] the inactiveness of the cell is not caused by the photodegradation, but by the gradual desorption of 4AzA from a substrate surface, as suggested by the results that 4AzA on a silica surface is removed by washing with pure benzene. This led us to fabricate a cell with clean silica plates and a nematic liquid crystal dissolving 0.1 wt% of 4AzA to reach an adsorption equilibrium in it. An initial LC texture of the cell was planar and converted gradually into a homeotropic mode, as shown in Figure 2-9. This corresponds unequivocally to the adsorption of 4AzA onto a substrate surface and offers quite a convenient way to make up photoresponsive LC cells. After the completion of a homeotropic alignment, the cell was subsequently exposed to UV light to give a planar mode. This implies that a simple procedure leading to the fabrication of photoresponsive cells is performed by solely filling a cell made up of a couple of clean substrate plates with a nematic liquid crystal containing a photochromic amphiphile.

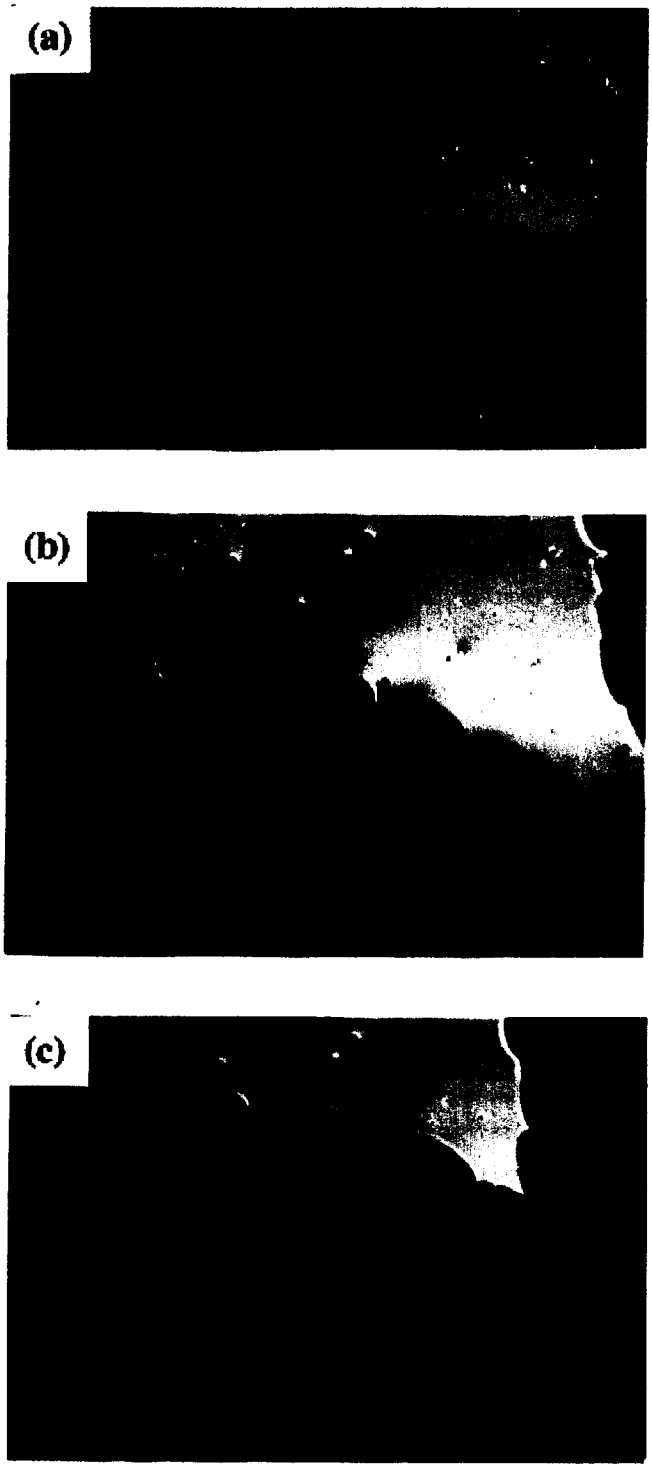

Figure 2-9 Polarized micrographs (×40) of a cell assembled with a couple of silica plates and filled in with DON-103 containing 0.1 wt% of 4AzA during being kept standing at room temperature. (a) 1 min, (b) 5 min and (c) 10 min after the cell assembly.

SUMMARY

In summary, azobenzenes having an amino residue show good adsorptivity on a silica surface, and adsorbed azobenzene molecules form a face-to-face aggregation. A silica surface adsorbing an azobenzene amphiphilic compound displays an ability to command the photoalignment of a nematic liquid crystal between homeotropic and planar modes. This provides a convenient procedure to fabricate photoresponsive LC cells simply by filling LC dissolving azobenzene amphiphiles between clean silica surfaces.

REFERENCES

1) K. Ichimura, T. Seki, Y. Kawanishi, Y. Suzuki, M. Sakuragi and T. Tamaki, in *Photo-reactive Materials for Ultrahigh density Optical Memory*, ed. M. Irie, Elsevier Science, Amsterdam, 1994, p55.

2) K. Aoki,T. Tamaki, T. Seki, Y. Kawanishi and K. Ichimura, *Langmuir*, **8**, 1007 (1992).

3) K. Ichimura, H. Akiyama, K. Kudo and N. Ishizuki, *Liq. Cryst.*, **20**, 423 (1996).

4) K. Ichimura, H. Akiyama, N. Ishizuki and Y. Kawanishi, *Makromol. Chem., Rapid Commun.*, **14**, 813 (1993).

5) C.-H. Chiang, N.-I. Liu and J. L. Koenig, *J. Colloid and Interface Sci.*, **86**, 26 (1982).

6) C.-H. Chiang, H. Ishida and J. L. Koenig, *J. Colloid and Interface Sci.*, **74**, 396 (1980).

7) O. K. Johannson, F. O. Stark, G. E. Vogel and R. M. Fleischmann, *J. Composite Mater.*, **1**, 278 (1967).

8) T. Shioiri, K. Ninomiya, and S, Yamada, *J. Am. Chem. Soc.*, **94**, 6203 (1972).

9) M. Shimomura, R. Ando and T. Kunitake, *Ber. Bunsen-Gel. Phys. Chem.*, **87**, 1134 (1983).

10) T. Seki, M. Sakuragi, Y. Kawanishi, T. Tamaki, R. Fukuda and K. Ichimura, *Langmuir*, **9**, 211 (1993).

11) a) Y. Kawanishi, T. Tamaki, M. Sakuragi, T. Seki, Y. Suzuki and K. Ichimura, *Langmuir*, **8**, 2601(1992); b) Y. Kawanishi, T. Tamaki, M. Sakuragi, T. Seki and K. Ichimura, *Mol. Cryst. Liq. Cryst.*, **218**, 153 (1992).

12) Y. Kawanishi, T. Seki and K. Ichimura, *ACS Symp. Ser.*, **537**, 453 (1994).

Chapter 3

Photocontrolled Dispersibility of Colloidal Silica by Surface Adsorption of a Calixresorcin[4]arene having Azobenzene Groups

INTRODUCTION

In Chapter 2, adsorption behavior of azobenzenes having an aminoalkyl residue onto a silica surface was described. Silica plates adsorbing the azobenzene bearing an aminoalkyl residue were employed to achieve the surface-assisted photoregulation of alignment of a nematic liquid crystal between homeotropic and planar modes.

The stability of dispersions of colloidal silica is of great practical importance. It depends on various factors including dispersion media, pH, additives such as inorganic salts, surface-active reagents and polymers, and results from molecular interactions between colloidal surfaces and solvent molecules. As Chapter 1 shows, in order to improve the dispersibility in organic solvents, chemical modification of the silica surface has been undertaken by polymer adsorption, graft polymerization, silylation and esterification of surface silanols to render the surface organophilic. So far, however, little attention has been paid to regulating colloidal stability in organic solvents by external stimulation, without the aid of additives.

It is well-known that the *trans*-to-*cis* photoisomerization of azobenzene causes a marked change in the hydrophobicity of the molecule because of a large dipole moment developed across the azo bond. *cis*-Azobenzene has a large dipole moment of 3.1 D in contrast to the much smaller value of *trans*-azobenzene (0.5 D or less).[1] Many reports have demonstrated that the properties of material can be photocontrolled by using the polarity-changeable azobenzene molecules. In a solution of a polymer with azobenzene side chains, light-induced changes affect the solution viscosity,[2,3] the sol-gel transition,[4] solubility,[5] and so on. Therefore, it would be expected that the dispersibility of colloidal silica can be photoregulated by surface treatment with photochromic azobenzene molecules.

The following conditions would be required for the optimization of a polarity change due to the geometrical photoisomerization of azobenzenes on a silica surface. First, the molecular axes of azobenzene molecules tethered to a silica surface orient in the same direction as much as possible, so that cancellation of the dipole moment of the chromophores is expected to be minimized. Secondly, an azobenzene chromophore is substituted with an alkyl residue at the p-position to enhance the hydrophobicity of the *trans* isomer. Considering these conditions, the author noted the unique molecular structure of a crown conformer of calix[4]resorcinarene (CRA) which possess eight phenolic OH groups on the lower rim of the cyclic skeleton, whereas four alkyl residues are attached to the upper rim.[6] Thus, CRA is a cyclic amphiphile and expected to adsorb readily onto a polar silica surface through hydrogen bonds. The molecular design based on these consideration led us to prepare CRA having p-butylazobenzene residues at the upper rim (4-AzCRA in Figure 3-1).

In this Chapter, the author will propose a photochemical approach for controlling the dispersibility of colloidal silica by surface adsorption with drastic polarity-changeable azobenzene molecules as a novel photoresponsive system.

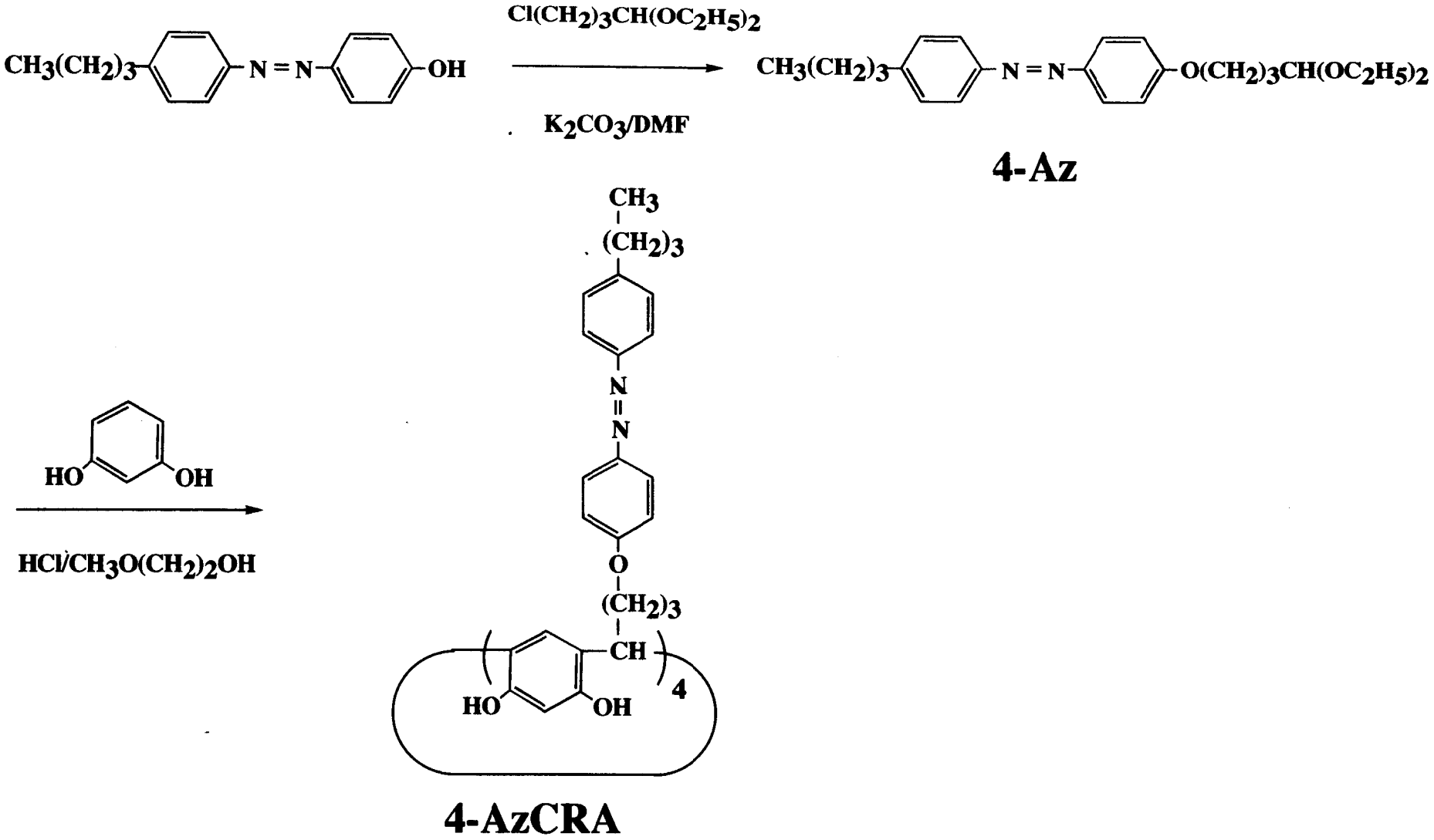

Figure 3-1 Synthetic pathways of 4-Az and 4-AzCRA

EXPERIMENTAL

Materials

Silica Particles

Monodispersed silica particles were a gift from Tokuyama Corp. ; diameter 150 nm, BET surface area 48 m^2/g.

4-[4-(4-butylphenylazo)phenoxy]butanal diethylacetal (4-Az)

A mixture of 1.50 g of 4-butyl-4'-hydroxyazobenzene, 1.10 g of 4-chlorobutanal diethylacetal and 3.0 g of powdered potassium carbonate in 23 ml of DMF was stirred for 8 h at 80 ℃. The reaction mixture was treated with 50 ml water and 50 ml hexane to separate the organic layer which was washed with water, followed by drying over magnesium sulfate. Evaporation of the solvent afforded a crystalline mass which was purified by chromatography on silica gel using a 9 : 1 mixture of hexane and ethyl acetate as eluent to give 1.79 g (76.1 % yield) of orange plates, mp. 38.5-40.5 ℃. ^{1}H-NMR ($CDCl_3$) : δ =0.95 (3H, t, $CH_3(CH_2)_3$), 1.24 (6H, t, CH_3CH_2O-), 1.06 (4H, br., $CH_3(CH_2)_2CH_2$-), 1.90 (4H, br., -$OCH_2(CH_2)_2CH$-), 2.70 (2H, t, Ph-CH_2CH_2-), 3.57 (4H, m, -OCH_2CH_3), 4.06 (4H, m, -OCH_2CH_2-), 4.65 (1H, t, CH), 6.9-8.0 (8H, m, Ar). Calcd. for $C_{24}H_{34}N_2O_3$: C; 72.33, H; 8.60, N;7.03%. Found: C;71.62, H;8.63, N;6.94%.

2,8,14,20-Tetrakis{3-[4-(4-butylphenylazo)phenoxy]propyl}-4,6,10,12,16,18,22,24-octahydroxycalix[4]arene (4-AzCRA)

A solution of 3.00 g of 4-Az and 0.83 g of resorcinol in 50 ml of 2-methoxyethanol containing 2 ml of conc. hydrochloric acid was stirred for 8 h at 80 ℃. After standing at room temperature for one day, the precipitated orange crystals were collected by filtration, washed successively with ethanol and water and finally with ethanol, and dried *in vacuo* to yield 1.28 g of crude product. Recrystallization from a mixed solvent of ethanol and chloroform gave 0.99 g of orange crystals which did not melt below 300 ℃. MS[M^+H]=1666. ^{1}H-NMR ($CDCl_3$) : δ =0.91 (12H, t,

CH_3), 1.34 (8H, m, CH_2), 1.58 (8H, m, CH_2), 1.86 (8H, br. s, CH_2), 2.47(8H, br. s, CH_2), 2.61 (8H, br. t, Ar-CH_2), 4.07 (8H, br. s, ArO-CH_2), 4.45 (4H, br. s, CH), 6.17(4H, br. s, Ar-H_b), 6.94(8H, d, Ar-H of azobenzene), 7.19 (8H, d, Ar-H of azobenezene), 7.32 (4H, br. s, Ar-H_c), 7.75(16H, dd, Ar-H of azobenzene), 9.45 (4H, br. s, OH) 9.71(4H, br. s, OH). Calcd. for $C_{104}H_{112}N_8O_{12}$: C;74.97, H;6.78, N;6.73%. Found: C;74.53, H;6.62, N;6.64%.

Adsorption of Azobenzenes

Silica particles adsorbed with two different amounts of 4-AzCRA were prepared (CRA-CS1 and CRA-CS2). The adsorption of on the surface of silica particles was carried out as follows. To a dispersion of silica particles (0.50 g) in chloroform (10 ml) was added 55.4 mg (for CRA-CS1) or 300 mg (for CRA-CS2) of 4-AzCRA, and the mixture was stirred for 1 h at room temperature. After being centrifuged, the supernatant was discarded. The residual colloidal silica was washed repeatedly with toluene, then rinsed with cyclohexane until no UV absorption bands of 4-AzCRA were observed in the supernatant cyclohexane, and dried at 60 ℃ under vacuum for 8 h. The amount of adsorbed 4-AzCRA was determined by means of electronic absorption measurement in a cyclohexane dispersion using the absorption coefficient (ε) of 4-AzCRA : 113000 $M^{-1}cm^{-1}$ at 350 nm. Average densities were estimated to be one 4-AzCRA molecule in a silica surface area of 21nm^2 for CRA-CS1 and 9nm^2 for CRA-CS2, respectively. The densities are quite low for both cases, when compared with a cross-sectional area of an azobenzene moiety of 0.25 nm.

Silica particles with adsorbed 4-Az (Az-CS) were also prepared by the same procedure. The absorption spectra of Az-CS dispersed in cyclohexane were recorded using cyclohexane as a reference. The average density was estimated to be one 4-Az molecule in an area of 16nm^2 using ε : 30000 $M^{-1}cm^{-1}$ for 4-Az.

Photoirradiation

The photochromism experiments were carried out by irradiation with 365 nm and 440 nm light at room temperature using a Jasco CRM-FA irradiator equipped with a 2-kW xenon arc lamp with

a monochromator. Absorption spectra were taken on a diode-array spectrometer (Hewlett Packerd HP8452A).

Sedimentation Measurement

Surface-modified silica particles (200 mg) were dispersed in 100 ml of carbon tetrachloride or cyclohexane. A sample (4 ml) of each dispersion was placed in a cell (10 mm ×10 mm × 50 mm) and exposed to 365-nm light. The dispersion was shaken and subsequently placed in the cell holder of a spectrometer and allowed to stand at room temperature. The cell was exposed to the probe light through a circular window of diameter 7 mm, which was set on a cell wall 15 mm from the bottom of the cell as shown in Figure 3-2, to measure the absorbance at an isosbestic point (304 nm) during the sedimentation.

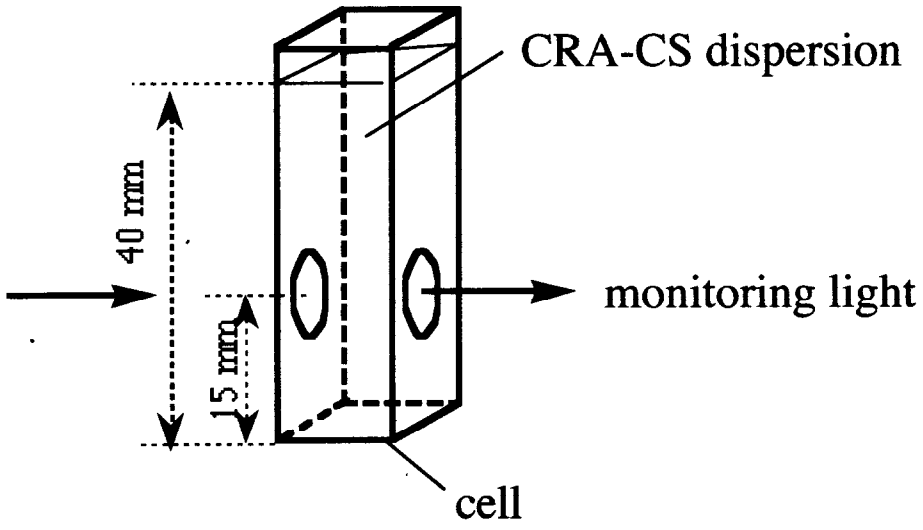

Figure 3-2 A cell for the photoinduced sedimentation of azo-modified colloidal silica.

Physical Measurements

Scanning electron microscope photographs were taken by a JEOL JSM-6400F.

RESULTS AND DISCUSSION

Preparation and Surface Adsorption of a Calixarene with Azobenzene Residues

It has been reported that CRA is readily prepared by the condensation of resorcinol with an aldehyde in ethanol containing hydrochloric acid.[7,8] The formation of a crown conformer needs prolonged heating[7] because the thermodynamically stable crown isomer is formed selectively as a result of acid-catalyzed isomerization of the other conformers. The reaction of resorcin with an equimolar amount of an azobenzene acetal (4-Az) in ethanol in the presence of hydrochloric acid resulted in the precipitation of a product at an early stage of heating so that the transformation into the crown compound was inefficient. In order to enhance the solubility of the condensation product, the solvent was replaced by 2-methoxyethylethanol to carry out the reaction in a homogeneous solution at an elevated temperature. On cooling the reaction mixture, 4-AzCRA was precipitated and purified conveniently by recrystallization. A spot of 4-AzCRA on a silica gel TLC plate did not move at all with less polar eluent solvents, suggesting that the cyclic compound adsorbs firmly on a silica surface. Structural elucidation was carried out by means of NMR spectroscopic studies. The phenolic OH groups of 4-AzCRA were separated at δ 9.45 and 9.71, respectively, because half of the OH groups are subjected to intramolecular hydrogen bonding to stabilize the cyclic structure.[8] The signals of two hydrogen atoms of benzene rings (H_b and H_c in the structural presentation) originated from resorcin are well separated and appear at δ 6.17 and 7.32, respectively, indicating that the molecule has C_{4v} symmetry.

Absorption Spectra of 4-Az and 4-AzCRA

Monodisperse colloidal silica particles of diameter 150 nm were employed here because of their large surface area which will adsorb a sufficient amount of 4-AzCRA, and because of the availability of a transparent dispersion in cyclohexane owing to good refractive index matching which enabled us to carry out spectroscopic analysis. The adsorption was performed in a chloroform solution because of good solubility of the calixarene, followed by washing out with toluene. For

comparison, a monomer model, 4-Az, was also subjected to the adsorption experiment.

Figures 3(a)and 3(b) show the absorption spectra of the colloidal silica particles modified with 4-Az and 4-AzCRA, respectively, which were dispersed in cyclohexane. The n-π^* transitions of both 4-Az and 4-AzCRA adsorbed on silica particles are blue-shifted so that the absorption bands appear as a shoulder at *ca.* 420 nm. It should be noted that the n-π^* absorbance of 4-AzCRA is smaller than that for 4-Az. The blue shift is ascribed to hydrogen bonding between the azo group and silanols and/or water molecules on the silica surfaces. As discussed later (in Chapter 6 and 7), the increase in the n-π^* absorbance can be reasonably explained in terms of the distortion of azobenzene moiety which leads to the mixing of forbidden n orbitals with allowed p orbitals.[9,10] Therefore, 4-Az molecules on silica particles are intimately adsorbed on the silica surface through hydrogen bonds between the azo group and silanols, which cause the mixing of n orbitals of the azo group with the π orbitals. On the other hand, 4-AzCRA molecules adsorbed a silica surface display no marked molecular deformation since it is very likely that the physical adsorption is mainly due to the hydrogen bonding between the phenolic OH groups, which are oriented in the same direction, and the silanol groups on the silica surface. A structural model of these two azobenzene chromophores on the surface of silica are shown in Figure 3-4.

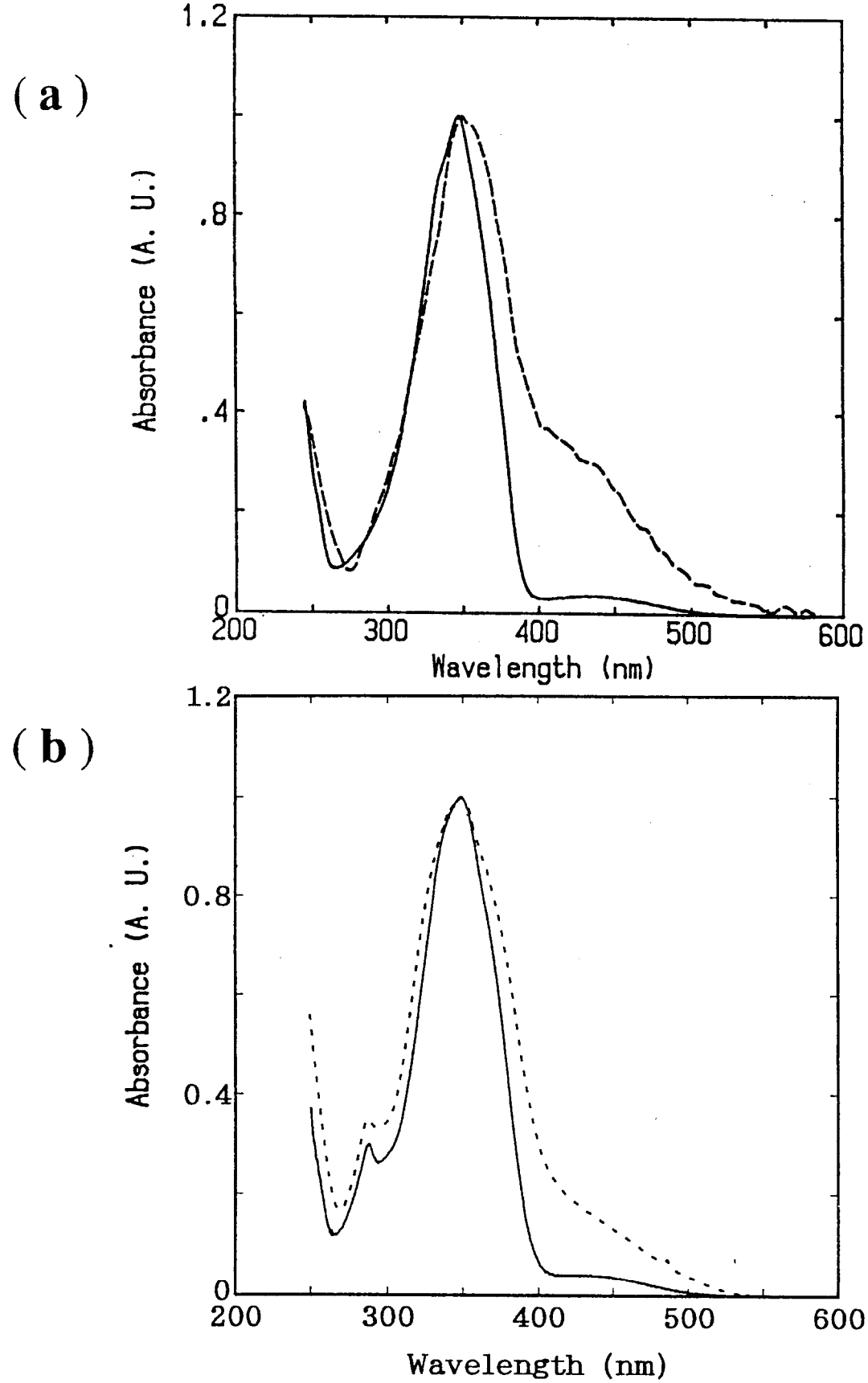

Figure 3-3 Absorption spectra of azobenzenes. (a) (——) 4-Az in a cyclohexane solution and (– – –) 4-Az adsorbed on silica particles dispersed in cyclohexane. (b) (——) 4-AzCRA in THF and (– –) 4-Az adsorbed on silica particles dispersed in cyclohexane.

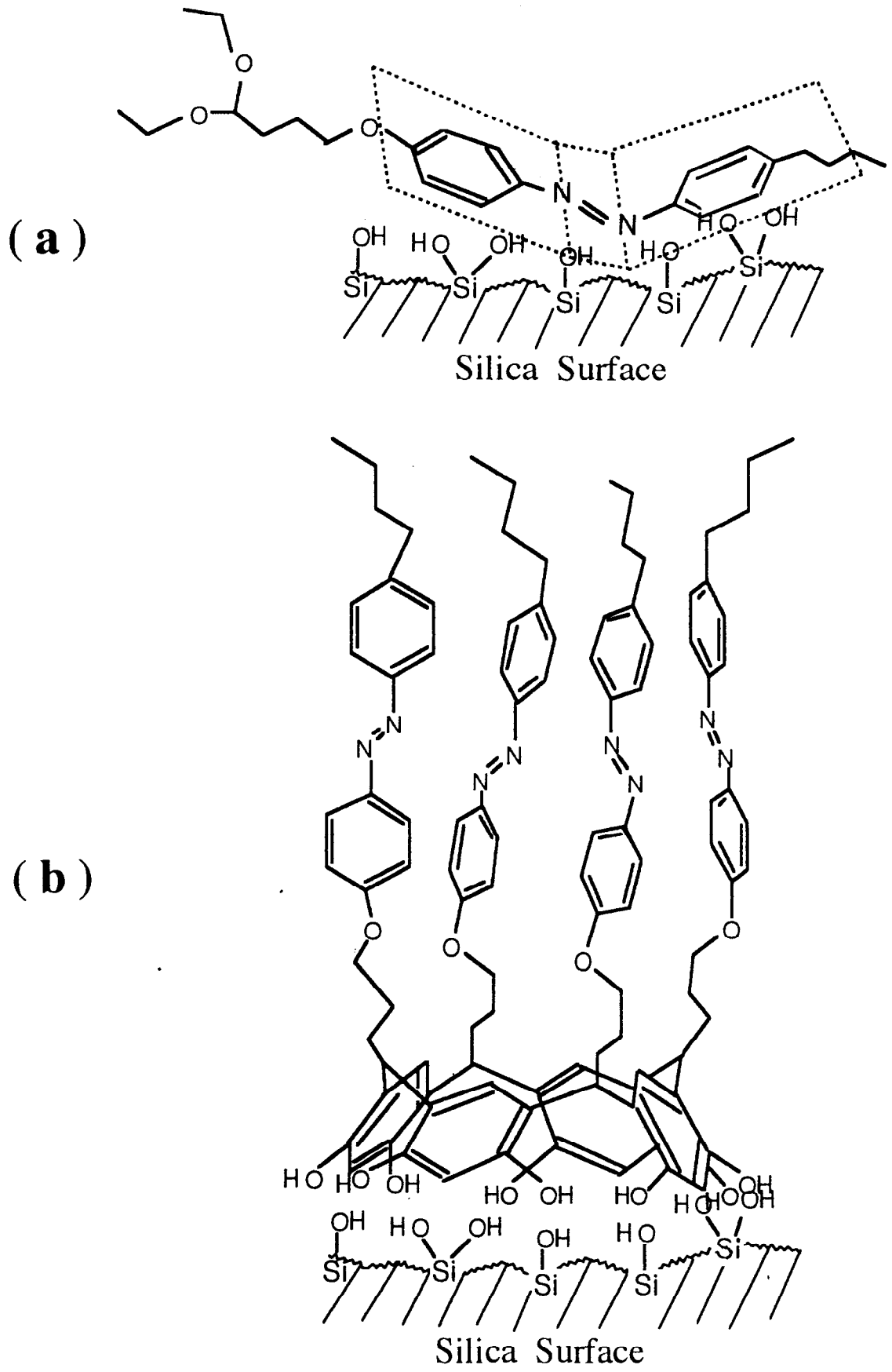

Figure 3-4 Illustrative representation of (a) 4-Az and (b) 4-AzCRA on a silica surface.

Photocontroll Aggregation of Silica Particles Physisorbed with 4-AzCRA

In order to obtain a transparent dispersion, carbon tetrachloride (n = 1.457) and cyclohexane (n = 1.426) meet the requirements for refractive index matching with silica (n = *ca.* 1.45) and are convenient for following the photochromic reaction of the modified silica particles spectroscopically. The desorption of 4-AzCRA from the silica surface was found to be negligible because essentially no UV absorption band due to the chromophore was detected in the supernatant obtained by centrifuging dispersions before and after the photoisomerization. As shown in Figure 3-5, the *trans*-to-*cis* photoisomerization of 4-AzCRA on silica particles went almost to completion without being affected by the surface adsorption. The appearance of isosbestic points indicates that the *trans*-to-*cis* photoisomerization proceeds without any side reactions.

The sedimentation behavior of silica particles with different surface densities of 4-AzCRA (CRA-CS1 and CRA-CS2) was determined by following the decrease in the absorbances at an isosbestic point (304 nm) appearing during the photochromic reaction of dispersions of the particles. A monitoring light was passed through a cell (*ca.* one-third of the way up) filled with the dispersion. Figure 3-6 shows the absorbance changes of dispersions in non-polar solvents showing good refractive-index matching before and after UV irradiation. In carbon tetrachloride, UV irradiation resulted in fact in the enhancement of sedimentation of azo-modified silica particles while the sedimentation rate was influenced by the degree of surface coverage with 4-AzCRA (Figures. 3-6(a)and 3-6(b)) . The slower rate for CRA-CS2 clearly reflects the stabilizing effect of surface 4-AzCRA on the dispersion owing to its hydrophobicity.

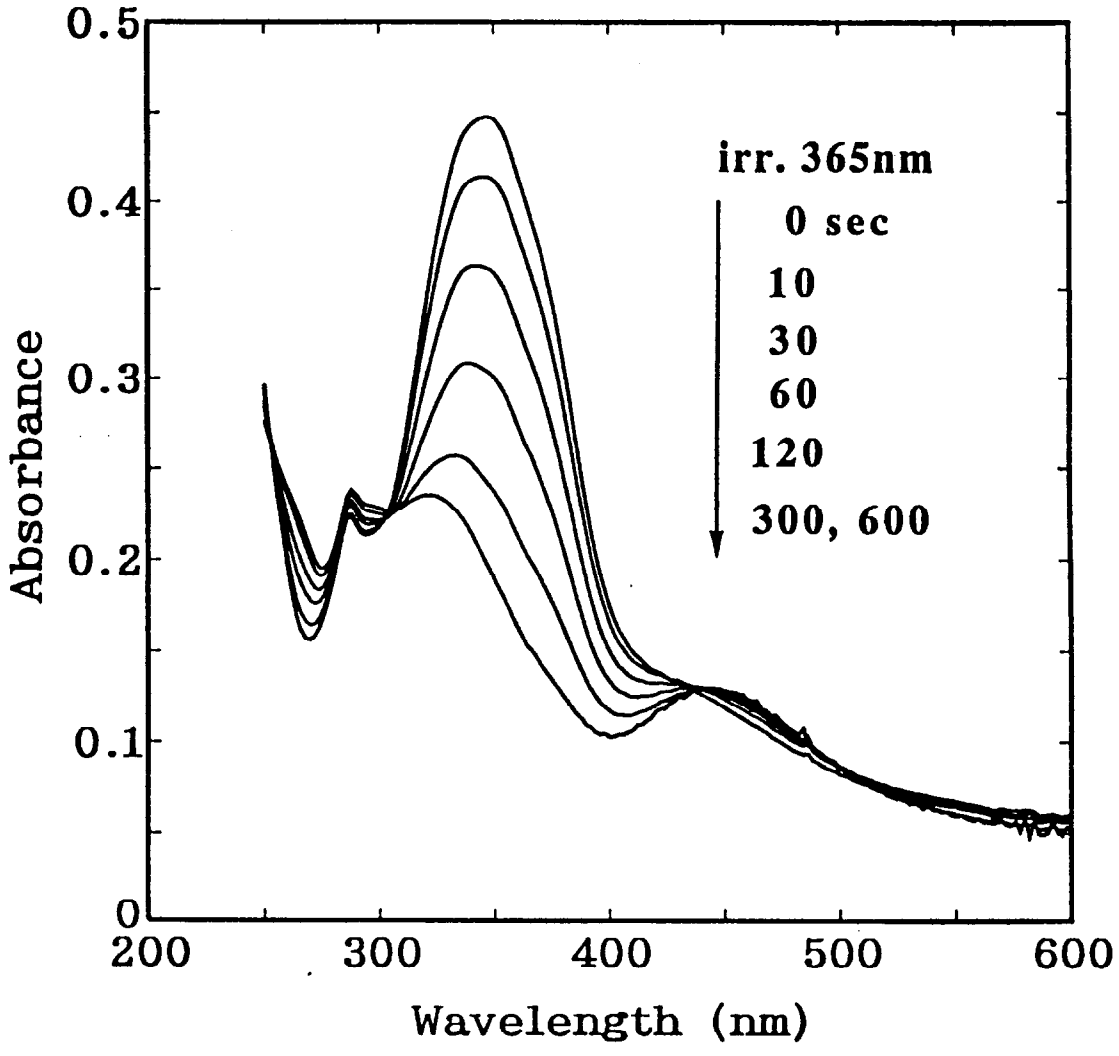

Figure 3-5 Change in absorption spectra of a dispersion of silica particles adsorbing 4-AzCRA during 365 nm light irradiation at room temperature.

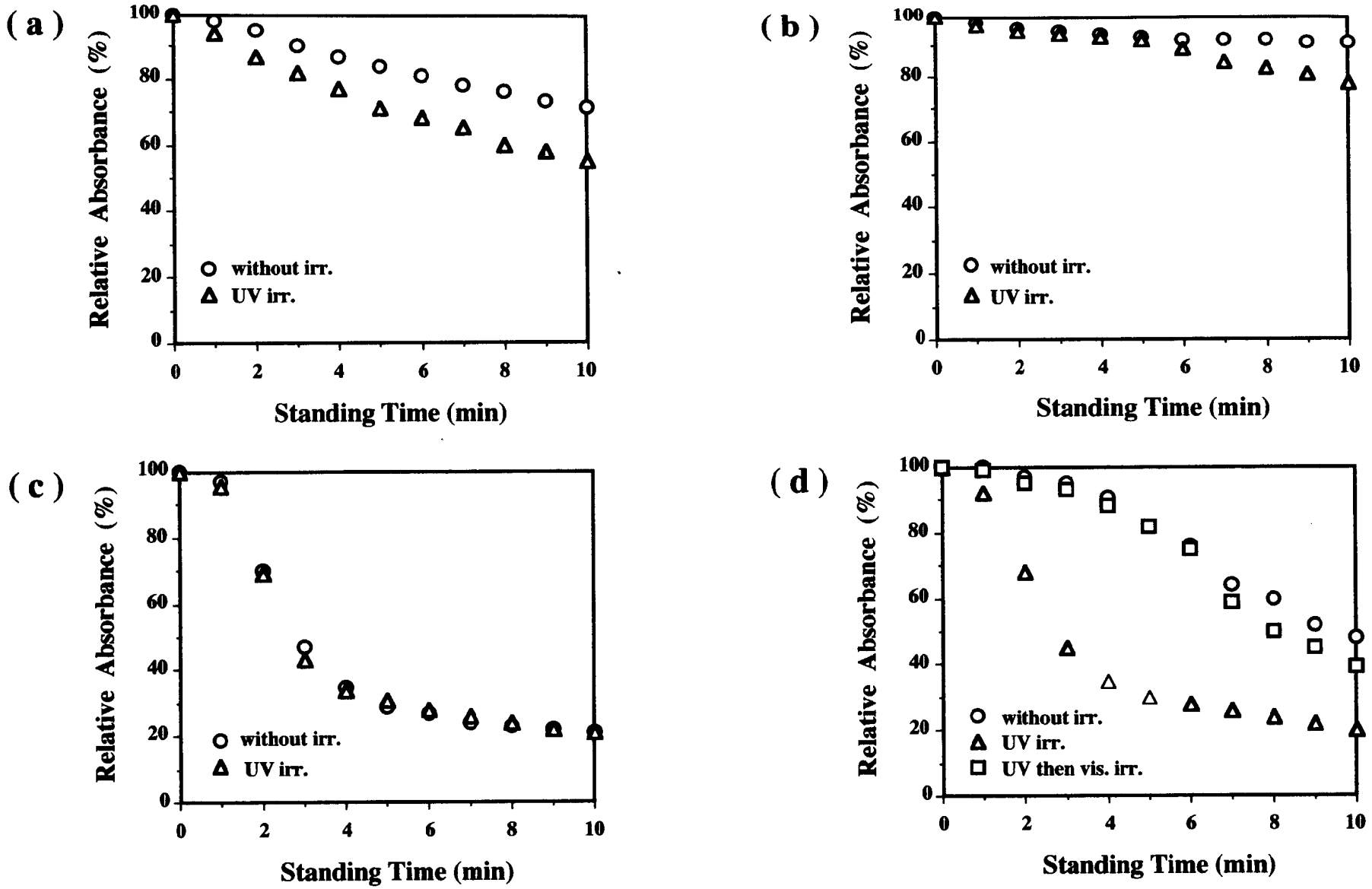

Figure 3-6 Sedimentation behavior of colloidal silica adsorbing 4-AzCRA; (a) CRA-CS1 in carbon tetrachloride, (b) CRA-CS2 in carbon tetrachloride, (c) CRA-CS1 in cyclohexane, (d) CRA-CS2 in cyclohexane.

Much more unequivocal results were obtained when silica particles were dispersed in cyclohexane. Although the sedimentation took place relatively rapidly and was not affected by UV-photoirradiation(Figure 3-6(c)), the rate of sedimentation of CRA-CS2 was reduced owing to greater surface coverage with azobenzene. As shown in Figure 3-6(d), the sedimentation is markedly accelerated by UV-irradiation. The reversion of the *cis* to the *trans* form with 440 nm light irradiation regenerated a light-yellow dispersion after ultrasonical treatment, leading to sedimentation behavior similar to that of the original dispersion. This implies that dispersion and precipitation are interchangeable by means of surface photoisomerization. It should be noted here that surface coverage with 4-AzCRA is quite low, at 21nm^2 and 9 nm^2 per 4-AzCRA molecule for CRA-CS1 and CRA-CS2, respectively. The base area of the cylindrical CRA skeleton is ca. 1.3nm^2 according to a π -A isotherm measurement on a water surface, being in line with that estimated with use of a space-filling molecular model.[11,12] In the case of CRA-CS1, such a low surface density of azobenzene displays no stabilizing effect on the dispersion so that the aggregation of particles occurs readily after ultrasonical treatment.

The different sedimentation behaviour of cyclohexane and carbon tetrachloride is interpreted as follows. [13] The sedimentation rate (υ) of spherical particles of a diameter D is expressed as the Stokes equation:

$$\upsilon = \frac{(\rho - \rho_0)gD^2}{18\eta}$$

where ρ and ρ_0 are the densities of the particle and the solvent (which has viscosity η), respectively, and g is gravitational acceleration. The slow sedimentation in carbon tetrachloride (ρ_0= 1.584 g/cm^3 at 25 ℃) is brought about, at least partially, as a result of the smaller density difference ($\rho - \rho_0$) when compared with that for cyclohexane (ρ_0= 0.774 g/cm^3 at 25 ℃).

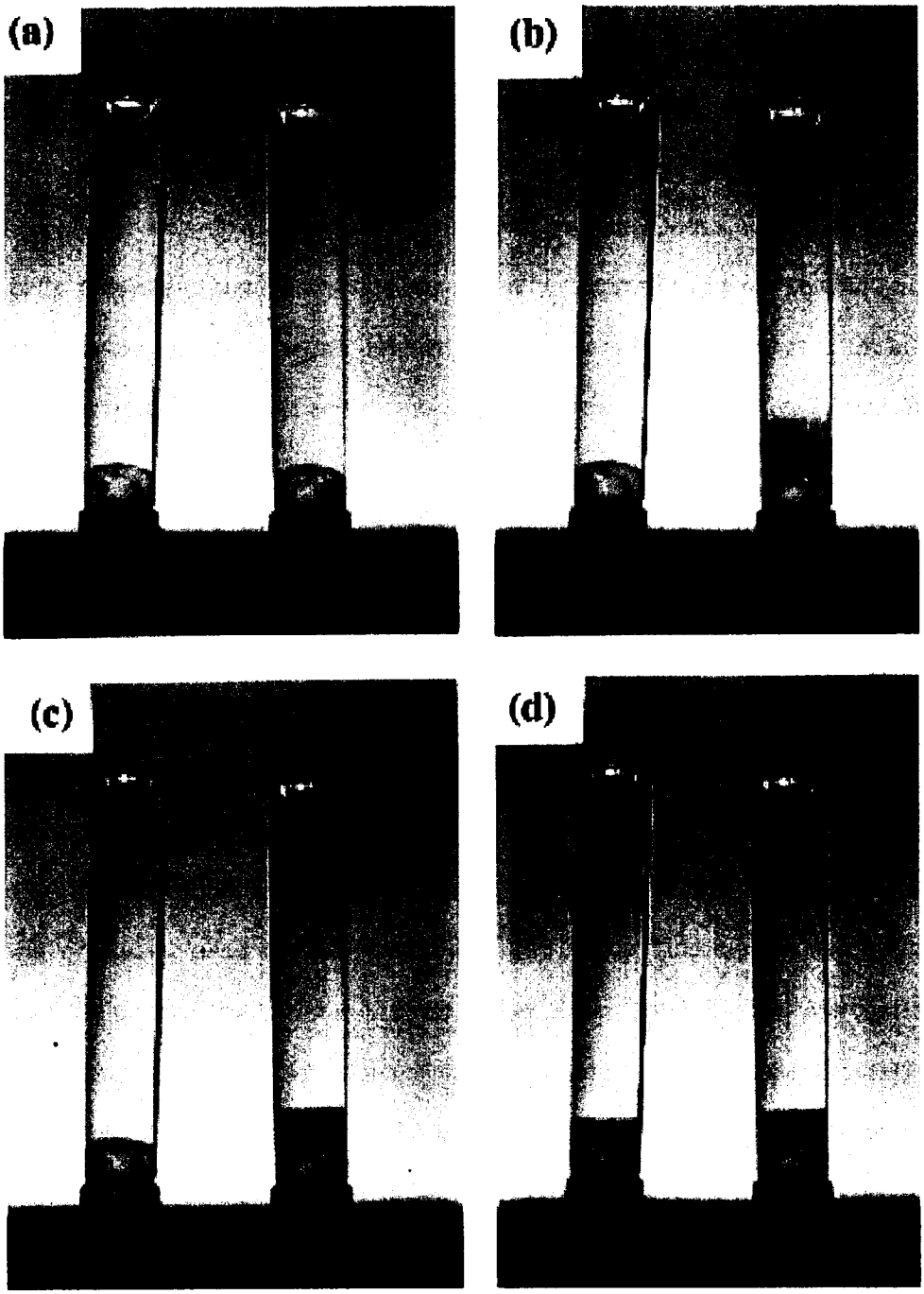

Figure 3-7 Pictures of a CRA-CS2 dispersion in cyclohexane (concentration: 2.0 g/L) in microtubes (inner diameter 6 mm, length 50 mm): (a) 0 min standing; (b) 2 min standing; (c) 5 min standing;, (d) 15 min standing. The right- and left-hand tubes in each picture are the dispersion with and without UV irradiation, respectively.

The photoinduced enhancement of particle sedimentation of CRA-CS2 is ascribable to the drastic increase in the surface polarity owing to the conversion from *trans*-azobenzene to *cis*-azobenzene with more polar character. Closely related work has been reported on the UV induced precipitation of a polystyrene with azobenzene derivatives as pendant groups in cyclohexane, because of the decrease in the polymer-solvent interaction caused by the generation of polar pendant groups.[14,15] UV irradiation induces the change in surface polarity, which causes abrupt reduction of the interaction between silica surface and the non-polar solvent molecules, resulting in an attractive force between the silica particles.

Figure 3-7 shows photographs of dispersions of CRA-CS2 in cyclohexane. The sedimentation of yellow particles was observed when a dispersion was exposed to UV light and subsequently kept standing at room temperature. After sedimentation was complete, the sample was irradiated with 440 nm light to reverse the *trans*-form to *cis*-form. A homogeneous dispersion was obtained again with the aid of ultrasonic treatment, thereby displaying reversible alternation between dispersed and aggregated states of silica particles.

Figure 3-7 also shows that the volume of the *cis*-form precipitate is approximately double that of the *trans*-form precipitate after 15 min standing in the dark. This implies that the *cis*-form precipitate has a highly porous structure due to flocculation of the particles. This was confirmed by scanning electron microscopy of samples prepared by evaporating a solvent of the dispersion before and after UV irradiation. As shown in Figure 3-8, after UV irradiation the particles form highly porous aggregates.

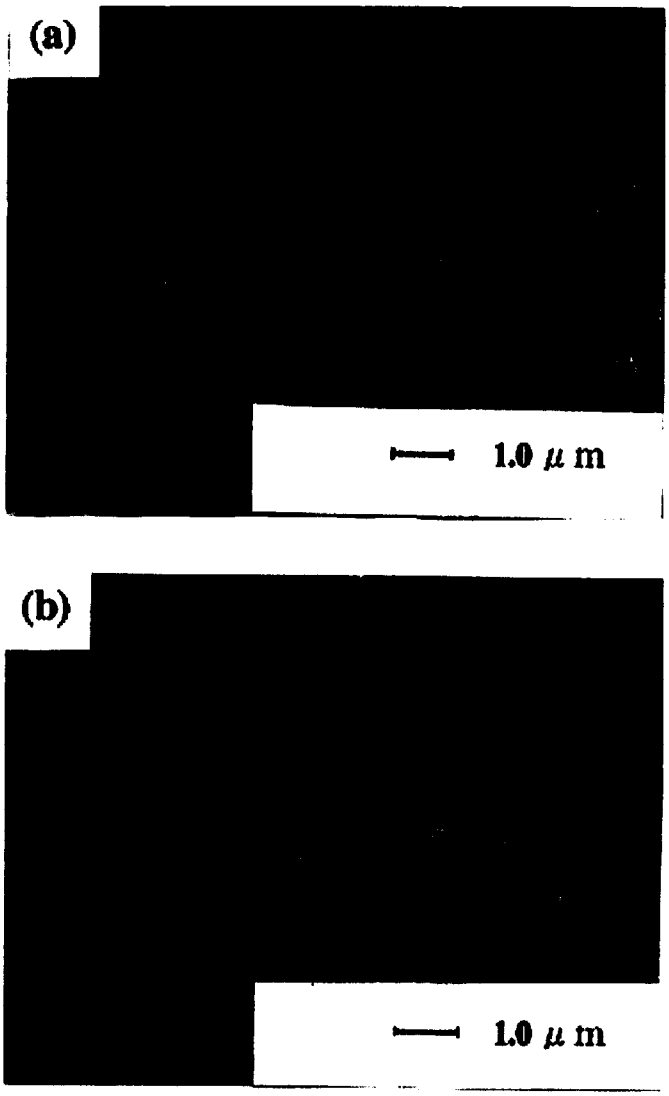

Figure 3-8 Scanning electron micrographs of CRA-CS2; (a) before and (b) after UV irradiation.

SUMMARY

In summary, a novel carlixresorcin[4]arene having four p-butylazobenzene residues sprouted from an upper rim of the cyclic framework was prepared to be subjected to adsorption on a surface of colloidal silica particles. UV irradiation of a homogeneous dispersion of surface-modified silica particles in cyclohexane enhanced the sedimentation owing to the increase in surface polarity, leading to the formation of porous precipitates. Subsequent visible light irradiation regenerated a dispersed state, displaying the photocontrol of the reversible alternation between dispersed and aggregated states of silica particles.

This provides a novel system for molecular amplification of photonic information.

REFERENCES

1) D. J. W. Bullock, C. W. N. Cumper and I. Vogel, *J. Chem. Soc.*, 5316 (1965).

2) M. Irie, Y. Hirano, S. Hashimoto and K. Hayashi, *Macromolecules,* **14,** 262 (1981).

3) M. Irie and T. Suzuki, *Makromol. Chem., Rapid Commun,* **8,** 607 (1987).

4) M. Irie and R. Iga, *Macromolecules,* **19,** 2480 (1986).

5) H. Yamamoto and A. Nishida, *Bull. Chem. Soc. Jpn.*, **61,** 2201 (1988).

6) J. Vicens and V. Bohmer, Calixarenes: *A Versatile Class of Macrocyclic Compounds,* Kulwer Academic Press, Dordrech, 1991.

7) A. G. S. Hogberg, *J. Am. Chem. Soc.*, **102,** 6046 (1980).

8) Y. Aoyama, Y. Tanaka and S. Sugahara, *J. Am. Chem. Soc.*, **111,** 5397 (1989).

9) M. Ueda, H.-B. Kim, T. Ikeda and K. Ichimura, *Chem. Mater.*, **4,** 1229(1992).

10) M. Ueda, H.-B. Kim, T. Ikeda and K. Ichimura, *J. Non-Cryst. Solids,* **163,** 125 (1993).

11) K. Kurihara, K. Ohta, Y. Tanaka, Y. Aoyama and T. Kunitake, *Thin Solid Films,* **179,** 21 (1989).

12) K. Ichimura, M. Fujimaki, Y. Hayashi, K. Kudo, unpublished results.

13) M. Ueda, H.-B. Kim, K. Ichimura, *J. Mater. Chem.*, **4**, 883 (1994).

14) M. Irie and H.Tanaka, *Macromolecules,* **16**, 210 (1983).

15) M. Irie and W. Schnabel, *Macromolecules*, **18**, 394 (1985).

Chapter 4

Photocontrolled Dispersibility of Colloidal Silica by Surface-modification with a Spirobenzopyran

INTRODUCTION

In the Chapter 3, the photoisomerization of a novel calix[4]resorcinarene (4-AzCRA) adsorbed on silica particles triggers reversible dispersion/sedimentation cycles due to the change in the surface polarity. The *trans*-to-*cis* photoisomerization of the azobenzene molecules brings about a decrease in the affinity between the particle surfaces and the non-polar solvent molecules, resulting in the aggregation of silica particles which lead to sedimentation.

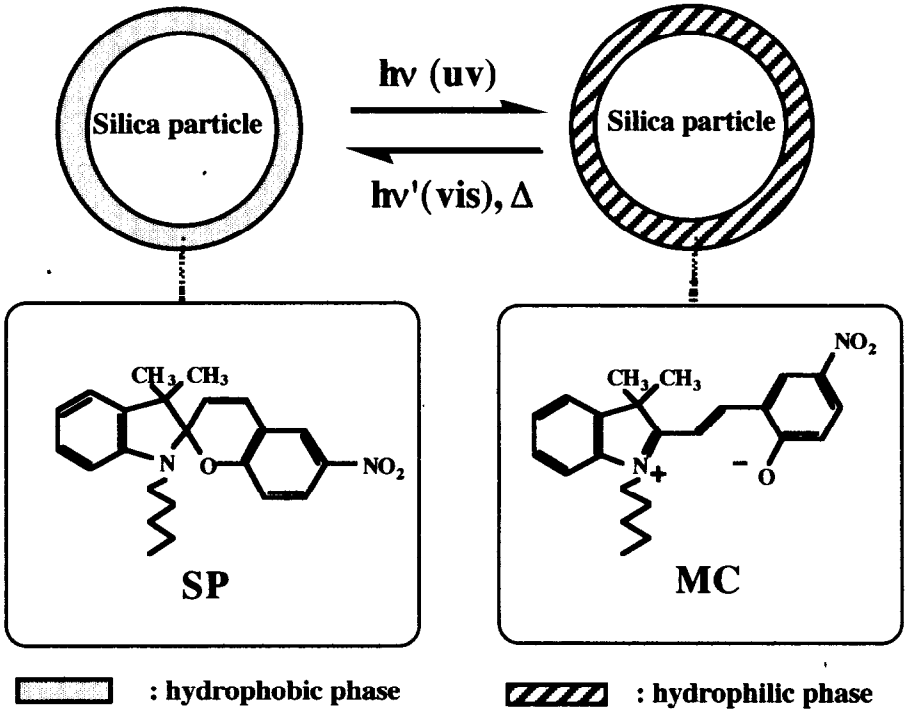

Figure 4-1 Polarity change of colloidal silica surface by light stimulation.

In this system, the photoactive molecules are reasonably referred to as " commander molecules" since their photofunctionality does not arise from the spectroscopic modification in the visible range, but from triggering the alteration in the surface polarity.

Transformation of spiropyran (SP) into merocyanine (MC) is also accompanied by a drastic increase in polarity.[1] Hence, the author expected that the surface polarity of colloidal silica could be controlled photochemically by SP molecules on the surface, leading to macroscopic change between aggregated and dispersed states of the colloidal silica.

In this Chapter, the author will demonstrate another photochemical approach for controlling the dispersibility of colloidal silica by surface treatment with a photochromic spirobenzopyran that displays a drastic polarity change upon UV irradiation due to photoisomerization to a zwitterionic structure (Figure 4-1).

EXPERIMENTAL

Materials

Silica Particles

Monodispersed silica particles were a gift from Tokuyama Corp., diameter = 150 nm and BET surface area = 48 m^2/g. Spirobenzopyran-modified particles (SPCS10) and a model spiropyran (SP10) were prepared according to Figure 4-2.

Spiropyrans

1'-(1-Carboxydecyl)-3',3'-dimethyl-6-nitrospiro[2H-1-benzopyran-2,2'-indoline] (CDN)

This was prepared according to the literature with slight modification.[2] 1-(1'-Carboxydecyl)-3,3,-dimethylindolenium iodide (25.84 g; 0.075 mol) and 5-nitrosalicylaldehyde (12.53 g; 0.075 mol) was heated in methyl ethyl ketone (200 ml) in the presence of piperidine (6.71 g; 0.083 mol) at 70 ℃ for 3 h to yield crystals (9.99 g; 27 %) of mp 121-122℃ which were recrystallized repeatedly from acetonitrile. Found: C, 69.99; H, 7.60; N, 5.51%. Calcd. for $C_{29}H_{36}O_5N_2 \cdot 1/4H_2O$: C, 70.07; H, 7.40; N, 5.64%. ^{1}H-NMR ($CDCl_3$) δ : 1.23 (3 H, s, $\mathbf{CH_3}$-C-CH_3), 1.27 (3 H, s, CH_3-C-$\mathbf{CH_3}$), 0.8～1.9 (16 H, m, -CH_2-), 2.33 (2 H, t, -CH_2-C=O), 3.14 (2 H, t, -CH_2-N), 5.85 (1 H, d, CH=C), 6.5～7.3 (6 H, m, CH=C and ArH), 7.9～8.1 (2 H, m, ArH). IR (KBr) 2930, 1700, 1500, 1330, 1270 cm^{-1}.

1'-(N-Propylcarbamoyldecanyl)-3',3'-dimethyl-6-nitrospiro[2H-1-benzopyran-2,2'-indoline] (SP10).

Spiropyrancarboxylic acid (CDN) (1.48g; 3.0 mmol) was condensed with a slight excess of propylamine (0.195g; 3.3 mmol) in dichloromethane (30 ml) with the aid of dicyclohexylcarbodiimide (DCC) (0.681 g; 3.3 mmol) to give pale-yellow crystals (0.40 g; 25 %) of mp = 97-98 ℃, which were recrystallized repeatedly from ethanol. Found: C, 71.05; H, 8.38; N, 7.73%. Calcd. for $C_{32}H_{43}O_4N_3 \cdot 1/2H_2O$: C, 70.82; H, 8.17; N, 7.74%. ^{1}H-NMR ($CDCl_3$) δ : 0.8～1.0 (3H, t, $HNCH_2CH_2\mathbf{CH_3}$), 1.23 (3 H, s, CH_3-C-$\mathbf{CH_3}$), 1.27 (3 H, s, $\mathbf{CH_3}$-C-CH_3), 0.8～1.9 (18H, m, -CH_2- and $NHCH_2\mathbf{CH_2}CH_3$), 2.18 (2H, t, -CH_2-C=O), 3.0～3.4 (4H, m, -CH_2-N and $NH\mathbf{CH_2}CH_2CH_3$), 5.85 (1H, d, CH=C), 6.5～7.3 (6H, m, CH=C and ArH), 7.9～8.1 (2H, m, ArH). IR (KBr) 2920, 1650, 1510, 1340, 1275 cm^{-1}.

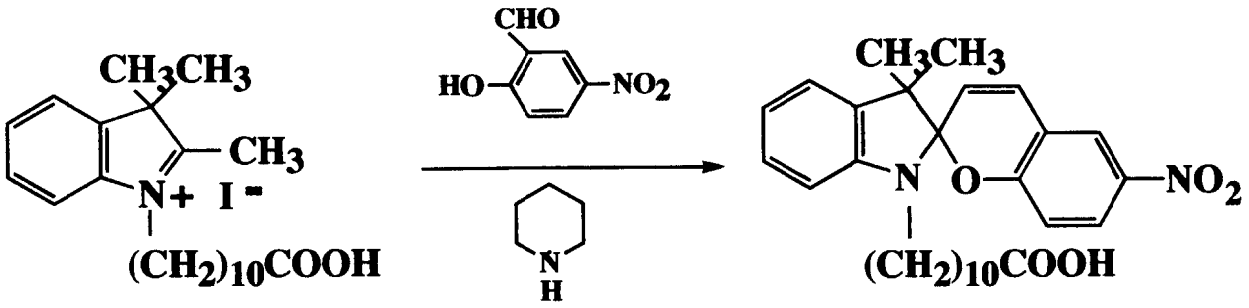

CDN

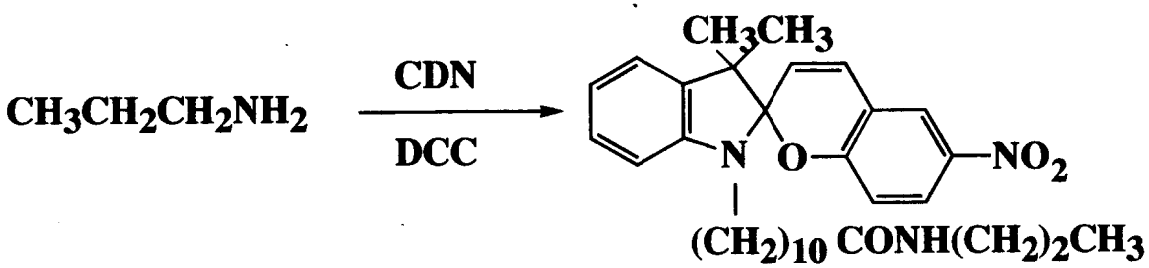

SP10

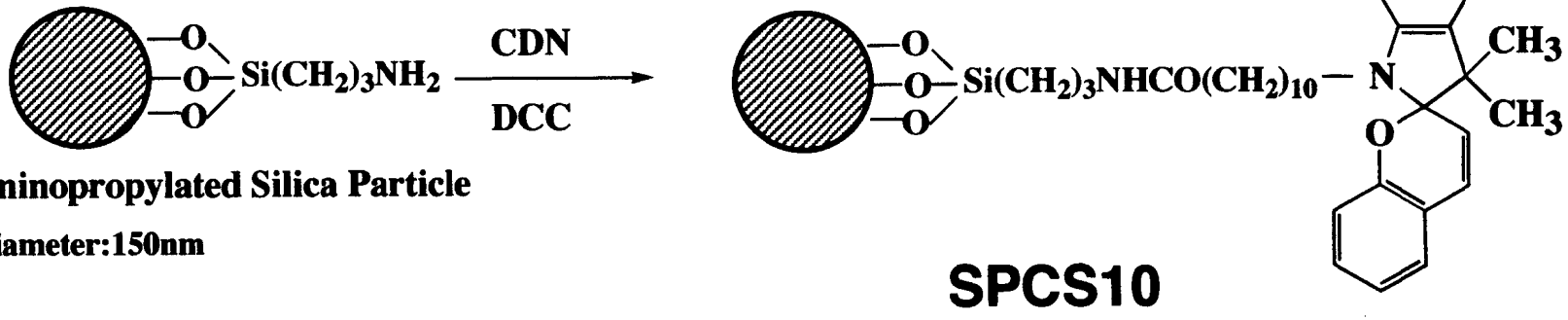

Aminopropylated Silica Particle

diameter:150nm

SPCS10

Figure 4-2 Synthetic pathways of SP10 and SPCS10

Surface Modification of Colloidal Silica

Aminopropylated silica particles were prepared by the reaction of 3-aminopropyltriethoxysilane with colloidal silica after the method of Hörner and Ziegler.[3] To a suspension of the aminated particles (0.50 g) in dichloromethane (15 ml) was added 0.246 g (0.50 mmol) of the spiropyrancarboxylic acid (CDN) and 0.124 g (0.60 mmol) of DCC, and the suspension was stirred at 5 ℃ for 6 h, followed by stirring overnight at room temperature. After centrifugation of the mixture, the supernatant was discarded. Residual silica particles (SPCS10) were washed repeatedly with methanol and tetrahydrofuran by the centrifugation-decantation cycles and dried finally at 60 ℃ *in vacuo* for 10 h. The amount of the chemisorbed SP was determined by measuring electronic absorption spectra of the particles dispersed in chloroform, which shows good refractive index matching with the silica.

Photoirradiation

The photochromic experiments were carried out by irradiation with 365 and 552 nm light at room temperature using a Jasco CRM-FA irradiator (2 kW xenon arc lamp with a monochromator). Absorption spectra were taken on a diode-array spectrometer (Hewlett-Packard HP8452A).

Sedimentation Measurement

SPCS10 (200 mg) was dispersed in 100 ml of carbon tetrachloride, cyclohexane and chloroform, respectively. Each dispersion (4 ml) was put in a cell (10 mm × 10 mm × 50 mm) and exposed to 365 nm light. The colored dispersion was shaken and then moved to a cell holder placed in the spectrometer and allowed to stand at room temperature. The cell was exposed to a probe light through a circular window of a diameter of 7 mm, which was set on a cell wall 15 mm from the bottom of the cell, to measure the absorbance at the isosbestic point (346 nm) during the sedimentation.

Physical Measurements

Scanning electron microscopy photographs were taken with a JEOL JSM-6400F, and particle size distributions were measured in ether by a dynamic light-scattering method with a laser particle analyzer (Otsuka electronics LPA-3000).

RESULTS

Surface Photochromism

A spiropyran (SP) derivative having a triethoxysilyl residue was required the dry-heat treatment for attachment to the silica surface [4], which may induce irreversible aggregation of colloidal silica. Therefore, the surface modification involves two steps in the present work: aminopropylation and subsequent chemical modification with SP bearing a carboxy group (CDN) under milder reaction conditions (Figure 4-2). The author employed monodisperse silica particles of diameter 150 nm, which is quite small, so that rapid sedimentation is prevented, although centrifugal separation is readily achieved to isolate surface-modified particles.

In order to obtain a transparent dispersion, ethylene glycol (n = 1.432), chloroform (n = 1.443), carbon tetrachloride (n = 1.457) and cyclohexane (n = 1.426) meet the requirement for refractive index matching with silica (n = *ca.* 1.45) and are convenient for following the photochromic reaction of the modified particles spectroscopically. The average density was estimated to be one SP molecule per 160 $Å^2$ area of the colloidal silica surface, from BET measurements and an absorbance of SP for a dispersion in chloroform at 343 nm under the assumption that the molar absorption coefficient $\varepsilon = 11000\ mol^{-1}cm^{-1}$ is not affected by the surface binding.

The photochromic behavior of SP-modified particles (SPCS10) was very dependent on the nature of the solvent. Figure 4-3 shows the change in absorption spectra of a model spiropyran (SP10) and SPCS10 in ethylene glycol during 365 nm light irradiation. In the case of SP10 (Figure 4-3(a)), the stable form in the dark is the merocyanine (MC) form; this was bleached upon irradiation with 365 nm light, showing reversed photochromism,[5] the MC form with a highly polar character being more

thermally stable than the ring-closed SP form in polar solvents. In contrast, SP bound on the colloidal surface shows the normal photochromism in ethylene glycol (Figure 4-3(b)). Furthermore, λ_{max} for the MC form on the surface is shifted *ca.* 30 nm to longer wavelength compared with that of SP10.

Irradiation of SPCS10 in carbon tetrachloride with UV light showed a spectral change quite different from that of SP10 (Figure 4-4). As shown in Figure 4-4(a), there are two peaks, at 570 and 608 nm, for SP10 due to MC aggregation, while purple-colored SPCS10 after UV irradiation possesses a single peak at 570 nm (Figure 4-4(b)). The same behavior was observed in cyclohexane. In chloroform, a single absorption band in the visible region appeared for both SPCS10 and SP10 at 573 nm and 580 nm, respectively, indicating normal photochromism without formation of any MC aggregate.

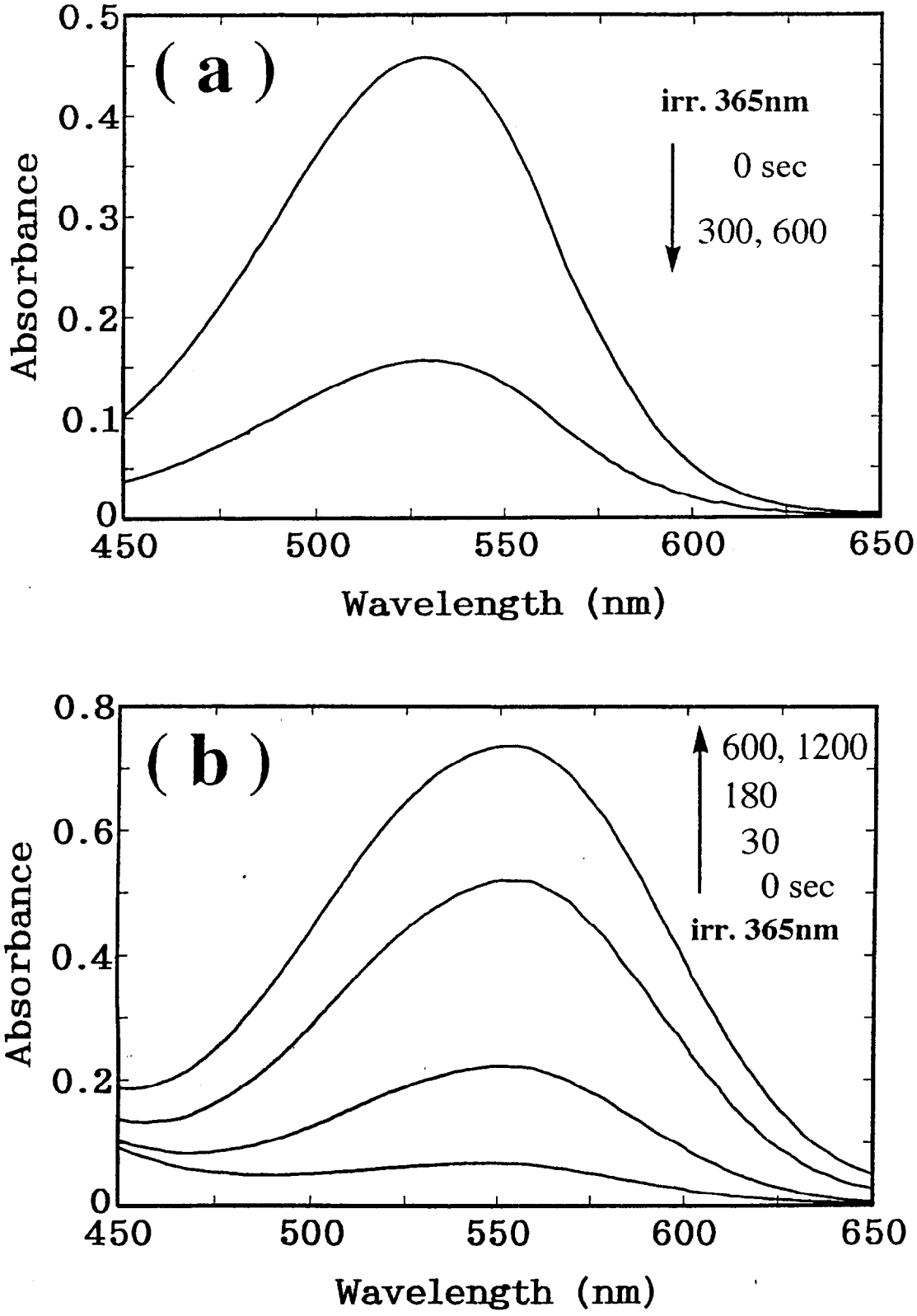

Figure 4-3 Absorption spectral change upon irradiation with 365 nm light at room temperature of: (a) a solution of SP10 (5.0×10^{-5} mol/L), (b) a dispersion of SPCS10 (1.0 g/L) in ethylene glycol.

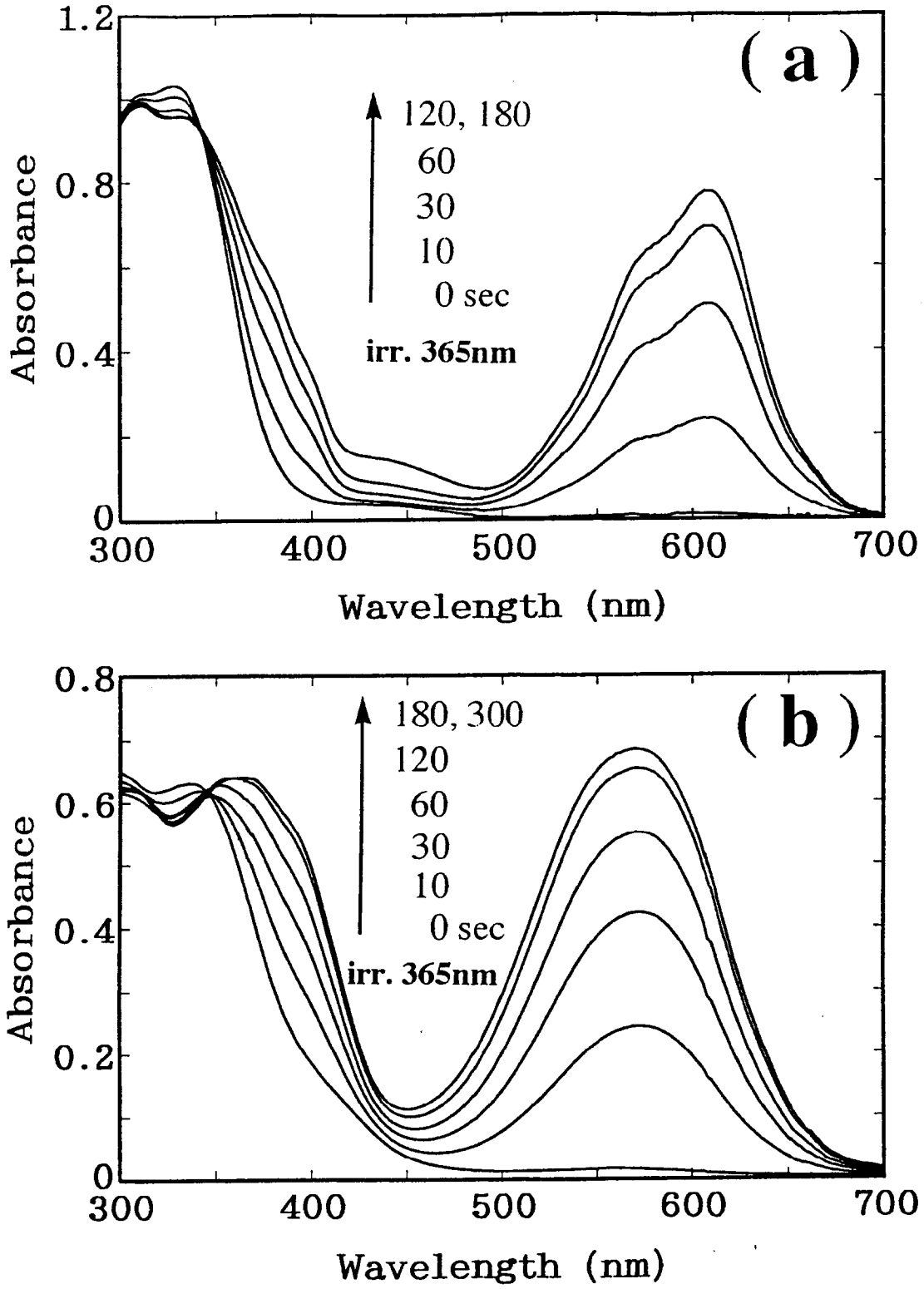

Figure 4-4 Absorption spectral change upon irradiation with 365 nm light at room temperature of: (a) a solution of SP10 (5.0×10^{-5} mol/L), (b) a dispersion of SPCS10 (1.0 g/L) in carbon tetrachloride.

Reversible Photoaggregation of Silica Particles

As shown in Figure 4-5, sedimentation of purple particles was observed, when a dispersion of SPCS10 in carbon tetrachloride was exposed to UV light and subsequently kept standing at room temperature. After sedimentation was complete, the sample was irradiated with 552 nm light under sonication to reverse the MC form to the pale-yellow SP form. A homogeneous dispersion was obtained again thereby displaying reversible alternation between dispersed and aggregated states of silica particles.

Figure 4-5 also shows that the volume of the precipitate reduces by approximately half after prolonged standing in the dark, accompanied by partial bleaching of the MC color. This implies that the colored precipitate has a highly porous structure due to the flocculation of the MC particles, which is then converted into the more compressed SP form having reduced particle interactions. This was confirmed by scanning electron microscopy of samples prepared by evaporating a solvent of the dispersion before and after UV irradiation. As shown in Figure 4-6, after UV irradiation the particles form highly porous aggregates.

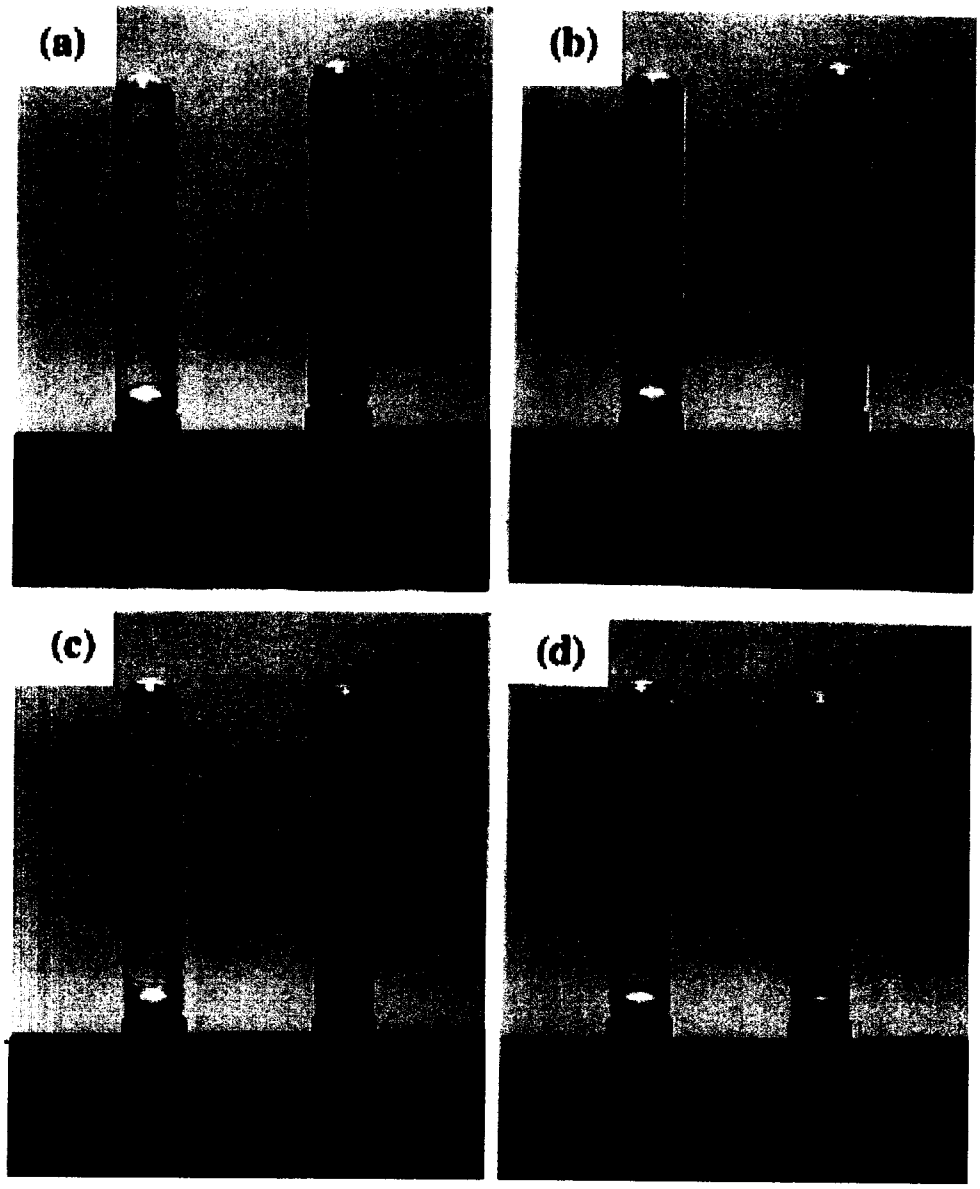

Figure 4-5 Pictures of SPCS10 dispersed in carbon tetrachloride (concentration: 1.0 g/L) in microtubes (inner diameter, 6 mm; length, 50 mm): (a) 0 min standing, (b) 5 min standing, (c) 1 h standing, (d) 12 h standing. Right (left) tube is the dispersion with (without) UV irradiation, respectively.

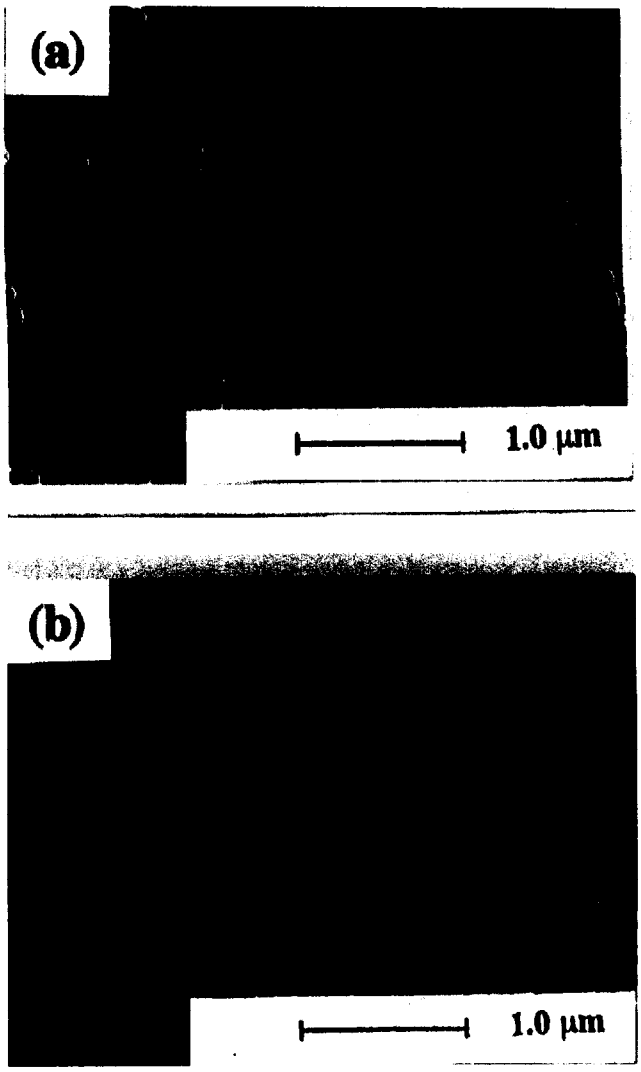

Figure 4-6 Scanning electron micrographs of the SP-modified colloidal silica: (a) before and (b) after UV-irradiation.

The author attempted to measure the particle size distribution by means of dynamic light-scattering to evaluate the dispersibility of the original particles and to follow the dynamic process of the aggregation of UV-exposed particles. Measurements for the dispersion in carbon tetrachloride were unsuccessful owing to very weak light scattering due to good index matching. Thus, the size distribution was measured in a diluted dispersion in ether with a lower refractive index, and the results are shown in Figure 4-7. The size distribution is centered at *ca.* 700~800 nm, indicating that the particles are not monodispersed in the solvent, resulting in aggregation. In fact, a concentrated dispersion in this solvent was strongly opaque, reflecting the formation of larger aggregated substances. Exposure of the ether dispersion to UV light brings about a shift in the distribution so that there appear much larger particles centered at *ca.* 24000 nm, confirming the photoinduced enhancement of the particle aggregation. However, this technique is not appropriate for evaluating photoinduced aggregation behavior quantitatively since the sedimentation of UV-exposed particles took place in ether during the light scattering measurements.

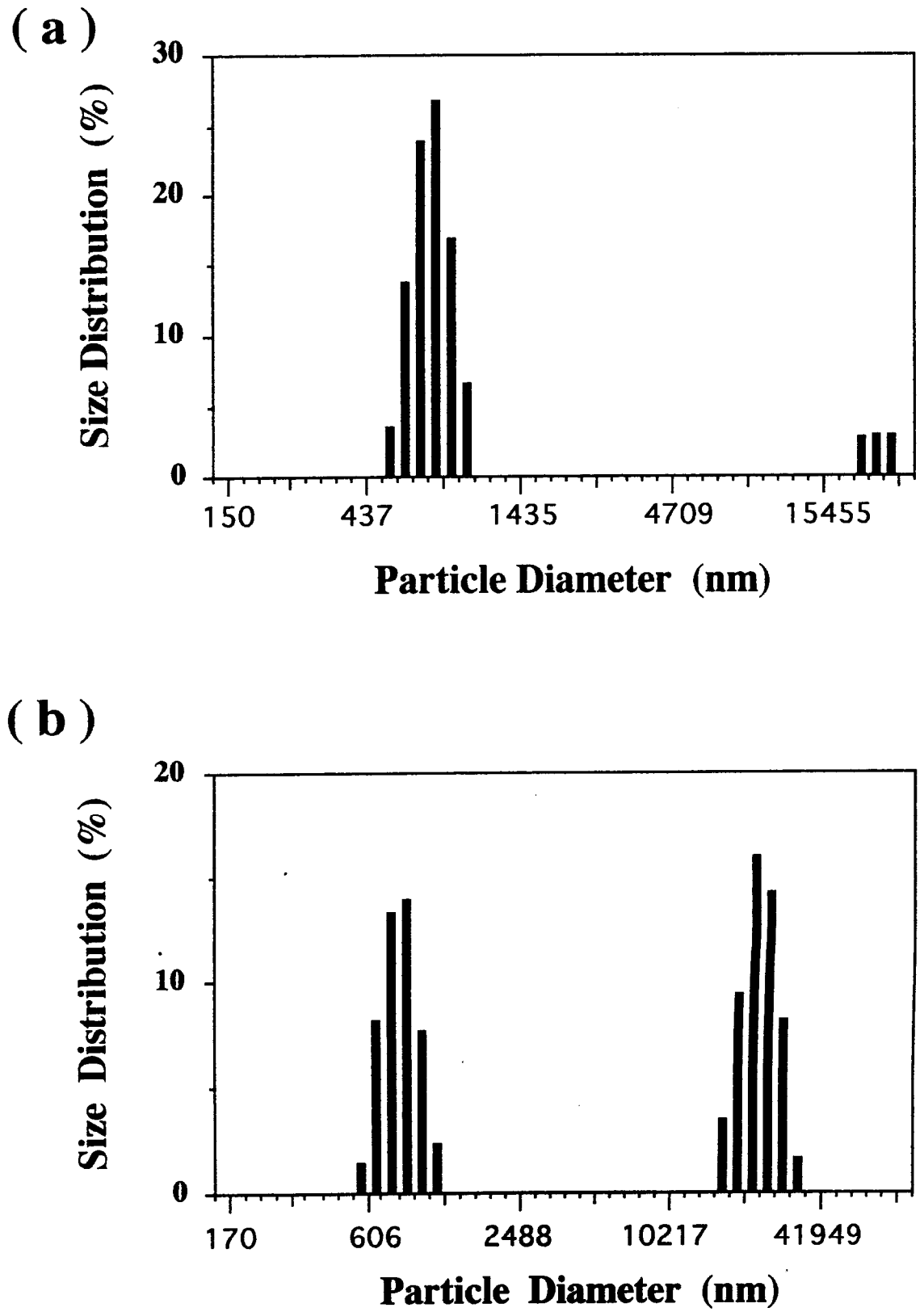

Figure 4-7 Particle size distributions of the SP-modified colloidal silica dispersed in ether (1.0×10^{-2} g/L): (a) before and (b) after UV irradiation.

Photochemically Enhanced Sedimentation

The sedimentation of SPCS10 particles was monitored by following the decrease in absorbance at an isosbestic point appearing during the photochromic reaction. A monitoring light beam was passed through a cell (*ca.* one-third of the way up) filled with the dispersion. Figure 4-8 shows the absorbance changes of the dispersions in non-polar solvents showing good refractive-index matching before and after UV irradiation.

In carbon tetrachloride, the rate of sedimentation is markedly enhanced by UV irradiation (Figure 4-8(a)), confirming the result shown in Figure 4-5. Reversion of the MC form of the UV-exposed particles to the SP form with 552 nm light under sonication regenerated a pale-yellow dispersion which had a sedimentation rate similar to that of the original dispersion, implying that dispersion and precipitation are interchangeable by means of the surface photochromic reaction.

Different behavior was observed for dispersions in cyclohexane and chloroform. As seen in Figure 4-8(b), SPCS10 particles show relatively rapid sedimentation in cyclohexane during the early stages of standing. In contrast, when they are dispersed in chloroform, the dispersion stability increases remarkably, and even UV photoirradiation did not affect sedimentation (Figure 4-8(c)).

The effect of lecithin, a naturally occurring amphiphilic compound, was also examined. Three types of SPCS10 dispersion in carbon tetrachloride were prepared by dissolving lecithin so that the molar ratios of SP : lecithin were 100 : 1, 1 : 1 and 1 : 100. It was found that after UV irradiation purple dispersions were dramatically stabilized when more than an equimolar amount of lecithin was added to the dispersion, and no colored precipitation occurred even on prolonged standing. This lecithin effect was also observed for dispersion in cyclohexane.

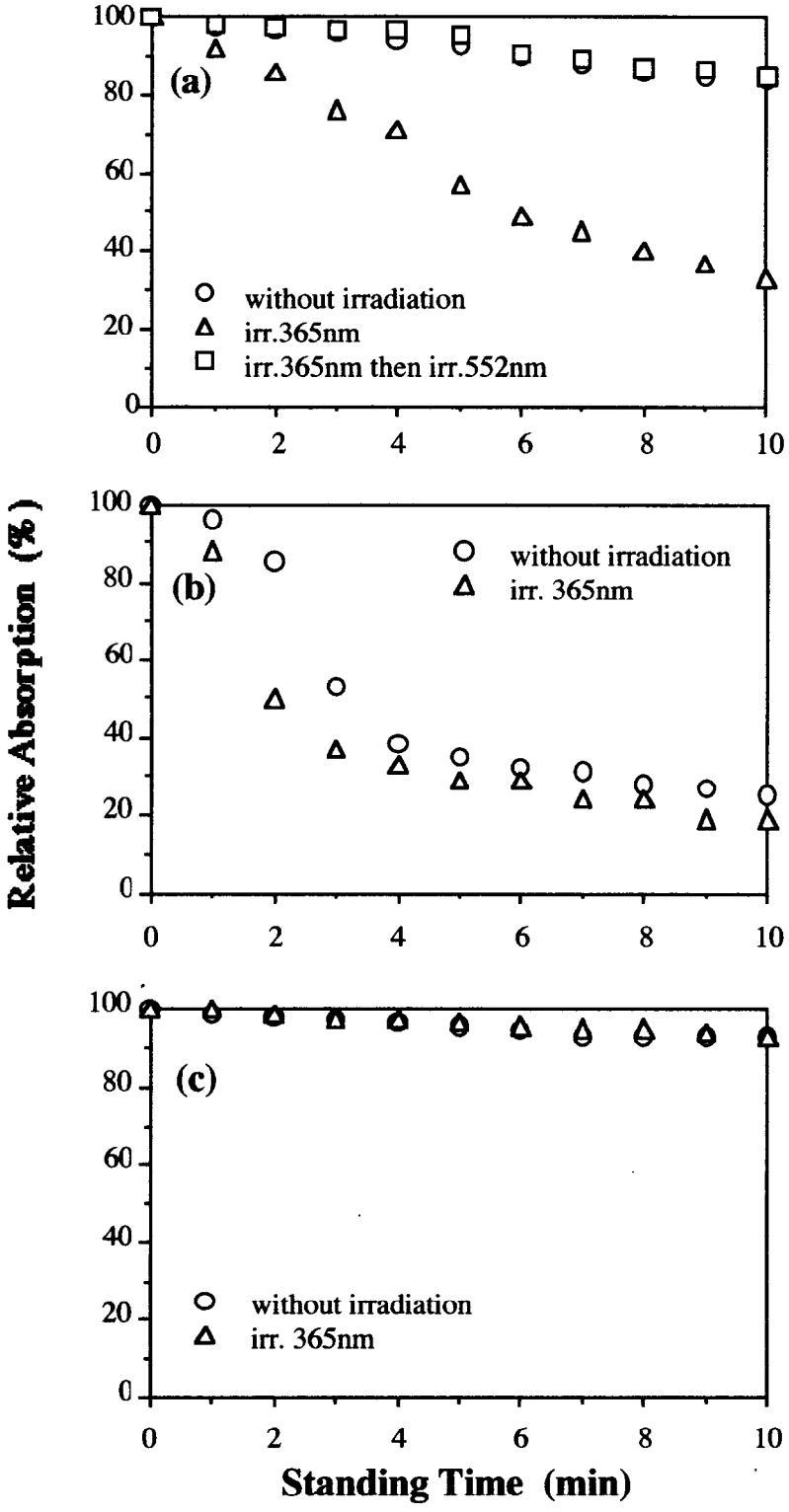

Figure 4-8 Sedimentation behavior of SPCS10 at room temperature; (a) in carbon tetrachloride, (b) in cyclohexane, (c) in chloroform.

DISCUSSION

SP is converted from the stable colorless form to a metastable colored zwitterionic MC form upon UV irradiation, which is then reversed to SP upon visible light irradiation or thermal treatment (Figure 4-1). The absorption maximum of MC is so sensitive to the nature of the medium that this kind of solvatochromism[6] can provide information on the microenvironmental polarity. According to Flannery,[7] in polar solvents a complex probably forms between the zwitterion and solvent molecules, and this complex formation stabilizes the colored form; this is in contrast with non-polar environments.[7] This suggests that the SP moiety on the silica surface is surrounded by a less polar microenvironment, possibly due to the hydrophobic decamethylene spacer chains, and the complex formation of MC units with polar solvent molecules seems to be inhibited in the present system possibly because SP units are not exposed directly to the ethylene glycol phase. This is in marked contrast to the observations that a nitrospirobenzopyran (6-nitro BIPS) displays reverse photochromism when the compound is physically adsorbed on silica gel[5] in cyclohexane, and that some spiropyrans incorporated in silica glasses prepared by the sol-gel method show the reverse photochromism.[8] The surface photochromism of SPCS10 indicates that the highly polar silica surfaces were rendered relatively hydrophobic as a result of the chemical modification.

Photogenerated MCs have been reported to form molecular aggregates comprised of SP and MC forms in non-polar solvents.[9-12] According to Krongauz *et al.*, a 1:1 dimer of SP and the corresponding merocyanine exhibits a λ_{max} of 515 nm, whereas the 2 : 1 or 3 : 1 oligomers have a λ_{max} of 610 nm in methylcyclohexane.[11] Hence, the absorption band at the longer wavelength of photoirradiated SP10 can be ascribed to the blue aggregates consisting of an oligomer [(SP)n(MC)] whereas the shorter wavelength absorption band at 570 nm is assignable to monomeric MC.[12] The exclusive appearance of the absorption band due to a monomeric MC in SPCS10 is quite reasonable since the average distance between the photochromic units is 12.6 Å, too large to form stable molecular aggregates. The fact that there is no blue-shifted absorption band of MC due to the molecular aggregation in Figure 4-4(b) implies that there is no intimate molecular interaction of MCs among

colloidal particles.

The sedimentation rate (υ) of spherical particles of a diameter D is expressed as the Stokes equation:

$$\upsilon = \frac{(\rho - \rho_0)gD^2}{18\eta}$$

where ρ and ρ_0 are the densities of the particle and a solvent with a viscosity η, respectively, and g is gravitational acceleration. Although the discussion is rather semiquantitative, owing to the lack of information concerning to the size and shape of particle aggregates at present, the considerably different behavior between carbon tetrachloride and chloroform can be ascribed to the difference in D, since the density of carbon tetrachloride (ρ_0= 1.584 g/cm^3 at 25 ℃) is rather greater than that of chloroform (ρ_0= 1.480 g/cm^3 at 25 ℃) so that the contribution of $\rho - \rho_0$ to the sedimentation is relatively small. In other words, the SPCS10 particles are aggregated in carbon tetrachloride to form larger secondary particles to enhance the sedimentation. It is very probable that the aggregation of particles in the non-polar solvent reflects that the surface covered with SP moieties is not sufficiently non-polar because the photochromic unit possesses a polar nitro substituent and two heteroatoms in the ring-closed molecular framework. Conversely, this kind of surface property may induce good solvation with chloroform to lead to a relatively stable dispersion. The stable dispersion of the UV-exposed particles in chloroform is also ascribable to the good solvation. The rapid sedimentation in cyclohexane (ρ_0= 0.774 g/cm^3 at 25 ℃) is brought about, on the contrary, at least partially as a result of the greater difference in density ($\rho - \rho_0$) when compared with that for carbon tetrachloride.

As stated above, the enhanced sedimentation of SPCS10 is ascribable to the drastic increase in the surface polarity owing to the conversion from SP to monomeric MC with zwitterionic character. Closely related work was reported on UV-induced precipitation of a polystyrene having spirobenzopyran derivatives as pendant groups in cyclohexane because of the decrease in the

polymer-solvent interaction by the generation of polar pendant groups.[13] UV irradiation induces the change in surface polarity, which causes abrupt reduction of the interaction between less polar SP units and non-polar solvent molecules to result in an attractive force between the silica particles.

As Figure 4-9 shows schematically, the ionic interaction of MC units on the surface consequently brings about flocculation and sedimentation. This mechanism is in line with the stabilizing effect of lecithin on the dispersibility. Amphiphilic lecithin molecules with zwitterionic character are adsorbed immediately on the MC-covered surface because of the ionic interaction to make the surface highly hydrophobic as shown in Figure 4-10. The specific role of lecithin has been demonstrated by the fact that the dispersion stabilization is achieved by addition of an equimolar amount of the amphiphile.

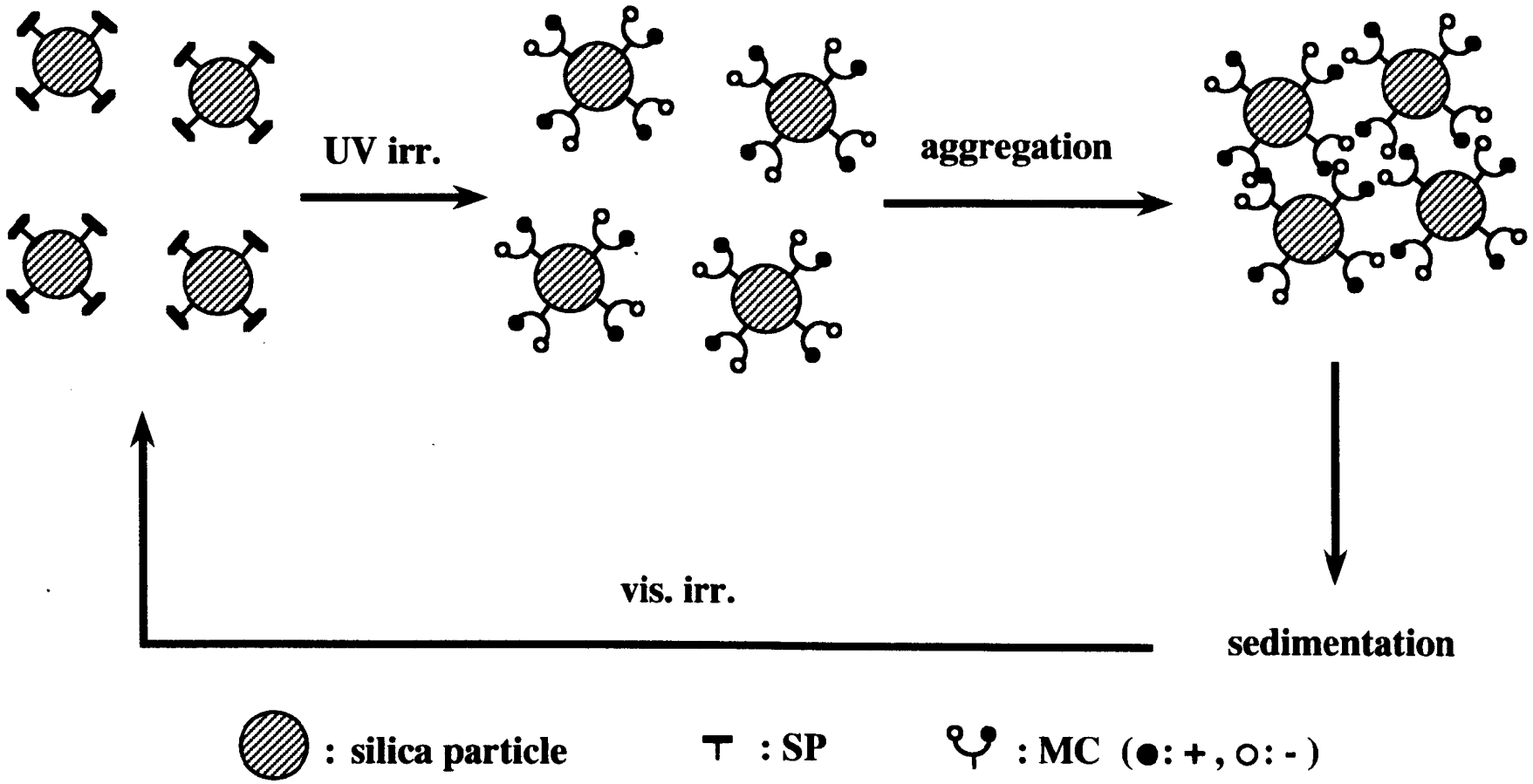

Figure 4-9 Representation of reversible sedimentation of colloidal silica particles covered with a photochromic spiropyran.

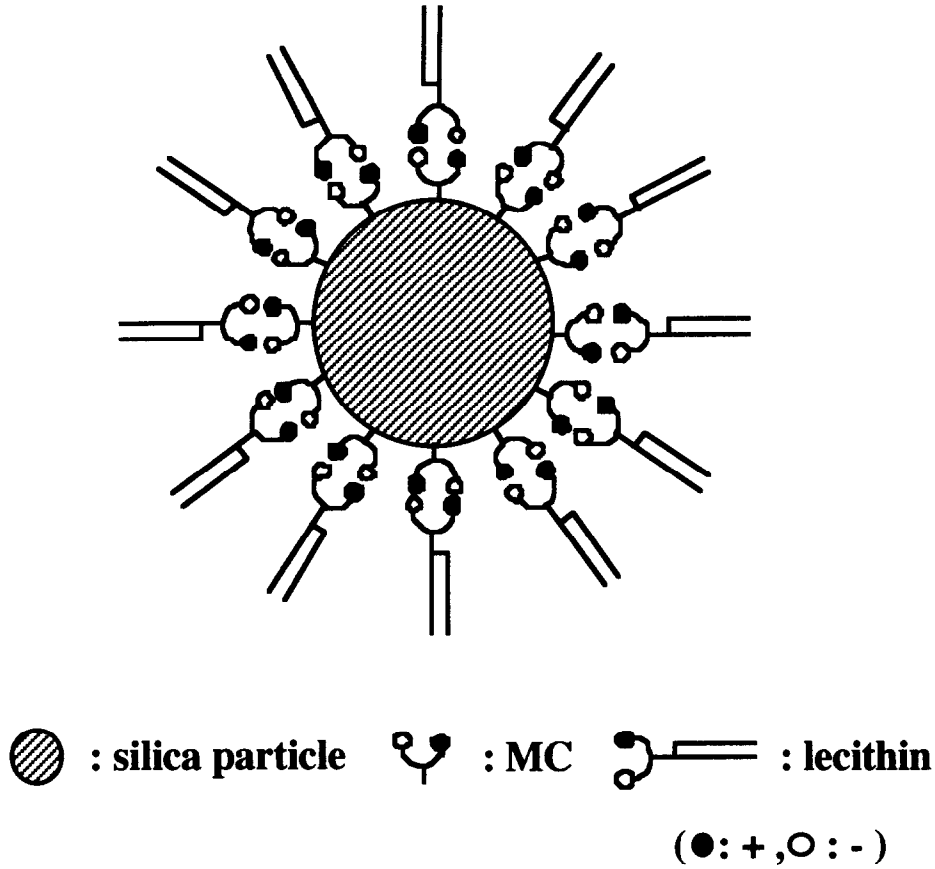

Figure 4-10 Representation of the effect of addition of lecithin.

SUMMARY

An SP moiety bound on the surface of colloidal silica demonstrates the normal photochromism which is, however, quite different from that in an ethylene glycol solution and in physically adsorbed states on silica surfaces or walls; in the latter, reversed photochromism is observed because of stabilization of the zwitterionic MC form located in a highly polar environment. This means that the microenvironmental polarity of the photochromic units is markedly reduced to improve the dispersibility of the surface-modified silica particles in non-polar solvents. Although aggregation

of the particles occurs to some extent, UV irradiation to convert SP into MC on the surface results in an increase in the size of the aggregates.

Reversible control of the modified colloidal silica between sedimentation and dispersion was induced unequivocally in carbon tetrachloride by alternate irradiation with UV and visible light to cause the surface photochromism. The photoinduced sedimentation is triggered by the decrease of the affinity between the particle surface and the non-polar solvents accompanied by the increase in its surface polarity, resulting in the aggregation of particles which cause the flocculation, leading to the colored precipitate with high porosity. Similarly to Chapter 3, the photochromic silica colloid provides a novel photoresponsive system in which photoinduced molecular structural alteration is converted into macroscopic dispersibility change.

REFERENCES

1) E. Fischer and J. Hirshberg, *J. Chem. Soc.*, 4522 (1952).

2)K. Namba and S. Suzuki, *Bull. Chem. Soc. Jpn.*, **48**, 1323 (1975).

3)L. Horner and H. Ziegler, *Z.'Naturforsch., Teil B*, **42**, 643 (1987).

4)K. Ichimura, Y. Hayashi, K. Goto and N. Ishizuki, *Thin Solid Films*, **235**, 101 (1993).

5)T. R. Evans, A. F. Toth and P. A. Leermakers, *J. Am. Chem. Soc.*, **89**, 5060 (1967).

6)R. C. Bertelson, in *Photochromism*, Ed. G. H. Brown, Wiley, New York, 1971 p.45.

7)J. B. Flannery, *J. Am. Chem. Soc.*, **90**, 5660 (1968).

8)D. Levy and D. Avnir, *J. Phys. Chem.*, **92**, 4734 (1988).

9)V. A. Krongauz and A. A. Parshutkin, *Photochem. Photobio.*, **15**, 503 (1972).

10)V. A. Krongauz, S. N. Fishman and E. S. Goldburt, *J. Phys. Chem.*, **82**, 2469 (1978).

11)V. A. Krongauz and E. S. Goldburt, *Nature (London)* , **271**, 43 (1978).

12)H. Sato, H. Shinohara, M. Kobayashi and T. Kiyokawa, *Chem. Lett.*, 1205 (1991).

13)M. Irie, T. Iwayanagi and Y. Taniguchi, *Macromolecules*, **18**, 2418 (1985).

Chapter 5

Photochromic Behavior of a Spirobenzopyran Chemisorbed on a Colloidal Silica Surface

INTRODUCTION

In Chapter 4, the author demonstrated that the dispersibility of colloidal silica particles in non-polar solvents can be controlled by surface chemisorption with a photochromic spirobenzopyran (SP) having a decamethylene spacer. The surface photochromism leads to a reversible change between aggregation and dispersion of colloidal silica owing to modification of the affinity of the particle surface for non-polar solvent molecules as a result of an increase in its surface polarity.

Apart from the photofunctinalization of materials based on a photoinduced polarity change,[1] a photochromic SP is often employed as an indicator for the estimation of microenvironmental factors[2] such as polarity, viscosity and the free volume of polymers, based on the following two reasons.[3,4] First, the zwitterionic MC is characterized by a negative solvatochromism which results in a considerable shift of the absorption wavelength in the visible region. The thermal MC→SP isomerization rate is also solvent dependent. These facts provide us with useful information concerning the microenvironmental polarity of MC-located sites. Secondly, the MC→SP thermal isomerization rate is also very sensitive to environmental steric effects. The photoisomerization from SP to MC involves scission of the C-O pyran bond to form a *cis*-MC, followed by geometrical isomerization leading to the zwitterionic *trans*-isomer with a coplanar structure.[5] This large change in molecular shape must be highly susceptible to steric constraints of surrounding matrices.[2, 6, 7] In view of these properties, the photochromic behavior of an SP chemisorbed on a silica surface can act as an effective photoprobe to reveal the characteristics of inorganic surfaces.

In this Chapter, the thermal reverse isomerization kinetics of SP attached to a silica surface through two different methylene spacers (SPCS2 and SPCS10 in Figure 5-1) were studied and

compared with those of their model compounds (SP2 and SP10 in Figure 5-1) in various solvents in order to elucidate the surface environment. The photoinduced control of the dispersibility of the SP-modified colloidal silica will be also discussed.

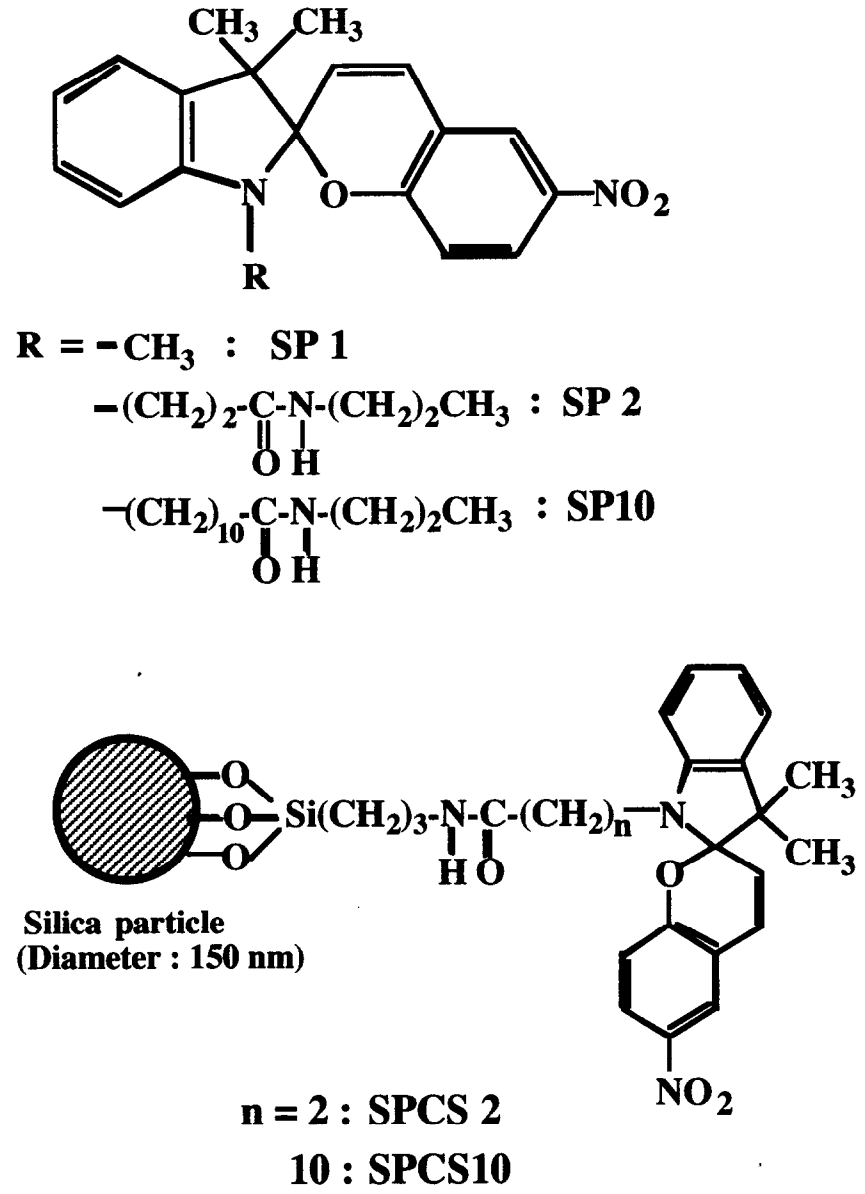

Figure 5-1 Chemical structures of spiropyranes and surface modified colloidal silica

EXPERIMENTAL

Materials

Silica particles

Monodispersed silica particles were a gift from Tokuyama Corp., having a diameter= 150 nm and BET surface area= 48 m^2g^{-1}.

Spirobenzopyrans (SP1, SP2 and SP10)

1',3',3'-Trimethyl-6-nirobenzo[2*H*-1-benzopyran-2,2'-indoline] (SP1) was purchased from Tokyo Kasei Corp. and recrystallized repeatedly from ethanol. 1'-(*N*-Propylcarbamoyldecyl)-3',3'-dimethyl-6-nitrospiro[2*H*-1-benzopyran-2,2'-indoline] (SP10) was prepared by reaction of the corresponding spiropyrancarboxylic acid with *n*-propylamine with the aid of dicyclohexylcarbodiimide (DCC) as described in Chapter 4. 1'-(*N*-Propylcarbamoylethyl)-3',3'-dimethyl-6-nitrospiro[2*H*-1-benzopyran-2,2'-indoline] (SP2) was synthesized in a similar manner. The product was purified by repeated recrystallization from an ethanol-water mixture, mp 149-150 ℃. Anal. Calcd. for $C_{23}H_{27}N_3O_4$: C, 67.46; H, 6.65; N, 10.26 %. Found: C, 67.68; H, 6.58; N, 10.11 %. ^{1}H-NMR ($CDCl_3$) δ :0.85 (3 H, t, -NHCH$_2$CH$_2$C**H**$_3$), 1.15 (3 H, s, CH$_3$-C-C**H**$_3$), 1.27 (3 H, s, C**H**$_3$-C-CH$_3$), 1.3-1.6 (2 H, m, -NHCH$_2$C**H**$_2$CH$_3$), 2.2-2.7 (2 H, m, NCH$_2$C**H**$_2$C=O), 3.0-3.3 (2 H, m, -NHC**H**$_2$CH$_2$CH$_3$), 3.3-3.9 (2 H, m, NC**H**$_2$CH$_2$C=O), 5.3-5.6 (1 H, br., N**H**CH$_2$CH$_2$CH$_3$), 5.85 (1 H, d, CH=C), 6.6-7.4 (6 H, m, CH=C and ArH), 7.9-8.1 (2 H, m, ArH). IR (KBr) 2970, 1640, 1480, 1340, 1275 cm^{-1}.

Photochromic Silica Particles (SPCS2 and SPCS10)

Chemisorption of SP on colloidal silica was performed by the reaction of aminopropylated silica particles with SP bearing a carboxyl group ((CH$_2$)$_n$COOH: n= 2, 10) at the indole nitrogen atom in the presence of DCC as described in Chapter 4. The aminopropylated silica particles were prepared by the reaction of 3-aminopropyltriethoxysilane with colloidal silica.[8] For both SPCS2 and SPCS10, the average density of chemisorbed SP was estimated to be one SP molecule per 1.60 nm^2 area of the silica

surface, from BET measurements and UV-VIS spectroscopy. The amount of SP absorbed on the silica was measured by dispersing the colloidal silica in chloroform, which shows good refractive index matching with the particles.

Kinetic Measurements

In order to monitor the photochromic reaction of the modified silica particles spectroscopically, SPCS2 and SPCS10 were dispersed in ethylene glycol (n = 1.432), chloroform (n = 1.443), carbon tetrachloride (n = 1.457) and cyclohexane (n = 1.426), respectively. These solvents meet the requirement for refractive-index matching with silica (n ≒ 1.45) to give a transparent dispersion. The kinetics of the thermal MC→SP decoloration were determined using a diode-array UV-VIS spectrometer (Hewlett-Packard HP8452A) by monitoring changes in absorbance at the visible absorption maximum (λ_{max}) immediately after sufficient UV irradiation with 365 nm light using a Jasco CRM-FA irradiator (2kW xenon arc lamp with a monochromator). All measurements of the thermal MC→SP isomerization were carried out in the dark at 20 ℃. Thermodynamic constants (Ke) for the equilibrium between the colorless SP form and the colored MC form, *i.e.*, Ke=[MC]/[SP], are required to determine the decoloration rate constants. Ke was estimated to be < 0.01 in the present systems by the use of a reported molar extinction coefficient, ε, for the MC form of SP1 in polar solvents ($\varepsilon = 3.5 \times 10^4$ dm^3 mol^{-1} cm^{-1}).[3] Under such conditions, the thermal decoloration rate constants could be directly estimated from the decrease in the absorbance at λ_{max} with sufficient accuracy.

RESULTS

Photochromism of Model Compounds

The thermal MC→SP decoloration rate is affected markedly by the polarity of the surrounding medium[3,4] and the photogenerated MC form shows strong solvatochromism. In this context, the solvent effect on both phenomena was confirmed for SP2 and SP10 as model compounds for surface SP on colloidal silica. The thermal bleaching rate for SP1, SP2 and SP10 in various solvents was fitted excellently by first-order kinetics.

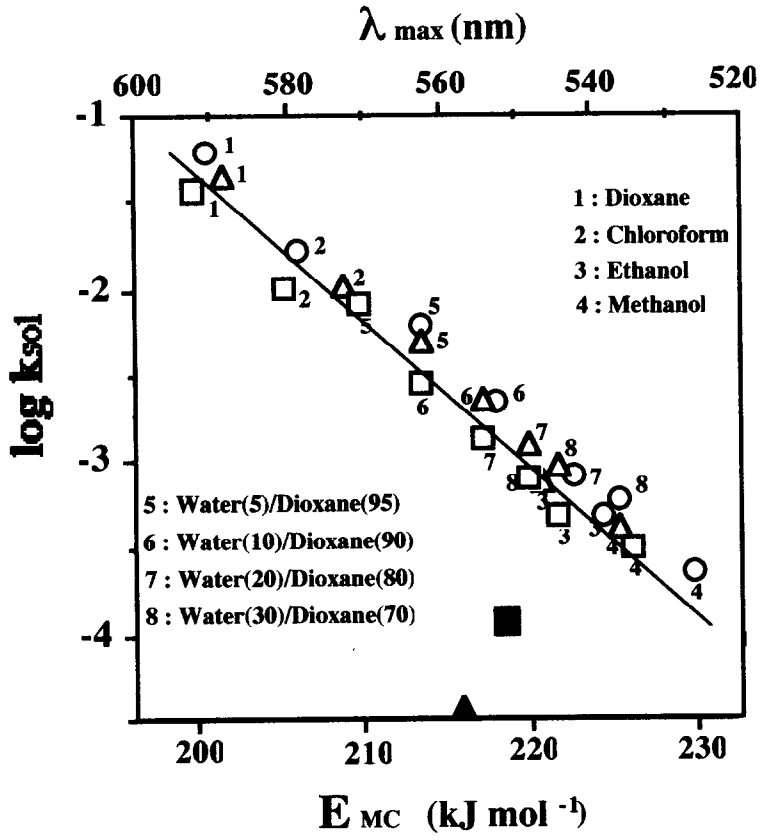

Figure 5-2 Logarithm of first-order decoloration rate constant at 20 ℃ *vs.* electronic transition energy in various solvents. (○) SP1; (△) SP2; (□) SP10; (▲) SPCS2 in ethylene glycol, (■) SPCS10 in ethylene glycol.

Figure 5-2 shows plots of the logarithm of the first-order rate constant (K_{sol}) *vs.* the electric transition energy of MC (E_{MC}). The slopes of the linear relationship between K_{sol} and E_{MC} for SP2 and SP10 are completely superimposable with that of SP1. This indicates that the amide group in the polymethylene spacers [-$(CH_2)_n$-; n=2 or 10] linked to the N position of SP has no influence on the photochromic behavior.

In ethylene glycol, the three spirobenzopyran derivatives (SP1, SP2 and SP10) showed reversed photochromism. In such a situation, as described in Chapter 4, the MC form is bleached upon irradiation with 365 nm light and is more stable than the SP form in the dark because the zwitterionic structure with a highly polar character forms a complex with the polar solvent molecules; this complex formation stabilizes the colored form.[3)]

Photochromism on a Colloidal Silica Surface

The photochromic silica particles (SPCS2 and SPCS10) showed normal photochromism in ethylene glycol in sharp contrast to the solution photochromism. The visible absorption maxima of photoformed MCs on the colloidal silica showed red-shifts up to *ca.* 30 nm when compared with those of the corresponding model compounds (SP2 and SP10). This implies that the SP moiety on the silica surface is situated in a relatively less polar microenvironment and that the complexation of MC units with the polar solvent molecules seem to be inhibited in the present system because the MC moieties are not directly exposed to the ethylene glycol phase.

Figure 5-3 shows the spectral changes of the photopumped MC of SPCS10 in the dark in ethylene glycol at 20 ℃. The visible absorption band corresponding to the MC diminished slowly with time with no change in the spectral shape. The fading reaction was well described by first-order kinetics, as shown in Figure 5-4. SPCS2, with a shorter spacer connecting SP to the surface, gave a similar result. These facts suggest that the thermal decoloration of the MC units on the silica surface occurs homogeneously. In marked contrast to this, UV irradiation of SPCS10 in carbon tetrachloride showed a spectral change quite different from that of the model compound (SP10), as described in Chapter 4.

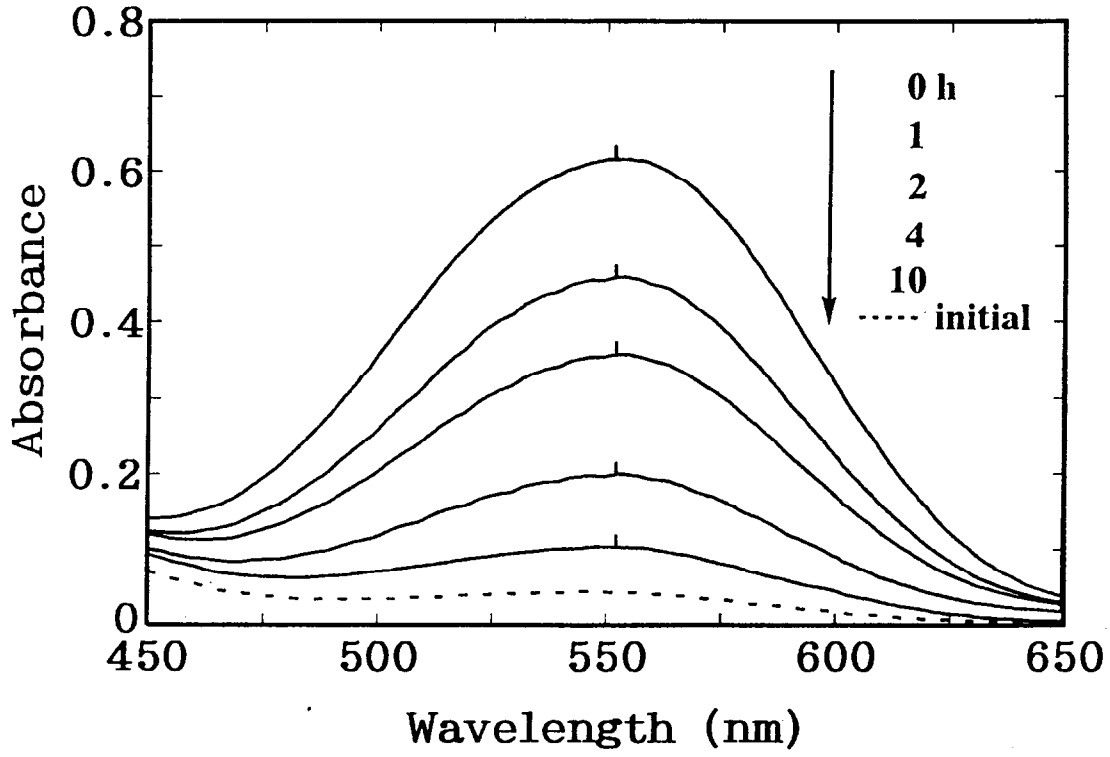

Figure 5-3 Change in absorption spectra of photoformed MC of SPCS10 in the dark in ethylene glycol at 20 ℃.

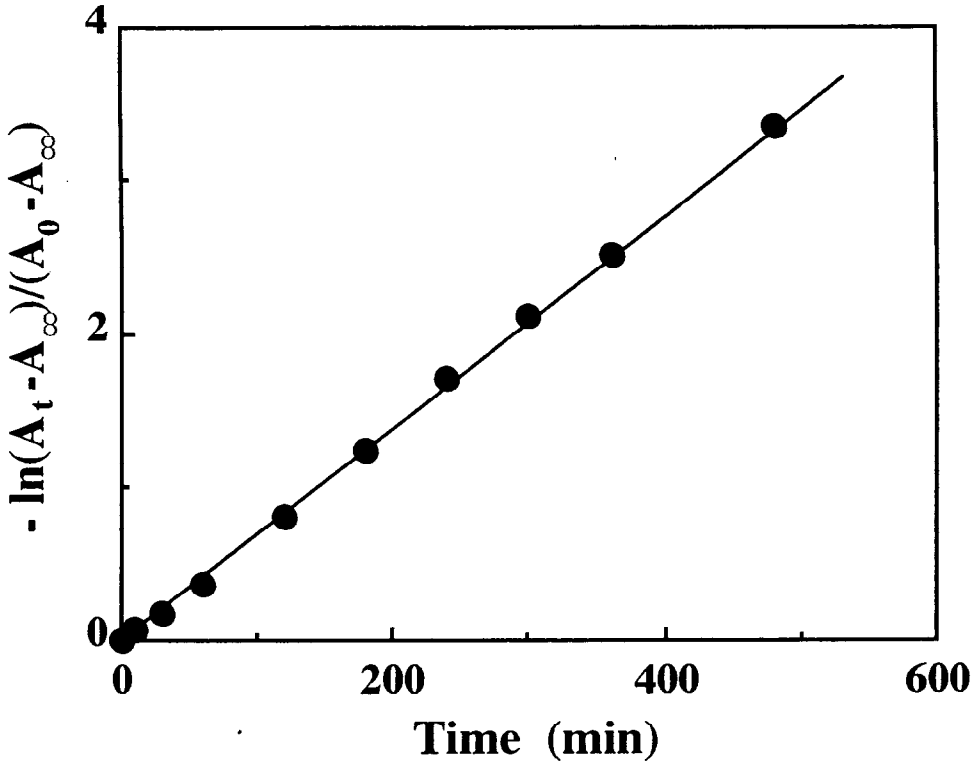

Figure 5-4 First-order plots for the thermal MC→SP isomerization of SPCS10 in ethylene glycol at 20 ℃. Solid line is the single first-order fit to the data.

For SP10, there were two peaks at 570 nm and 608 nm which were assigned to monomeric MC and SP-MC aggregation, respectively. On the other hand, purple silica particles (SPCS10) dispersed in the same solvent possessed a single absorption maximum at 570 nm. The same behavior was observed in cyclohexane. In the case of chloroform, a single absorption band was observed in the visible region for both the model compound in solution and the photochromic colloidal silica in a dispersion, indicating normal photochromism with no aggregation to form oligomers [(SP)n(MC), n=2 or 3] asserted by Krongauz *et al.*[9] SPCS2 and its model compound (SP2) also gave similar results.

On thermal bleaching of the photochromic silica particles, the spectral change observed in ethylene glycol was different from those in the non-polar solvents. Figure 5-5 shows the change in absorption spectra of the photoformed MC of SPCS10 in chloroform in the dark at 20 ℃. A blue shift of the absorption maximum from 573 nm to 554 nm occurred during the reverse isomerization of MC. Such a spectral shift during the bleaching was also observed in carbon tetrachloride and cyclohexane. A similar result was observed for SPCS2. The results are compiled in Table 5-I. The thermal decoloration process in the non-polar solvents did not obey first-order kinetics, in contrast to the case in ethylene glycol stated above.

Such a deviation from single first-order kinetics was observed frequently in glassy polymer matrices and can be explained in terms of treating the thermal decoloration as a dispersive first-order process.[10, 11] It has been demonstrated that the following equation holds over the entire observation time-frame for this dispersive process:

$$\log [-d (\ln A_t)/dt] = (\alpha - 1) \log t + \log \kappa$$

where α is defined as the dispersive parameter ($0 < \alpha < 1$) and κ is a constant. Figure 5-7 shows typical plots of log [-d (ln A_t)/dt] *vs.* log t for the thermal decoloration of SPCS10. No linear relationship was obtained.

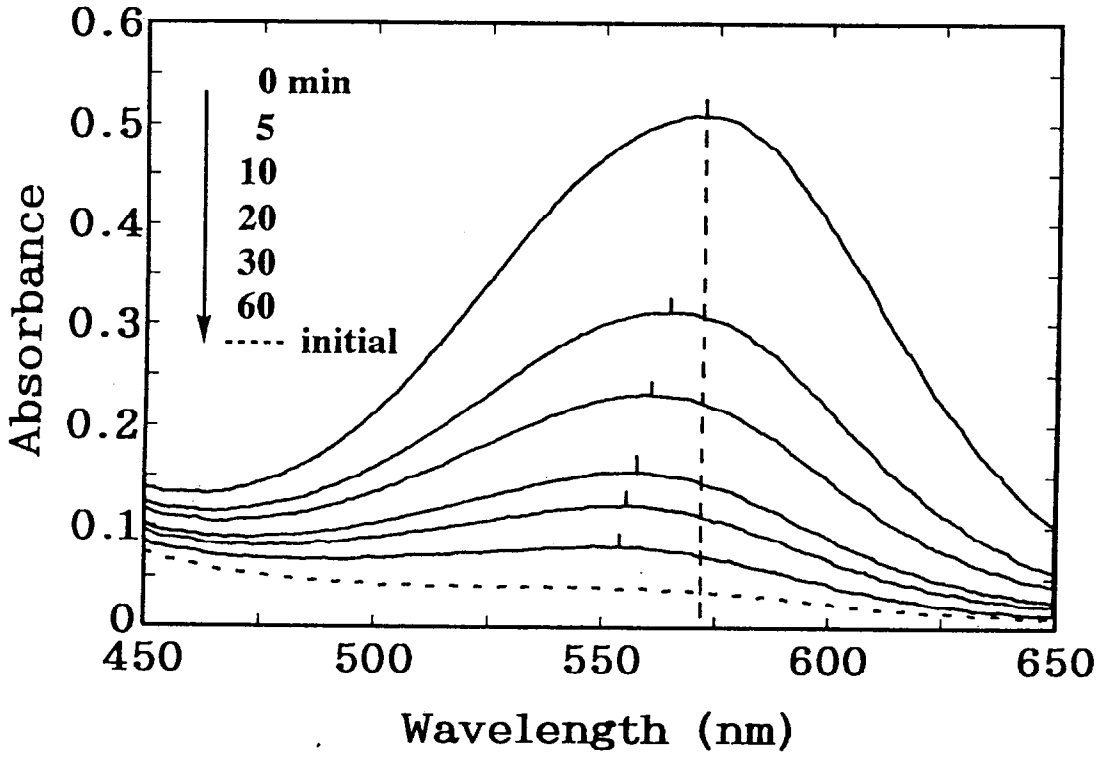

Figure 5-5 Change in absorption spectra of photoformed MC of SPCS10 in the dark in chloroform at 20 ℃.

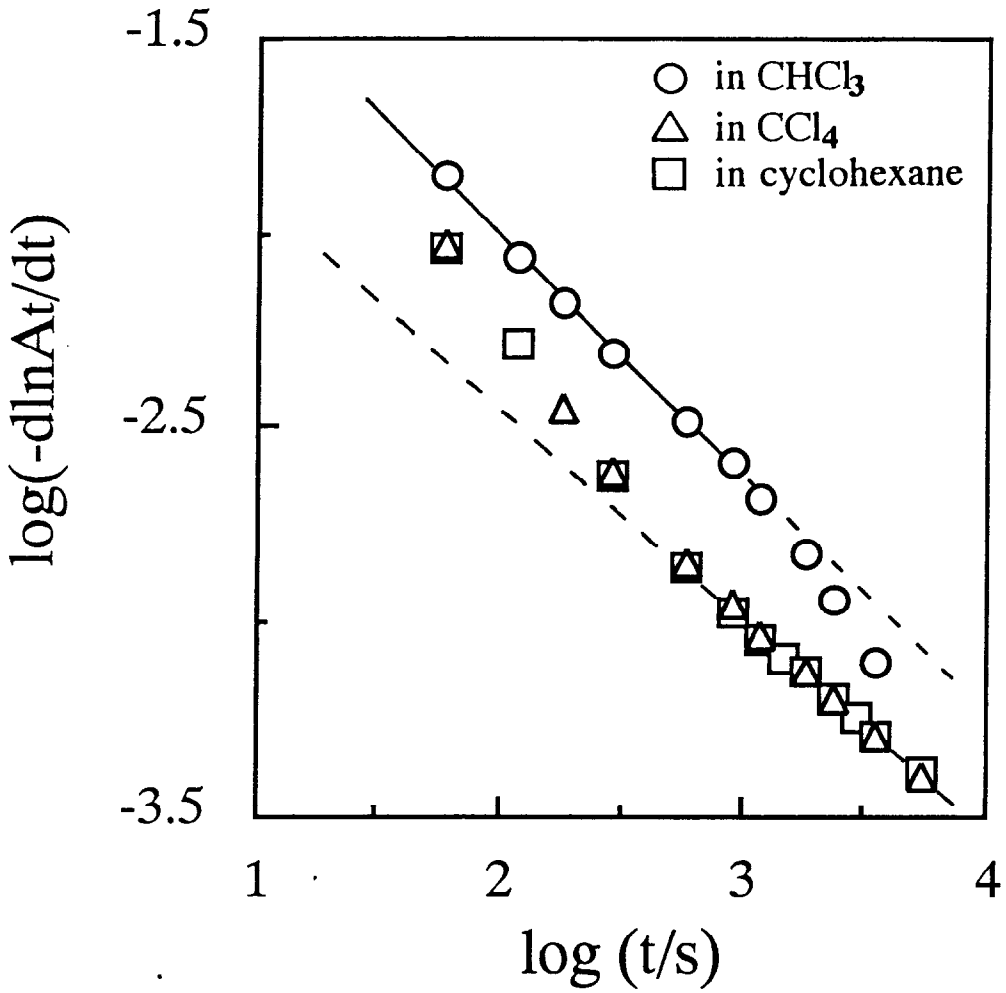

Figure 5-6 Dispersive process plots for the thermal MC→SP isomerization of SPCS10 in chloroform (○), carbon tetrachloride (△) and cyclohexane (□).

An alternative description of MC bleaching is the superposition of two first-order rate processes expressed by the following equation:

$$\frac{A_t - A_\infty}{A_0 - A_\infty} = F e^{-Kf} + (1 - F) e^{-Ks}$$

where F and (1 - F) are fractions of MC moieties decaying faster with a rate constant Kf and slower with Ks, respectively. Figure 5-7 suggests that the thermal decoloration of MC can be described satisfactorily according to the superposition of two first-order rate processes. The rate constants and F values were obtained by fitting the experimental curves and summarized in Table 5-I.

TABLE 5 - I

Thermal decoloration rates of spirobenzopyran chemisorbed silica particles (at 20 ℃)

Species	Solvent	λ_{max} (nm)	$10^4 \times K$ (S^{-1})	F
SPCS2	$CHCl_3$	576→560	5.2^f	0.55
			0.61^s	
	CCl_4	570→555	7.5^f	0.46
			0.33^s	
	Cyclohexane	578→563	7.3^f	0.44
			0.50^s	
SPCS10	$CHCl_3$	573→554	42^f	0.63
			13^s	
	CCl_4	573→560	18^f	0.44
			1.6^s	
	Cyclohexane	580→566	11^f	0.44
			2.1^s	

f: fast process, s: slow process.

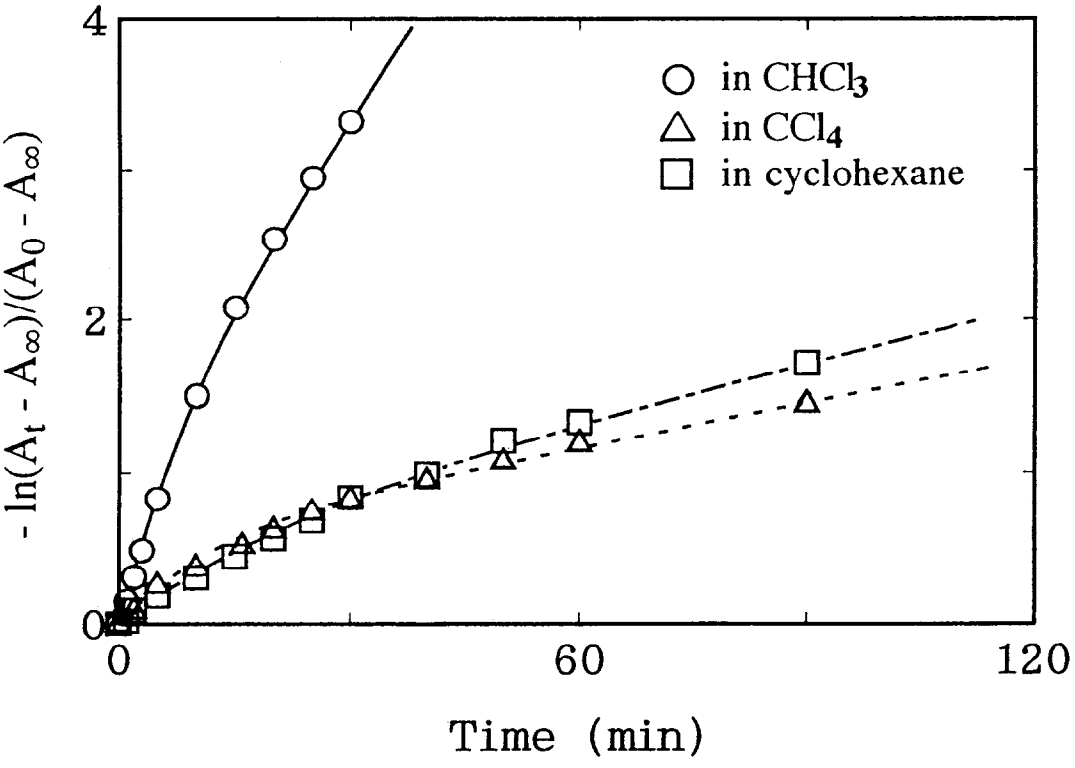

Figure 5-7 First-order plots for the thermal MC→SP isomerization of SPCS10 in chloroform (○), carbon tetrachloride (△) and cyclohexane (□). Solid or broken lines indicate the bimodal first-order fit.

DISCUSSION

The properties of MC attached to colloidal silica dispersed in ethylene glycol are different from those in non-polar solvents. The absorption maxima of the MCs are anomalously blue-shifted in this solvent. According to the negative solvatochromism of MC, the microenvironmental polarity of the surface-bound MC is dispersed in ethylene glycol is estimated to be approximately equivalent to that of a 1:9 water-1,4-dioxane mixture for SPCS2 and a 3:7 water-1,4-dioxane mixture for SPCS10. The more polar nature of the latter suggests that the MC units on SPCS10 are effectively exposed to an outer phase of polar ethylene glycol. The considerable deviation of the plots for both SPCS2 and SPCS10 from the linear relationship between K_{sol} versus E_{MC}, as shown in Figure 5-2, reflects the retardation of the first-order bleaching reaction. The suppressive effect of the surface attachment of MC on the reverse isomerization is more marked for SPCS2, in which the SP units are linked with the shorter spacer. It is likely that the longer spacer of SPCS10, which has good flexibility, causes an increase in the mobility of the chromophore units which enhances the relaxation of the constraint during the isomerization, accompanied with a drastic molecular shape change. A closely related effect was discussed by Labsky *et al.* who linked an SP to a polymeric backbone through an alkylene spacer.[12] According to their data, the thermal decoloration of the photoformed MC of a polymer in solution obeys first-order kinetics, and elongation of the spacer causes an enhancement of the mobility of the SP groups, leading to an increase in the rate constant of the thermal bleaching process.

Concerning the polar nature of silica surfaces, Lochmuller *et al.* studied the microenvironment of the surface with the aid of time-dependent luminescence measurements of a pyrene photoprobe chemically bound to silica particles in contact with different solvents.[13, 14] The long-lived monomer lifetimes for tetrahydrofuran and methanol as well as the longest excimer rise time for tetrahydrofuran supported the idea that polar solvents with hydrogen-bonding capability effectively disrupt a structured water multilayer[15, 16] by displacing water molecules, except for those firmly bound to surface silanols by organic molecules.[13] Therefore, it is very likely that water-miscible ethylene glycol may expel adsorbed water layers to make MC residues so free that they exist in a homogeneously polar

microenvironment. This leads to the first-order decoloration kinetics.

In contrast to the case in ethylene glycol, the thermal bleaching in non-polar solvents showed a bimodal exponential decay accompanied by a change of λ_{max} of the MC (Table 5-I). This type of thermal decoloration process has been reported in solutions of homopolymers substituted with SP[17,18] and surfactant vesicle systems incorporating SP units.[19-21] Goldburt *et al.* studied the MC→SP isomerization of homopolymers of a methacrylates, an acrylate and a styrene having a SP group connected with flexible alkylene spacers.[17,18] They observed a superposition of two exponential decays in non-polar solvents such as benzene or toluene and concluded the presence of two (stacked and unstacked) types of MC displaying different absorption bands at 560 and 580 nm.[17] They also mentioned that the relative intensity of λ_{max} of MC changed during the photocoloration and thermal decoloration processes. In the case of SP chemisorbed on a silica surface, however, the pumping spectra had a single absorption maximum in carbon tetrachloride and cyclohexane as mentioned above, indicating the presence of a single MC species on the surface. This is simply because the MC units are attached to the silica surface at an average distance of *ca.* 1.3 nm for both SPCS2 and SPCS10 to inhibit the aggregation of the chromophores. Therefore, it is reasonable to ascribe the blue shift of MC attached to SPCS2 and SPCS10 during thermal isomerization to the existence of reaction sites with different polarity contributing to the shift in λ_{max}, just as in the case of vesicle systems. Seki *et al.* have shown that the thermal decoloration of MC having an octadecyl chain (SP-18) embedded in dioctadecyldimethylammonium bromide vesicles can be described as a bimodal first-order kinetic process and that the single absorption maximum for MC of SP-18 gradually shifts to shorter wavelengths with time in the dark, indicating that the MC units should be located in the different microenvironmental polarity arising from the existence of distributed solubilization sites in the bilayer matrix.[19]

For water-immiscible solvents, the solvent molecules are unable to interact with the silica surface so that the structured water layer on the silica surface is not modified. The blue shift of MC on colloidal silica particles dispersed in non-polar solvents reflects a hydrophilic microenvironment owing to the water layer on the surface. The MC units with a polar character show so low an affinity to

non-polar solvent molecules that molecular mobility is restricted. This may allow the MC moiety to distribute into a heterogeneous microenvironment with variant polarity. For water-insoluble solvents, (1-F) values may correspond to MC units neighboring on an inner water layer, leading to the blue shift. F values may reflect MC units which are subject to solvation at an outer molecular layer, resulting in the red shift. As shown in Table 5-I, the F values in carbon tetrachloride and cyclohexane are smaller than those in chloroform for both SPCS2 and SPCS10.

In contrast to the stable dispersion of UV-exposed SPCS2 or SPCS10 in chloroform, UV irradiation induces flocculation causing the sedimentation of colored colloidal silica in carbon tetrachloride and cyclohexane as described in Chapter 4. This means that a fraction of the MC interacted with an outer solvent phase is assignable to F and a dominant factor determining whether the UV-exposed photochromic silica is dispersed in non-polar solvents.

SUMMARY

(i) Elongation of the methylene spacer linking SP to the silica surface causes an increase in the thermal decoloration rate because of an enhancement of the mobility of the end-photochromic moiety.

(ii) Dispersion of SP-modified colloidal silica in ethylene glycol results in the single first-order decay of photoformed MC because of efficient solvation which assures a homogeneous microenvironment on the silica surface.

(iii) Water-insoluble solvents force the MC moiety to distribute into a heterogeneous microenvironment with variant polarity to bring about the bimodal first-order kinetics of the thermal reversion of MC.

REFERENCES

1) E. Fisher and J. Hirshberg, *J. Chem. Soc.*, 4522 (1952).

2) V. A. Krongauz, in *Photochromism Molecules and System* Eds. H. Dürr and H. Bouas-Laurent, Elsevier, Amsterdam, 1990, p. 793.

3) J. B., Jr. Flannery, *J. Am. Chem. Soc.*, **90**, 5660 (1968).

4) B. Nadolski, P. Uznanski and M. Kryszewski, *Makromol. Chem. Rapid Commun.*, **5**, 327 (1984).

5) R. C. Bertelson, in *Photochromism* Ed. G. H. Brown Chap. 3, Wiley, New York, 1971.

6) M. Kryszewski and B. Nadolski, *J. Chem. Soc., Faraday Trans. II.*, **76**, 351 (1980).

7) G. Smets, *Advances in Polymer Science*, **50**, 17 (1983).

8) L. Hörner and H. Ziegler, *Z. Naturforsch., Teil B*, **42**, 643 (1987).

9) V. A. Krongauz and E. S. Goldburt, *Nature (London)*, **271**, 43 (1978).

10) R. Richert and H. Bassler, *Chem. Phys. Lett.*, **116**, 302 (1985).

11) T. Tsutsui, A. Hatakeyama, S. Saito and M. Irie, *Chem. Phys. Lett.*, **132**, 563 (1986).

12) J. Labsky, I. Koropecky, S. Nespurek and J. Kalal, *Eur. Polym. J.*, **17**, 309 (1981).

13) C. H. Lochmuller, A. S. Colborn, M. L. Hunnicutt and J. M Harris, *J. Am. Chem. Soc.*, **106**, 4077 (1984).

14) C. H. Lochmuller and M. L. Hunnicutt, *J. Phys. Chem.*, **90**, 4318 (1986).

15) S. A. Mitchell, *Chem., Ind. (London)*, 924 (1966).

16) R. P. W. Scott and S.Traiman, *J. Chromatogr.*, **196**, 193 (1980).

17) E. Goldburt, F. Shvartsmann, S. Fishman and V. Krongauz, *Macromolecules*, **17**, 1225 (1984).

18) E. Goldburt and V. Krongauz, *Macromolecules*, **19**, 247 (1986).

19) T. Seki and K. Ichimura, *J. Colloid Interface Sci.*, **129**, 353 (1989).

20) T. Seki and K. Ichimura, *Macromolecules*, **23**, 31 (1990).

21) C. J. Drummond, D. N. Furlong and G. Georgaklis, *J. Chem. Soc. Faraday Trans.*, **86**, 3913 (1990).

Chapter 6

Photoisomerization of an Azobenzene in Sol-Gel Glass Films

INTRODUCTION

As described in Chapter 1, detailed information on the microscopic environment of organic molecules embedded in a matrix of silica gel glass by the sol-gel process has not been fully clarified since little is known about the mobility of organic molecules in the silica cage and about the interaction between the silica cage and the guest molecules. On the other hand, many studies have been dealt with the photochemical *trans*-to-*cis* isomerization and thermal *cis*-to-*trans* isomerization of azobenzene chromophores molecularly dispersed in polymer films.[1-8] While photoisomerization in dilute solution occurs by a single rate process, its initial portion in the solid films may be fitted by two separate rate processes, *i. e.*, the first is as fast as in dilute solutions and is followed by a slow second process. The fractional amount of the first part decreases with physical aging, but increases with temperature, plasticization, or tensile deformation.[6] This fraction has been related to the number of regions where local free volumes are greater than a critical size necessary for the photoisomerization of the azobenzene group.[7] Azobenzene molecularly dispersed in polymer film has rather small critical free volume needed for isomerization, and hence photochemical- and thermal- isomerizations of azobenzene at room temperature are generally regarded as being chemically controlled even in polymer matrices below T*g*. Thus, the distribution of local free volume in polymers has been characterized by using these photochromic probe molecules.[3, 4]

Hence, incorporation of molecularly dispersed azobenzene chromophores in the sol-gel glass matrices is a useful method for studying the characteristics of reactions in the silica cage, since the reaction rates of photoexcited molecules are expected to reflect the rigidity of the matrix. In this Chapter, the author studied the photoinduced *tran* -to-*cis* isomerization under steady-state irradiation at 365 nm and the thermal *cis*-to-*trans* isomerization of an azobenzene derivative in sol-gel films prepared

under varying conditions in order to estimate the rigidity of the sol-gel glass matrix compared with a polymer matrix.

EXPERIMENTAL

Materials

MHAB was synthesized from 4-hydroxy-4'-methoxyazobenzene by the Williamson method (Figure 6-1). The product was purified by repeated recrystallization from a toluene/hexane (9:1) mixture to give light-yellow crystals of MHAB; melting point 156 ℃ in a 34 % yield. ^{1}H-NMR (CDCl3) δ : 3.9 (3H, s, -OCH_3), 3.9-4.3 (4H, m, -CH_2CH_2-), 6.9 (2H, d, ArH), 7.1 (2H, d, ArH), 7.9 (4H, d, ArH); IR (KBr): 3300, 2950, 1590, 1500, 1250, 840 cm^{-1}. Anal. Calcd. for $C_{15}H_{16}O_3N_2$: C, 66.16; H, 5.92; N, 10.29. Found: C, 66.01; H, 5.86; N, 10.54. Tetraethyl orthosilicate (TEOS) purchased from Tokyo Kasei Kogyo Corp. was used without further purification. Ethanol, ether, tetrahydrofuran (THF) , dimethylsulfoxide (DMSO), and water were of spectroscopic grade. Poly(methyl methacrylate) (PMMA, Mn=1.0×10^5, Tg = 105 ° C) was obtained from Wako Pure Chemical Corp.

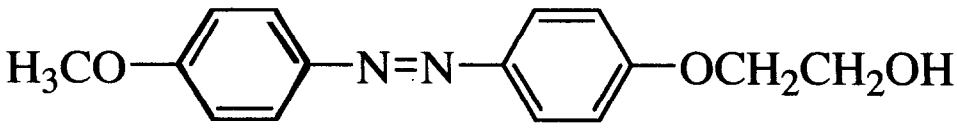

Figure 6-1 Structure of 4-methoxy-4'-(2-hydroxyethoxy)azobenzene (MHAB).

Sample Preparation

Sol-gel films were prepared on quartz substrates. To obtain good homogeneous wetting of the substrate surface, it has to be clean. The substrates were immersed for 24 h in a neutral detergent

solution and then agitated ultrasonically in concentrated HNO_3 for 10 min, washed with distilled water, and dried at 120 ℃ for 60 min.

Various techniques to prepare sol-gel films have been reported.[9-12] The author selected the dip-coating technique. A quartz substrate was immersed into a metal alkoxide solution and pulled up vertically at a rate of 3.33 mm/s and allowed to stand for 1 min, followed by heating at 60 ℃ for 2 h, or at 110 ℃ for 15 h. Three coating solutions with different ratios of TEOS: water were prepared (solution A: $[H_2O]/[Si(OC_2H_5)_4]=2$; solution B:$[H_2O]/[Si(OC_2H_5)_4]=1$; solution C:$[H_2O]/[Si(OC_2H_5)_4]=4$). The thin film coating from solution A was obtained as follows: A mixture of 7.50 g (0.036 mol) TEOS, 5.05 g (0.112 mol) of ethanol, 1.30 g (0.072 mol) of water, and 0.0003 mol of MHAB was stirred, and 0.55 g of concentrated HCl was added to this mixture as a hydrolytic catalyst. The mixture was stirred for 2 h at room temperature, and 7.20 g of ether was added. Before coating, the mixture was kept standing for 1 h at room temperature. Solution B and C were prepared in the same way.

The PMMA film was prepared by solvent-casting onto a quartz substrate from a 10 wt % PMMA solution containing 0.004 mol/L of MHAB in THF. The film was kept at room temperature for 6 h and then heated *under vacuo* at 70 ℃ for 12 h to remove residual solvent.

Measurements of Photoisomerization and Thermal Isomerization

A sample film was irradiated at 365 nm from a Jasco CRM-FA irradiator (2-kW xenon arc lamp with a monochromator) at room temperature for the measurements of the *trans*-to-*cis* photoisomerization of MHAB. Absorbance measurements were made with a Hitachi UV-320 spectrometer. To measure the thermal *cis*-to-*trans* isomerization, the irradiation was discontinued after reaching the photostaionary state, and the sample was moved to the thermostated sample holder placed in the spectrometer to follow the absorbance at the absorption maximum of the *trans* isomer.

Reference experiments for the *trans*-to-*cis* photoisomerization and thermal isomerization of MHAB in a dilute solution were carried out in ethanol or DMSO. The concentration of MHAB in the solutions was adjusted so as to give the same absorbance as in the thin film sample at the absorption maximum.

RESULTS AND DISCUSSION

Absorption Spectra in Sol-Gel Films

Since azobenzene itself was scarcely soluble in the coating solutions for sol-gel films, MHAB bearing hydrophilic substituents was used in order to enhance the solubility. Absorption spectra of MHAB before and after UV-irradiation were measured in ethanol, ethanol/water (1:9) mixture solution, PMMA and the sol-gel film (solution A, heating condition: 110 ℃, 15 h) and are shown in Figure 6-2. A shoulder at somewhat longer wavelength than that of π-π* absorption band is observed in a 10 % ethanol aqueous solution and in the sol-gel film of *trans*-MHAB, in contrast to that in ethanol. Wyman *et al.* ascribed the shoulder in 10 % ethanol aqueous solution to the formation of a hydrogen bond between the azo group and water molecule [13] causing the blue shift of the n-π* transition. In the case of the sol-gel film, the shift of the absorption band may be owing to the hydrogen bond between the azo group and Si-OH at the surface of silica matrix. Some reports have demonstrated hydrogen bonding between organic molecules doped in sol-gel glasses and silanol groups which surround the molecules.[14,15] Another possibility is the effect of a hydrogen bond between the azo group and residual water molecules in silica matrix. The latter interpretation is less reasonable because the shoulder of absorption spectrum was not altered in intensity even after the sample was heated *under vacuo* at 200 ℃ for 12 h to remove residual water.

Trans to Cis Photoisomerization at Room Temperature

Figure 6-2 shows that the photoisomerization rate of MHAB on irradiation with 365-nm light depends on the reaction media. Using eq (6-1), the *cis* fraction ([cis]/[trans]$_0$) in the photostationary state under various conditions were estimated and are summarized in Table 6-I. Here, [cis] and [trans]$_0$ denote the concentration of the *cis*-isomer in the photostationary state and that of the *trans*-isomer before UV irradiation, respectively, ε_{cis} and ε_{trans} are the absorption coefficients, whereas A_0 and A are the absorbances at λ_{max} before and after UV irradiation:

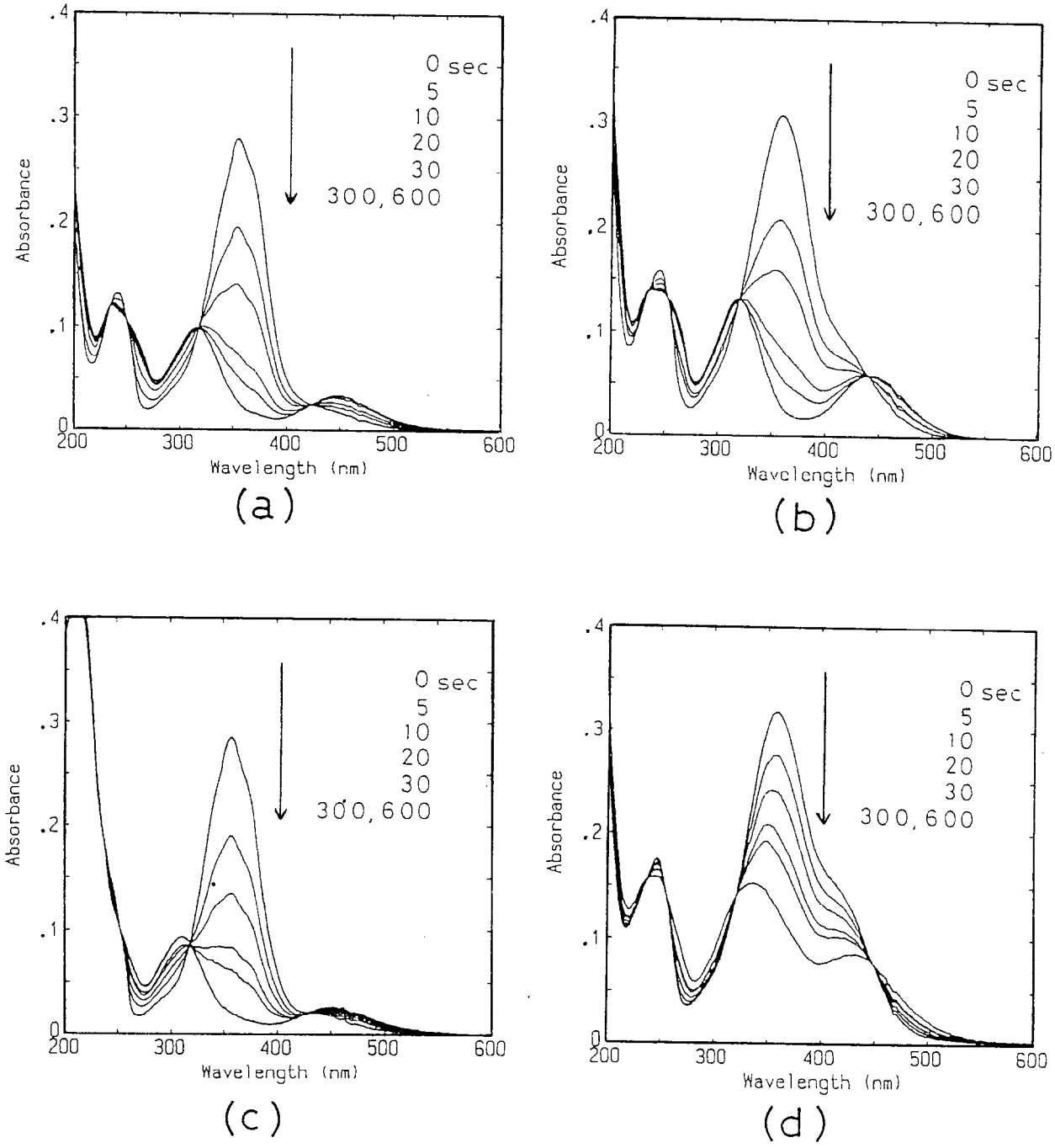

Figure 6-2 Change in UV spectra of trans-MHAB during 365 nm light irradiation at room temperature: (a) in ethanol, (b) in a 1:9 mixture of ethanol and water, (c) in PMMA and (d) in a sol-gel film (solution A, heating condition: 110 ° C, 15 h).

Table 6-I

Photochemical Conversion of MHAB

matrix	*cis* fraction in a photostationary state (%)
ethanol	93
10 % ethanol aqueous solution	92
PMMA	93
sol-gel film (solution A, heating condition: 110 ° C, 15 h)	60
sol-gel film (solution A, heating condition: 60 ° C, 2 h)	64
sol-gel film (solution B, heating condition: 60 ° C, 2 h)	82
sol-gel film (solution C, heating condition: 60 ° C, 2 h)	61

$$[\text{cis}] = \frac{1 - A/A_0}{1 - \varepsilon_{\text{cis}}/\varepsilon_{\text{trans}}} [\text{trans}]_0 \qquad (6\text{-}1)$$

Table 6-I shows that the final *cis* fraction in the sol-gel film is much less than in ethanol and PMMA. The *cis* fraction in the photostationary state in a 10 % ethanol aqueous solution, which resulted in spectra similar to those in the sol-gel films, is almost the same as in ethanol, suggesting that the formation of the hydrogen bond between the azo group and silanol groups has no effect on the final *cis* fraction. In addition, it is not likely that residual solvents (water and ethanol), ethoxysilyl and silanol groups which exist in the sol-gel glass alter photophysical properties of MHAB considerably to quench the photoisomerization, because the *trans*-to-*cis* photoisomerization proceeds in a sol solution as well as in an ethanol solution. Hence, it may be noted that photoisomerization of *trans*-MHAB is suppressed in the sol-gel film owing to the rather small critical free volume available in this matrix (Table 6-I). Such an effect of the free volume was reported for azobenzene in a polycarbonate film at extremely low temperature[1] and for azonaphthalene in cross-linked epoxy resins at room temperature.[2] However, the quenching of the photoisomerization of azobenzene in the polycarbonate is considerably relaxed at ambient temperature to result in a conversion to the *cis*-isomer similar to that in PMMA or

polystyrene.[1-8] This suggests that the partial suppression of the *trans*-to-*cis* photoisomerization in the sol-gel films is caused by the highly cross-linked network, which is more rigid than the polymer matrices at room temperature.

Quinson *et al.* have measured the radius of pores of the wet silica gel by thermoporometry.[16] The pore radius distribution of a wet gel prepared by the sol-gel process is very narrow and centered at around 25 Å, and the shape factor indicates cylindrical interconnected pores. The pore size of the xerogel (dry gel) should be smaller than that of the wet gel. Scherer *et al.* have demonstrated that the pore diameter distribution of the xerogels prepared by acidic hydrolysis is very wide below 40 Å.[17]

The free volume which is required for the *trans*-to-*cis* photoisomerization of photoprobes is the volume swept out by the van der Waals area of the displacing group. Victor and Torkelson have calculated these sweep volumes of several photoactive compounds [3] after the method of Bondi,[18] and estimated the free volume needed by azobenzene to isomerize as 127 $Å^3$. The sweep volume of MHAB is larger than that of azobenzene because of the presence of substituents. Some portion of MHAB molecules may exist at least partially in the pores with much smaller size (probably the pore diameter below *ca.* 10 Å) in sol-gel films, and the photoisomerization can then not to take place.

According to Horie *et al.*, [1] when the *trans*-azobenzene with an initial concentration of $[t]_0$ is irradiated at 365 nm, the change in *trans*-azobenzene concentration, [t], approaching its equilibrium value, $[t]_\infty$, is given by

$$\ln \frac{[t]_0 - [t]_\infty}{[t] - [t]_\infty} = \frac{[t]_0}{[t]_0 - [t]_\infty} A \cdot t = \frac{[t]_0}{[t]_\infty} (B + K) \cdot t \qquad (6\text{-}2)$$

where A, B, and K are the rate constants for the *trans*-to-*cis* photoisomerization, the *cis*-to-*trans* photoisomerization, and the thermal *cis*-to-*trans* isomerization, respectively.

The first-order plots according to eq (6-2) for the *trans*-to-*cis* photoisomerization of MHAB in ethanol, PMMA and the sol-gel film (solution A, heating condition: 110 ° C, 15 h) at room

temperature are shown in Figure 6-3. The reaction is first-order in solution, whereas in PMMA and in the sol-gel film it deviates from first-order kinetics. The degree of the rate reduction in the sol-gel film was more marked than in PMMA. This also suggests that the sol-gel matrix is more rigid than the polymer matrix.

Thermal Cis to Trans Isomerization in Sol-Gel Films

The thermal *cis*-to-*trans* isomerization of MHAB in the sol-gel films and in DMSO was followed at 40 and 60 ° C. DMSO was employed here as a high boiling point solvent in order to avoid a change in the concentration of the azobenzene during the spectroscopic measurement.

The thermal *cis*-to-*trans* isomerization follows first-order kinetics:

$$\ln \frac{[t]_{H\infty} - [t]_{H0}}{[t]_{H\infty} - [t]} = K \cdot t \qquad (6\text{-}3)$$

where [t] is the *trans*-azobenzene concentration, $[t]_{H0}$ and $[t]_{H\infty}$ are the concentration of the *trans* isomer of the azobenzene in the photostationary state and after the thermal reversion is completed, respectively. First-order plots for the thermal *cis*-to-*trans* isomerization of MHAB at 40 and 60 ° C in the sol-gel films (solution A, heating condition: 110 ° C, 15 h) and in the solution are shown in Figure 6-4.

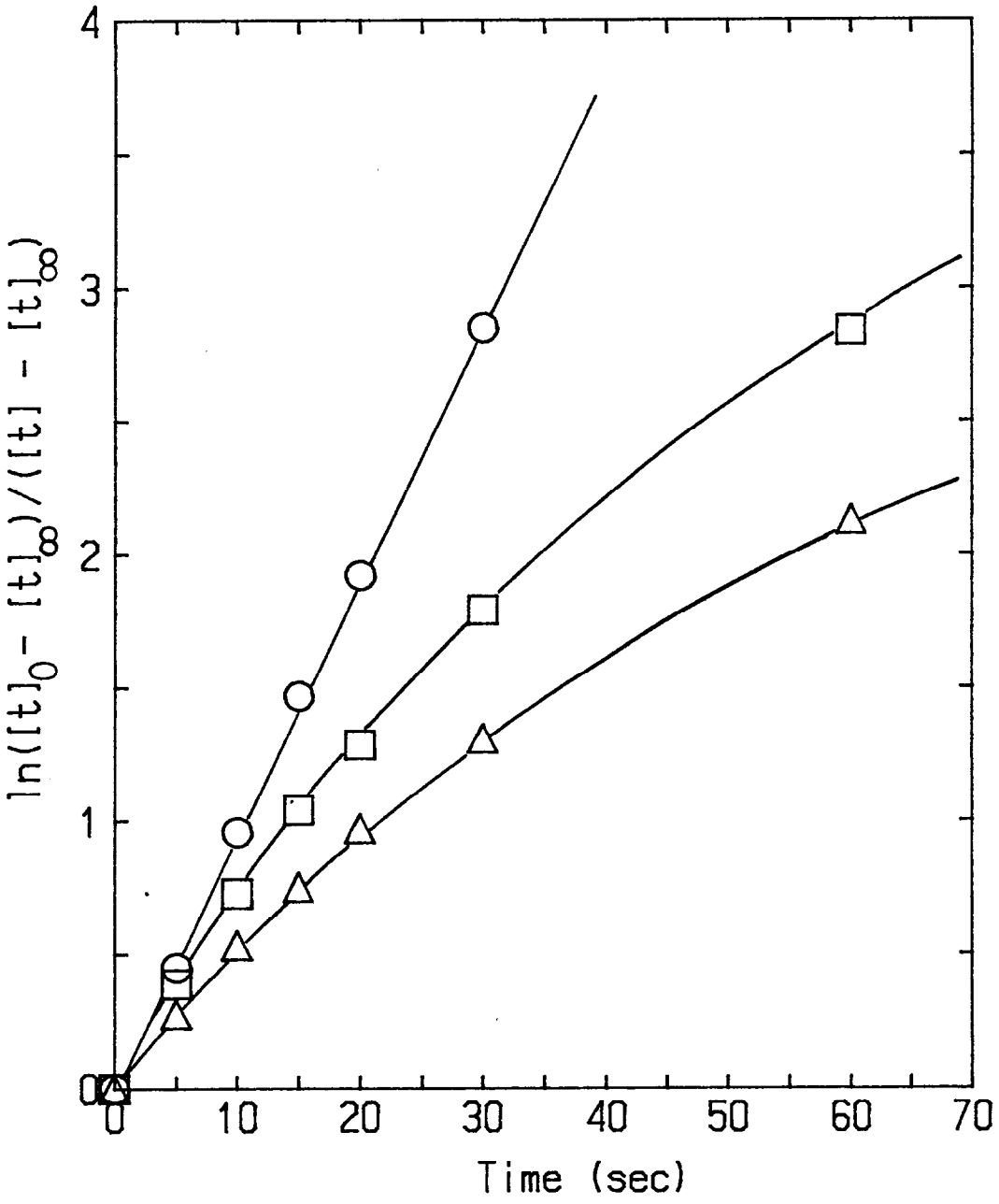

Figure 6-3 First-order plots for trans → cis photoisomerization of MHAB at room temperature: in ethanol (○), in PMMA (□) and in a sol-gel film (△) (solution A, heating condition: 110 ° C, 15 h).

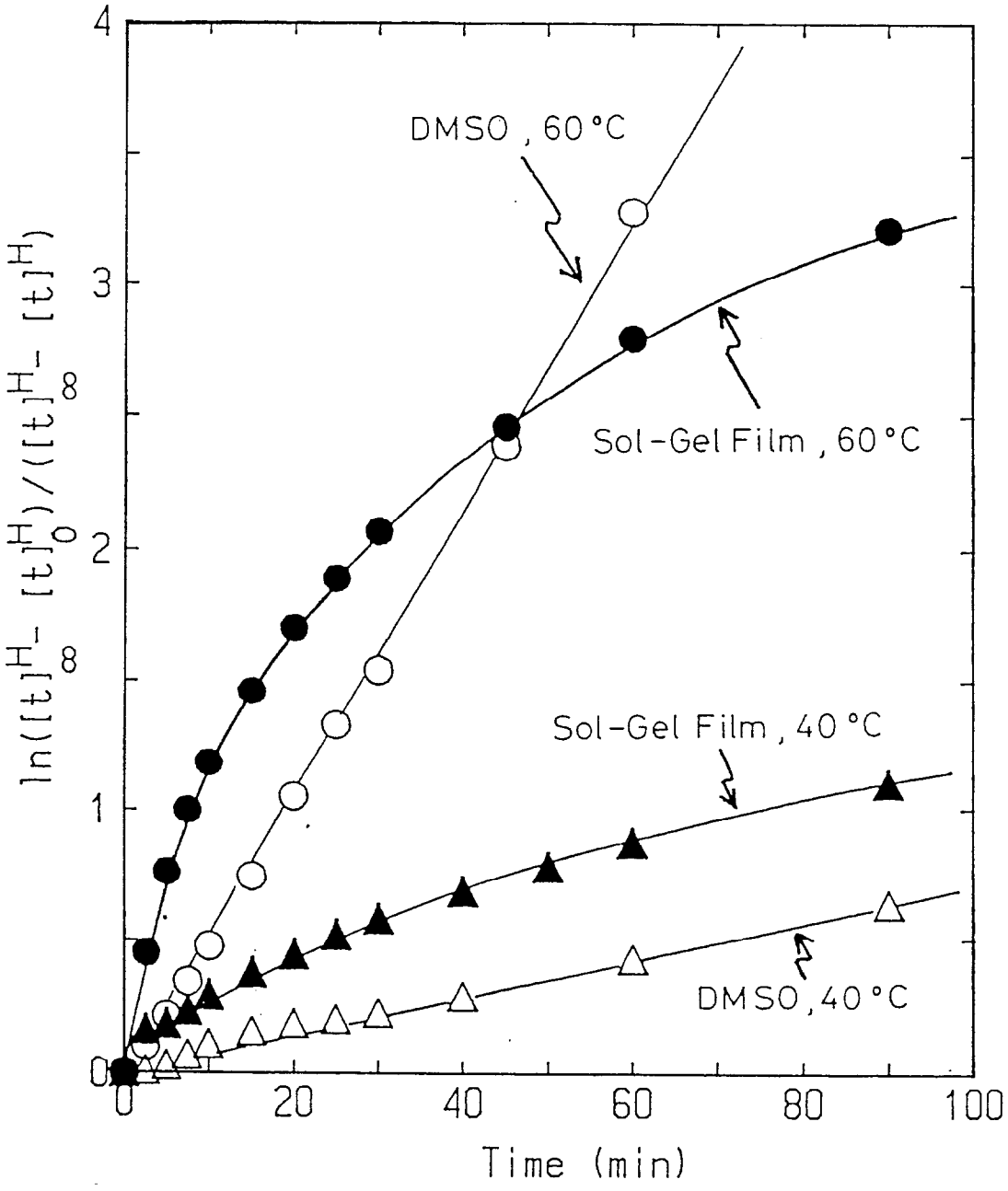

Figure 6-4 First-order plots for thermal cis → trans isomerization of MHAB: (△) in DMSO at 40 ° C, (○) in DMSO at 60 ° C, (▲) in a sol-gel film (solution A, heating condition: 110 ° C, 15 h) at 40 ° C and (●) in a sol-gel film (solution A, heating condition: 110 ° C, 15 h) at 60 ° C.

The reaction proceeds by first-order kinetics in solution whereas in the sol-gel films the reaction is initially faster than in solution and decreases gradually with time. Such a thermal reversion kinetics in the sol-gel films was not eventually affected by additional heating, indicating that there is no remarkable change in the composition at the pore walls and in the pore size distribution. Such a rate enhancement in the beginning of the thermal isomerization was also observed in polymer matrices and attributed to residual strain in the *cis*-azobenzene produced by UV irradiation.[19] In analogy with polymer matrices, in the sol-gel matrix a part of the *cis* isomer is produced in a strained conformation and can revert more easily to the *trans* isomer than the relaxed *cis* species. The low rate of reaction, at 60 ° C in the terminal phase of the thermal isomerization in the sol-gel film may be ascribed to the interaction between MHAB molecule and the silica matrix (*e.g.*, the hydrogen bond between MHAB and silanol groups).

These results, in conjunction with the composition of the photostationary state, suggest that MHAB in the sol-gel glass contains three fractions. In the first the local free volumes are smaller than a critical size necessary for the photoisomerization. In the second fraction the reaction can take place but the produced *cis* isomer is in a strained conformation. In the third fraction the reaction rate is lower than in solution because of the interaction between MHAB and the silica matrix.

Dependence of the Matrix Rigidity on the Preparative Method

The sol-gel process is composed of two reactions, the hydrolysis of metal alkoxides and polycondensation. These reactions are influenced markedly by the preparative conditions (*e. g.*, preparation composition, catalyst (acid / base), reaction temperature, *etc.*)[20-23] and determine the matrix rigidity of sol-gel glasses. Brinker and his colleagues[24] have studied of the hydrolysis and condensation to give a silica gel made by a two-step process.[25] The first step consists of hydrolysis under acidic condition (pH = 0.3) with the reactants added in a molar ratio of TEOS/alcohol/H_2O/HCl = 1/3/1/0.0007. This causes a rapid hydrolysis, but the reaction cannot go to completion because of the substoichiometric quantity of water, resulting in the formation of lightly cross-linked polymers. The second step (additional water plus acid) resulted in completely hydrolyzed polymers. As given in

Table 6-I, the *cis* fraction at the photostationary state depends on the water content. Although the *cis* fraction is low when $[H_2O]/[TEOS] \geqq 2$, the content of water ($[H_2O]/[TEOS]=1$) favors the *cis*-isomer formation.

The thermal isomerization is also affected by the water content. Figure 6-5 shows first-order plots for the thermal *cis*-to-*trans* isomerization of MHAB in the sol-gel films at 60 ° C under various preparative conditions. Films prepared under different heating conditions (● and ○), exhibited almost the same thermal isomerization reaction rates, suggesting that the matrix rigidity in the sol-gel glasses prepared from solution A is scarcely altered by changing the annealing condition. However, in the sol-gel film prepared from solution B, the first-order (△) is different from the others, *i. e.*, the reaction rate of MHAB in the sol-gel film prepared from the low water content solution is higher.

The gel formed from a solution with such a low water content is weakly cross-linked and linear polymeric in nature since the hydrolysis reaction does not proceed to completion.[25-27] Consequently, the sol-gel film prepared from solution B, may have a more weakly cross-linked structure leading to effective *cis*-to-*trans* isomerization.

Absorption spectra of MHAB in the sol-gel films prepared from solution B and solution C are shown in Figure 6-6. The solid lines and dotted lines show the spectra of the *trans* form and the photostationary state, respectively. The shape of the absorption spectra of the *trans* form in the sol-gel film prepared from solution B is quite similar to that in ethanol (Figure 6-2(a)). The shoulder arising from the formation of hydrogen bond between the azo group in MHAB and silanol group in silica matrix is scarcely recognized. Under such a low water concentration condition a large quantity of residual $Si\text{-}OC_2H_5$ groups remains on the surface of silica matrix.[28] The *trans*-to-*cis* photoisomerization goes almost to completion since the silica matrix may be weakly cross-linked. However, in the case of the sol-gel film prepared from solution C, the final *cis* fraction is lower because of the highly cross-linked structure formed after complete hydrolysis (Figure 6-6(b)). In Figure 6-5, the first-order plot of MHAB in the sol-gel film prepared from solution C (□) is similar to that in the sol-gel film prepared from solution B (○). This is probably because the total reaction of the sol-gel process is insensitive to a $[H_2O]/[TEOS]>2$.

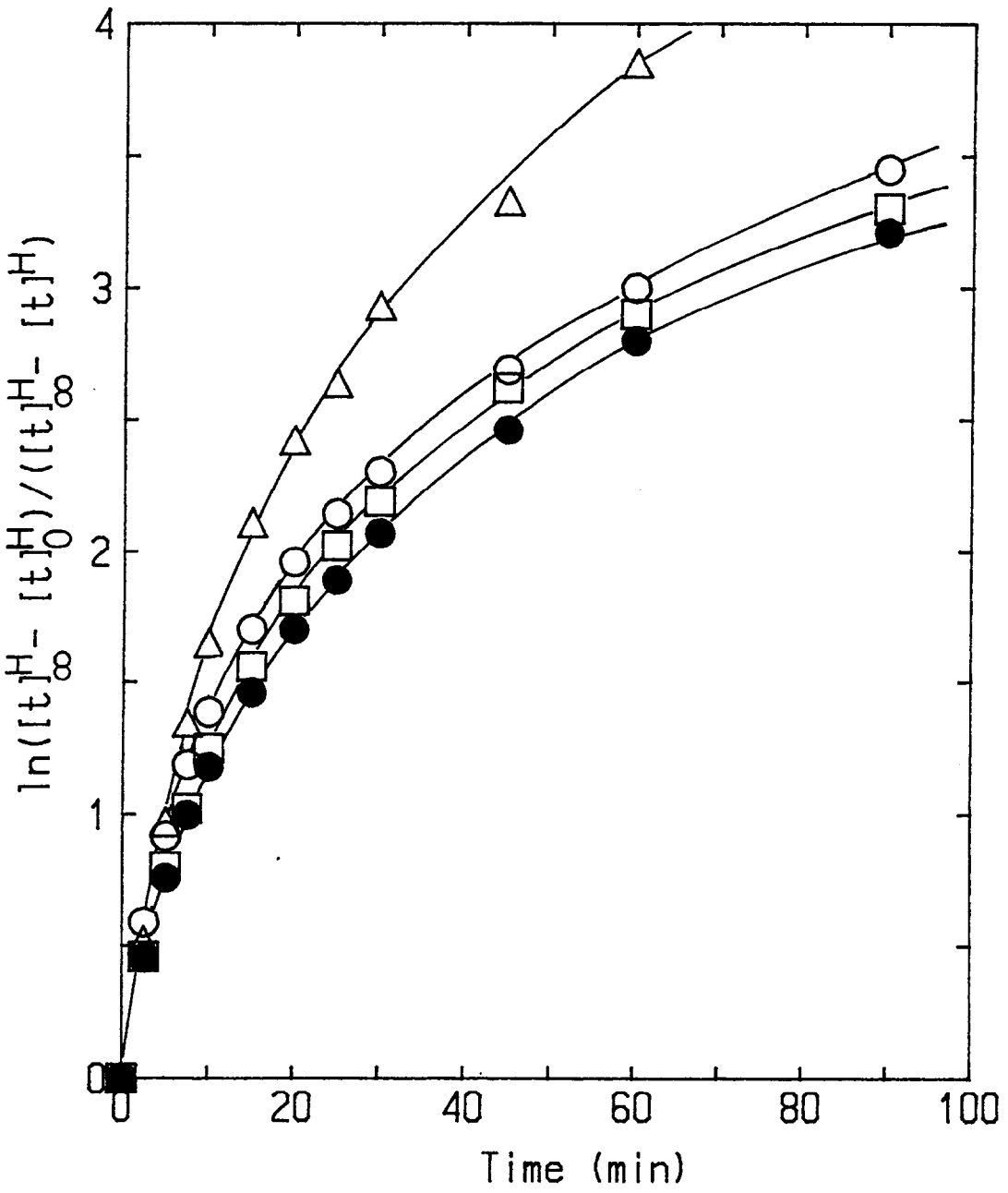

Figure 6-5 Preparation condition dependence of the first-order plots for thermal cis → trans isomerization of MHAB in sol-gel films at 60 ° C. The preparation conditions were as follows:

(●) solution A, heating condition: 110 ° C, 15 h . (○) solution A, heating condition: 60 ° C, 2 h.

(△) solution B, heating condition: 60 ° C, 2 h. (□) solution C, heating condition: 60 ° C, 2 h.

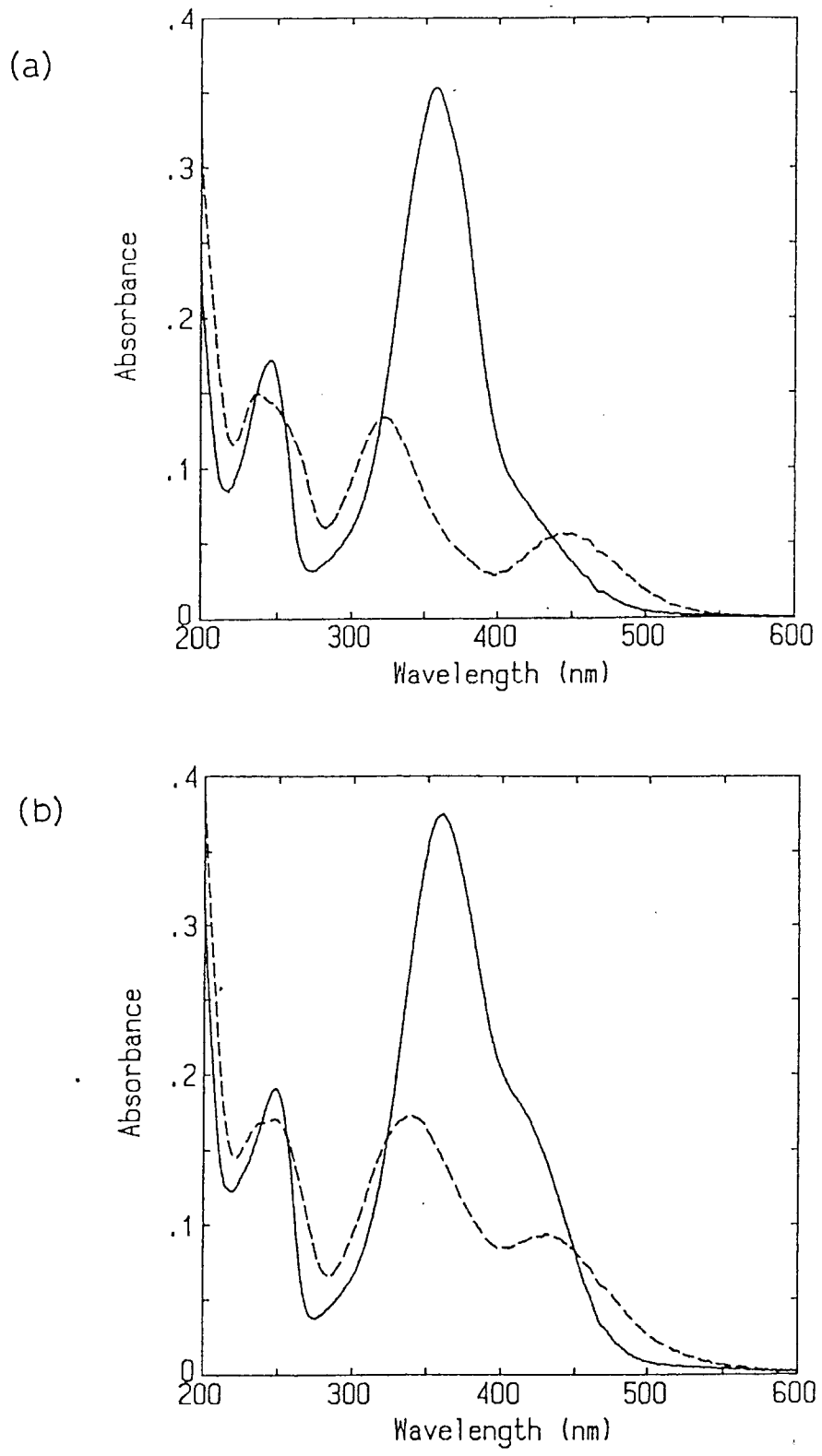

Figure 6-6 Absorption spectra of MHAB: (a) (——) in a sol-gel film (solution B, heating condition: 60 ° C, 2 h) and (- - - -) after prolonged irradiation with a UV light, (b) (- - - -) in a sol-gel film (solution C, heating condition: 60 ° C, 2 h) and (——) after prolonged irradiation with a UV light.

SUMMARY

The following conclusions can be drawn about the isomerization behavior of the azobenzene derivative in the sol-gel films:

(1) Hydrogen bonds are formed between the azo group in azobenzene probe and silanol group in sol-gel glass matrix whose films were prepared with a relatively high water concentration ($[H_2O]/[TEOS] \geqq 2$).

(2) The azobenzene probes in the sol-gel glass are of three types when the glass is prepared from a solution of $[H_2O]/[TEOS]=2$. (a) At sites with smaller pores in which the *trans*-to-*cis* photoisomerization is quenched, (b) at sites in which the *cis* isomer is formed in a strained conformation enhancing the thermal reversion, (c) at sites in which the thermal reversion rate is reduced by the hydrogen bond between the guest molecule and silanol groups.

(3) The rigidity of the matrix in sol-gel glass depends on the water content of the solution from which it was prepared. In the case of $[H_2O]/[TEOS]=1$, the photoisomeriation takes place readily in a sol-gel film possibly because of inefficient network formation.

REFERENCES

1) I. Mita , K. Horie and K. Hirao, *Macromolecules*, **22**, 558 (1989).

2) T. Naito, M. Kunishige, T.Yamashita, K. Horie and I. Mita, *React. Polym.*, **15**, 185 (1991).

3) J. G. Victor and J. M. Torkelson, *Macromolecules.*, **20**, 2241 (1987).

4) J. S. Royal, J. G. Victor and J. M. Torkelson, *Macromolecules.*, **25**, 729 (1992).

5) J. W. Priest and M. M.Sifain, *J. Polym. Sci. Part A-1*, **9**, 3161 (1971).

6) L. Lamarre and C. S. P. Sung, *Macromolecules.*, **16**, 1729 (1983).

7) C. S. P. Sung, I. R. Gould, and N. J. Turro, *Macromolecules.*, **17**, 1447 (1984).

8) W.-C. Yu, C. S. P. Sung and R. E. Robertson, *Macromolecules,* **21**, 355 (1988).

9) M. Yamane, S. Aso and T. Sakaino, *J. Mater. Sci.*, **13**, 865 (1978).

10) H. Dislich and E. Hussman, *Thin Solid Films*, **77**, 129 (1981).

11) H. Dislich, *J. Non-Cryst. Solids*, **57**, 371 (1983).

12) S. Sakka, K. Kamiya, K. Makita and Y. Yamamoto, *J. Non-Cryst. Solids*, **63**, 223 (1984).

13) W. R. Brode, I. L. Seldin, P. E. Spoerri and G. M. Wyman, *J. Am. Chem. Soc.*, **77**, 2762 (1955).

14) K. Matsui, T. Matsuzuka and H. Fujita, *J. Phys. Chem.*, **93**, 4991 (1989).

15) A. Levy, D. Avnir and M. Ottolenghi, *Chem. Phys. Lett.*, **121**, 223 (1985).

16) J. F. Quinson, J. Dumas and J. Serughetti, *J. Non-Cryst. Solids*, **79**, 397 (1986).

17) C. J. Brinker and G. W. Schaefer, in *Ultrastructure Processing of Ceramics, Glass, and Composites* Eds. L. L. Hench and D. R. Ulrich, John Wiley& Sons, New York, 1984, p. 43.

18) A. Bondi, *J. Phys. Chem.*, **68**, 441 (1964).

19) C. S. Paik and H. Morawetz, *Macromolecules*, **5**, 171 (1972).

20) S. Sakka and K. Kamiya, *J. Non-Cryst. Solids*, **42**, 403 (1980).

21) C. J. Brinker and G. W. Scherer, *J. Non-Cryst. Solids*, **70**,301 (1985).

22) G. W. Scherer, *Yogyo Kyokaishi*, **95**, 21 (1987).

23) L. L. Hench and J. K. West, *Chem. Rev.*, **90**, 33 (1990).

24) C. J. Brinker, K. D. Keefer, G. W. Schaefer, R. A. Assink, B. D. Kay and C. S. Ashley, *J. Non-Cryst. Solids*, **63**, 45 (1984).

25) K. D. Keefer, in *Better Ceramics through Chemistry*, Eds. C. J. Brinker, D. E.Clark and D. R. Ulrich, North-Holland, New York, 1984, p. 15.

26) D. W. Schaefer and K. D. Keefer, in *Better Ceramics through Chemistry*, Eds. C. J. Brinker, D. E.Clark and D. R. Ulrich, North-Holland, New York, 1984, p. 1.

27) J. B. Blum and J. W. Ryan, *J. Non-Cryst. Solids*, **81**, 221 (1986).

28) A. H. Boonstra and C. A. M. Mulder, *J. Non-Cryst. Solids*, **105**, 201 (1988).

Chapter 7

Photoisomerizability of an Azobenzene Covalently Attached to Silica-Gel Matrix

INTRODUCTION

In Chapter 6, a hydrophilic azobenzene derivative, 4-methoxy-4'-(2-hydroxyethoxy)-azobenzene (MHAB) was used as a photochromic probe to reveal the microenvironment of silica film matrices. The results indicate the presence of hydrogen bonding interaction between the azo group and silanol groups and suppression of photoisomerization at least partially due to the highly cross-linked network structure entrapping the molecules. The fact that the major part of the azobenzene was able to photoisomerize freely in a xerogel implied that these probing molecules exist in pores without steric constraint.

If doping with other photoactive molecules in silica matrices brings about the same situation, a large part of these molecules appears to be located in state quite similar to that in fluid phase without essential perturbation of the chemical or physical properties. Conversely, if a major part of photoactive molecules is frozen in silica-gel matrices due to the highly cross-linked network to reduce the translational motion, specific physicochemical properties would be expected.

This chapter deals with the effect of covalent bond formation between a doping azobenzene moiety and silica-gel matrices on the geometrical isomerization. Figure 7-1 shows the azobenzene derivatives employed in this chapter. MTAB and DTAB possess silylating unit(s) for binding covalently to silica matrix. The author expected that the introduction of silylation units at both sides of the azobenzene enhances considerably suppression of reactivity of the chromophore.

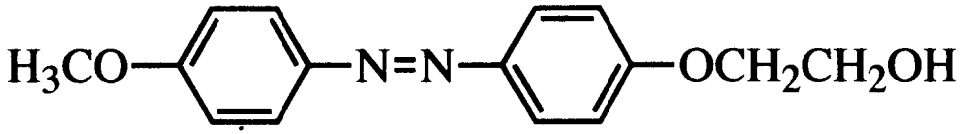

MHAB

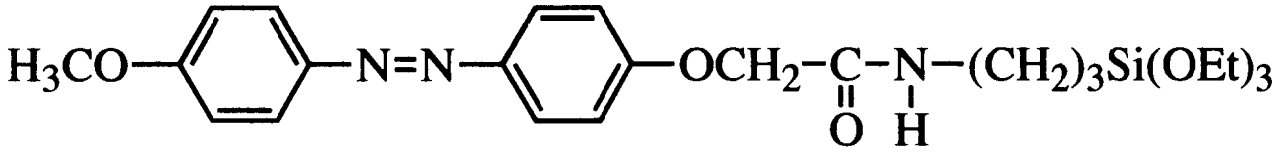

MTAB

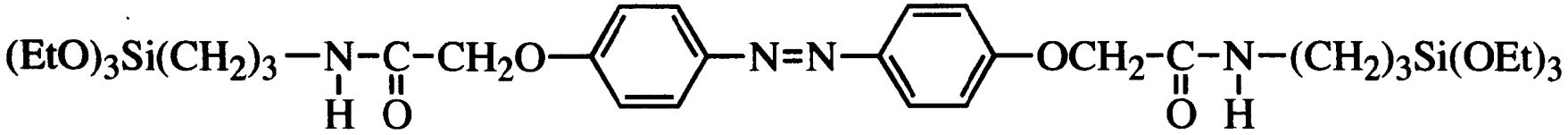

DTAB

Figure 7-1 Chemical structures of azobenzene derivatives

EXPERIMENTAL

Materials

Tetraethyl orthosilicate (TEOS, Tokyo Kasei Kogyo Corp.) was used without further purification. Ethanol, tetrahydrofuran (THF), dimethyl sulfoxide (DMSO), and water were of spectroscopic grade.

4-Methoxy-4'-(2-hydroxyethoxy)azobenzene (MHAB) was prepared as described in Chapter 6. The other azobenzenes were prepared according to the reaction scheme in Figure 7-2.

4-Methoxy-4'-carboxymethoxyazobenzene was synthesized by reaction of 4-methoxy-4'-hydroxyazobenzene with ethyl bromoacetate, followed by alkaline hydrolysis. 4,4'-Bis(carboxymethoxy)azobenzene was prepared by reaction of the corresponding dihydroxyazobenzene with ethyl bromoacetate, followed by alkaline hydrolysis.

4-Methoxy-4'-(*N*-(3-triethoxysilylpropyl)carbamoylmethoxy)azobenzene (MTAB) was prepared by adding dicyclohexylcarbodiimide (DCC, 1.19g; 4.76 mmol) to an ice-cooled solution of the azobenzenecarboxylic acid (1.50 g; 5.24 mmol) and 3-aminopropyltriethoxysilane (APTS, 1.28 g; 5.76 mmol) in dichloromethane (20 ml). The mixture was stirred for 6 h at room temperature. Precipitated urea was removed by filtration, followed by evaporating the solvent under reduced pressure. The residue was recrystallized from toluene/hexane to give purified MTAB (yield 27 %, melting point 130 ℃): ^{1}H-NMR (CDCl3) δ : 0.5-0.8 (2H, m, -CH_2Si), 1.2 (9H, t, OCH_2CH_3), 1.5-1.9 (2H, m, NH-$CH_2CH_2CH_2$-), 3.3-3.5 (2H, m, NH-CH_2), 3.8 (6H, q, OCH_2CH_3), 3.9 (3H, s, OCH_3), 4.5 (2H, s, -OCH_2-), 6.6-6.9 (1H, m, NH), 6.9 (2H, d, ArH), 7.1 (2H, d, ArH), 7.9 (4H, d, ArH); IR (KBr) 3290, 2950, 1650, 1250, 1110, 840 cm^{-1}. Anal. Calcd. for $C_{24}H_{35}O_6N_3Si$: C, 58.87; H, 7.20; N, 8.58 %. Found: C, 58.87; H, 7.34; N, 8.71 %.

The conventional DCC condensation of the azobenzene dicarboxylic acid with APTS gave a very poor 4,4'-bis(*N*-(3-triethoxysilylpropyl) carbamoylmethoxy) azobenzene (DTAB) yield.

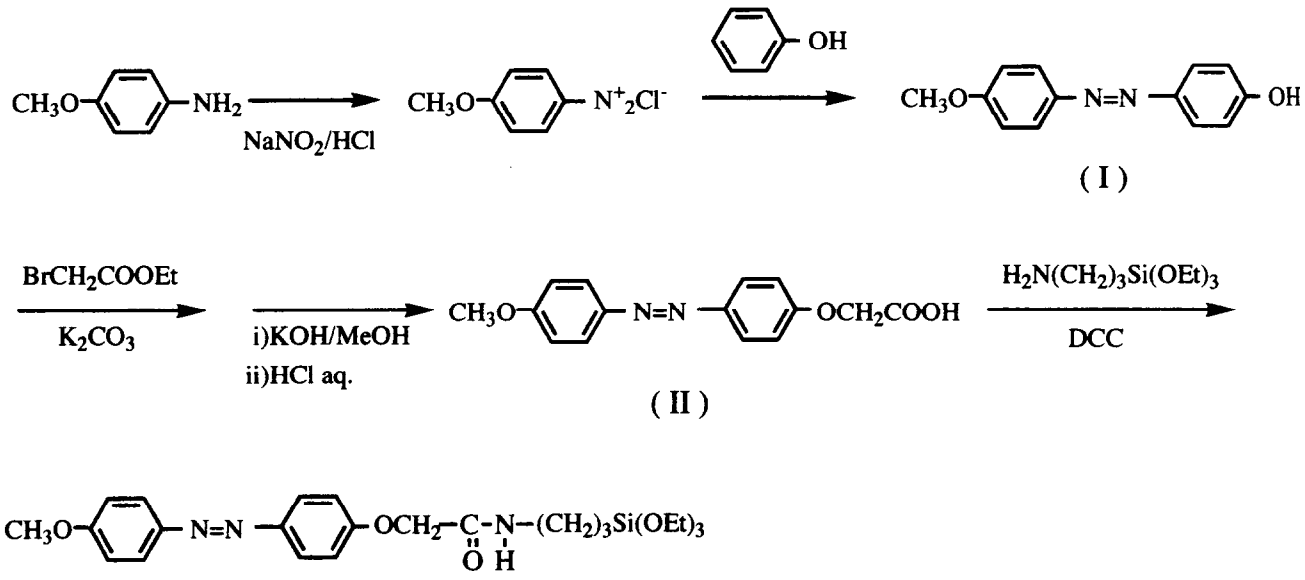

MTAB

(Scheme I)

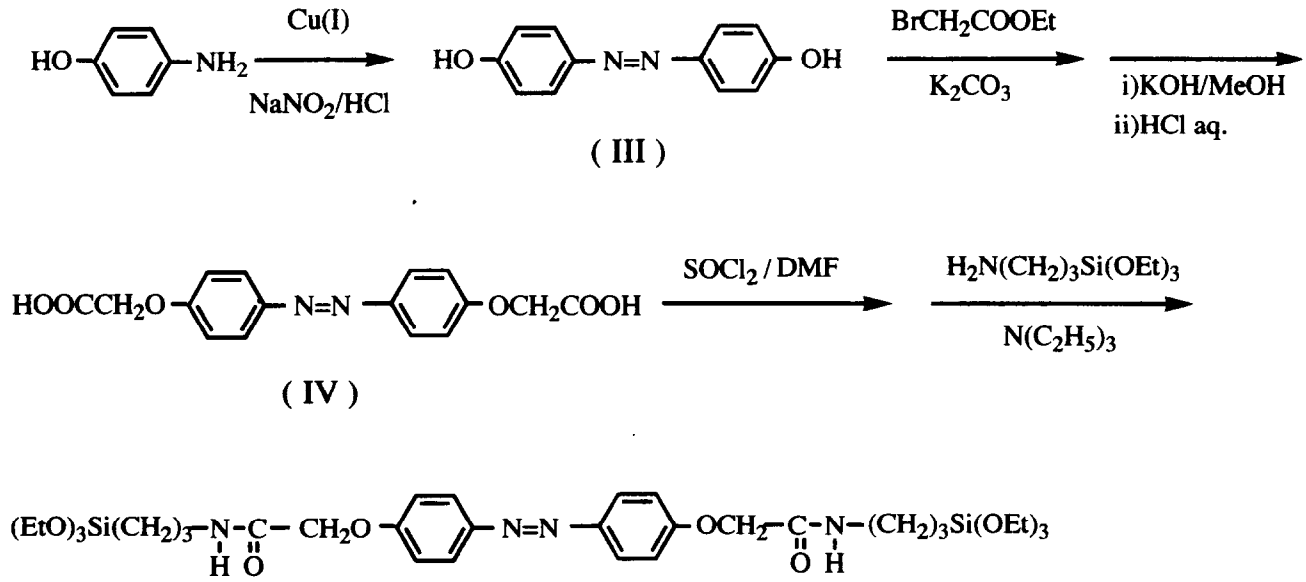

DTAB

(Scheme II)

Figure 7-2 Synthetic pathways of MTAB(Scheme I) and DTAB(Scheme II).

As consequence, a few drops of DMF and thionyl chloride (0.53g; 4.4 mmol) was added to the azobenzenedicarboxylic acid (0.61 g; 2.0 mmol) dissolved in dry benzene (10 ml). The mixture was refluxed for 3 h, and after cooling to room temperature the solution was evaporated under reduced pressure. The residue dissolved in dry benzene (10 ml) was added to a solution of APTS (0.98 g; 4.4 mmol) and triethylamine (0.46 g; 4.4 mmol) in benzene (10 ml). The mixture was stirred for 30 min at room temperature. After the precipitate was removed by filtration, the filtrate was evaporated under reduced pressure. The product was recrystallized from benzene/hexane to give DTAB (yield 72 %, melting point 121 ℃: ^{1}H-NMR ($CDCl_3$) δ : 0.5-0.8 (4H, m, -CH_2Si), 1.2 (18H, t, OCH_2CH_3), 1.5-1.9 (4H, m, NH-$CH_2CH_2CH_2$-), 3.3-3.5 (4H, m, NH-CH_2), 3.8 (12H, q, OCH_2CH_3), 4.6 (4H, s, -OCH_2-), 7.0 (4H, d, ArH), 7.9 (4H, d, ArH); IR (KBr) 3290, 2950, 1660, 1250, 1090, 840 cm^{-1}. Anal. Calcd. for $C_{34}H_{56}O_{10}N_4Si$: C, 55.41; H, 7.66 ; N, 7.60 %. Found: C, 55.44; H, 7.86; N, 7.57 %.

Sample Preparation

Sol-gel films were prepared on quartz substrates by using the technique described in previous chapter. A mixture of TEOS, water and ethanol (molar ratio 1:2:3), in which an azobenzene derivative was dissolved, was used as a coating solution. The films obtained were heated at 110 ℃ for 15 h. Poly (methylmethacrylate) (PMMA) films were prepared by solvent-casting on quartz substrates from a 10 wt % PMMA solution containing an azobenzene derivative in THF. The films were kept at room temperature for 6 h and then heated *in vacuo* at 70 ℃ for 15 h to remove residual solvent.

Measurements

Measurements of photoisomerization and thermal isomerization were conducted as described previous chapter. A sample film was irradiated at 365 nm in a Jasco CRM-FA irradiator (2 kW xenon arc lamp with monochromator) at room temperature. The absorption spectra were measured by a Hitachi UV-320 spectrometer. The irradiation was stopped after reaching the photostationary states and the sample was moved to a temperature-controlled sample holder placed in the spectrometer to follow the absorption spectra during the *cis*-to-*trans* isomerization.

RESULTS AND DISCUSSION

All azobenzenes gave similar spectra and the same absorption coefficient (ε =21000 $M^{-1}cm^{-1}$) in ethanol, while λ_{max} (π-π*) of MHAB, MTAB, and DTAB were 354, 353, and 351 nm, respectively (Figure 7-3(a)). They also showed the *trans*-to-*cis* photoisomerization and *cis*-to-*trans* thermal reversion in solution. These observations confirm that triethoxysilyl group(s) linked with azobenzene moiety have no effect on photophysical or photochemical properties of the azobenzene unit. Analogous spectra were also obtained in PMMA thin films.

Azobenzene itself was scarcely soluble in the coating solution for sol-gel films. The azobenzene derivatives employed here, however, were more soluble owing to the hydrophilic substituents and triethoxysilyl group(s). During the sol-gel process, triethoxysilyl group(s) was hydrolyzed to condense with the growing silica matrix to result in the fixation of the one or both sides of the azobenzene unit to the silica matrix. Attempts to extract MTAB and DTAB from the silica films in methanol failed, supporting the view that azo-chromophores are covalently fixed. Homogeneous optically transparent sol-gel films were obtained and no aggregation of the azobenzene derivatives was observed during the sol-gel processes.

Figure 7-3(b) shows absorption spectra of the azobenzene derivatives in sol-gel films. The π-π* absorption band around 353 nm in the glass films appears at the wavelength similar to that observed in ethanol (Figure 7-3(a)) or in PMMA, suggesting that the azobenzene derivatives are dispersed monomolecularly since the band should suffer wavelength shift if the intermolecular interaction of the azo-chromophores occurs. A striking feature of Figure 7-3(b) is the appearance of a shoulder around 420 nm for all azobenzenes entrapped in sol-gel films. The shoulder is assignable to blue-shifted n-π* caused by hydrogen-bonding interaction between the azo group and Si-OH groups and /or bound water molecules on the surface of silica matrix, since the marked blue shift was previously confirmed in an aqueous solution (Figure 6-2 in Chapter 6). Some reports have demonstrated the formation of a hydrogen bond between organic molecules and silanol groups which surround the molecules in sol-gel glasses.[1, 2)]

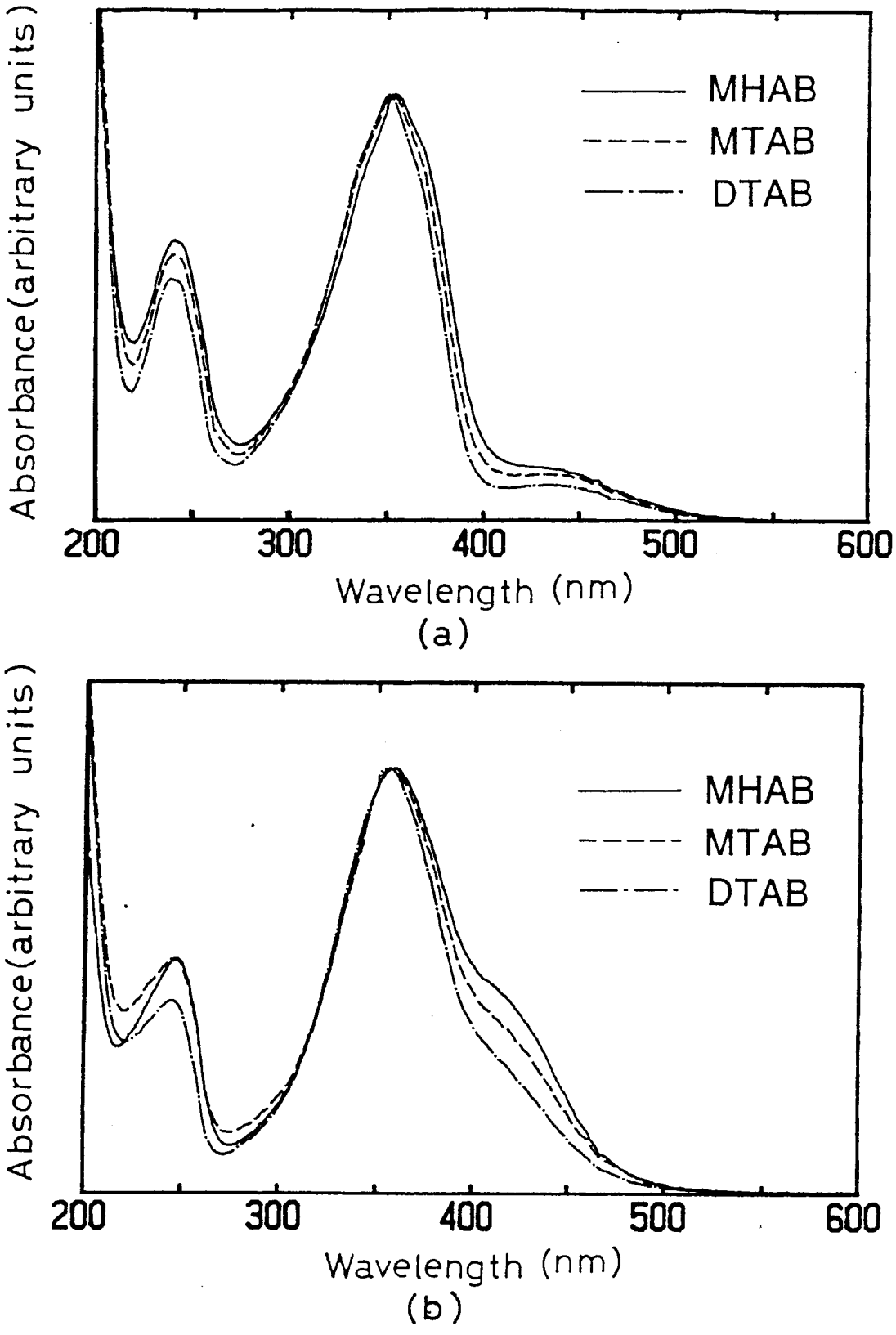

Figure 7-3 Absorption spectra of azobenzene derivatives: (a) in ethanol, (b) in sol-gel films

It should be noted that the relative height of absorbance, A_{420}, of the three azobenzenes at around 420 nm in the sol-gel films is larger than that for MHAB in an aqueous solution and decreases in the order: MHAB > MTAB > DTAB. Values for MHAB in an aqueous solution, MHAB, MTAB and DTAB in sol-gel films were 0.26, 0.46, 0.37 and 0.26, respectively, for a ratio of A_{420} to A_{353} (absorbance at 353 nm) as a measure of the relative intensity of the n-π^* transition. Although DTAB is assumed to be entrapped by the covalent bond formation at the both end of the chromophore inside silica matrix, the absorption spectrum of the chromophore is unexpectedly similar to that in an aqueous solution. This suggests that the spectroscopic behaviors can not be understood solely in terms of hydrogen bond formation.

The small absorption coefficient of azobenzene in the visible is due to the symmetry forbidden n-π^* transition. Reduction of coplanarity of the azobenzene moiety brings about mixing of n-orbitals with π-orbitals to result in the increase in the n-π^* absorption coefficient.[3] This explains why a *cis*-azobenzene with distorted structure has a larger n-π^* absorption coefficient because of the steric hindrance of both phenyl rings, as compared with the *trans* counterpart which possesses planar structure. The same situation is applied to the *trans* isomer-itself. It has been shown that an azobenzene cyclophane displays an anomalously larger absorption coefficient for the n-π^* transition because the chromophore is bent due to the steric hindrance.[4] These facts and theoretical considerations lead to the assumption that the larger A_{420}/A_{353} values reflect the reduction of the coplanarity of the azobenzene chromophore. MHAB, in particular, may be subjected to molecular deformation at least partially because of the strong physical adsorption upon the silica wall through hydrogen bonds between the azo group and silanols which causes mixing of the n-orbitals of the azo group with the π-orbitals. The azo-chromophore of DTAB is isotropically surrounded by silica so that as no marked molecular deformation exists. The azobenzene moiety derived from MTAB is of the intermediate nature. Structural models of the azobenzenes in the sol-gel matrix are illustrated in Figure 7-4.

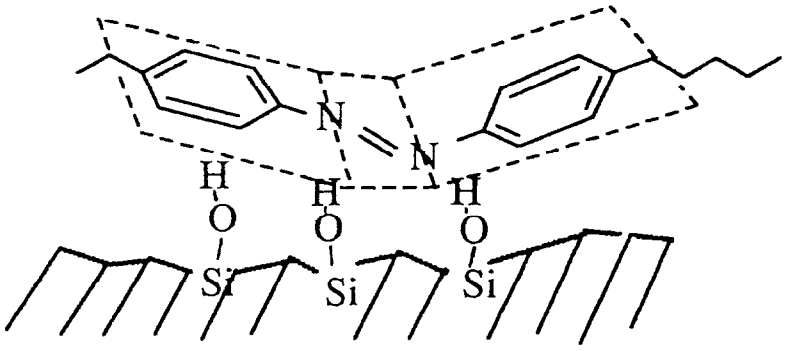

(a) MHAB

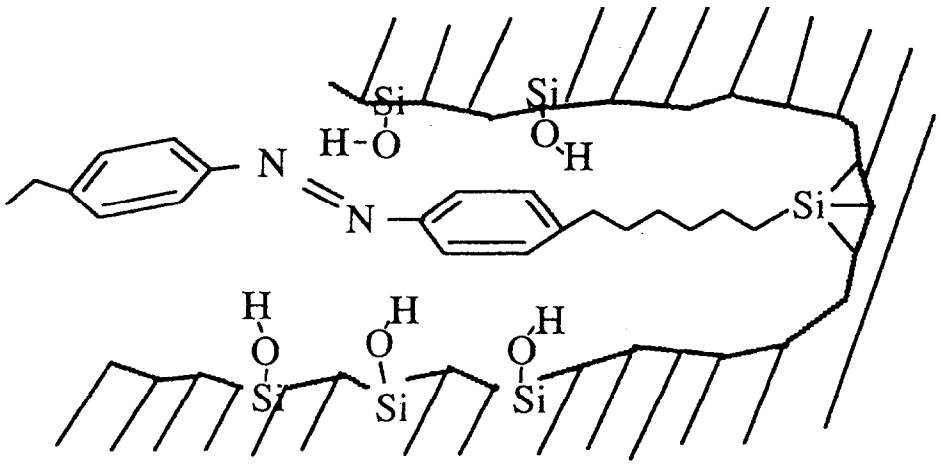

(b) MTAB

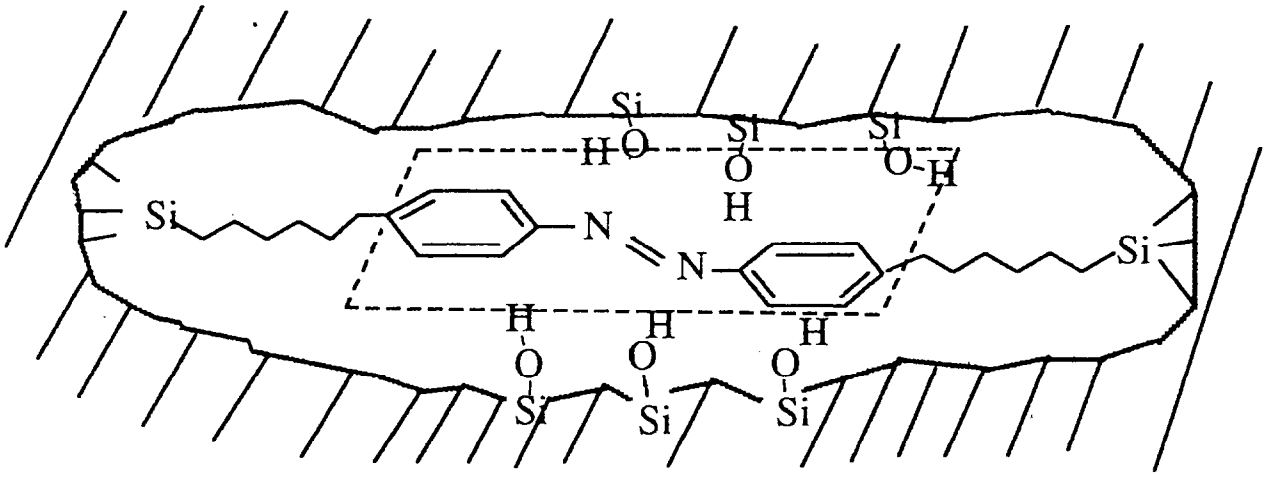

(c) DTAB

Figure 7-4 Structural formula of the three azobenzene derivatives in sol-gel films.

Figure 7-5 shows the change in absorption spectra of the azobenzene derivatives in sol-gel films upon 365 nm photoirradiation. The absorbance around 350 nm decreased and the absorbance around 410 nm increased, indicating the *trans*-to-*cis* photoisomerization occurred in the sol-gel matrices. The appearance of isosbestic points indicates that the *trans*-to-*cis* photoisomerization proceeds without side reaction. Similar changes in absorption spectra were also observed in ethanol or PMMA, while the *cis* fraction in a photostationary state and the photoisomerization behavior were different from those in the sol-gel matrix.

The *cis* fractions (f_{cis} = [cis]/[trans]$_0$) of the azobenzene derivatives in a photostationary state are given by

$$f_{cis} = [cis]/[trans]_0 = \frac{1 - A/A_0}{1 - \varepsilon_{cis}/\varepsilon_{trans}}, \qquad (7\text{-}1)$$

where [cis] is the concentration of the *cis*-isomer in the photostationary state and [trans]$_0$ is the *trans*-isomer concentration before UV irradiation. A_0 and A are the absorbances at λ_{max} before and after 365 nm irradiation, summarized in Table 7-I.

The values of f_{cis} in ethanol were almost identical. It is clear that the silyl group(s) linked with azobenzene unit has no effect on the photoisomerization. Similarly, the values of f_{cis} in PMMA were almost identical to those in ethanol, and 91 - 93 % of the *trans*-isomer isomerizes to the *cis*-isomer. Many studies have dealt with the *trans*-to-*cis* photoisomerization of azobenzene chromophores in solid films of polymers such as PMMA,[5] polycarbonate,[6] polystyrene,[7] epoxy resin,[8] with results similar to ours. These suggest that the PMMA matrix network is coarse enough for molecular motion required for photoisomerization of the azobenzene derivatives even though the azobenzenes have triethoxysilyl group(s).

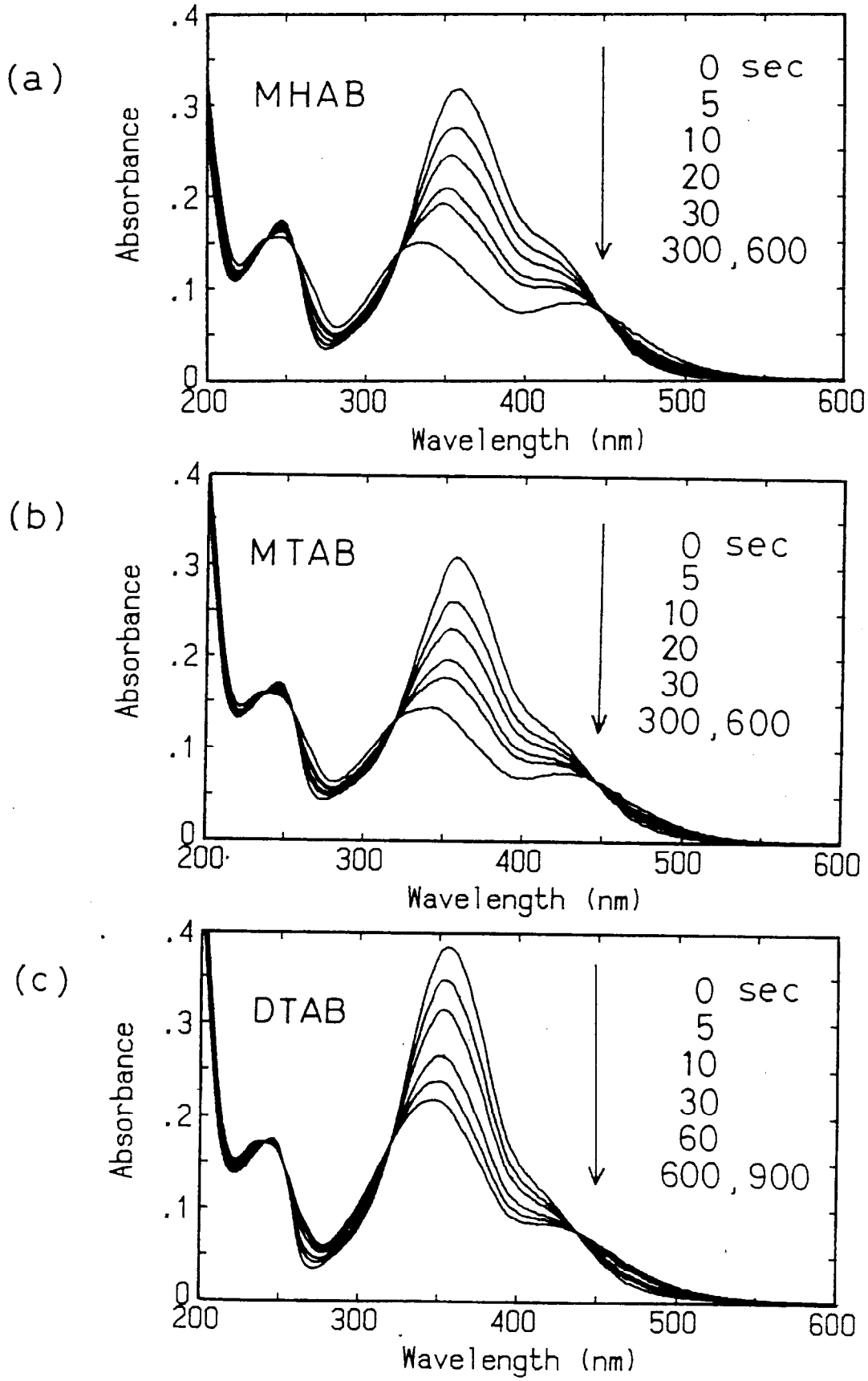

Figure 7-5 Change in UV spectra of trans-azobenzene in a sol-gel film during 365 nm light irradiation at room temperature: (a) MHAB, (b) MTAB, (c) DTAB.

In sol-gel films, the values of f_{cis} were much less than those in ethanol or PMMA, whose order was MHAB = MTAB > DTAB. The results suggest that the partial suppression of the *trans*-to-*cis* photoisomerization is caused by the highly cross-linked network of silica matrix as shown in Chapter 6 and fixation of both sides of the azobenzene of DTAB by silylation restrict molecular motion needed for *trans*-to-*cis* photoisomerization.

The kinetics for *trans*-to-*cis* photoisomerization of azobenzene is expressed by

$$\ln \frac{[t]_0 - [t]_\infty}{[t] - [t]_\infty} = \frac{[t]_0}{[t]_0 - [t]_\infty} = k_{t\text{-}c} \cdot t \qquad (7\text{-}2)$$

where [t], $[t]_0$, and $[t]_\infty$ are the *trans*-isomer concentrations at a given irradiation time, t, before irradiation and in the photostationary state.[6] The rate constant, $k_{t\text{-}c}$, is for the *trans*-to-*cis* photoisomerization. Results obtained for all three azobenzene derivatives in ethanol, PMMA, and sol-gel films plotted according to eq (7-2) are shown in Figure 7-6.

The first-order plots fell in the same line in ethanol, regardless of the azobenzene derivatives. However, the reactions in PMMA deviated from the first-order kinetics, whose slopes were smaller than in ethanol (MHAB = MTAB > DTAB). Such phenomena are characteristic of amorphous polymers, particularly below Tg, and could be due to restriction of segment motion and heterogeneous distribution of local free volume at the reaction sites.[6-8] The lower rate of the photoisomerization of DTAB reflects that the sweep volume of DTAB is larger than that of MHAB or MTAB. In sol-gel films, the first-order plots displayed downward curvature similar to those in PMMA, but the slopes were much smaller, particularly for DTAB. The data shown in Figure 7-6 and Table 7-I indicate that photoisomerization of MTAB in sol-gel matrix is roughly the same as that of MHAB despite connecting one side of the azobenzene moiety to the sol-gel matrix. Photoisomerization is eventually not affected by fixing one side probably because of the relatively long flexible chain.[9]

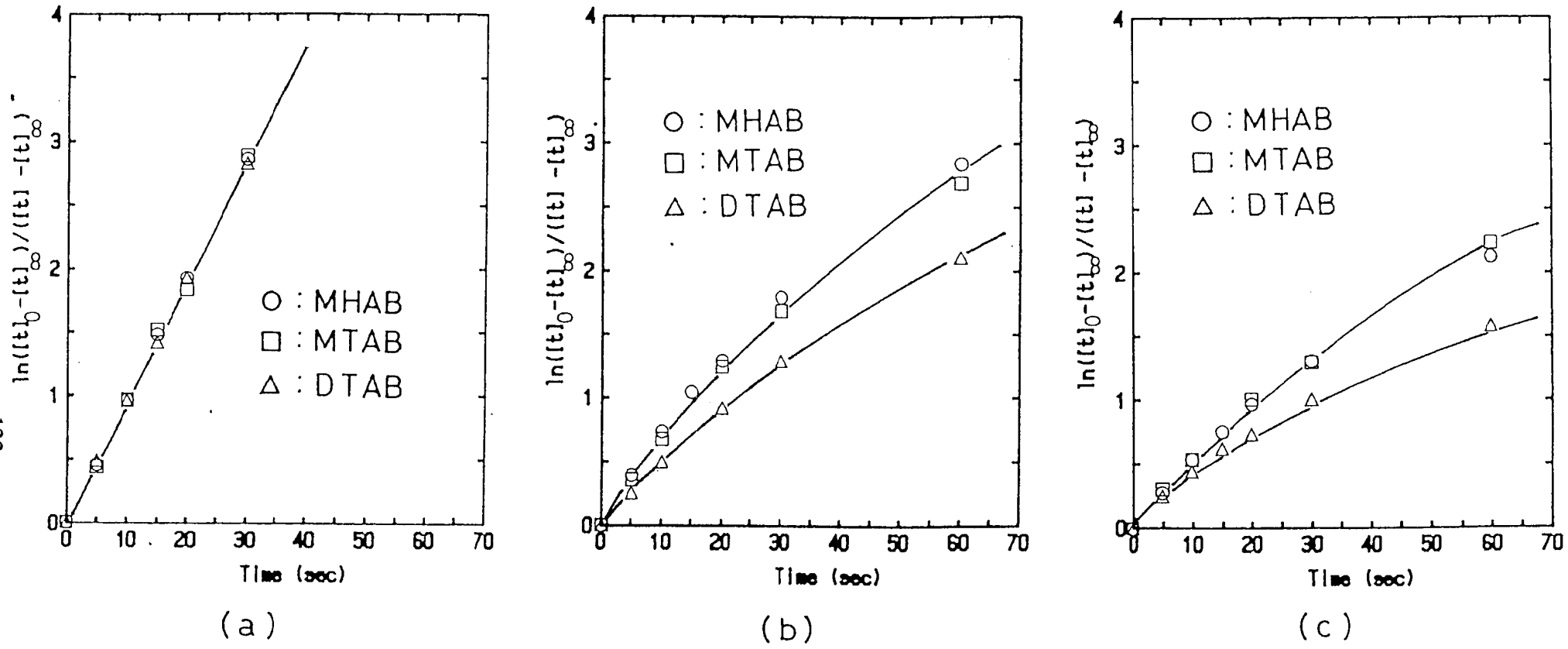

Figure 7-6 First-order plots for trans → cis photoisomerization of azobenzene derivatives at room temperature: (a) in ethanol, (b) in PMMA, (c) in sol-gel films. Errors are within the size of the symbols.

Table 7-I

Photochemical Conversion of Azo Compounds

	f_{cis} (%)		
Species	ethanol	PMMA	sol-gel film
MHAB	93	93	60
MTAB	94	94	60
DTAB	95	91	42

Sung and co-workers have studied free volume environments at different sites in polystyrene by incorporating azobenzene chromophores at sites in chain ends, in the chain center, and in the side chain on a polystyrene backbone, and compared with the result for doped azobenzenes.[10, 11] They showed that the photoisomerization of the center-labeled azobenzene occurred to a smaller extent, mainly due to the smaller free volume. Hence, it is concluded that the photoisomerization of DTAB is much suppressed in the sol-gel film owing to fixation of both sides of the azobenzene moiety to the sol-gel matrix.

In the sol-gel matrix and DMSO, thermal *cis*-to-*trans* reversions of azobenzene derivatives were studied at 60 ℃. DMSO was used here as a non-volatile solvent to avoid change in concentration of the azobenzene derivatives during measurement. The results shown in Figure 7-7 are of the form of first-order plots:

$$\ln \frac{[t]_{H\infty} - [t]_{H0}}{[t]_{H\infty} - [t]} = k_{c\text{-}t} \cdot t \qquad (7\text{-}3)$$

where [t] is the *trans* azobenzene concentration at time, t, and $[t]_{H0}$ and $[t]_{H\infty}$ are concentration of *trans*-isomer in the photostationary state before and after thermal reversion, respectively. The rate constant, $k_{c\text{-}t}$, is for the thermal *cis*-to-*trans* reversion.

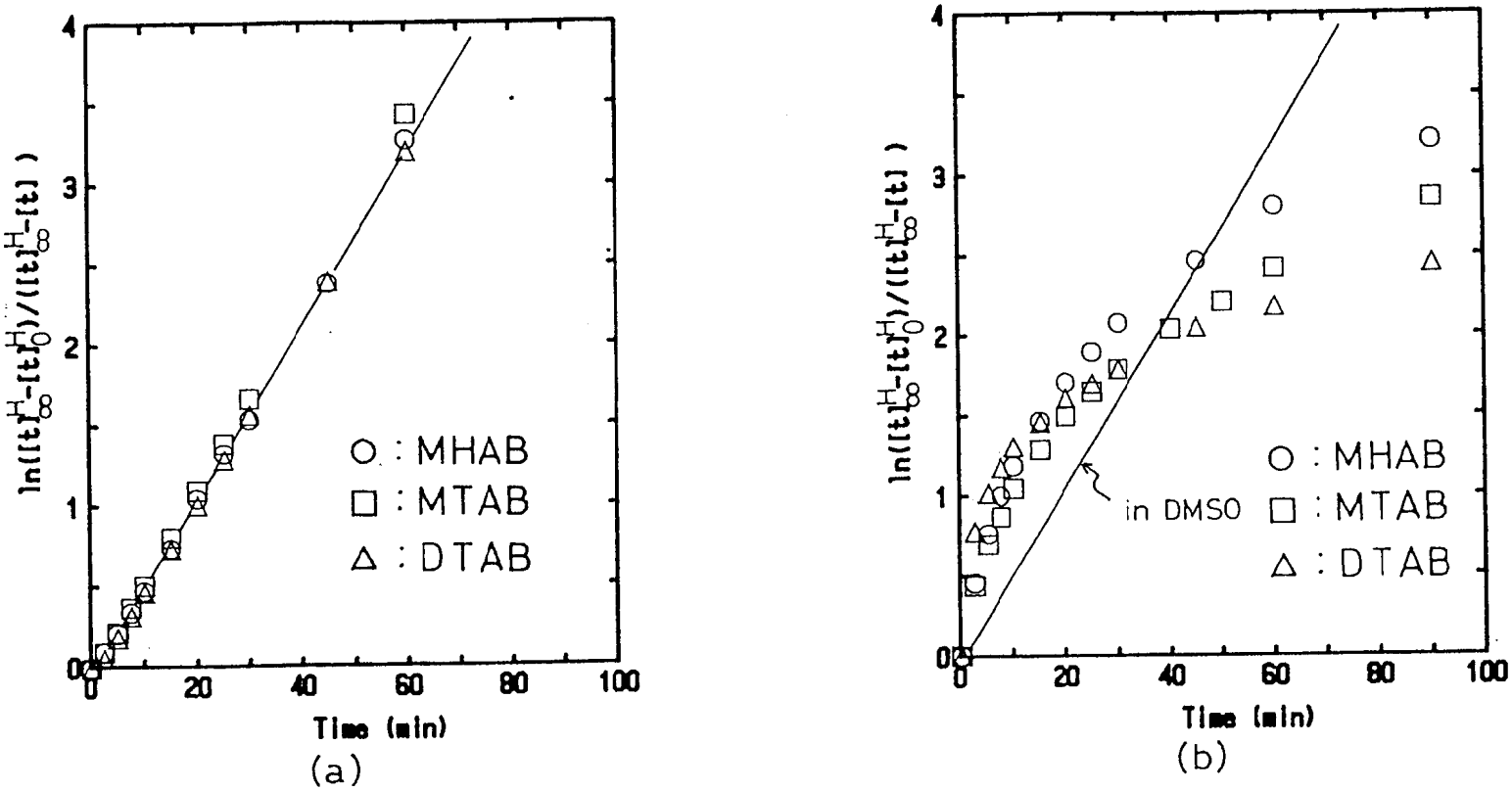

Figure 7-7 First-order plots for thermal cis → trans isomerization of azobenzene derivatives at 60 ℃: (a) in DMSO, (b) in sol-gel films. Errors are within the size of the symbols.

The reaction in DMSO proceeded via first-order kinetics, and the values of k_{c-t} for three azobenzene derivatives were identical (Figure 7-7(a)). The triethoxysilyl group(s) did not affect thermal reversion in solution. In sol-gel films (Figure 7-7(b)), the reaction was initially faster than in solution and decreased gradually with time. Such a rate enhancement at an earlier stage of thermal reversion has been observed in polymer matrices and attributed to residual strain in the *cis*-isomer in the silica matrix produced by UV irradiation because the *cis*-isomer in a strained conformation could revert more easily to the *trans*-isomer than the relaxed *cis* species.[12] The lower reversion rate in the terminal phase may be ascribed to interaction between azobenzene derivatives and the silica matrix. The degree of the rate reduction is different with respect to these three probes, and the rate decreases in the order DTAB > MTAB > MHAB. It is considered that these differences occur due to fixing the azo-chromophore to the silica matrix.

SUMMARY

The n-π^* absorption band of azobenzene chromophore is affected by the nature of silica matrix, by contrast with the π-π^* transition which is not dependent on fluid as well as solid media. The hydrogen bond formation between the azo group and silanols and/or water molecules bound on the silica wall results in blue shift of the n-π^* absorption band. The relative intensity of the blue-shifted band was affected by the nature of bond of the azo-chromophore to the silica matrix. MHAB doped in the matrix without covalent band formation displayed anomalously large n-π^* band intensity because of absorption of the chromophore on the silica wall to induced molecular structure deformation which reduced the coplanarity of the chromophoric system.

Photochemical or thermal isomerization of the azobenzene in solutions was not affected by introduction of triethoxysilyl group(s). In the silica matrix, the *trans*-to-*cis* photoisomerization was suppressed, and the *cis*-isomer produced was in a strained conformation. Fixation of both sides of the azobenzene unit to the silica matrix enhanced the suppression effect to quench photoisomerization of about 60 % of azobenzene units. This supports the view that molecular motion of azobenzene unit

is highly restricted because of the cross-linked silica network.

REFERENCES

1) K. Matsui, T. Matsuzuka and H. Fujita, *J. Phys. Chem.*, **93**, 4991 (1989).

2) A. Levy, D. Avnir and M. Ottolenghi, Chem. *Phys. Lett.*, **121**, 223 (1985).

3) J. Fabian and H. Hartmann, in *Light Absorption of Organic Colorants*, Springer, Berlin, 1980, p. 50.

4) N.Tamaoki, K. Koseki and T. Yamaoka, *Angew. Chem., Int. Ed. Engl.*, **29**, 105 (1990).

5) J. S. Royal , J. G. Victor and J. M. Torkelson, *Macromolecule*, **25**, 729 (1992).

6) I. Mita, K. Horie and K. Hirao, *Macromolecule*, **22**, 558 (1989).

7) T. Naito, M. Kunishige, T. Yamashita, K. Horie and I. Mita, *React. Polym.*, **15**, 185 1991).

8) T. Naito, K. Horie and I. Mita, *Macromolecules*, **24**, 2907 (1991).

9) M. Ueda, H.-B. Kim, T. Ikeda and K. Ichimura, unpublished data.

10) C. P. S. Sung, I. R. Gould and N. J. Turro, *Macromolecules*, **17**, 1447 (1984).

11) W.-C. Yu, C. S. P. Sung and R. E. Robertson, *Macromolecules*, **21**, 355 (1988).

12) C. S. Paik and H. Morawetz, *Macromolecules*, **5**, 171 (1972).

Chapter 8

Photochemical and Thermal Isomerization of Azobenzene Derivatives in Sol-Gel Bulk Materials

INTRODUCTION

There are two methods to yield metal oxide glasses doped with organic molecules as shown in Figure 8-1. The first consists of putting a thin layer of a sol-gel solution on a substrate to form a thin film, followed by drying for relatively short period, whereas bulk glasses are formed by the second method in which a sol-gel solution is slowly evaporated at ambient temperature to give monolithic glass preventing crack formation.

Brinker *et al.* have studied the differences in the structure and properties between sol-gel bulk material and sol-gel thin film utilizing gas adsorption on surface acoustic wave substrate and showed that the structure of films is considerably more compact than that of the bulk xerogels prepared from identical precursors.[1-3] Several reports demonstrated the reason for the microstructural difference between bulk materials and thin films.[1-3] In the film-forming process, the rapid evaporation of solvents forces the chemical precursors into a close proximity with each other and accelerates the condensation reaction significantly. This causes the capillary pressure huge due to the small pores to cause further densification the matrix.[4-6] The slow vaporization of the bulk systems, on the contrary, allows the structure to stiffen in the early drying stage so that the pores are larger and the capillary pressure smaller.[1-3]

Several studies were concerned with the photophysical properties of organic dye molecules in bulk glass and thin film.[7-9] However, there have been few systematic investigations to reveal the difference in chemical behavior of the doped organic molecules ascribed to the microstructural differences between the bulks and the films.

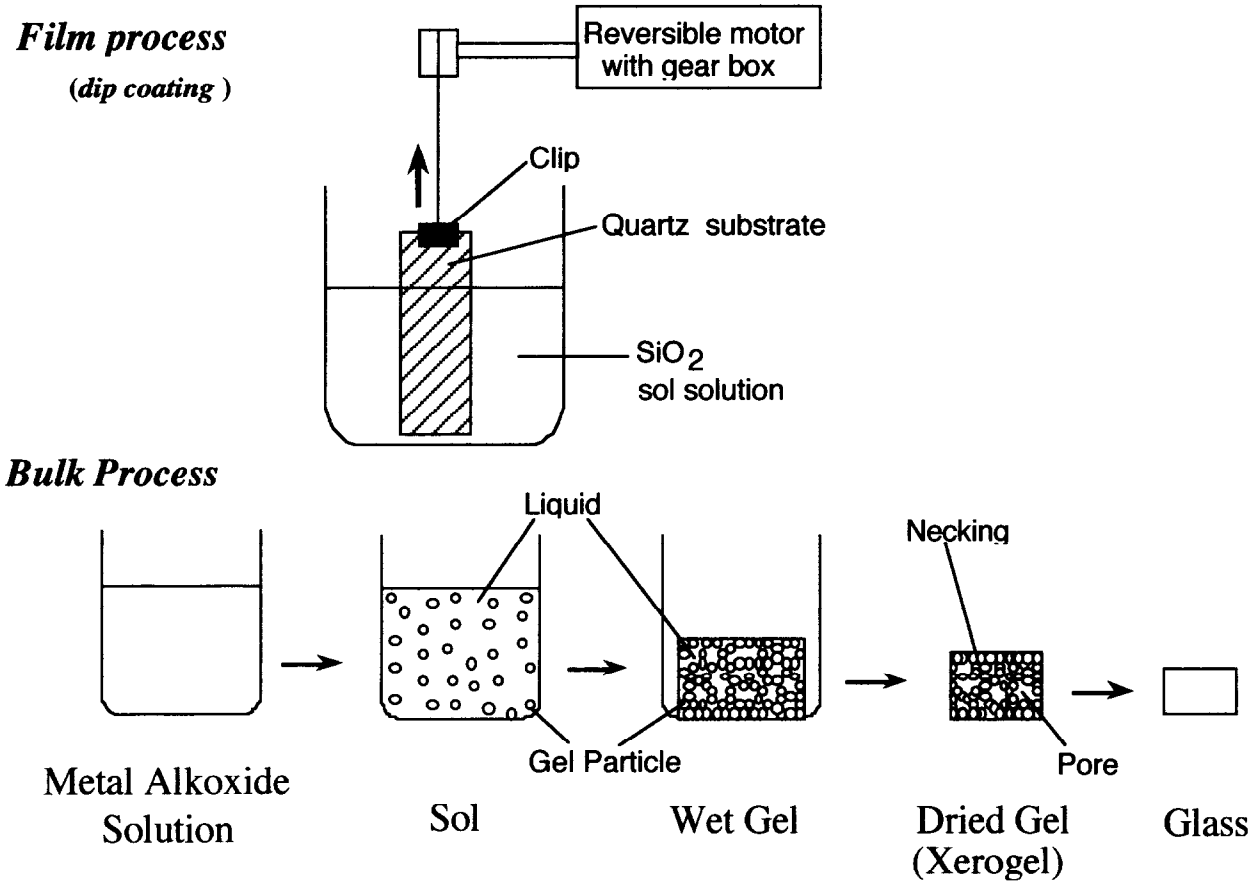

Figure 8-1 Film process and Bulk process

The photoinduced *trans*-to-*cis* isomerization and thermal *cis*-to-*trans* isomerization of azobenzene derivatives in sol-gel silica films were demonstrated in Chapter 6 and 7, taking account of the fact that this type of photochromic compounds is sensitive to the microenvironment and extensively employed as a photoreactive probe to estimate the free volume and rigidity of solid polymers. The results are summarized as follows:

(1) The *cis* fraction of a photostationary state in a sol-gel film was much smaller than in poly(methyl methacrylate) (PMMA), an organic glass, suggesting that the free volume in sol-gel silica films is smaller than in PMMA films.

(2) In a sol-gel film, attachment of the chromophore to silica through a single covalent bonding had slight effect on photochemical as well as thermal isomerizations, whereas the photoisomerization

was markedly suppressed when an azobenzene is fixed to the silica matrix at both ends of the chromophore.

The major concern of this chapter is to disclose outstanding differences in microenvironmental structures between a monolithic silica bulk and a silica film by means of evaluating the reactivity of doped azobenzenes as probe molecules.

EXPERIMENTAL

Materials

Tetraethyl orthosilicate (TEOS), purchased from Tokyo Kasei Kogyo Corp., was used without further purification. Ethanol, diethyl ether, dimethyl sulfoxide (DMSO), cyclohexane and water were of spectroscopic grade. 4-Methoxy-4'-(2-hydroxyethoxy) azobenzene (MHAB), 4-methoxy-4'-(*N*-(3-triethoxysilylpropylcarboxymethoxy)azobenzene (MTAB), 4,4'-bis(*N*-(3-triethoxysilylpropyl)-carbamoylmethoxy)azobenzene (DTAB), poly(methyl methacrylate) (PMMA) films, and sol-gel films doped with these azobenzene probes were prepared as described in Chapter 7. The thickness of the sol-gel film was calculated to be *ca.* 200 nm with use of absorbances of the azobenzenes under the following assumptions; all TEOS is converted into silica, the density of the film is 2.0, and the absorption coefficient of azobenzenes are not affected by embedding. Monodisperse silica particles (a BET surface area: 48 m^2, particle diameter: 150 nm) were obtained from Tokuyama Corp.

Sample Preparation

Sol-gel Process

The composition to prepare sol-gel bulks by the hydrolysis of TEOS catalyzed by hydrochloric acid in ethanol was the same as a film-coating solution (TEOS : H_2O : ethanol = 1 : 2 : 3 in molar ratio). MHAB, MTAB and DTAB were dissolved in ethanol at 7.0×10^{-5} mol/L, respectively. The mixtures were stirred for 2 h at room temperature. Subsequently, a 10 ml portion of each mixture was poured into a flat Petri dish (inner diameter 42 mm; height 23 mm), the surface of which was

treated with octadecyltriethoxysilane in advance. The Petri dishes were covered with an aluminum foil and left to gel at room temperature for 3 days. After gelation the aluminum foil was perforated with a few holes (diameter 1 mm) and then with additional holes on subsequent days. After 30 days, the bulk gels were heated at 60 ℃ for 24 h and at 110 ℃ for 30 h to give monolithic crack-free bulk samples containing the azobenzene derivatives (diameter 27 mm, thickness 1.2 mm).

Physisorption of MHAB on the Surface of Silica Particles

The physisorption of MHAB on the surface of silica particles was carried out as follows: To a dispersion of the silica particles (0.50 g) in chloroform (25 ml) was added 218 mg of MHAB, and the mixture was stirred for 1 h at room temperature. After being centrifuged, the supernatant was discarded. The residual colloidal silica was repeatedly washed with cyclohexane and dried at 60 ℃ *under vacuo* for 10 h. The amount of physisorbed MHAB was determined by means of electronic absorption measurement using the absorption coefficient of MHAB =21000 $M^{-1}cm^{-1}$ at 354 nm. An average density was estimated to be one MHAB molecule in 600 $Å^2$ on the silica surface.

Chemisorption of MTAB on the Surface of Silica Particles

Chemisorbed MTAB silica particles were prepared by the reaction of MTAB with surface silanols of silica particles according to the method of Hörner *et al.*[10] with a slight modification. To a dispersion of the silica particles (0.50 g) in dry benzene (15 ml) was added 539 mg of MTAB, and the mixture was refluxed for 48 h. After centrifugation, the supernatant was discarded. Residual silica particles were washed repeatedly with benzene and methanol and dried at 60 ℃ *in vacuo* for 10 h. An average density of the azobenzene was one MTAB molecule in 500 $Å^2$ on the silica surface.

Measurements

For the *trans*-to-*cis* photoisomerization, a sample was irradiated at 365 nm by using a Jasco CRM-FA irradiator equipped with a 2-kW xenon arc lamp and a monochromator at room temperature. Absorbance measurement was made on a Hitachi UV-320 spectrometer. Azo-modified silica particles

were dispersed in cyclohexane because of the good refractive index matching. The thermal *cis*-to-*trans* isomerization were carried out at 60 ℃ and followed spectroscopically at the same temperature.

RESULTS

Absorption Spectral Changes during Drying Process

Three types of azobenzene having the same chromophoric system were incorporated in silica glass to survey the effect of covalent attachment on the photoactive probe behavior to obtain microstructural information of bulk silica matrices. Ethanolic solutions of TEOS and the corresponding azobenzene were acidified by hydrochloric acid to result in the hydrolysis and subsequent gelation, followed by gradual evaporation of solvents to yield gelled silica in the conventional way. The solutions turned red on acidification due to the protonation of the azobenzene which is a very weak base (pKa = -2.95 for *trans*-azobenzene). [11] Figure 8-2 shows the change in absorption spectra of MHAB as a typical example in a bulk system during the drying process. The bulk sample possesses absorption maximum (λ_{max}) at 499 nm assignable to the protonated form even after heat treatment at 60 ℃ for 24 h. Upon additional heating at 110℃ for 30 h, the color of the sample became light yellow, and λ_{max} was shifted to 353 nm, indicating the completion of the deprotonation.

For comparison, silica glass films doped with the azobenzenes were prepared by use of the same solutions according to the so-called dip-coating technique.[12] A quite different color change behavior was observed for sol-gel films. Although a thin silica film coated on a quartz plate by means of the dip coating method was red, the color turned light yellow within 10 min when the plate was heated at 60 ℃. Actually, the absorption spectrum of the thin film was superimposed upon that of a free azobenzene after heating at 60 ℃ for 2 h (Figure 6-6 in Chapter 6).

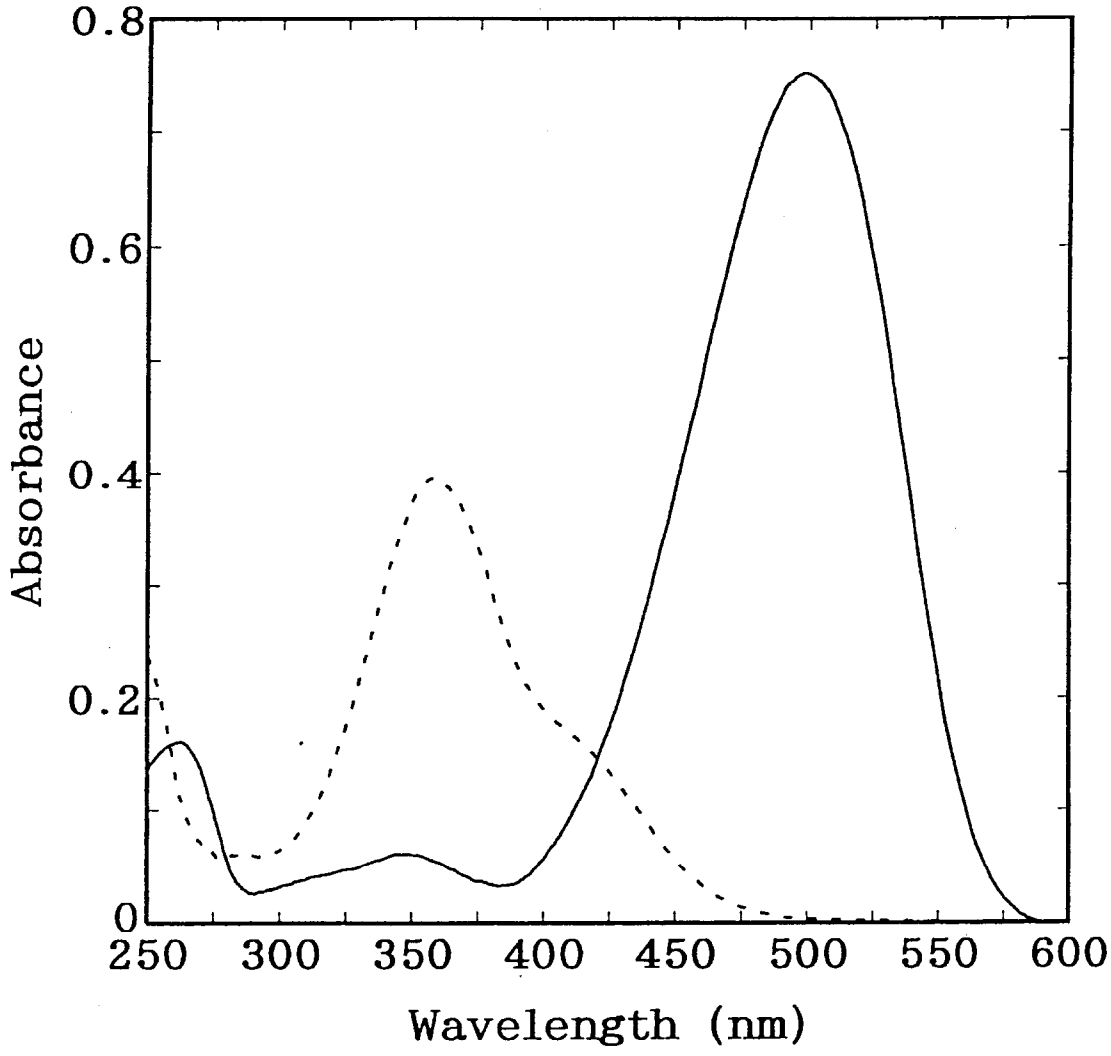

Figure 8-2 Change in absorption spectra of MHAB during drying stage of a sol-gel bulk: heating at 60 ℃ for 24 h (——) and then additional heating at 110 ℃ for 30 h (- - - - -).

Trans-to-Cis Photoisomerization in Bulk Glasses

After confirming the formation of free base azobenzenes by heat treatment, monolithic bulk plates were exposed to UV light at 365 nm. Figure 8-3(a) shows the spectral change of MHAB in a bulk glass. MTAB gave a similar result, implying that a single covalent attachment of the azo chromophore plays no role in the photoisomerizability. In contrast to our previous observation that the photoconversion into the *cis*-isomer is restricted in a sol-gel film, the transformation of the *trans*-isomer in the bulk glass took place quite efficiently without any disturbance. This suggests that the azo chromophores are not incorporated in the silica network but rather localized on walls of porous structures to ensure free volumes for the molecular structural changes. To confirm this assumption, MTAB and MHAB were treated with colloidal silica particles to cover the silica surface with the azobenzene chromophore physically as well as chemically and to review the photoisomerizability. Monodisperse colloidal silica of a diameter of 150 μ m was employed because of the large surface area to adsorb a sufficient amount of the chromophore and the availability of a transparent dispersion in cyclohexane owing to good refractive index matching which enabled us to carry out spectroscopic analysis.

Parts (b) and (c) of Figure 8-3 show the absorption spectra of dispersions of colloidal silica particles physisorbed with MHAB and chemisorbed with MTAB respectively before and after UV irradiation. The n-π* transition of the azobenzene chromophores adsorbed on silica particles is blue-shifted so that the absorption band appears as a shoulder at around 420 nm. The blue shift is ascribed to hydrogen bonding between the azo group and silanols and/or water molecules on the silica surfaces as described in Chapter 6 and 7. The absorption spectral shapes of the colloidal silica bear a close resemblance to that of the bulk (Figure 8-3(a)). Therefore, the azobenzenes on silica particles are intimately adsorbed on the surface since the blue shift is observed even in the non-polar cyclohexane.

Furthermore, the n-π* absorption of the forbidden transition is enhanced in these cases when compared with solution spectra. As discussed in Chapter 7, the increase in the n-π* absorption coefficient can be reasonably explained in terms of the distortion of azobenzene moiety which leads to the mixing of forbidden n orbitals with allowed π-orbitals. In other words, the ratio of the n-π*

absorbance (A_n) to the π-π* absorbance (A_π) can be assumed to be a measure of the extent of molecular distortion of azobenzene chromophoric systems. Although A_n values involve a certain inaccuracy because of the overlap with A_π, the absorbances at 420 nm were employed for A_n values for semiquantitative discussion. The absorbance ratios (A_n/A_π) for the bulk, physisorbed particles and chemisorbed particles were 0.42, 0.31, and 0.26, respectively. These values imply that the molecular distortion due to the surface adsorption appears most markedly in the bulk glass, whereas the chemisorbed chromophore seems to be distortion-free since the A_n/A_π value equals to that in a solution of 1 : 9 mixture of ethanol and water.

As shown in parts (b) and (c) of Figures 8-3, the *trans*-to-*cis* photoisomerization of azobenzene chromophores on the silica particles went almost to completion without being affected by the strong adsorption on the surface. This means that the photoisomerization of the azobenzene immobilized in silica matrices takes place readily as long as the azo-chromophores are bound on the wall of porous silica sol-gel bulk matrices.

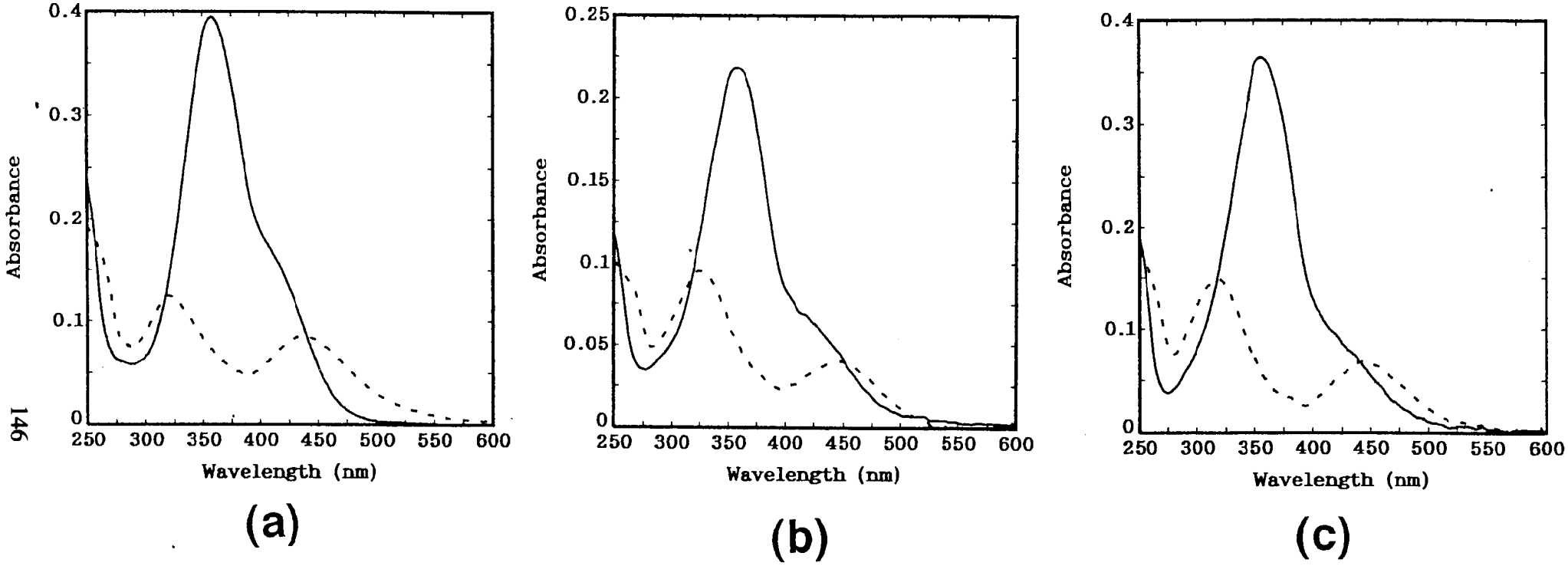

Figure 8-3 Absorption spectra of azobenzenes: (a) MHAB in a sol-gel bulk, (b) MHAB physisorbing on the surface of silica particles in cyclohexane (concentration: 0.83 g / L), (c) MTAB chemisorbing on the surface of silica particles in cyclohexane (concentration: 1.0 g / L). Solid lines and broken lines indicate before and after prolonged irradiation with a UV light, respectively.

Thermal Isomerization

To obtain further information on the mobility of the azobenzene moieties in the bulk glasses, the author studied the kinetics of the thermal *cis*-to-*trans* isomerization. The thermal *cis*-to-*trans* isomerization is expressed by first-order kinetics according to the following relation:

$$\ln \frac{A_{H\infty} - A_{H0}}{A_{H\infty} - A_{Ht}} = K \bullet t \qquad (8\text{-}1)$$

where K is the rate constant for the thermal isomerization. A_{H0}, A_{Ht}, and $A_{H\infty}$ are observed absorbances in the peak of the π-π^* band of the respective *trans*-isomers at subscript times. These absorbances are substantially proportional to concentrations of the *trans*-isomer in view of the low extinctions of the corresponding *cis* forms at the monitoring wavelength.

In a DMSO solution, as described in Chapter 7, the reaction proceeds by first-order kinetics and the slopes (K) of three azobenzene derivatives were the same. First-order plots for the thermal isomerization of three azobenzenes in PMMA films and in the sol-gel bulks and films at 60 ℃ are shown in Figure 8-4. In PMMA films, the shapes of the plots are similar with regard to all three probes. The reaction deviates from a straight line gradually with time, and the degree of the rate reduction is in the following order; MHAB < MTAB < DTAB (Figure 8-4(a)). The results suggest that the thermal *cis*-to-*trans* isomerization can be retarded by the steric restriction of PMMA matrix. This reduction order can be explained in terms of the size of the sweep volume required for the thermal *cis*-to-*trans* isomerization (MHAB < MTAB < DTAB). On the other hand, a different behavior of the rate between the derivatives was observed in sol-gel bulks (Figure 8-4(b)). The reaction of MHAB follows first-order kinetics just as in solution, which implies that the isomerization is not affected by a matrix of sol-gel bulk. While the rate of MTAB slows down with time, the isomerization of DTAB proceeds faster than in solution in the beginning and decreases after that.

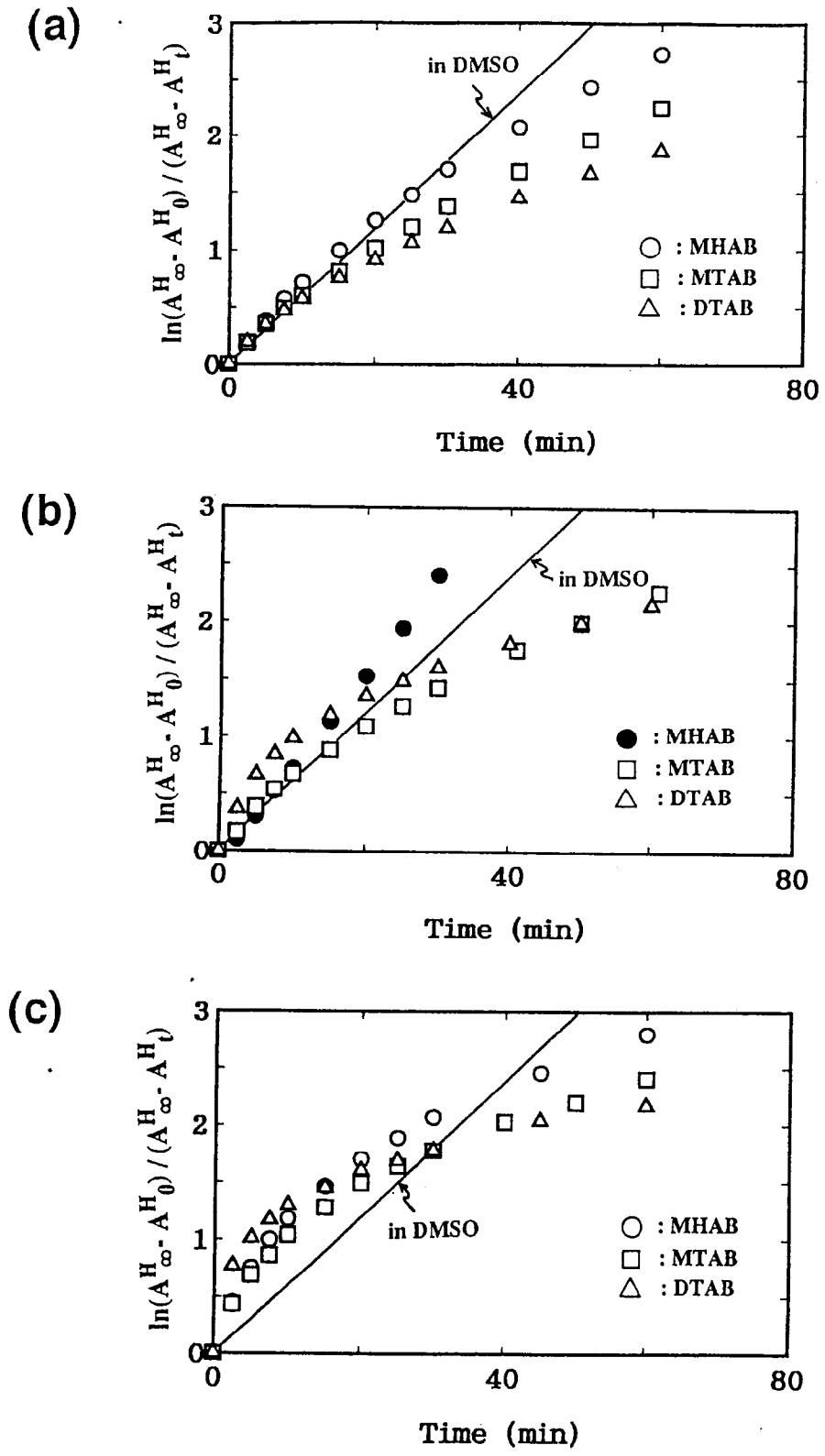

Figure 8-4 First-order plots for the thermal cis-to-trans isomerization of azobenzene derivatives at 60 ℃: (a) in PMMA; (b) in sol-gel bulks; (c) in sol-gel films.

The straight solid lines are plots in DMSO. Experimental errors are within the symbols.

DISCUSSION

The n- π * transition absorption band afforded a 2-fold information concerning microenvironmental polarity and location of the chromophore. As stated above as well as in Chapters 6 and 7, a considerable blue shift of the absorption band indicates hydrogen bond formation of the azo group. Furthermore, the enhancement of the blue-shifted absorbance in the bulk matrix may reflect the strong adsorption of the azo chromophore on walls of highly porous silica.

Some reports dealt with the photochromic behavior of a fulgide and spiropyranes in sol-gel bulk.[13-17] However, these photochromic compounds seem to be inappropriate to estimate the rigidity of the matrix since the molecular movement associated with these 6 π electrocyclic reactions is very small and the photochromism of spiropyrans is too markedly affected by the polarity of matrices. In this respect, for more detailed discussion based on the photochemical behavior of azobenzene as a photoprobe, the *cis* fractions in the photostationary state (f_{cis}) on the surface of silica and in the sol-gel bulks were estimated by using eq (8-2) and summarized in Table 8-I. The f_{cis} values in sol-gel films and in PMMA obtained in Chapter 7 are also listed in Table 8-I. A_0 and A stand for the absorbance at λ_{max} before and after UV irradiation whereas ε_{cis}, ε_{trans} denote the molar absorption coefficients of the *cis* and the *trans* isomers at λ_{max}, respectively.

$$f_{cis} = \frac{1 - A / A_0}{1 - \varepsilon_{cis} / \varepsilon_{trans}} \qquad (8\text{-}2)$$

As Table 8-I shows, the *trans*-to-*cis* photoisomerization goes almost to completion even though azobenzene probes are adsorbed on the surface of silica. This suggests that the final *cis* fraction is affected predominantly by micropore size of the silica matrix. The *cis* fractions in a photostationary state of three azobenzenes in the sol-gel bulks are much larger than those of the corresponding azobenzenes in the sol-gel films. This implies that there are differences in the structure

and properties between sol-gel thin films and sol-gel bulk materials; micropore size or free volume of the bulk material is markedly larger than that of the sol-gel film.

There was no marked difference in the photoisomerizability between MHAB and MTAB in the sol-gel bulks. However, the *cis* formation was considerably reduced for DTAB, just as in the case of a sol-gel thin film. The suppression of the photoisomerizability is obviously ascribable to the fixation of both ends of the azobenzene chromophore to silica matrix through Si-O bondings. Such a effect was not observed in PMMA films in which DTAB is entrapped only physically.

Table 8-I

Photochemical Conversion of Azo Compounds

	f_{cis} (%)			
Species	PMMA	Surface of silica particle*	Sol-gel film	Sol-gel bulk*
MHAB	93	87	60	91
MTAB	94	90	60	86
DTAB	95	—	42	66

* The experimental errors are within ± 2 %.

Thermal isomerization analysis disclosed a striking feature of the bulk that the reaction of MHAB in a sol-gel bulk obeys first-order kinetics which is very close to that in the solution phase (Figure 8-4(b)). This result also, in conjunction with the photoisomer composition of the photostationary state, suggests that the pore of the sol-gel bulk materials is so large as to cause essentially no suppressive effect on the isomerization of the azobenzene molecules inside the silica cage. This is in decided contrast with the facts that the thermal isomerization deviates from the first order kinetics not only in silica films but also even in polymeric matrices including a PMMA solid unless the reactions are carried out above their glass transition temperatures. Unexpectedly, the rate was rather slightly higher than that in the solution. This may reflect probably the alteration of the molar extinction coefficient of

the azo-chromophore entrapped in the matrix to lead to a slight overestimation of the rate.

In sol-gel films, the non-linear first-order plots of the *cis*-to-*trans* isomerizations of MTAB were almost the same as those of MHAB (Figure 8-4(c)). On the other hand, in the sol-gel bulk materials, the rate for the thermal isomerization of MTAB differs from that of MHAB, and the rate deviated from the first-order kinetics and slowed down gradually with time. These results support the idea that the steric restriction due to smaller pores governs the reactivity in sol-gel films preferentially. Consequently, the reverse isomerization behavior of azobenzene moiety fixed in sol-gel films through a single covalent bond does not differ markedly from that of the chromophore fixed in sol-gel films at the both sides. Contrary to this, the isomerization behavior in the bulk materials is influenced by the fixation mode of the chromophore more evidently since the pores of the matrix are large than those in sol-gel films so that the free molecular motion is considerably suppressed by attachment of the chromophore on a silica wall. The thermal isomerization of DTAB in the sol-gel bulk is initially faster than in a solution because the photogenerated *cis* isomer has a strained conformation[18] and decreases gradually with time. A similar phenomenon was observed for these azobenzenes in sol-gel films.

As mentioned above, spectroscopic changes clearly show that the evaporation process is much faster in the film formation than in the bulk formation. As a result, the structure of film becomes more dense than those of the corresponding bulk xerogel prepared from the identical precursor.

SUMMARY

The behavior of azobenzenes as probe molecules in sol-gel silica matrix have revealed that bulk materials differ from silica films markedly in the following points.

(1) Azobenzene hydrochlorides, which are formed by protonation with hydrochloric acid from the hydrolysis of TEOS, are subjected to the deprotonation during the backing for drying of sol-gel silica. The deprotonation takes place in bulk materials much slower than in sol-gel films.

(2) Comparison of absorption spectra of azobenzenes in bulk materials with those adsorbed on colloidal silica particles reveals that the probe molecules are adsorbed more strongly on the silica wall of bulk material so that the molecular frame is distorted although the free volume for the photoisomerization is sufficiently ensured.

(3) The first-order kinetics of the thermal isomerization of the photoinduced *cis* isomer reveals that the steric restrictions to suppress the molecular motion increases in the following order; sol-gel bulk < PMMA < sol-gel film. In particular it should be noteworthy that the *cis*-to-*trans* thermal isomerization of MHAB obeys first-order kinetics even though the probe compound is entrapped in solid bulk material, reflecting much larger free volumes in the sol-gel bulk silica matrix so that the isomerizations of azo chromophore take place as readily as in solution. These may lead to a novel conclusion that reactions, at least unimolecular reactions, of organic molecules entrapped physically in bulk materials does not undergo suppressive effect caused by silica matrices.

REFERENCES

1) C. J. Brinker, A. J.; Hurd and K. J. Ward, in *Ultrastructure Processing of Advanced Ceramics*; Eds. J. D. Mackenzie and D. R. Ulrich, Wiley, New York, 1988, P. 223.

2) C. J. Brinker, A. J.; Hurd, G. C. Frye, K. J. Ward and C. S. Ashley, *J. Non-Cryst. Solids,* **121**, 294 (1990).

3) C. J. Brinker, A. J.; Hurd, G. C. Frye, P. R. Schunk and C. S. Ashley, *Nippon Seramikkusu Kyokai Gakujutsu Ronbunshi*, **99**, 862 (1991).

4) L. E. Scriven, in *Better Ceramics Through Chemistry III*, Eds. C. J. Brinker, D. E. Clark and D. R. Ulrich, Mater. Res. Soc., Pittsburgh, PA, 1988, p. 717.

5) C. J. Brinker, G. C. Frye, A. J. Hurd and C. S. Ashley, *Thin Solid Films*, **201**, 97 (1991).

6) C. J. Brinker, A. J. Hurd, P. R. Schunk, G. C. Frye and C. S. Ashley, *J. Non-Cryst. Solids,* **147/148**, 424 (1992).

7) R. Gvishi and R. Reisfeld, *J. Non-Cryst. Solids*, **128**, 69 (1991).

8) C. Burgdorff, H.-G. Lohmannsroben and R. Reisfeld, *Chem. Phys. Lett.*, **197**, 358 (1992).

9) H. Inoue, T. Iwamoto, A. Makishima, M. Ikemoto and K. Horie, *J. Opt. Soc. Am. B*, **9**, 816 (1992).

10) L. Hörner and H. Ziegler, *Z. Naturforsch., B: Chem. Sci.*, **42**, 43 (1987).

11) F. Gerson, E. Heilbronner, A. van Veen and B. M. Wepster, *Helv. Chim. Acta.*, **43**, 1889 (1960).

12) S. Sakka, K. Kamiya, K. Mikita and Y. Yamamoto, *J. Non-Cryst. Solids*, **63**, 223 (1984).

13) V. R. Kaufman, D. Levy and D. Avnir, *J. Non-Cryst. Solids*, **82**, 103 (1986).

14) D. Levy and D. Avnir, *J. Phys. Chem.*, **92**, 4734 (1988).

15) D. Levy, S. Einhorn and D. Avnir, *J. Non-Cryst. Solids*, **113**, 137 (1989).

16) K. Matsui, T. Morohoshi and S. Yoshida, *MRS Int'l. Mtg. on Adv. Mats.*, **12**, 203 (1989).

17) D. Preston, J.-C. Pouxviel, T. Novinson, W. C. Kaska, B. Dunn, J. I. Zink, *J. Phys. Chem.*, **94**, 4167 (1990).

18) C. S. Paik and H. Morawetz, *Macromolecules*, **5**, 171 (1972).

Chapter 9

Photochemical Behaviors of Tethered Dianthryl Compounds in Sol- Gel Glass

INTRODUCTION

In Chapter 6, 7, and 8, the author reported the photochemical and thermal isomerization of hydrophilic azobenzene derivatives when used as photochromic probes to reveal microenvironments within sol-gel matrices. The azo-groups are hydrogen bonded in inorganic matrices, and both the retardation of the photoisomerization and the deviation from linear first-order kinetics of the thermal reversion process are markedly influenced by the preparation conditions of sol-gel silica and also molecular structures of azo-photoprobes; this reflects the entrapment of organic molecules in the highly cross-linked network structures.

Anthracene photodimerizes upon UV irradiation and recovers again upon exposure of the dimer to light of a shorter wavelengths.[1)] This chapter deals with the intramolecular photodimerization of 1, 3-bis(9-anthryl)propane-1-ol (BAP) and bis(9-anthrylmethyl)amine (BAA) (Figure 9-1) in sol-gel silica matrices, however, two points were noted, in particular. First, in contrast to azobenzenes, which hydrogen bond to the silica walls, the aromatic hydrocarbon chromophores are entrapped in the inorganic matrices without the formation of hydrogen bonds with the surface silanol residues so that the extent of the photodimerization is directly affected by the free volumes of the inorganic matrices. Secondly, anthracene when used as a photoprobe possesses dual characteristics that reflect the rigidity of the solid matrices; the intramolecular photodimerization is accompanied by a much larger molecular structural change whereas the photoinduced dissociation of photodimers requires a very small free volume in the reaction matrices. The purpose of this chapter is to obtain further information on the mobility of the organic molecules embedded within the sol-gel matrices. Studies of competitive photooxidation behavior of the anthracenes were also made to reveal the permeation of atmospheric

oxygen into the inorganic matrices.

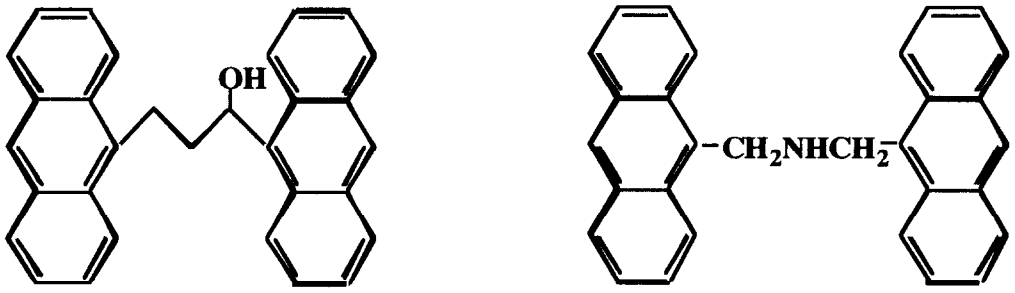

BAP **BAA**

Figure 9-1 Chemical structures of 1,3-bis(9-anthryl)propane-1-ol (BAP) and bis(9-anthrylmethyl)amine (BAA)

EXPERIMENTAL

Materials

Tetraethyl orthosilicate (TEOS) and tetramethyl orthosilicate (TMOS) were purchased from Tokyo Kasei Kogyo Corp. and used without further purification. Methanol, ethanol, ether, tetrahydrofuran (THF) and water were of spectroscopic grade. Poly(methyl methacrylate) (PMMA, Mn = 1.0 × 10^5, Tg = 105 ℃) was obtained from Wako Pure Chemical Corp. Poly(vinyl alcohol) (PVA; degree of polymerization = 2000, degree of saponification = 98.5-99.4 mol %) was available from Nippon Gosei Kagaku Kogyo Corp. 1, 3-Bis(9-anthryl)propane-1-ol (BAP) was prepared according to the literature.[2)]

Bis(9-anthrylmethyl)amine (BAA)

BAA was prepared according to the reaction scheme in Figure 9-2. To a methanol-THF (1:1) mixture (50 ml) containing 1,3-bis(9-anthryl)-2-azapropene[3)] (1.0 g, 2.5 mmol) was added a few drop

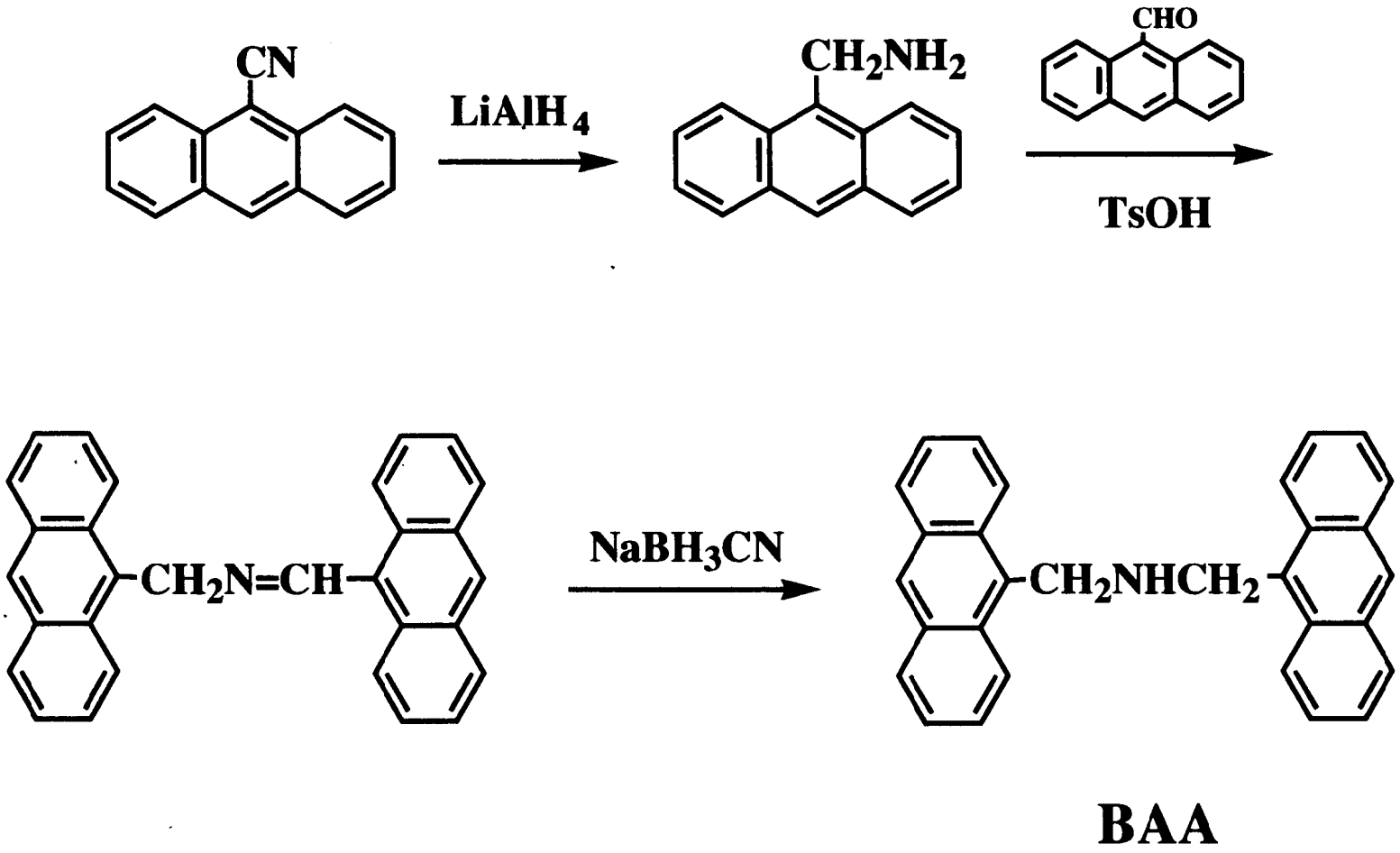

Figure 9-2 Synthetic pathway of BAA

of concentrated HCl and sodium cyanoborohydride (0.30 g, 4.8 mmol). After stirring the mixture for 1 h at room temperature, the solvent was evaporated off under reduced pressure. To the residual mass was added 2 wt% aqueous NaOH, and the resulting solution was extracted twice with chloroform. The organic layers were combined, washed twice with a saturated aqueous NaCl solution, and dried over anhydrous potassium carbonate. After filtration, the solvent was evaporated off, and the residue repeatedly recrystallized from ethanol to give light-yellow crystals of BAA · $1/2C_2H_5OH$; mp 192-194 ℃ in a 77% yield. ^{1}H-NMR ($CDCl_3$) δ : 1.2 (1.5H, t, CH_3CH_2OH), 3.6-3.9 (1H, q, CH_3CH_2OH), 4.9 (4H, s, $-CH_2-$), 7.3-8.4 (18H, m, aromatic). IR (KBr): 2830, 1620, 1440, 890, 725 cm^{-1}. Anal. Calcd. for $C_{30}H_{23}N$ · $1/2C_2H_5OH$: C, 88.54; H, 6.23; N, 3.33 %. Found: C, 88.23; H, 5.93; N, 3.12 %.

Intramolecular photodimerization of BAA

A degassed solution of BAA (20.0 mg, 5.0×10^{-5} mol) in THF (250 ml) was irradiated in a Pyrex vessel with UV (300 nm $< \lambda <$ 390 nm) light using a 500 W super-high-pressure mercury lamp and a Toshiba cut-off filter (UV-D36A) for 30 min. After confirmation of the disappearance of the absorption band corresponding to the anthracene ring (*vide infra*), the solvent was evaporated off to give the intramolecular photodimer (DBAA) in the form of a powder.

Sample Preparation

The sol-gel bulk materials doped with either BAA or DBAA were prepared by the hydrolysis of TMOS, without catalyst, according to the procedure reported by Yamane *et al.*[4] A mixture of 9.7 ml of TMOS, 4.8 ml of H_2O and 12.0 ml of methanol/chloroform (9 : 1) solution containing BAA or DBAA at a concentration of 5.0×10^{-5} mol/L was stirred for 1 h at room temperature. A 10 ml portion of the mixture was poured into a cylindrical glass container (*id*, 46 mm; *h*, 60 mm), the surface of which had been previously treated with octadecyltriethoxysilane. The container was covered with aluminum foil having in it several holes (*d*, 1 mm), and the solution was left to gel at room temperature for 5 days. After gelation the aluminum foil was perforated with additional holes. After 14 days, the bulk gel was heated at 30 ℃ for 5 days and subsequently at 60 ℃ for 24 hr to give the monolithic

crack-free bulk sample containing BAA or DBAA (*d*, 20 mm; *thickness*, 3 mm).

Sol-gel films were prepared on quartz plates by using the so-called dip-coating technique as described in Chapters 6 - 8. A mixture of TEOS, water, concentrated HCl, ethanol and ether (molar ratio of TEOS: water: ethanol = 1:2:3), in which BAP was dissolved, was used as the coating solution. The films obtained were heated at 110 ℃ for 15 hr. The thickness of the sol-gel film was calculated to be *ca.* 100 nm, using the UV-absorbance of BAP with the following assumptions;(i) all TEOS is converted into silica, (ii) the density of the film is 2.0, and (iii) the absorption coefficient of BAP is not affected by embedding.

PMMA films were prepared by solvent-casting onto quartz substrates from a 10 wt % PMMA solution containing 5.0 x 10^{-3} mol/L of BAA or DBAA in THF. They were kept at room temperature for 2 h and then heated *in vacuo* at 70 ℃ for 8 h.

PVA film was overcoated onto a sol-gel film by spin-coating in order to act as an oxygen barrier.

Measurements

The photodimerization and photodissociation in the solid matrices was carried out by irradiation at room temperature with 365 nm or 285 nm light at a constant intensity; a Jasco CRM-FA irradiator equipped with a 2-kW xenon arc lamp and a monochromator was used. Electronic absorption measurements were made with a Hitachi UV-320 spectrometer.

RESULTS AND DISCUSSION

Photocyclodimerization of BAP and BAA in Solutions

In an aerated diluted solution, anthracene undergoes both photodimerization and photooxidation upon irradiation with 365 nm light, as shown in Figure 9-3. A number of bichromophoric systems, in which two anthryl rings are connected by a flexible chain, have been prepared in order to cause preferential photodimerization, even with a diluted solution, so as to gain novel photochromic molecules.[5,6] Use of bichromophoric anthracene as a photoactive probe for elucidating the microstructures of silica matrices may have a dual significance. First, the intramolecular photodimerization of the dianthryl compound requires a much larger molecular structural change than that of azobenzenes so that the estimation of a larger free volume in a sol-gel silica matrix can be made.

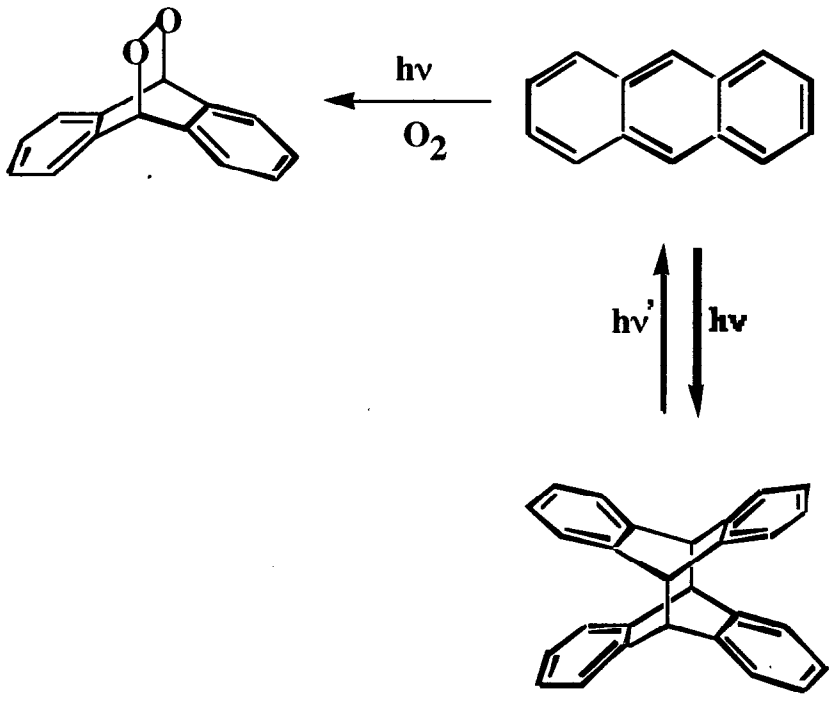

Figure 9-3 Photodimerization and photooxidation of anthracene.

Secondly, photo-induced reversibility between the dissociation and photodimerization of an intramolecular photodimer may provide a clue for use in estimating smaller free volume in silica matrices as the reversibility will be canceled if the free volume is so large that the photodissociated anthracene moieties separate.

For the present purpose, BAP and BAA was employed because of their effective photodimerizability and their hydrophilic characters (due to the presence of either a hydroxyl or amino group) both of which are favorable for dissolution in a solution to give sol-gel matrices. Figure 9-4 shows the change in absorption spectra of BAA in an aerated ethanol solution during 365 nm light irradiation for the dimerization and subsequent 285 nm light irradiation for the monomerization. The characteristic absorption spectrum of BAA disappeared completely after prolonged irradiation with 365 nm light and was restored upon irradiation with 285 nm light. This reversible spectral change confirms that the intramolecular photocyclodimerization in BAA takes place efficiently and that the resulting photodimer (DBAA) reverts to BAA upon exposure to 285 nm light. In this reversal process, the amount of BAA recovered does not reach that of the initial absorbance as both DBAA and BAA absorb the incident light thus leading to a photostationary state. BAP exhibited similar spectral changes in an aerated ethanol solution, which corresponded to the intramolecular photodimerization and photodissociation. As expected from Hirayama's rule for excimer fluorescence,[7] an efficient photocyclomerization takes place when a saturated three-membered chain links two anthracene moieties. Both BAA and BAP conform with this.

Because the solubility of BAA in polar solvents is enhanced by acidification to form a hydrochloride salt (BAA-HCl), UV irradiation was undertaken to check the photochemistry of BAA-HCl. Contrary to our expectation, the absorbances of BAA-HCl in a diluted solution partially decreased (*ca.* 85 %) upon UV irradiation, and the absorption bands corresponding to the remaining anthracene framework were almost unchanged even after prolonged irradiation in degassed ethanol. After neutralization of a UV irradiated solution in order to recover BAA, subsequent UV irradiation with 365 nm light resulted in no further alteration of the absorption spectrum. In contrast to this, the intramolecular photodimerization of BAP was not affected by addition of HCl. These points indicate

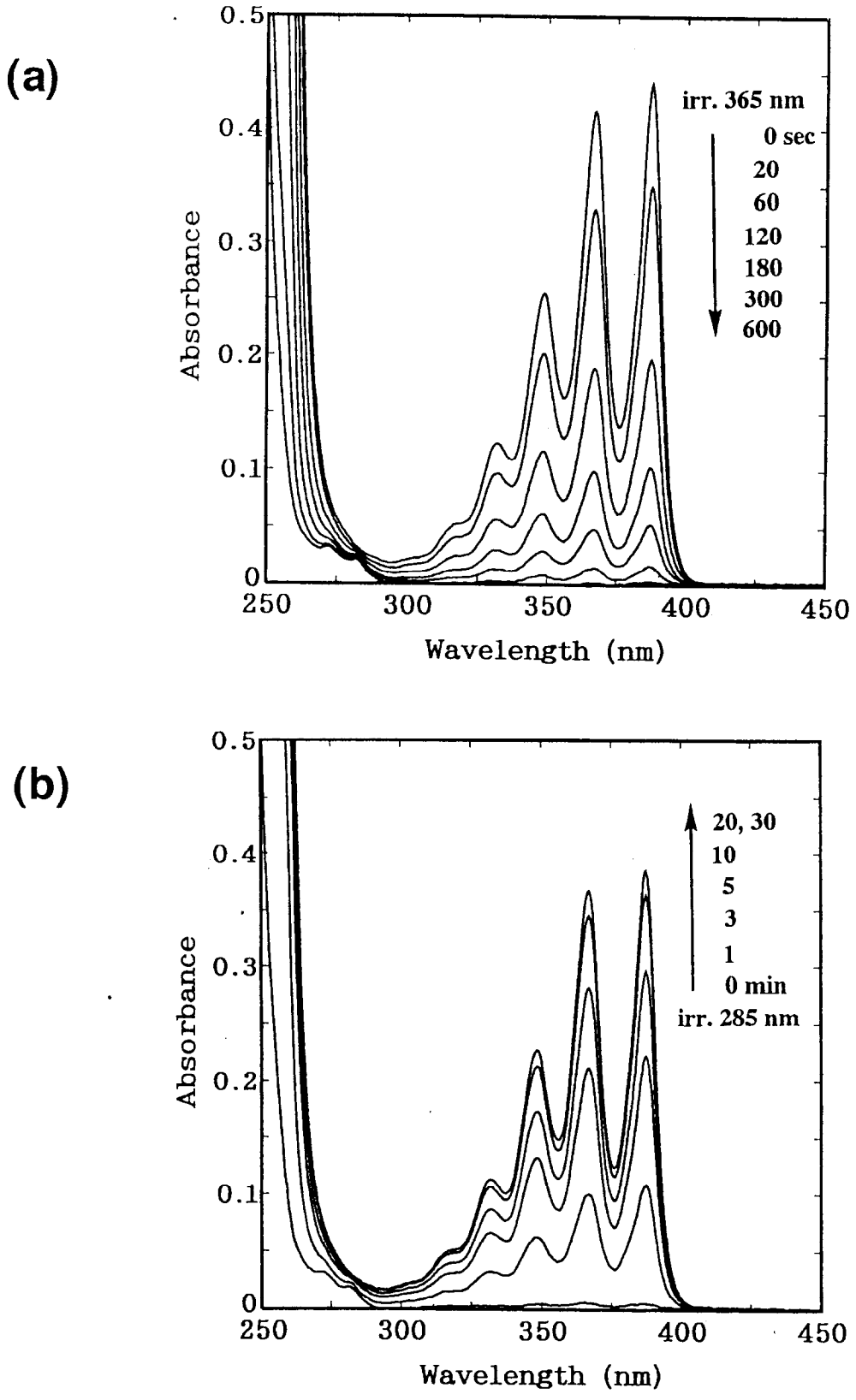

Figure 9-4 Changes in UV spectra of BAA in ethanol (a) during 365 nm light irradiation and (b) subsequent irradiation at 285 nm.

that the photodimerization of BAA under acidic conditions is accompanied by irreversible photocleavage of the spacer linking the two anthracene rings, which inhibits intramolecular dimerization.

Photochemical Behaviors of BAP in Sol-gel Film

A sol-gel coating film is so thin that a photoprobe has to be adequately soluble in the coating solution so as to obtain a film that has an appropriate absorbance. Unfortunately, BAA was only sparingly soluble in the sol-gel starting solution. However, with BAA-HCl, although the solubility is improved, it suffers from an irreversible side photoreaction that results in bond cleavage. BAA was employed as a very low concentration dopant for monolithic sol-gel glasses prepared under neutral conditions without the addition of aqueous hydrochloric acid as hydrolytic catalyst. BAP could, to some extent, be dissolved in an alkoxide solution and photodimerized without decomposition, even in the presence of HCl. This bichromophoric compound was used as a probe in sol-gel films prepared under acidic condition.

Figure 9-5 (a) shows changes in the UV spectra of BAP in a sol-gel film during 365 nm light irradiation at room temperature. The characteristic absorption bands of BAP gradually diminished with increasing irradiation time and disappeared almost completely when the film was irradiated for 35 min. In sharp contrast to the solution behavior, no characteristic band of BAP reappeared upon exposure to 285 nm light. This fact led us to assume that BAP undergoes preferential photooxidation rather than photodimerization upon irradiation with 365 nm light in the sol-gel film. Concerning the mobility of encapsulated organic molecules in sol-gel films, the author have already demonstrated that the degree of the photoisomerization of an azobenzene derivative was much smaller than that in solution because of the steric restriction of the matrix (Chapter 6-8). As intramolecular photodimerization, in which two anthracene rings come together, requires a much larger molecular movement than that for the isomerization of azobenzene, the dimerization must be considerably suppressed by the networked matrix and, consequently, photooxidation occurs predominantly. As Figure 9-5(b) shows, the photoinduced decrease in the absorption bands corresponding to the anthryl moiety in the sol-gel film

is considerably reduced by overcoating the film with a PVA film, which acts as a n oxygen barrier owing to the very low permeability of oxygen. These results support the fact that the disappearance of the absorption bands due to the anthracene in the sol-gel film is ascribable not to photodimerization, but to irreversible photooxidation of BAP.

The diffusion coefficient of oxygen through a fully densified sol-gel silica coating on Si and on SiC is known to be very small, $D < 10^{-14}$ $cm^2 s^{-1}$ at 750 ℃, indistinguishable from that through thermally grown SiO2.[8] If mass transport of oxygen is limited by the xerogel matrix, similarly, oxidative degradation of organic molecules incorporated in sol-gel matrices should be markedly retarded. As described in Chapter 8, the structure of sol-gel films is considerably more compact and dense than that of sol-gel bulk materials. The present observations reveal that even organic molecules encapsulated in such a dense sol-gel film react easily with externally diffused oxygen. Schutte *et al.* have demonstrated that an inorganic environment derived from the sol-gel technique does not enhance the thermal or oxidative stability of 2,4-dinitroaniline in coatings.[9] These results indicate that the sol-gel silica matrices do not provide significant protective measures against oxidation of the organic molecules embedded in the silica films. However, it has been reported that the photostability of Rhodamine 6G (R6G) is enhanced by incorporation in a sol-gel glass.[10] The bleaching process of the dye may depend on the nature of solvent or matrix and on the presence of other reactive species, such as oxygen.[11] From these findings, the photostabilization of R6G in the sol-gel glass may be assumed not to be due to the shielding from atmospheric oxygen but due to other factors.

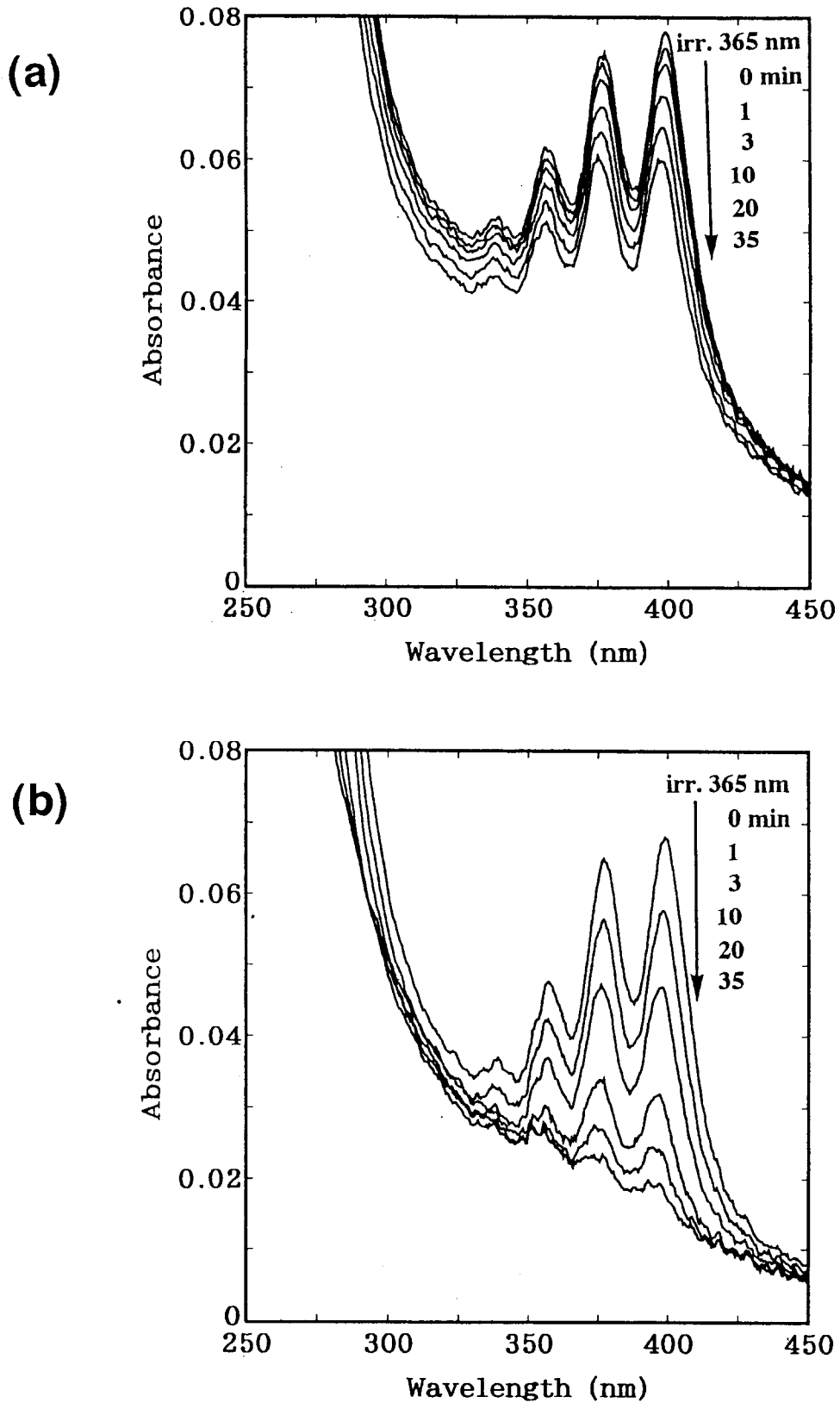

Figure 9-5 Changes in UV spectra of BAP in a sol-gel film during 365 nm light irradiation (a) with and (b) without a PVA film coating.

Photochemistry of BAA and Photodissociated DBAA in PMMA

Because BAP does not act as a photodimerization probe in the solid matrices, an intramolecular photodimer was entrapped in solids in order to generate two anthryl units by irradiation with light at a shorter wavelength. The photodimerized BAP was not suitable for this purpose because it is only slightly soluble. This led us to the use of DBAA-BAA system owing to the acceptable solubility of the photodimer. Figure 9-6(a) shows spectral changes of BAA in PMMA upon exposure to 365 nm light and subsequent exposure to 285 nm light. The photochemical regeneration of the anthryl group did not take place, just as for BAP in a sol-gel film, suggesting that the predominant photochemistry is not photodimerization, but irreversible photooxidation. Thus, in analogy with a sol-gel film matrix, BAA molecules are frozen in a PMMA matrix leading to the suppression of the conformational alteration required for the intermolecular photoreaction.

A closely related piece of work has been described by Tran-Cong and co-workers,[12] who studied photocyclomerization of bis(9-anthrylmethyl)ether in polystyrene film, in which a fraction (5-10 %) intramolecular photodimerization occurred, the rest did not have a suitable conformation for the cycloaddition. This is consistent with our experimental results.

Chandross and co-workers[13,14] demonstrated that two anthracene molecules with a face-to-face arrangement, termed a sandwich dimer, were formed in rigid glasses of methylcyclohexane by photodissociation of the photocyclodimer upon irradiation with 254 nm light at 77 K. In this system, only a small fraction of the sandwich dimer can be reversed photochemically back to the cycloadduct. This means that the face-to-face arrangement of major part of the sandwich pairs is distorted away from the symmetrical geometry (even at a low temperature) because of the instability of sandwich dimer in the ground state. The resulting preferred arrangement of two aromatic molecules resembles that in a unit cell of anthracene crystals.[15] However, if two anthracene rings of the intramolecular photodimer (DBAA) are forced to remain close to each other and can come together in a solid matrix, the reversible photodimerization will occur easily upon irradiation with 365 nm light. Figure 9-6 (b) shows the results. A PMMA film doped with DBAA was pre-irradiated with 285 nm light to generate anthryl groups, followed by exposure to 365 nm light to result in the monotonous decrease in

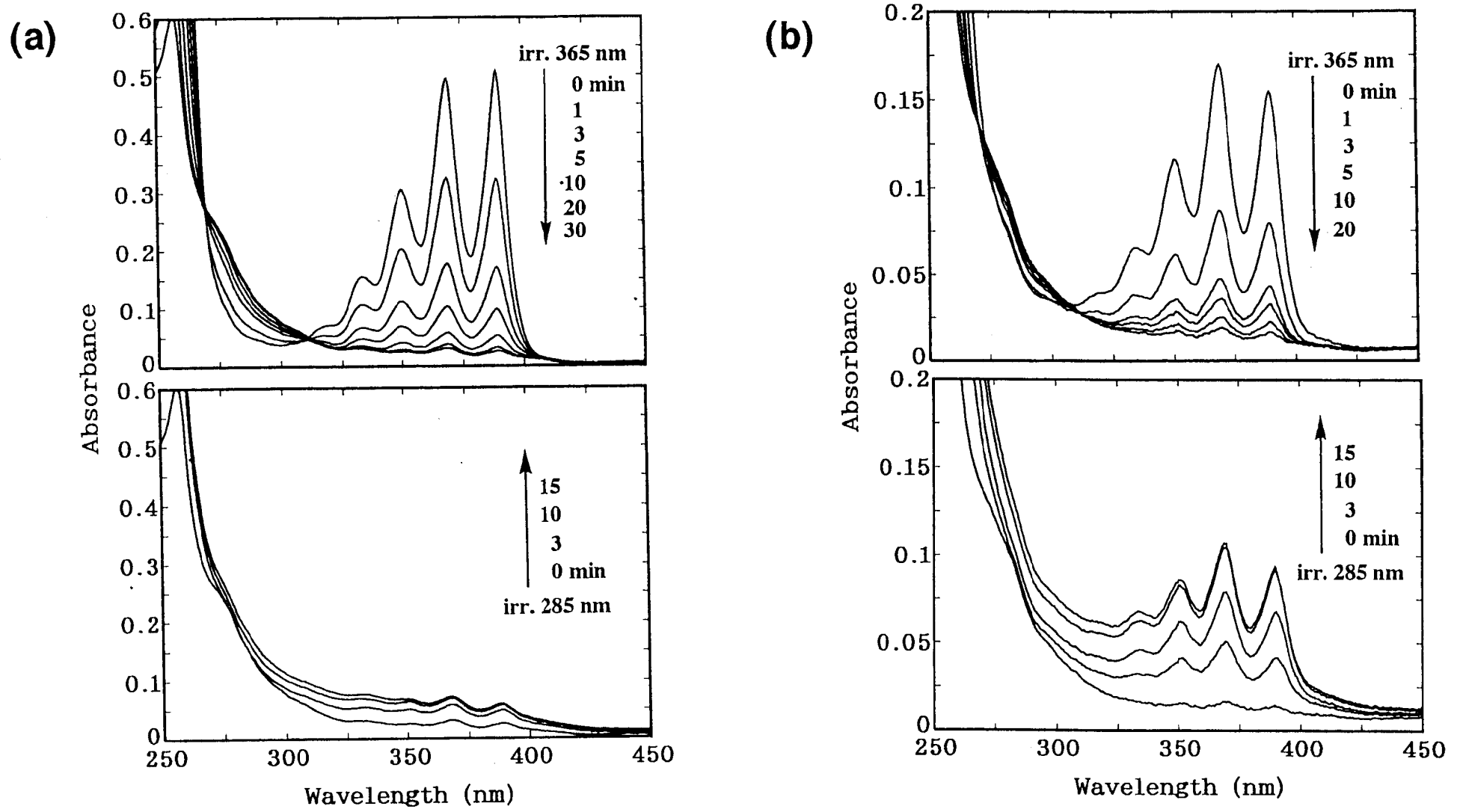

Figure 9-6 Changes in UV spectra of bichromophoric anthracene in PMMA films: (a) BAA ; (b) DBBA dissociated by pre-irradiation with 285 nm light. Upper panels, during 365 nm light irradiation, lower panels, subsequent irradiation with 285 nm light.

the absorbance of the aromatic moiety [Figure 9-6 (b), upper panel]. In contrast to the photochemical behavior of BAA [Figure 9-6 (a), lower panel], the characteristic vibronic bands corresponding to anthryl groups became noticeable upon a second irradiation with 285 nm light [Figure 9-6 (b), lower panel]. These results imply two of the anthracene groups of photodissociated DBAA remain in proximity to each other as a result of the matrix rigidity of PMMA (even at room temperature) this then affords a preferential conformation for the reversible photodimerization.

Photochemistry of BAA and Dissociated DBAA in Sol-Gel Bulk Materials

The reversibility of intramolecular photoisomerization of both BAA and DBAA was determined in sol-gel bulk materials. The absorbance of the anthryl units has been adjusted to be similar to those in PMMA matrix in order to provide a reasonable comparison. As shown in Figure 9-7 (a), the regeneration of the anthryl moiety from photo-irradiated BAA was markedly suppressed upon exposure to 285 nm light in a similar way to that in a PMMA film. For DBAA, which was first photodissociated upon irradiation with 285 nm light and then subsequently illuminated with 365 nm light in monolithic silica, the photochemical behavior [Figure 9-7 (b), lower panel] resembles that of PMMA [Figure 9-6 (b), lower panel]. This implies that the face-to-face arrangement of two photodissociated anthracene rings is maintained at least partially in sol-gel silica. Judging from the absorbances of the photochemically recovered chromophore, the efficiency of photodissociation in monolithic silica is far less than *ca.* 50% and is lower than that in PMMA in which 58% of the photodimer reverts to the anthryl groups.

In order to compare the rigidity of the matrix of a sol-gel bulk material with that of a PMMA film, the decrease in the absorbance at 390 nm of both BAA and photodissociated DBAA during the course of 365 nm irradiation were plotted as a function of the irradiation time, see in Figure 9-8. The disappearance processes of the chromophore involves both intramolecular photodimerization and photooxidation, as stated above. As photooxidation depends on the concentration of oxygen in the matrices, the difference in the consumption rate for the anthryl groups between those of BAA and those of photodissociated DBAA, in the same matrix, upon 365 nm light irradiation obviously reflects the

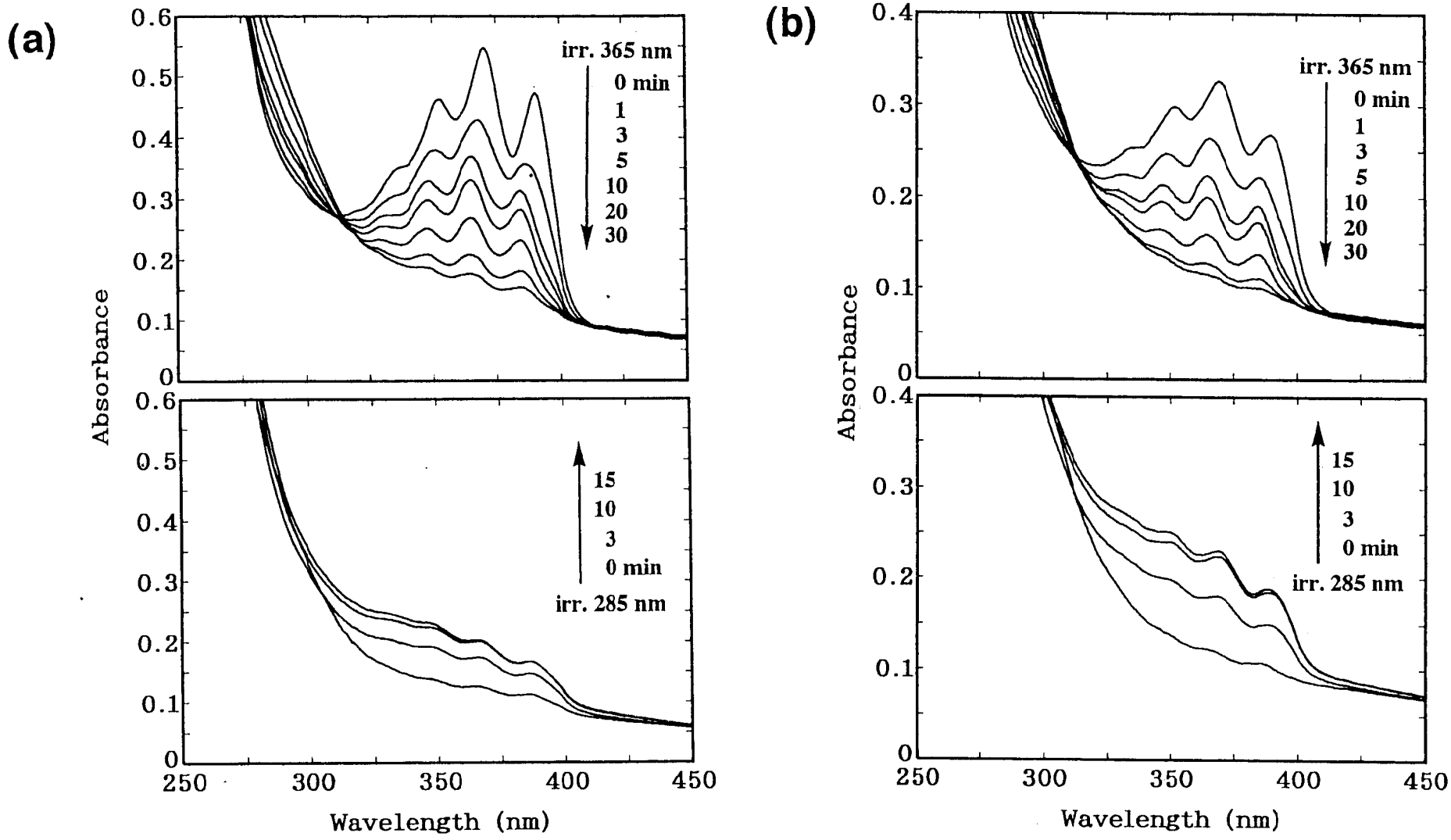

Figure 9-7 Changes in UV spectra of the chromophoric anthracene in the sol-gel bulk materials: (a) BAA ; (b) DBAA dissociated by pre-irradiation with 285 nm light. Upper panels, during 365 nm light irradiation; lower panels, subsequent irradiation with 285 nm light.

difference in the efficiency of the photodimerization. In a PMMA matrix, the disappearance of photodissociated DBAA takes place considerably faster than that of BAA. However, there was no marked difference observed between BAA and dissociated DBAA in the sol-gel bulk materials. This suggests that the face-to-face conformation of the dissociated photodimer is more readily relaxed in the inorganic materials than in the organic matrix. In other words, the steric restriction to suppressing molecular motion is rather larger in PMMA than in sol-gel bulk materials. This is in line with the above-mentioned observation that the anthracene moiety is more efficiently recovered upon 285 nm light irradiation in PMMA than in a monolithic silica.

In Chapter 8, the author described the photochemical and thermal isomerization of hydrophilic azobenzene derivatives in sol-gel films and bulk materials prepared from the same starting solution, and a comparison was made with their isomerization behaviors in PMMA. Kinetic studies of thermal *cis*-to-*trans* isomerization revealed that the steric restriction suppressing the molecular motion of the embedded probes increased in the following order; sol-gel bulk material < PMMA < sol-gel film. The present results, using anthracene probes, are consistent with the results in Chapter 8 and indicate that the molecular motion of embedded organic compounds is assured in sol-gel monolithic silica owing to its porous structure.

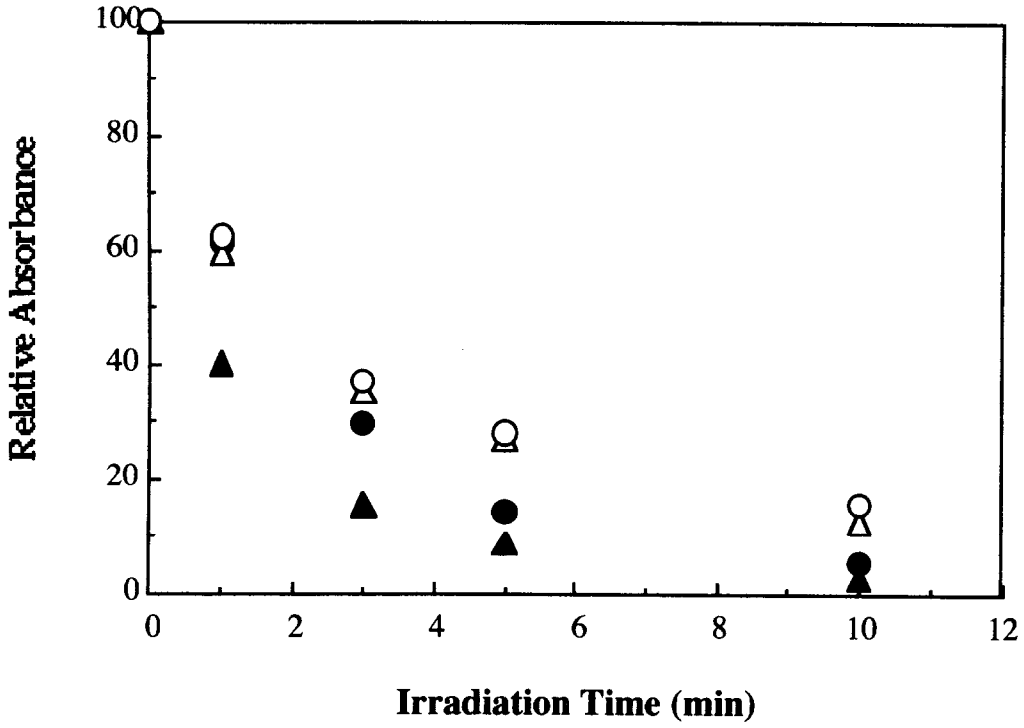

Figure 9-8 Decrease in the absorbance at 390 nm of anthryl groups: (a) in PMMA (●, BAA; ▲, dissociated DBAA), (b) in the sol-gel bulk materials (○, BAA; △, dissociated DBAA).

SUMMARY

The following conclusions can be drawn by studies on the reversible photodimerization and the photooxidation behaviors of anthracene probes in sol-gel glass and PMMA.

(1) The bichromophoric anthracenes undergo photooxidation in preference to intramolecular photodimerization in both sol-gel glass and PMMA because of the steric constraint of their matrices.

(2) The organic molecules entrapped within sol-gel silica are easily photooxidized by atmospheric oxygen that has permeated through the matrix.

(3) The steric constraint in the sol-gel bulk matrix is rather smaller than that of PMMA.

REFERENCES

1) H. Bouas-Laurent and J.-P. Desvergne, in *Photochromism Molecules and System*, ed H. Durr and H. Bouas-Laurent, Elsevier, Amsterdam, 1990, p. 561.

2) K. Itoh, T. Ikeda, S. Tazuke and T. Shibata, *J. Phys. Chem.*, **96**, 5759 (1992).

3) M. Hartmann and M. Rathe, *Z. Chem.*, **19**, 373 (1979).

4) M. Yamane, S. Aso and T. Sakaino, *J. Mater. Sci.*, **13**, 865 (1978).

5) H. Bouas-Laurent, A. Castellan and J.-P. Desvergne, Pure *Appl. Chem.*, **52**, 2633 (1980).

6) J.-P. Desvergne, H. Bouas-Laurent, F. Lahmani and J. Sepiol, *J. Phys. Chem.*, **96**, 10616 (1992).

7) F. Hirayama, *J. Chem. Phys.*, **42**, 3163 (1965).

8) J. Schlichting, *J. Non-Cryst. Solids*, **63**, 173 (1984).

9) C. L. Schutte, K. W. Williams and G. M. Whitesides, *Polymer*, **34**, 2909 (1993).

10) D. Avnir, D. Levy and R. Reisfeld, *J. Phys. Chem.*, **88**, 5956 (1984).

11) I. P. Kaminov, L. W. Stulz, E. A. Chandross and C. A. Pryde, *Appl. Opt.*, **7**, 1563 (1972).

12) H. Yoshizawa, K. Ashikaga, M. Yamamoto and Q. Tran-Cong, *Polymer*, **30**, 534 (1989).

13) E. A. Chandross, *J. Chem. Phys.*, **43**, 4175 (1965).

14) E. A. Chandross, J. Ferguson and E. G. McRae, *J. Chem. Phys.*, **45**, 3546 (1966).

15) J. Ferguson, *Chem. Rev.*, **86**, 957 (1986).

Chapter 10

Summary

This thesis deals with the presentation of novel functionality and characteristics of photochromic organic-inorganic hybrids. As discussed in Chapter 1, though various properties such as adhesion, wetting, and colloid stabilization have been advanced by surface-modification with organofunctional chlorosilane or alkoxysilane on inorganic surface, scarcely attention has been paid to integrate properties of inorganic materials with the unique function of organic chemistry. So, the author explored the novel possibilities of silicas/organic composite by two different approaches, *i. e.*, by placing organic photochromic molecules *onto* and *into* silica matrices. In the first half of this thesis (Chapters 2-5), the author examined the functionality of silicas by means of surface-modification *onto* silica surface. In the second half (Chapters 6-9), the author investigated microenvironmental structures *into* sol-gel silica matrices by evaluating the reactivity of doped organic photochromic probes.

(Chapters 2-5: Functionality of Silica by Surface-modification with Photochromic Compounds)

Azobenzenes having an amino residue show good adsorptivity on a silica surface through a hydrogen bonding, as reported in Chapter 2. A silica surface adsorbing the azobenzene amphiphilic compound displays an ability to command the photoalignment of a nematic liquid crystal between homeotropic and planar modes. This provides a convenient procedure to fabricate photoresponsive LC cells simply by filling LC dissolving azobenzene amphiphiles between clean silica surfaces.

In Chapter 3, a novel carlixresorcin[4]arene (4-AzCRA) having four p-butylazobenzene residues sprouted from an upper rim of the cyclic framework was prepared to be subjected to adsorption on a surface of colloidal silica particles. UV irradiation of a homogeneous dispersion of surface-modified silica particles in cyclohexane enhanced the sedimentation owing to the increase in surface polarity, leading to the formation of porous precipitates. Subsequent visible light irradiation

regenerated a dispersed state, displaying the photocontrol of the reversible alternation between dispersed and aggregated states of silica particles. This provides a novel system for molecular amplification of photonic information.

Another attempt of photocontrolled aggregation of colloidal silica was made by chemisorption on the silica surface with photochromic spirobenzopyran (SP), as mentioned in Chapter 4. Reversible control of the modified colloidal silica between sedimentation and dispersion was induced unequivocally in carbon tetrachloride by alternate irradiation with UV and visible light to cause the surface photochromism. The photoinduced sedimentation is triggered by the decrease in the affinity between the particle surface and the non-polar solvent molecules. The increase in the surface polarity of silicas upon UV irradiation induces the aggregation of particles which causes the sedimentation, leading to the colored precipitate with high porosity.

Apart from the photofunctionality of materials based on a photoinduced polarity change, a photochromic SP is often employed as an effective photoprobe for estimation of microenvironmental factors such as polarity, viscosity and the free volume of polymers. In Chapter 5, the thermal reverse reaction kinetics of SP attached to a silica surface through two different methylene spacers was studied in order to reveal the characteristics of the inorganic surfaces. Dispersion of SP-modified colloidal silica in ethylene glycol results in the single first-order decay of photoformed MC because of efficient solvation to assure a homogeneous microenvironment on the silica surface. On the other hands, water-insoluble solvents force the merocyanine (MC) moiety to distribute into a heterogeneous microenvironment with variant polarity to bring about the bimodal first-order kinetics of the thermal reversion of MC. The blue shift and the bimodal first-order kinetics have been interpreted as a partitioning of the MC moiety between two distinctive residential sites with different polarity: an inner region with the higher polarity faced to an adsorbed water layer lying on the silica surface and an outer region exposed to a organic solvent phase. The fraction of MC interacted with an outer solvent phase is a dominant factor determining whether the UV-exposed photochromic silica is dispersed in non-polar solvents.

(Chapters 6-9: Characteristic of Trapped Molecules in Sol-Gel Silica Matrices)

Aiming at investigation the rigidity of the sol-gel glass matrix, the behaviors of the photoinduced *trans*-to-*cis* isomerization and the thermal *cis*-to-*trans* isomerization of an azobenzene derivative in sol-gel films were mentioned in Chapter 6. Hydrogen bonds are formed between the azo group in the azobenzene probe and silanol group in sol-gel glass matrix whose films were prepared with a relatively high water concentration ($[H_2O]/[TEOS] \geqq 2$). The hydrogen bond formation between the azo group and silanols bound on the silica wall results in blue shift of the n-π^* absorption band. The relative intensity of the blue-shifted band was affected by the nature of bond of the azo-chromophore to the silica matrix. The azobenzene probes in the sol-gel glass can be divided into the following three types when the glass is prepared from a solution of $[H_2O]/[TEOS]=2$. (a) At sites with smaller pores in which the *trans*-to-*cis* photoisomerization is quenched, (b) at sites in which the *cis* isomer is formed in a strained conformation enhancing the thermal reversion, (c) at sites in which the thermal reversion rate is reduced by the hydrogen bond between the guest molecule and silanol groups. It was found that the rigidity of the matrix in sol-gel glass depends on the water content of the solution from which it was prepared. In the case of $[H_2O]/[TEOS]=1$, the photoisomerization takes place readily in a sol-gel film possibly because of inefficient network formation. The *cis* fraction in the photostationary state in sol-gel films was much smaller than in PMMA. This suggests that the sol-gel film matrix is more rigid than PMMA.

The major purpose of Chapter 7 is to investigate the effect of covalent bond formation between a doping azobenzene moiety and silica-gel matrices on the geometrical isomerization. The author expected that the introduction of silylation units at both sides of the azobenzene enhances considerably suppression of reactivity of the chromophore. The introduction of one triethoxysilyl group had a slight effect on both photoisomerization and thermal reversion in sol-gel films. Fixation of both sides of the azobenzene unit to the silica matrix enhanced the suppression effect to quench photoisomerization of about 60 % of azobenzene units. This supports the view that molecular motion of azobenzene unit is highly restricted because of the cross-linked silica network.

The major concern of Chapter 8 is to disclose outstanding differences in microenvironmental structures between a monolithic silica bulk and a silica film by means of evaluating the reactivity of doped azobenzenes as probe molecules. The results implied that the pores in the sol-gel bulks are larger than those in the sol-gel films. In particular, it should be noted that the *cis*-to-*trans* thermal isomerization obeys first-order kinetics even though the probe compound is entrapped in solid bulk material, reflecting much larger free volumes in the sol-gel bulk silica matrix so that the isomerizations of azo chromophore take place as readily as in solution, whereas the isomerization in a glass film deviated from the first kinetics. These may lead to a novel conclusion that reactions, at least unimolecular reactions, of organic molecules entrapped physically in bulk materials does not undergo suppressive effect caused by silica matrices. The steric constraint due to the matrix decreased in the following order:

sol-gel films > PMMA > sol-gel bulks.

In Chapter 9, the reversible photodimerization and the photo-oxidation behaviors of anthracene probes in the sol-gel glass and PMMA were investigated to confirm the above-mentioned results. Studies of competitive photooxidation behavior of the anthracenes were also made to reveal the permeation of atmospheric oxygen into the inorganic matrices. The following conclusions can be drawn by this studies;

(1) The bichromophoric anthracenes undergo photooxidation in the preference to intramolecular photodimerization in both sol-gel glass and PMMA because of the steric constraint of their matrices.

(2) The organic molecules entrapped within sol-gel silica are easily photooxidized by atmospheric oxygen that has permeated through the matrix.

(3) The steric constraint in the sol-gel bulk matrix is rather smaller than that of PMMA.

Recently, attractive features have been reported on glass-entrapped molecules which react with externally applied chemical reagents through the porous network of the material. Such a highly porous, transparent matrix provides a variety of applications such as solid ion exchangers, bioactive materials, chemical sensors, recyclable catalyst, GDLC (glass dispersed liquid crystal), and so forth as described in Chapter 1. It seems that above-mentioned applications could be imparted essentially by only using the sol-gel bulk process because such systems need the material having a sufficient pore size to allow the permeation of substrate molecules into silica matrix. For practical applications, a delicate balance should be necessary between good isolation by matrices on one hand and sufficient accessibility of the entrapped molecules to reactants on the other.

LIST OF PUBLICATIONS

Chapter 2.

" Alignment Photoregulation of a Nematic Liquid Crystal by Surface Adsorption of Aminoalkylated Azobenzenes "

M. Ueda, K. Kudo and K. Ichimura, *Israel J. Chem.*, **36**, 371 (1996).

Chapter 3.

" Photocontrolled Dispersibility of Colloidal Silica by Surface Adsorption of a Calix[4]resorcinarene having Azobenzene Groups "

M. Ueda, N. Fukushima, K. Kudo and K. Ichimura, *J. Mater. Chem.*, **7(4)**, 641 (1997).

Chapter 4.

"Photocontrolled Aggregation of Colloidal Silica"

M. Ueda, H.-B. Kim, and K. Ichimura, "*Advanced Materials '93, II/A: Biomaterials, Organic and Intelligent Materials*" , eds. H. Aoki, *Trans. Mat. Res. Soc. Jpn.*, (Elsevier Science B. V., 1994) p. 327.

"Photocontrol of Dipersibility of Colloidal Silica"

M. Ueda, H.-B. Kim, and K. Ichimura, *Mater. Lett.*, **20**, 245 (1994).

"Photocontrolled Aggregation of Colloidal Silica"

M. Ueda, H.-B. Kim, and K. Ichimura, *J. Mater. Chem.*, **4(6)**, 883(1994).

Chapter 5.

"Photochromic Behaviour of a Spirobenzopyran Chemisorbed on a Colloidal Silica Surface"

M. Ueda, K. Kudo, and K. Ichimura, *J. Mater. Chem.*, **5(7)**, 1007(1995)

Chapter 6.

"Photoisomerization of an Azobenzene in Sol-Gel Glass Films"

M. Ueda, H.-B. Kim, T. Ikeda, and K. Ichimura, *Chem. Mater.*, **4**, 1229 (1992).

Chapter 7.

"Photoisomerizability of an Azobenzene Covalently Attached to Silica-Gel Matrix"

M. Ueda, H.-B. Kim, T. Ikeda, and K. Ichimura, *J. Non-Cryst. Solids*, **163**, 125 (1993).

Chapter 8.

"Photochemical and Thermal Isomerization of Azobenzene Derivatives in Sol-Gel Bulk Materials"

M. Ueda, H.-B. Kim, and K. Ichimura, *Chem. Mater.*, **6**, 1771 (1994).

Chapter 9.

"Photochemical Behaviour of Tethered Dianthryl Compounds in Sol-Gel Glass"

M. Ueda, H.-B. Kim, T. Ikeda, and K. Ichimura, *J. Mater. Chem.*, **5(6)**, 889 (1995).

ACKNOWLEDGMENTS

This work was achieved at Tokyo Institute of Technology, where the author got the appropriate direction and advice by Professor Kunihiro Ichimura. The author would like to express sincere gratitude to Professor Kunihiro Ichimura for his valuable guidance and encouragement throughout the duration of this study. This work would have been impossible without his guidance.

I wish to express my grateful appreciation to Professor Tomiki Ikeda for his helpful discussion and encouragement and also to Associate Professor Takahiro Seki for his helpful support.

I am indebted to Dr. H.-B. Kim of Hokkaido University and Dr. Kazuaki Kudo of Tokyo University for their helpful discussion.

I gratefully acknowledge to Managing Director Dr. Koshi Kusumoto of Tokuyama Corp. for his encouragement and giving me the opportunity for this research, and to Section Chief Dr. Naoki Mikami of Tokuyama Corp. for his heartfelt support.

In addition, grateful acknowledgment is made to all members of Ichimura -Seki laboratory for their kind assistance and encouragement.

Finally, I sincerely express my hearty thanks to my parents, my lovely wife, my pretty daughter and son for their affectionate encouragement and understanding to this work.

上田雅英

Masahide Ueda
Tokuyama Corporation
July 2000